Design and Development of an Arsenic Removal Filter using Indigenous Materials

Thesis submitted

in partial fulfilment of the requirement for the degree of

Doctor of Philosophy

by

Sandip Mondal

DEPARTMENT OF CIVIL ENGINEERING

INDIAN INSTITUTE OF TECHNOLOGY GUWAHATI

GUWAHATI – 781039, INDIA

JANUARY 2013

Design and Development of an Arsenic Removal Filter using Indigenous Materials

Thesis submitted

in partial fulfilment of the requirement for the degree of

Doctor of Philosophy

by

Sandip Mondal

Regd. No. 05610408

DEPARTMENT OF CIVIL ENGINEERING

INDIAN INSTITUTE OF TECHNOLOGY GUWAHATI

GUWAHATI – 781039, INDIA

JANUARY 2013

DEDICATION

This thesis is dedicated to my parents

Mr. Gurudas Mondal

&

Mrs. Purnima Mondal

and especially my wife

Soumika Mondal

who have stood by me patiently all these years

Indian Institute of Technology, Guwahati

Candidate's Declaration

I hereby declare that the work presented in this thesis is original to the best of my knowledge, except as acknowledged in the text. This material has not been submitted, either in whole or in part, for degree at any university.

Sandip Mondal

Registration No. 05610408
Research Scholar
Department of Civil Engineering
IIT Guwahati

Indian Institute of Technology, Guwahati

Certificate

This is to certify that the thesis entitled "**Design and Development of an Arsenic Removal Filter using Indigenous Materials**" submitted by Sandip Mondal (Registration No.05610408) to the Indian Institute of Technology Guwahati for the degree of Doctor of Philosophy is a record of bonafide research work carried out by him under my supervision and guidance. The thesis work, in my opinion, has reached the requisite standard fulfilling the requirement for the award of the degree of Doctor of Philosophy. This work has not been submitted earlier for the award of any degree or diploma to the best of my knowledge and belief.

(Supervisor)
Chandan Mahanta
Professor
Department of Civil Engineering
Indian Institute of Technology
Guwahati

ACKNOWLEDGEMENT

I am indebted to many people who helped me over the years in this research work and it is my privilege to acknowledge them.

First and foremost I would like to thank my supervisor Prof. Chandan Mahanta, for his encouraging support, inspiration, guidance, continued interests, valued suggestions and confidence he placed on me for carrying out this research work. His continuous guidance and support have made this thesis seeing the light of the day. I would also like to thank the Doctoral Committee members Prof. Arup Kumar Sarma, Dr. Mihir Kumar Purkait and Dr. Pranab Kumar Ghosh for their time, commitment and helpful suggestions all throughout.

I would like to express my gratitude to Prof. S.K Deb (Head, Civil Engineering Department) and in-charges of the Environmental Engineering Laboratory Dr. Saswati Chakraborty, Dr. Sharad Gokhale and Dr. P.K. Ghosh for the help and facilities provided for completion of this research work.

Thanks are also due to all the faculty and staff members of the Department of Civil Engineering, the Library and the Administration staff members of Indian Institute of Technology, Guwahati for their help in different forms at various stages of this work.

I am very much thankful to Jonali Saikia (Scientific Officer) and P. Pathak (Lab Technician) for their cooperation and help with equipments and resources during my experimental period in the Environmental Laboratory, Civil Engineering Department.

I would like to extend my sincere gratitude to my friends especially Lalsangzela Sailo, Wazir Alam and Pronob Jyoti Borah who have been there always, from field trips in remote places to assistance in the laboratory, under all conditions - my appreciations are countless for them. I would like to acknowledge the services rendered by Khagen Das and other PHED officials staff of Nalbari district of Assam for their assistance in the field work. I am thankful to Gopal Gobinda Pal for helping me to develop laboratory scale arsenic removal filter.

I would like to thank Debabrata Ghosh for his continuous support during my thesis work. I feel deep gratitude for my friends who have made my research experience

at IIT Guwahati unforgettable: Tapasda, Albino, Kamal, Minaxi, Rupak, Sachin, Barun, Amit, Arpit, Rajendra and Dakua with whom I shared my pains, sorrows, fun and laughter. It was impossible to imagine a life in the campus without them.

Most of all, I want to thank my family: my wife, mother, father and brothers who have been constant sources of encouragement, support, patience and love.

Most importantly I thank Almighty God whose blessings have helped me in achieving these strides in life.

Sandip Mondal

Abstract

Arsenic contamination of groundwater is considered to be one of the largest human hazards faced in the last two decades around world. In India, the groundwaters of Ganga- Meghna-Brahmaputra floodplains are highly affected with arsenic contamination. In order to assess the severity of newly discovered arsenic contamination in Assam, a study carried out jointly by UNICEF and PHED of Assam found that 18 districts were affected with arsenic contamination. Several conventional and non-conventional technologies have been proposed so far with variable success for aqueous arsenic remediation. Filtration being one of them in developing countries, filtration cost and sustainability are critical issues. Naturally and locally available materials in India, Vietnam, Bangladesh and China have been attempted as low-cost adsorbents, considering their arsenic sorption capacity. However for the Assam valley in Upper Brahmaputra floodplains, most of these technologies are not viable due to logistics, social acceptances, delivery and non-availability of identical media. For a local filter, there is always a need of examining the potential of local materials. To overcome the arsenic pollution in drinking water in remote areas of Assam, where even indigenous filter is not in use, the arsenic adsorption capacity of four different locally available materials *i.e.* sand, naturally oxidized iron scrap (NOIS) and red soil were examined. The main objective of the study was to develop a low cost treatment method keeping in mind the local needs and locally available materials to be used as filter media. For this, first a new area affected by arsenic contamination but so far not having any treatment system in place was identified, the extent of arsenic contamination was evaluated and finally an appropriate filtration technology was designed with local materials with detailed kinetic and simulation study that were simple yet efficient and affordable so that a most efficient filter system can be developed, specially catering to local need of the inhabitants of the study area.

Delineation of unsafe aquifers in the study area (Madhupur block of Nalbari district in Assam, India) was carried out to quantify geochemical properties of the groundwaters followed by investigating the adsorption characteristics of local low cost

adsorbents [i.e. sand, naturally oxidized iron scrap (NOIS), red soil and murum] to develop a suitable arsenic removal filter appropriate for the study area.

The geo-chemical characteristics of the groundwater along with the spatial distribution and variation of arsenic in the study area were evaluated in the beginning. Plots of major cations and anions in piper diagram revealed that the groundwater of the study area was predominately Ca-Na-HCO_3 type. The pH values of groundwaters varied from 6.20 to 7.40 with alkalinity values ranging from 110 to 220 mg L^{-1}. The groundwaters exhibited electrical conductivity ranging from 140 to 380 µS cm^{-1}; iron ranging from 3.3 to 19.3 mg L^{-1}; calcium ranging from 10.4 to 40.8 mg L^{-1}; sodium ranging from 11.0 to 37.0 mg L^{-1} and manganese ranging from 0.1 to 1.2 mg L^{-1}. Relatively low concentrations of nitrate ranging from 0.4 to 1.4 mg L^{-1}; sulphate ranging from BDL to 1.8 mg L^{-1}; phosphate ranging from 0.3 to 1.8 mg L^{-1} and fluoride ranging from BDL to 0.5 mg L^{-1} were noted. Spatial distribution showed that the groundwater of the study area was severely affected with arsenic contamination. Out of 48 samples, 98% samples exceeded the drinking water permissible limit of arsenic (10 µg L^{-1}) according to World Health Organization (WHO) guidelines, 88% samples contained arsenic beyond the BIS (Bureau of Indian Standards) permissible limit (IS 10500:1991) of 50 µg L^{-1} and 46% samples contained more than 100 µg L^{-1} of arsenic concentration. Statistical analysis of geochemical parameters corroborated that dissolution of major cations from the soil matrix elevated arsenic concentration in the groundwater system. As the groundwater chemistry indicated high reducing conditions, arsenic concentrations possibly increased due to buffering of manganese (ranging from 0.1 to 1.2 mg L^{-1}) at higher level of redox stages and Fe^{2+} might have precipitated as siderite ($FeCO_3$) and vivianite ($Fe_3(PO_4)_2 \cdot 8H_2O$) in the presence of high CO_3^{2-} and PO_4^{3-} ions. No significant correlations of arsenic were observed in case of pH and SO_4^{2-} but a positive correlation could be observed in case of HCO_3^{2-} and PO_4^{3-}. In reducing conditions, the arsenic and the phosphate desorb from the oxides. As the arsenic and phosphate have similarities in adsorption sites, arsenic could also be replaced by phosphate when higher levels of phosphates are present in the soil matrix. Seasonal variations of major ions were not significant. During winter season the arsenic concentration was quite high and maximum concentration was reached in the month of the March. There was no significant

depression (<10 µg L^{-1}) of arsenic concentration in the groundwater samples observed throughout the year; which underlined the requirement of immediate implementation of arsenic removal technology as a mitigation measure all round the year.

To develop an arsenic removal filter, adsorption capacity and sorption mechanism of the four different adsorbents (NOIS, sand, red soil and murum) were investigated with different operating parameters in both batch and continuous mode. Batch studies were performed to define the adsorption characteristics like pH, contact time, temperature, adsorbent dose and initial arsenic concentration for the removal of arsenic (200 µg L^{-1}) by adsorption onto the selected adsorbents. From the pH study, it was found that the adsorbents were efficient on adsorbing arsenic in acidic media. In alkaline condition, the adsorption capacities of the adsorbents decreased with increase of pH of solution. From the kinetic study, it was found that both arsenic species [As(III) and As(V)] for all adsorbents reached the equilibrium concentration within 2 hours. Adsorption kinetics of arsenic sorption followed Ho pseudo second order reaction model. The arsenic sorption process consisted of two phases. Initial rapid sorption was controlled by film diffusion whereas comparatively slower second phase of the adsorption process was controlled by intraparticle diffusion. The thermodynamic study showed that the adsorption processes of all adsorbents were exothermic in nature. The experimental equilibrium data obtained were applied to several isotherm models. Results revealed that the Freundlich isotherm was the best-fit model. From the interpretation of the equilibrium data, the isotherm models can be arranged in the order of excellent fit as Freundlich> Redlich-Peterson> Langmuir> Temkin. The maximum adsorption capacity (q_m) was found to be highest for NOIS [155.60 µg g^{-1} for As(III) and 245.10µg g^{-1} for As(V)]. Initial arsenic concentration of the solution affected the arsenic removal efficiency for the studied adsorbents. The concentration range of the coexisting ions found to be having negligible interference on arsenic adsorption onto the examined adsorbents. The batch studies ensured that the NOIS can be used as promising adsorbent for arsenic remediation in developing indigenous treatment technologies.

To examine the effect of arsenic sorption in continuous mode, column studies were performed for different bed depths, flow rates and with different strengths of arsenic challenged water. The bed depth of adsorbent in column strongly affected the effluent

quantity as well as the quality. Increasing the bed depth of adsorbent, volume of treated water at breakthrough was increased. The findings of the column study indicated that NOIS and murum could meet the desired breakthrough concentration (10 μgL^{-1}) for bed depth of 7.5 cm, which was the minimum bed depth used for column experiment but sand could not reach that level even with 45 cm bed depth for both As(III) and As(V) species. The adsorption capacity was higher for lower flow rate for all the studied adsorbents that was in agreement with the findings of published literature. This can be explained by the fact that at lower flow rate, the contact time is more, which results in low diffusion of solute into the pores of the sorbent. Breakthrough curve for lower inlet arsenic concentration appeared earlier than its higher inlet concentration. This is due to the fact that higher concentration of arsenic saturated the adsorbent bed early, thereby shortens the bed breakthrough time. The run time of column and the shape of breakthrough are most important characteristics for the design of the operating criteria of the arsenic removal filter. In this study, continuous mode column experimental data of the adsorbents were validated using BDST model, Thomas model, Yoon-Nelson model and Mass Transfer model. Except the theoretical breakthrough curve, all other models (BDST model, Thomas model and Yoon-Nelson model) well represented the column experimental data. The BDST model could predict the service time of column run for a given effluent concentration and loading rate, which was finally applied to design the pilot scale and field scale filter.

Co-precipitation test was performed to evaluate the arsenic removal efficiency due to conversion of ferrous to ferric iron in natural groundwater system. Results indicated that iron flocs can remove a certain percent of arsenic but cannot meet the desirable permissible limit.

Desorption or regeneration tests were performed to quantify the chemical requirement for recovering the arsenic from spent adsorbents. Results assured that 2 bed volume 0.5N NaOH solution can be use as eluent to regenerate the arsenic from spent adsorbents.

In the present study, a porous filter was developed to accommodate the adsorbents and water, to control the loading rate, to remove the arsenic and also to retain the suspended particles. To develop porous arsenic removal filter, initially circular porous

disks (CPDs) were prepared in laboratory scale using different proportion of red soil and wheat husk to optimize the porosity of the media. 0.55:1 proportion of wheat husk and red soil was found as most effective ratio for development of the porous media. Using this optimized ratio, an arsenic removal porous filter was developed. The filter consisted of two chambers with the volumetric capacity of 9.5 L of each. The lower portion was developed to collect and store the filtered arsenic free water. The lower portion of the upper chamber was made porous to filter the arsenic polluted water. 2.5 L of sand and 1 L of NOIS were placed inside the filter as filtration media and arsenic sorption media respectively. The requirement of NOIS for the adsorption of arsenic within the design period was estimated using the BDST model. Performance of the arsenic removal filter was evaluated using 200 µg L^{-1} of As(III) spiked solution. Results revealed that that the filter can treat 3780 L of arsenic challenged water before it reaches breakthrough (10 µg L^{-1}). Assuming a moderate Indian family consisting of 4 members and water consumption rate of each is 5 L per day, daily requirement of water is 25 L for the family. Thereby, it is ensured that the filter can serve arsenic free water for at least 5 months before regeneration of the adsorption (NOIS) media. The implementation cost of the filter was estimated to be Rs. 162.50. Cost of arsenic treatment comes to 4 paisa per liter if initial investment is not taken into account, assuming a two years life of the filter, annual investment on the filter is less than Rs. 100 which is affordable to the rural people of Assam. In the present study, the filter, which was finally designed with cheap and easily available local materials, is found to be affordable to villagers, can be easily made by villagers with the help of local potter, where the initial cost is less than Rs 200.

Contents

List of Figures

List of Tables

Abbreviations and Acronyms

AAS	Atomic Absorption Spectroscopy
ARF	Arsenic Removal Filter
BDL	Below Detectable Limit
BDST	Bed Depth Service Time
BGS	British Geological Survey
BIS	Bureau of Indian Standard
CPD	Circular Porous Disk
DPHE	Department of Public Health Engineering
EDX	Energy Dispersive X-ray
EMBT	Empty bed contact time
FESEM	Field Emission Scanning Electron Microscopy
FTIR	Fourier Transform Infrared Spectroscopy
GIS	Geographic Information System
GPS	Global Positioning System
ID	Internal Diameter of column (cm)
IITG	Indian Institute of Technology, Guwahati
MCL	Maximum contaminant limit
NOIS	Naturally Oxidized Iron Scrap
PHED	Public Health Engineering Department
SEM	Scanning Electron Microscope
UNICEF	United Nations Children's Fund
VGA	Vapor Generation Accessory
WHO	World Health Organization
XRD	X-ray Powder Diffraction System
XRF	X-ray Fluorescence Spectrometry
AA	Activated Alumina
Al	Aluminum
AB	Arsenobetaine
AC	Arsenocholine

As	Arsenic
As(III)	Trivalent Arsenic, Arsenite
As(V)	Pentavalent Arsenic, Arsenate
C	carbon
Ca	Calcium
Cl	Chloride
CO_3	Carbonate
Cu	Copper
DMA	Dimethylarsinate
DOC	Dissolved Organic Carbon
EC	Electrical Conductivity
e	Electron
F	Fluoride
Fe	Iron
GFH	Granular Ferric Hydroxides
HCO_3	Bicarbonate
K	Potassium
Mg	Manganese
MMA	Monomethylarsonate
Mn	Manganese
Na	Sodium
Nitrate	Nitrate
OH	Hydroxyl
ORP	Oxidation Reduction Potential
pHzpc	Point Of Zero Charge
PO_4	Phosphate
SO_4	Sulfate
TDS	Total Dissolved Solid
A_s	Surface area of adsorbent (m^2)
A_{ads}	Area of arsenic adsorbed in the breakthrough curve
b	Langmuir constant

CP	Column performance (%)
C_0	Initial arsenic concentration (μg L^{-1}),
C_a	Concentration of arsenic on adsorbent at equilibrium (μg L^{-1})
C_e	Equilibrium concentration of arsenic in solution (μg L^{-1})
C_s	Liquid-phase concentration at external sorbent surface (μg L^{-1})
C_t	Concentration of the arsenic spiked solution at time t (μg L^{-1}),
C_i	Constant related to thickness of the boundary layer (μg g^{-1})
C_t/C_0	Normalized arsenic concentration
C_{ads}	Arsenic adsorbed at time t in continuous mode (μg L^{-1})
C_B , C_F	Desired arsenic concentration at breakthrough (μg L^{-1})
F	Fraction of the solute
E	Free energy of sorption (kJ/mol)
k_1	First order rate constant (min^{-1})
k_{s1}	Pseudo first order adsorption rate constant (min^{-1})
k_2	Second order adsorption rate constant (min^{-1})
k_{s2}	Pseudo second order adsorption (g μg^{-1} min^{-1})
k_i	Intraparticle diffusion rate constant (μg g^{-1} $min^{-1/2}$)
k_f	Liquid film mass transfer coefficient (m^2s^{-1})
k_fA_s	Global external transport coefficient (m^3s^{-1})
k_0	Constant of proportionality
k_{Th}	Thomas rate constant (ml μg^{-1} min^{-1})
k_{YN}	Yoon-Nelson rate constant (min^{-1})
K_1	Adsorption rate constant (min^{-1})
K_a	Adsorption rate constant in continuous mode (L $\mu g^{-1}h^{-1}$)
K_{sorp}	Adsorption kinetic constant (L μg^{-1} min^{-1})
K_{des}	Desorption kinetic constant (min^{-1})
K_c	Thermodynamic equilibrium constant
K_F	Adsorption capacity of the adsorbent ($\mu g^{1-(1/n)}$ $L^{1/n}$ g^{-1})
K_R,	Redlich-Peterson isotherm constants
K_0	Temkin constant (L μg^{-1})
m	Mass of adsorbent (g)

M_{ads}	Total arsenic adsorbed by the column (µg)
N_0	Adsorptive capacity of adsorbent (µg L^{-1})
n	Freundlich empirical constant
q_e	Amount of arsenic adsorbed at equilibrium (µg g^{-1})
q_m	Maximum adsorption capacity of adsorbent (µg g^{-1})
q_t	Amount of arsenic adsorbed at time t (µg g^{-1})
Q	Volumetric flow rate of solution in continuous mode (ml min^{-1})
R	Universal gas constant (8.314Jmol^{-1}K^{-1})
R^2	The coefficient of determination
$RMSE$	Residual root mean square error
SE	standard error of estimate
t	Time (min)
t_s	Service time of column
T	Adsorption temperature (K)
V	Volume of sample (L)
V_t	Throughput volume (ml)
v	Linear flow velocity or loading rate of feed solution (cm h^{-1})
x	Bed depth of adsorbent in continuous mode (cm)
x_0	Critical bed depth of column bed (cm)
y_a	Average value of experimental data
y_c, y_p	Predicted or calculated value determined from model
y_e	Experimental value
α	Bangham constant (<1)
γ	Initial adsorption kinetic coefficient (Lµg^{-1}m^{-1})
ε	Polanyi potential related to equilibrium concentration
τ	Time required for 50% adsorbate breakthrough in column (min)
ΔG^o	Gibb's free energy of arsenic sorption (kJ mol^{-1})
ΔH^o	Enthalpy change of adsorption (kJ mol^{-1})
ΔS^o	Entropy change of adsorption (J mol^{-1}K^{-1})
ΔQ	Energy transmission during sorption of the sorbate (k J mol^{-1})

Chapter 1

INTRODUCTION

1.1 Background

Arsenic contamination in groundwater is considered to be one of the largest human hazards faced during the last two decades around the world (Barringer et al., 2011). The use of tubewells for water supply widely around the world in arsenic contaminated area is causing serious arsenic poisoning to large numbers of people (Mohan and Pittman Jr., 2007). Arsenic is generally found in minerals, rocks, soils and in the sediments as natural source. The most common arsenic bearing minerals are arsenopyrite, cobaltite, enargite, gersdorffite, löllingite, orpiment, pyrite, realgar and tennantite (Drahota et al., 2009). Fossil fuel, mineral deposits, mining wastes and geothermal areas are other sources through which arsenic can occur in ground water (Ng et al., 2003; Xie et al., 2011). Also, arsenic and its compounds are found in wastes from various industries like glassware, ceramic, dye, petroleum and refining metallurgical, insecticides, pesticides, fertilizers and inorganic chemicals which leach into ground water (Do Carmo Freitas et al., 2004; Barringer et al., 2011; Robert 2002). As water passes through the soil and rock formations, the arsenic bearing minerals are exposed to the atmosphere or groundwater and the aquifer gets contaminated with arsenic (Wang et al., 2006; Davis et al., 2009). The dissolution of arsenic from the minerals is dependent on the redox potential of the groundwater and the solubility of the minerals (Duker et al., 2005; Craw, 2005). The mobilization of arsenic into the groundwater system is controlled by coagulation, adsorption, oxidation and reduction reactions (Bhattacharya et al., 2011; Duker et al., 2005). Variable amounts of arsenic exist in the natural groundwater in both organic and inorganic form (Sabbatini et al., 2010). Arsenic is tasteless, odorless, colorless and very difficult to measure for the common people. It is highly toxic in nature, even at low concentrations, long-term exposure of arsenic via drinking water is

dangerous to human health (Camacho et al., 2011; Chen et al., 2011; Sharma and Sohn 2009). World Health Organization (WHO) set the guideline value 10 ppb (or 10 µg L^{-1}) for drinking purpose (Mohan and Pittman Jr., 2007; Devi et al., 2008). According to Bureau of Indian Standard (BIS), the desirable limit of arsenic in drinking water is 50 ppb (or 50 µg L^{-1}) without relaxation (IS 10500: 1991).

Arsenic contamination in groundwater is a worldwide problem. The groundwaters of 35 countries are affected with arsenic contamination. Only in Asia, more than 130 million people are consuming arsenic contaminated water (Chakraborti, 2011). In Asia, most arsenicosis affected countries are Cambodia, China, Inner Mongolia, Taiwan, Myanmar, Vietnam, Bangladesh, India, Nepal and Pakistan (Guha and Dasgupta, 2011; Brammer and Ravenscroft 2009; Mondal et al., 2008a, b). In India, Datta and Kaul (1976) first reported arsenic contamination in groundwater of some parts of Chandigarh, Haryana, Himachal Pradesh and Punjab. Dermatologist Saha identified the first arsenic patient with skin lesions on 6th July 1983 (Saha 1984; Garai et al., 1984). Garai et al., (1984) reported arsenic contamination in West Bengal after analyzing groundwater samples in some tubewells of 24th Paragana district where arsenic concentration was as high as 1250 µg L^{-1}. Kartinen and Martin (1995) confirmed that the Ganga valley in West Bengal was severely affected with arsenic contamination. The groundwaters in some part of Jharkhand, Assam, Uttar Pradesh, West Bengal and Bangladesh lying in Ganga-Meghna-Brahmaputra plains are also highly affected with arsenic (Ahamed et al., 2006). Arsenic contamination problem in Brahmaputra basin was identified at the last decade. At 2004, Singh et al. reported arsenic concentration in groundwater of Assam. In order to assess the severity of arsenic contamination in Assam, an extensive study was carried out jointly by United Nations Children's Fund (UNICEF) and Public Health Engineering Department (PHED) of Assam, in collaboration with Indian Institute of Technology (IIT), Guwahati (Mahanta et al., 2011). The report confirmed that 18 districts are contaminated with arsenic. The affected districts are Cachar, Jorhat, Barpeta, Karimganj, Sivasagar, Hailakandi, Goalpara, Dhubri, Sonitpur, Nalbari, Golaghat, Morigaon, Lakhimpur, Darrang, Dhemaji, Bongaigaon, Kamrup and Nagaon (Mahanta et al., 2008; Mahanta et al., 2009; Mahanta et al., 2011).

In India, groundwater is the major drinking water source in rural and semi urban areas due to non-availability of piped water supply. Therefore, arsenic contamination in groundwater poses a serious health hazard to its consumer. To overcome the problem of arsenic consumption via drinking water, it is better to switch from problematic source to safe alternate drinking water source. If however when no other safe alternative source is available, it is necessary to treat contaminated water. Several technologies have already been developed based on oxidation (Mondal et al., 2008), adsorption and co-precipitation (Meng et al., 2001), adsorption (Qu et al., 2009; Sahabi et al, 2009; Chen et al., 2010, Chowdhury et al., 2011), ion exchange (Kim et al., 2004; Chutia, 2009), membrane (Qu et al., 2009; Curko et al., 2011; Melita 2008) and electro-coagulation processes (Zhao et al., 2010) to remove arsenic from drinking water. Many of them are removing arsenic satisfactorily both at household and community level. However, water treatment cost is a vital issue for rural as well as for semi-urban mass because of their low earnings. Hence, researchers need to try to develop affordable arsenic removal filter as far as possible using locally available materials, which is cheap as well as has low operation cost. Some low cost treatment facilities have been already implemented in Bangladesh, Vietnam and West Bengal since arsenic problems were detected in these places decades ago. It has been however experienced that successful arsenic removal technologies need not necessarily succeeded in the villages of West Bengal and Bangladesh, unless it fitted into the rural circumstances and is well accepted by the consumers. The acceptability of technology to the rural people increase when it is operable and affordable by them. The people of rural and semi urban areas of Assam have adopted the idea of using sand filtration device for cleaner water (iron free). Sand filter can also remove arsenic from water up to a certain amount but it cannot remove it completely. Thus, the main objective of this research was to develop an arsenic removal filtration device which can be easily made locally with locally available materials, is efficient, sustainable yet easily operable and hence acceptable by the community. The objective was also to design the arsenic filtration device similar to the iron filters that people are already accustomed to and familiar with maintaining over long period through regeneration or replacement of adsorbent.

1.2 Thesis objective

The major objective was to develop a low cost treatment method keeping in mind the local need and locally available materials to be used as adsorbent cum filter media. For this, first a new area affected by arsenic contamination but so far not having any treatment system in place was identified, the extent of arsenic contamination was evaluated and finally an appropriate filtration technology was designed with local materials that were simple yet efficient and affordable. Delineation of unsafe aquifers in the study area (Madhupur block of Nalbari district in Assam, India) was carried out to quantify geochemical properties/parameters of groundwaters followed by investigating the adsorption characteristics of local low cost adsorbents (*i.e.* sand, naturally oxidized iron scrap (NOIS), red soil and murum) to develop a suitable arsenic removal filter for the study area. The investigations were carried out in the following sequence:

1. Assessing the extent of arsenic contamination and other key pollutants in the study area by testing ground water using laboratory methods and preparing spatial distribution database and variation of the arsenic using GIS.
2. Seasonal variation of arsenic and correlation with other water quality parameters.
3. Characterization of the selected adsorbents i.e. sand, red soil, NOIS and murum for arsenic sorption from aqueous solution.
4. Conducting kinetic and equilibrium study to determine the adsorption capacity of the adsorbents and establishment of sorption mechanism.
5. Optimization of adsorption capacity of the adsorbents for the removal of arsenic by conducting a series of batch experiments as function of pH, time, dose, temperature and coexisting ions (i.e. major ions, iron, bicarbonate, alkalinity, phosphate and sulfate).
6. Conducting column experiments to assess the adsorption capacity of NOIS, sand and murum as function of bed depth, flow rate and initial arsenic concentration.
7. Preparation of a porous medium using red soil and optimization of that medium as function of loading rate, arsenic and turbidity removal efficiency.

8. Design of a suitable low-cost domestic prototype filter for arsenic removal and evaluate the performance of this designed filter for the arsenic challenged water.

1.3 Thesis organization

While the primary goal of this thesis is to development of an arsenic removal filter using locally available materials for the contaminated area of Brahmaputra floodplains. The secondary goal of this thesis is to propose and validate a series of logical steps to determine whether the adsorbent materials are suitable for treating the groundwater to make it arsenic free. The goal and the objectives of the thesis are accomplished in sequential manner and delineated in corresponding chapters.

Chapter 2 presents a brief review on the geochemical properties and mobility of arsenic in the natural groundwater system. A brief discussion is made in this chapter to understand the health effect while arsenic consumed with the drinking water. A literature survey is carried out to distinguish the arsenic affected area in Brahmaputra floodplains as well as worldwide scenario as a whole. A brief discussion is made on the existing arsenic removal technologies that are in use around the world, with their advantages and limitations. The reason for considering the locally available materials as adsorbent for remediation of arsenic in the study area has been narrated here. Moreover, justification of use of sand, red soil, naturally oxidized iron scrap and murum as adsorbent for their advantages over other adsorbents have also been mentioned in this part of thesis.

Chapter 3 deals with the groundwater quality parameter estimation methods which are generally collected from study area (Nalbari district, Assam) at different time intervals. This chapter also deals with the preparation of the selected adsorbents, preparation of reagents, analytical methods and different batch & column experiments procedures. Preparation, development and optimization technique procedure is discussed in this chapter. The preparation development and testing of the arsenic removal filter is elaborately described at the end of this chapter.

Chapter 4 aims at delineation of the unsafe aquifer of the study area. Seasonal variation of arsenic, spatial distribution of arsenic and correlation of arsenic with other water quality parameters and elaborately discussed in this chapter.

Chapter 5 focuses on the characterization and optimization of the selected adsorbent. The experimental results of kinetic study, equilibrium study, effect of pH, effect of agitation speed, effect of co-ions, desorption and regeneration study elaborately discussed in this chapter to optimize the adsorbents and to determine the sorption mechanisms.

Chapter 6 discusses the finding from the column experimental results of the selected materials at different loading rate, bed depth and initial arsenic concentration. In this chapter, the column experimental results successfully modeled using different model to predict the bed life of the adsorbents at different operating condition.

Chapter 7 is aimed at the optimization and development of porous media. In this chapter, the arsenic removal filter using appropriate adsorbents is developed. The performance of the developed filter is examined with the help of arsenic challenged water. Cost analysis of the newly developed arsenic removal filter is carried out in this chapter.

Chapter 8 concludes the entire thesis work with findings in brief. It produces views on possible studies involving the developed arsenic removal filter for future modification or improvement.

Chapter 2

LITERATURE SURVEY

2.1 Introduction

The chapter objective is to perform literature survey to understand the risk of arsenic contamination in groundwater system. The chapter objective consists of a brief discussion on worldwide distribution of arsenic, its health impact and implemented arsenic removal technologies in different arsenic contaminated areas. Another objective of this part is also to justify the present research work.

2.2 Arsenic in natural environment

2.2.1 Geochemistry of arsenic

Arsenic is a naturally occurring 20th abundant trace element (Sabbatini et al., 2010), geogenic and ubiquitous in nature (Sidle, et al., 2001). It is present in the earth's crust and often forms inorganic compounds by combining with oxygen, chlorine and sulfur (Kartinen and Martin, 1995). It is generally present in igneous rocks (like ultrabasic, basalts, andesites, granitic, silicic and volcanic) and sedimentary rocks (like limestones, sandstones, phosphorites, shales and clay). This crystal-shaped metalloid element is brittle in nature, gray or tin white in color and Group-V element in the periodic chart. Its atomic number is 33 and the atomic weight is 74.9216, density 5.72 g cm^{-3} at 293K and first ionization energy 946.5 KJmole^{-1}. In the natural environment, it is rarely encountered as the free element, which can occur in four oxidation states (-3, 0, +3, +5), but the two predominant oxidation states common in drinking water are oxyanions of trivalent arsenic and pentavalent arsenic (Hem, 1985). Trivalent and pentavalent arsenic

is normally found in water as arsenic acid which ionizes according to the equations (Kartinen and Martin, 1995):

Arsenic (III)

$H_3AsO_3 \longrightarrow H^+ + H_2AsO_3^-$ pKa = 9.22 (2.1)

$H_2AsO_3 \longrightarrow H^+ + HAsO_3^{2-}$ pKa = 12.3 (2.2)

Arsenic (V)

$H_3AsO_4 \longrightarrow H^+ + H_2AsO_4^-$ pKa = 2.2 (2.3)

$H_2AsO_4^- \longrightarrow H^+ + HAsO_4^{2-}$ pKa = 7.08 (2.4)

$H_2AsO_4^{2-} \longrightarrow H^+ + AsO_4^{3-}$ pKa = 11.5 (2.5)

Arsenic is one of the members of elements those are termed as ′Heavy Metals′. A heavy metal is a member of a loosely defined subset of elements that exhibit metallic properties and are having a specific gravity that is at least 5 times the specific gravity of water. Toxic metals sometimes imitate the action of an essential element in the body, interfering with the metabolic process to cause illness. Heavy metals are in general toxic, but some heavy metals are essential to humans. Toxic metals can bio-accumulate in the body and in the food chain. Arsenic and many of its compounds are especially potent poisons. Arsenic disrupts (Adenosine tri-phosphate) ATP production through several mechanisms. ATP, coenzyme used as an energy carrier in the cells of all known organisms.

2.2.2 Sources of arsenic

Arsenic is found everywhere in soils, water bodies and air at different forms. In the atmosphere the availability of arsenic is mainly either due to volcanic eruptions or due to human activities. Coal burning in thermal power plant is one of the main human activities apart from mining activities passes arsenic in the atmosphere. Volatilization of arsenic from arsenical waste dumps is also reason for the presence of the same. The major arsenic minerals found in nature are shown in Table 2.1 High concentrations of arsenic are found in a variety of environments. These include both oxidizing (under

conditions of high pH) and reducing aquifers and areas affected by geothermal, mining and industrial activity (Smedley and Kinniburgh, 2002).

Table 2.1. The major arsenic minerals occurring in nature (Smedley and Kinniburgh, 2002).

Minerals	Composition	Occurrence
Native Arsenic	As	Hydrothermal veins
Niccolite	NiAs	Vein deposits & norites
Realgar	AsS	Vein deposits, often associated with orpiment, clays & limestone, also deposits from hot springs
Orpiment	As_2S_3	Hydrothermal veins, hot springs, volcanic sublimation products
Cobaltite	CoAsS	High-temperature deposits, metamorphic rocks
Arsenopyrite	FeAsS	The most abundant As mineral, dominantly in mineral veins
Tennantite	$(Cu,Fe)_{12}As_4S_{13}$	Hydrothermal veins
Enargite	Cu_3AsS_4	Hydrothermal veins
Arsenolite	As_2O_3	Secondary mineral formed by oxidation of arsenopyrite, native arsenic and other As minerals
Claudetite	As_2O_3	Secondary mineral formed by oxidation of realgar, arsenopyrite and other As minerals
Scorodite	$FeAsO_4.2H_2O$	Secondary mineral
Annabergite	$(Ni,Co)_3(AsO_4)_2.8H_2O$	Secondary mineral
Hoernesite	$Mg_3(AsO_4)_2.8H_2O$	Secondary mineral, smelter wastes
Haematolite	$(Mn,Mg)_4Al(AsO_4)(OH)_8$	Secondary mineral
Conichalcite	$CaCu(AsO_4)(OH)$	Secondary mineral
Pharmacosiderite	$Fe_3(AsO_4)_2(OH)_3.5H_2O$	Oxidation product of arsenopyrite and other As minerals

2.2.3 Speciation of arsenic

Speciation of arsenic is used to improve knowledge of arsenic's physicochemical and biochemical interactions and also to evaluate toxicity risks. The toxicity and bioavailability of arsenic is highly dependent on form or species. Arsenic occurs in the environment in several oxidation states but in natural waters it is mostly found in an inorganic (Strawn et al., 2002) form as oxy-anions of trivalent arsenite [As(III)] or pentavalent arsenate [As(V)]. Organic forms of arsenic are rarely significant in groundwaters but may become very important in waters affected by industrial pollution (Smedley, 2007). Despite the fact that inorganic species are predominant in natural

waters, the presence of MMA and DMA has also been reported (Duker et al., 2005). The major arsenic species found in environmental and clinical samples are arsenite [As(III)], arsenate [As(V)], arsenious acids (H_3AsO_3, $H_2AsO_3^-$, $HAsO_3^{2-}$), arsenic acids (H_3AsO_4, $H_2AsO_4^-$, $HAsO_4^{2-}$), dimethylarsinate (DMA), monomethylarsonate (MMA), arsenobetaine (AB) and arsenocholine (AC) (Kumaresan and Riyazuddin, 2001). Speciation is also an important factor influencing the behavior of metal ions in aqueous solution, as well as adsorbed on metal oxide surfaces. Speciation refers to the chemical form in which a molecule or ion exists in solution, whether it is a monomer or polymer, an aqua or hydroxo complex, etc. Depending on the nature of the problem under study, multiple levels of speciation information may be needed, including: (1) the identity of the element, (2) the oxidation state, (3) the molecular chemical formula, and (4) the detailed molecular structure. The most commonly available species found in groundwater are arsenite and arsenate whose molecular configuration is given in the Fig. 2.1 below.

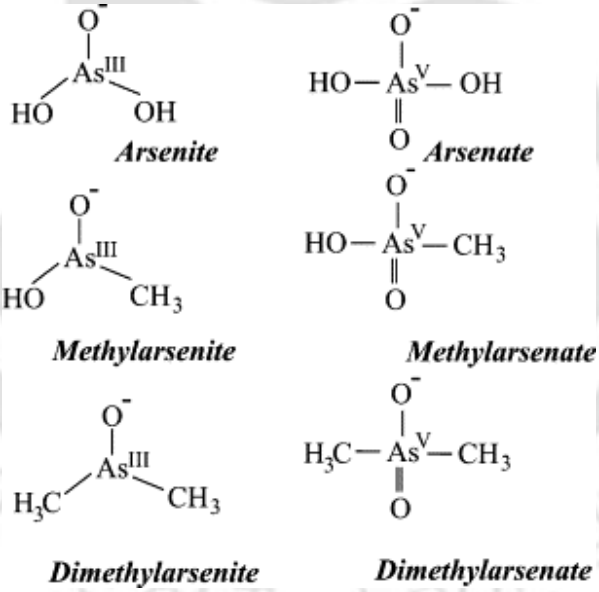

Fig. 2.1. Common species of arsenic in groundwater (Hung et al., 2004).

Vaclavikova et al. (2008) described that chemical reactions of target substances with water molecules, with dissolved inorganic and organic compounds and with surfaces of suspended particles are responsible for formation of "species". The species can be present as neutral, cationic and anionic molecules or they are solid-bound. They are decisive for the environmental behavior in aquatic systems and for their removal during

treatment. Heithmar et al. (2000) described that arsenic species which most likely to account for human exposure include: (i) inorganic arsenite and arsenate; (ii) methylated anionic species; iii) volatile arsenic hydrides and (iv) organoarsenic species in food.

2.2.4 Cause of arsenic contamination in groundwater

Extensive studies have been performed to investigate the sources and mobilization of arsenic due to severity of arsenic enrichment found in West Bengal and Bangladesh (Nath et al., 2008). Assam is also suffering from the same problem and sedimentological history of Brahmaputra valley is similar to those areas. According to BGS (2001), in Bangladesh arsenic problem arises mainly due to three unfortunate combinations of three factors (Ahmed, 2004): (1) source of arsenic (arsenic is present in the aquifer sediments), (2) mobilization (arsenic is released from the sediments to the groundwater) and (3) transport (arsenic is flushed in the natural groundwater circulation). According to this report, the original sources of arsenic existed as both sulphide and oxide minerals. Oxidation of pyrite in the source areas and during sediment transport would have released soluble arsenic and sulphate. The sulphate would have been lost to the sea but the arsenic, as As(V), sorbed by the secondary iron oxides formed. These oxides are present as colloidal-sized particles and tend to accumulate in the lower parts of the delta. Two prevailing hypotheses to describe the mobilization of arsenic into groundwater in Bangladesh are (Harvey et al., 2006): (1) pyrite oxidation (Fazal et al., 2001) and (2) oxy-hydroxide reduction (Horneman et al., 2004).

Py*rite oxidation hypothesis:* Arsenic is assumed to be present in certain sulphide minerals (pyrite) that are deposited within the aquifer sediments. Due to lowering of water table, arseno-pyrite is oxidized and arsenic is released. Arsenic can be re-adsorbed on Fe-hydroxide during the subsequent recharge period, the reduction of Fe-hydroxide releases arsenic into groundwater. In accordance with the hypothesis, the origin of arsenic rich groundwater is man-made, and would be a recent phenomenon (Karim et al., 2000).

Oxy-hydroxide reduction hypothesis: According to this hypothesis, arsenic is assumed to be present in high concentrations in alluvial sediments of sand grains coated with iron

hydroxide. The sediments were deposited in valleys eroded in the delta when the stream base level was lowered due to the drop in the sea level during the last glacial advance. Following upraise in the sea level, these sediments stream submerged and reduced. The reducing conditions would be enhanced by the organic matter deposited with the arsenic bearing Ferric hydroxide sediments and would lead to arsenic solubilization into groundwater. This oxy-hydroxide reduction hypothesis was first proposed by Nickson et al. (1997) and later supported by Fazal et al. (2001), Zheng and Horneman et al. (2004).

2.2.5 Factors controlling arsenic concentration and transport

Presence of higher concentrations of arsenic in groundwater has greater influence on arsenic speciation and mobility than the total concentration in soils. The arsenic solubility in water usually controlled by redox conditions, biological activity, pH, form of arsenic and adsorption reactions (Ahmed, 2004). Soil fractions, dissolved organic carbon (DOC) and oxides of Fe, Al and Mn effect on mobility of arsenic. Generally finer texture sediment contains more arsenic than sediments with coarser texture (Khan, 2000). To understand the mobility of arsenic in groundwater, the redox conditions and adsorption-desorption processes of the soil-water system must be understood. Arsenic adsorption depends on pH and redox condition. Change of pH in groundwater can promote the mobility of arsenic. The aqueous Arsenic concentration can be controlled by redox reaction by their effect on arsenic speciation and on adsorption-desorption reactions (Ahmed, 2004).

Natural geochemical and biological processes play critical role in controlling the fate and transformation of arsenic in the subsurface. Arsenite is thermodynamically unstable in aerobic environments and should oxidize to As(V) though in nature the transformation occurs slowly due to kinetic barrier to the reaction. Presence of other oxides such as FeO, Fe_2O_3, MnO_2 and even clay minerals shown to be capable of oxidizing As(III). Oxidation of As(III) to As(V) by microorganisms using oxygen as terminal electron acceptor has also been reported (Cheng et al., 2009).

Jonsson and Lundell (2004) stated that Redox processes could be mediated by microorganisms, which serve as catalysts in speeding up the reactions. These

microorganisms, mostly bacteria, use redox reactions in their respiratory process. In oxygen-rich environments, oxygen is the natural electron acceptor, but a number of other electron acceptors step in according to a distinct order when the previous electron acceptor has been consumed or nearly consumed (Fig. 2.2). The sequence begins with the consumption of O_2 and thereafter NO_3^- is used. MnO_2 dissolve by reduction to soluble Mn^{2+} and thereafter NH_4^+ is produced through ammonification. These processes are followed by reduction of hydrous ferric oxides to Fe^{2+}. Finally, SO_4^{2-} is reduced to H_2S and CH_4 is produced from fermentation and methanogenesis.

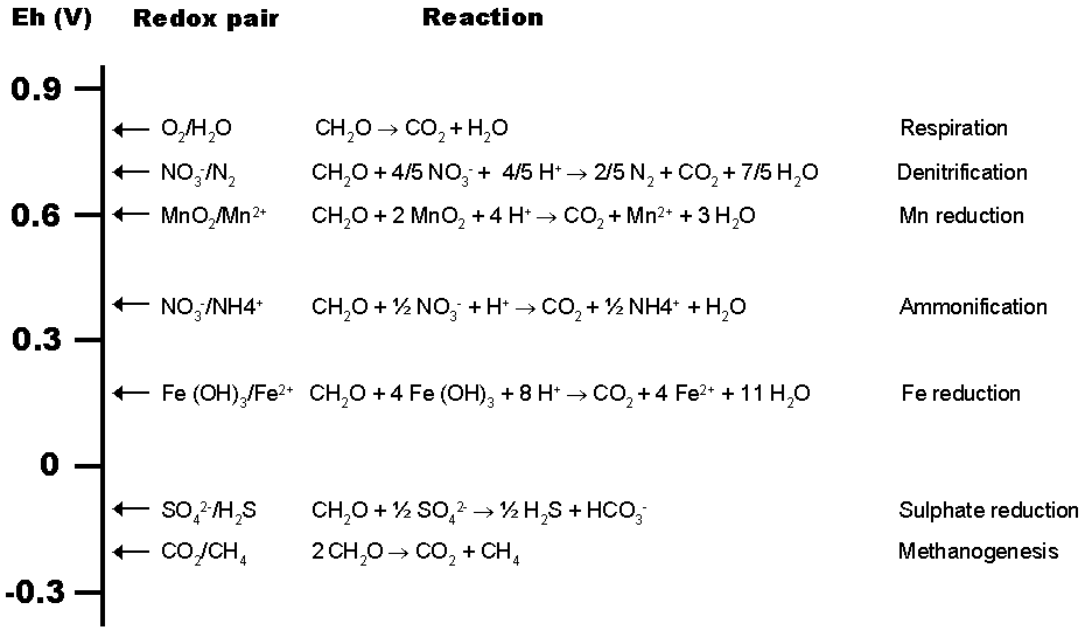

Fig. 2.2. Sequence of principal redox reactions for neutral pH groundwater (Jonsson and Lundell, 2004).

2.2.6 Mobility of arsenic

In addition to diverse toxicity of arsenic, the chemical forms of arsenic determine mobility in the environment. Therefore, new environmental regulations are being developed to specifically monitor for individual species of arsenic. Arsenic is generally present in ground water as an oxy-anion, either in the form of arsenite (H_3AsO_3) or as arsenate (H_3AsO_4) or both. The pH and Eh have a dominant effect on the chemistry of arsenic in ground water. Eh-pH diagram (Fig. 2.3) illustrates the fields of stability of

mineral or chemical species in terms of the activity of hydrogen ions (pH) and the activity of electrons (Eh).

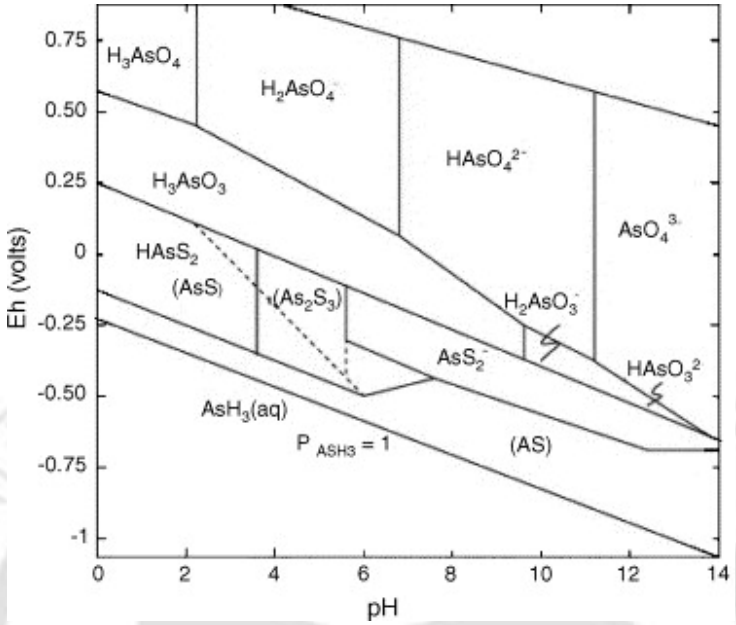

Fig. 2.3. Eh-pH diagram of arsenic species in the system As-O_2-H_2O at 25°C and 1 bar total pressure (Mohan, and Pittman Jr., 2007).

Consequently, the reactions as illustrated in the Eh–pH diagrams involve either proton transfer (hydrolysis) or electron transfer (oxidation or reduction) or both. The relation between Eh and arsenic concentration is linear and arsenic concentration goes up as Eh increases. In pH ranging from 2 to 11, release of arsenite and arsenate follow a pattern of substantial increase with decreasing pH (Haque et al., 2008). At lower pH values, metal ions (iron, manganese) get solublised releasing arsenic as shown in Fig. 2.3.

At high pH, the increased hydroxide concentrations displaced the arsenic species from binding sites in a ligand exchange type reaction. When it is an oxidizing condition (Eh 0.2-0.5 V), As(V) is found to be major species with solubility. Reducing condition (Eh<0.1 V) lead to mobilization, which is controlled by the dissolution of hydrous iron oxide. As(V) is co-precipitated with iron oxide and is released upon their solublisation.

2.3 Arsenic distribution in groundwater

2.3.1 Arsenic around the World

Four main geochemical processes trigger the natural release of arsenic from aquifer materials into groundwater, which are: (i) Reductive Dissolution; (ii) Alkali desorption; (iii) Sulfide oxidation and (iv) Geothermal process. Table 2.2 shows that these processes can occur in a wide range of geological environments.

Table 2.2. Brief description of natural geochemical processes that release arsenic to groundwater in different countries (UNICEF, 2008).

Process	Characteristic geochemical conditions	Generalized geological environment	Affected Countries	Additional information
Reductive dissolution	Anoxic groundwater; low levels of dissolved oxygen, nitrate (NO_3) and sulfate (SO_4); pH~7; high iron (Fe); also high manganese (Mn), ammonia (NH_4) and bi-carbonate (HCO_3).	Holocene Sediments deposited in floodplain areas of rivers draining geologically recent mountain chains.	Bangladesh, India, Vietnam, China, Cambodia, Hungary	May affect large areas. 64% of known occurrences of arsenic due to this process.
Alkali desorption	Oxic groundwater; pH ~ 8; low levels of iron (Fe). Possible elevated levels of other toxic ions such as F, B, Mo, Se.	Alluvium and bedrock aquifers.	Argentina, USA, Spain, China	May affect large areas.
Sulfide oxidation	Oxic groundwater; pH < 7(sometimes extremely acidic); high levels of sulfate (SO_4).	Areas where mineralization has taken place, often associated with rare metals, e.g., gold, tin.	Ghana, Thailand, USA	Usually localized, may be associated with lowering of water table due to extraction of groundwater.
Geothermal	High temperature groundwater; high chloride (Cl).	Areas of geothermal activity, i.e., geologically active, often associated with volcanic rocks.	Chile, China, Nicaragua	Usually localized.

Under natural conditions, the greatest range and the highest concentrations of arsenic are found in groundwater as a result of the strong influence of the water-rock interactions and the favorable physical and geochemical conditions in aquifers for the mobilization and accumulation of arsenic. Arsenic is particularly mobile at pH values

typically found in groundwater (pH: 6.5-8.5) under both oxidizing and reducing conditions (Anawar et al., 2004; UNISEF, 2008; Asta et al., 2009; Kar et al., 2010; Postma et al., 2010; Yamamura et al., 2009).

Severe cases of arsenic contaminated groundwater have been found in aquifers in India, Bangladesh, China, Nepal, Cambodia, Vietnam, Taiwan, Mongolia and Pakistan of Asia. In both North and South America also high arsenic contaminated aquifers have been located where contamination is due geogenic reasons. Groundwater arsenic contamination is found around the area called Great Hungarian Plain covering a part of Hungary and Romania in Europe as a natural source. The arsenic availability around the world is shown in the Fig. 2.4. An estimated 150 million people in 70 countries are at risk of ingesting unsafe levels of arsenic through drinking water (Brammer and Ravenscroft, 2009).

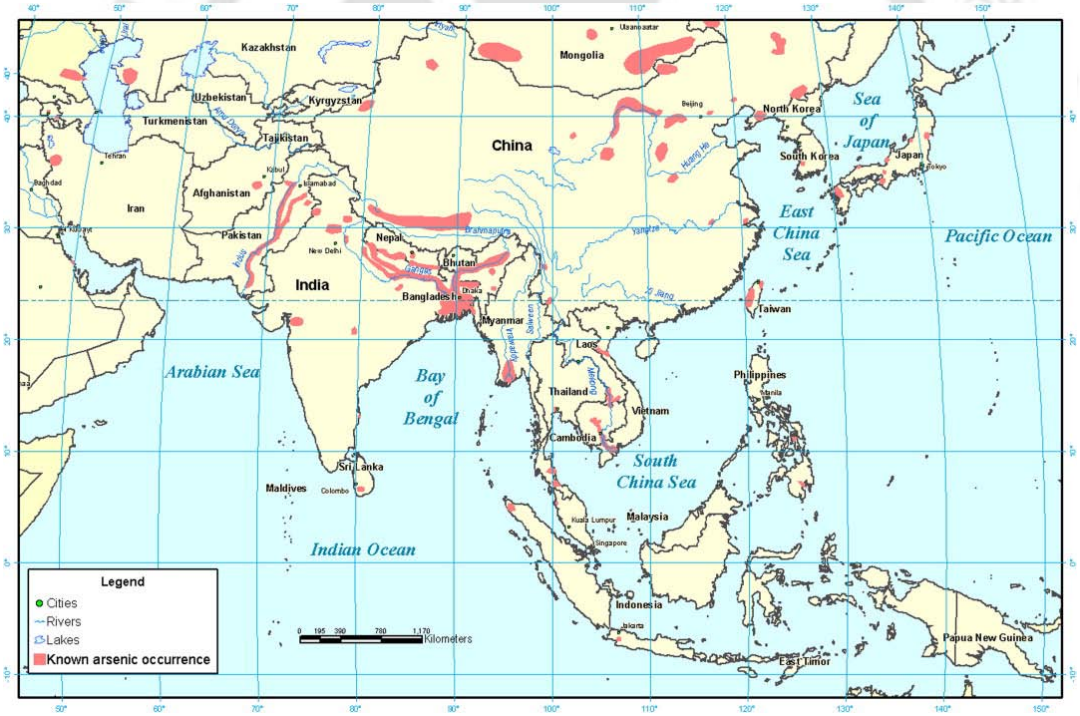

Fig. 2.4. Arsenic contamination situation across Asia (Brammer and Ravenscroft, 2009).

2.3.2 Arsenic in India

In the 1990s, scientists identified the source of the arsenic contamination: the Himalaya mountain range, where arsenic-laden rocks and sediments are carried

downstream along four major river systems -Ganges-Brahmaputra, Mekong, Irrawaddy and Red. In India, The Ganges and Brahmaputra basins are highly affected with arsenic. The major arsenic contaminated area i.e. West Bengal was first time reported in 1980. Apart from West Bengal, arsenic contamination in ground water has been found in the states of Bihar, Chhattisgarh, Uttar Pradesh and Assam. Concentrations of arsenic in groundwater exceeded 50 µg L^{-1} in some parts of Assam (18 of 24 districts), Tripura (3 of 4 districts), Arunachal Pradesh (6 of 13 districts), Nagaland (2 of 8 districts) and Manipur (1 of 9 districts).

The Brahmaputra floodplain area is highly contaminated with arsenic (Mahanta et al., 2011). In Assam, the maximum level of arsenic was found in Jorhat, Laksmipur, Nalbari, and Nagaon districts. In the flood plain area of Assam, i.e Barpeta, Dhemaji, Dhubari, Darrang, and Golaghat, arsenic was found in the range of 100-200 µg L^{-1} (Mukherjee et al, 2006). At first Singh (2004) stated that 20 districts of Assam are in the grip of high arsenic in groundwater. However, in a recent study, Mahanta et al. (2009) expressed that of presence of arsenic in the upper Brahmaputra floodplains, a relatively recent discovery but extensive study drinking water quality was made covering all the districts of Assam. It revealed presence of arsenic beyond permissible limit of 50 µg L^{-1} in 72 blocks out of 192 blocks spread over 22 districts. Enmark and Nordborg (2007) have carried out their field study on groundwater in Darrang and Bongaigaon districts of Assam. They found that more than 95% of their tested well water contained arsenic above 10 µg L^{-1} the MCL guideline laid down by WHO (World Health Organization). Out of these samples 30% of the samples contained arsenic beyond Indian National standard (IS 10500:1991) of 50 µg L^{-1}. Singh (2004) pointed that in flood plain area of Assam viz. Barpeta, Dhemaji, Dhubari, Darrang, and Golaghat, the arsenic was found in between 100-200 mgL^{-1}. Samples from 11 districts as reported by him contain arsenic in between 50-100 mgL^{-1}. Only three districts namely, Karbi Anglong, North Cachar Hills and Morigaon were free from arsenic contamination.

The Brahmaputra plain is, with a few exceptions, covered by young alluvial sediments, which are deposited from the great sediment load carried by the river and its tributaries. The minerals on the south and north side differ a lot. The north side is fed with sediments derived from the young Himalayas while the sediments on the south side

originate from the older Assam plateau. The gradient of the northern tributaries is steeper and the flows generally larger than in the southern tributaries. The steeper gradients, together with more easily eroded bedrock and larger flows, result in a higher sediment load from this part of the drainage area. The sedimentological history of the area is similar to the one in Bangladesh. Therefore conclusions about the source of arsenic found there are therefore thought to be applicable in Assam (Mahanta et al., 2009; Enmark and Nordborg, 2007).

2.4 Health impact of arsenic

Main route to exposure of human body to arsenic is either inhalation or ingestion. In human body there are four stages of reaction of arsenic when ingested by human body. These are classified as: i) Absorption; ii) Distribution; iii) Metabolism; iv) Excretion (Ahamed et al., 2006; Liu et al., 2002). Dermal contact is not reported to have any adverse effect on human life as cause for any disease. The route of inhalation is remote in normal situation to human except otherwise he/she is occupationally exposed to arsenic bearing material handling either in mines or in any smelting shop (Mazumder, 2003). IARC (International Agency for Research on Arsenic) has pointed out that with regard to absorption of arsenic through the skin; a few experimental studies indicate a low degree of systemic absorption. Morphological changes, cytotoxicity and inhibition of DNA and protein syntheses were found with in-vitro doses of As (III) as low as 10 $\mu g\ L^{-1}$ (Chakraborti, 2011; Kosnett, 1999). Thus, it seems probable that inorganic arsenic can be absorbed from the exterior, leading to a breakdown in skin barrier function. Concentration of arsenic in air is not a matter of concern for this thesis since it mainly deals with groundwater arsenic concentration and remedial measures (Milton and Rahman, 2002). However in brief, exposure due occupational reasons may lead to chest infection and even lung cancer to the miners and smelters, in some cases of skin infection (Rom et al., 1982; Taylor et al., 1989).

Ingestion of arsenic is through food and water that is being consumed in daily life. Many incidents of arsenic contamination of the environment have been reported in several countries of the world. The situation can have significant adverse influence on

health due to arsenic uptake in water and food especially by developing and rural populations who depend on local sources of food and water. Therefore, any arsenic geochemical anomaly may impact negatively on health (Duker et al., 2005).

Intake of inorganic arsenic to human body for a long period of time causes a health hazard termed as 'arsenicosis'. Arsenicosis is a general term used to identify several symptoms arises from toxic effect in human body (Signes-Pastor et al., 2008). The manifestations of arsenicosis include many non-specific clinical symptoms and a number of specific skin conditions (Rosenboom, 2004). The pathway of ingesting arsenic is mainly through drinking water and also from the crops irrigated with high arsenic groundwater. The more common non-specific symptoms (expressed in more than 10% of all cases) include numbness, dizziness, palpitations, fatigue, sleep disorders, anorexia and abdominal pain. Specific clinical signs include three types of skin changes (Chen et al., 2009; Mazumder et al., 1999; Siripitayakunkit et al., 1999):

1. *Keratosis*: A hardening of the skin into light yellow to brown nodules, often on the palms of the hand or the soles of the feet.
2. *Melanosis*: A pigmentation change taking the form of dark spots on both sides of the trunk, gradually spreading to the extremities; and
3. *Depigmentation*: Colourless spots the size of millet grain, up to densely clustered rain-drop sized spots, mostly on the trunk (Supapong et al., 2004).

Children are more susceptible arsenic toxicity and are more susceptible to cancer than adults at lower concentration of metal (Vahter, 1999; Moore et al., 1997). Zierold et al. (2004) stated that different researchers found that arsenic exposure is associated with lower verbal IQ and poorer long-term memory in children. A mechanism of action has not been identified, but perhaps long-term exposure to arsenic may interfere with the neurotransmitters associated with depression (ASTDR, 2007). Long term arsenic ingestion is a pattern of skin changes that include generalized hyperkeratosis and formation of hyperkeratotic warts or corns on the palms and soles, along with areas of hyperpigmentation interspersed with small areas of hypopigmentation on the face, neck, and back (ASTDR, 2007; Guha Mazumder et al., 2003, 2005). Among other symptom respiratory problem is found to the person (Guha Mazumder et al., 1999 2005; ASTDR, 2007). Researchers concluded that long-term arsenic exposure may induce hypertension

in humans (Rahaman et al., 1999; Abernathy et al., 2003). Inorganic arsenic is known to be a human carcinogen causing lung cancer by inhalation and skin cancer by ingestion (Hopenhayn-Rich et al., 2000; Ferreccio et al., 1999). Anemia and leukopenia are common effects of arsenic poisoning in humans, and have been reported following acute when consuming of inorganic arsenic through water intake (ASTDR, 2007). It showed that elevated risks for diabetes are associated for those exposed to arsenic in their drinking water (Abernathy, 2003).

The outward symptoms as can be in arsenic affected patients are shown in the Figure 2.5.

. Fig. 2.5. Arsenic patients with external symptoms (Chakraborti, 2011; Sampson et al., 2008).

2.5 Arsenic treatment technologies

Arsenic in groundwater is considered as one of the greatest menace to mankind. Groundwater contamination of arsenic above maximum concentration level (MCL) may be geogenic or due to local anthropogenic activity. Whatever reasons for the cause of contamination may be human sufferings are well documented in number of areas. Not only people face health related problems which affect them financially but socially arsenic affected families are isolated from mainstream of locality in a number of cases. With the spreading of arsenic affected regions around the world day by day, new technologies are emerging across the world. Scientists and technologists are trying to find out viable solution to combat the situation suitable for the areas in particular.

There are number of treatment methods for removal of arsenic from groundwater. Some of the methods are in large in size and some other in small in size to cater need of fewer people. Domestic level filters with variety of filter media are also in use at different places subject to the availability of ingredients needed for such filters. Inorganic arsenic occurs in groundwater mainly in trivalent and pentavalent form. In neutral solutions (pH: 6.5-8.5), the trivalent form is found as H_3AsO_3 (Smith et al., 1998). Treatment of arsenic contaminated groundwater with predominant As(III) species is considered to be a big obstacle in removal technologies for supply of arsenic safe water. However, the methods mostly used for arsenic contaminated water treatment all over the world are (Mohan and Pittman Jr., 2007):

i) Oxidation/chemical oxidation
ii) Coagulation/filtration process
iii) Membrane filtration
iv) Electroflocculation
v) Ion exchange
vi) Adsorption
vii) Indigenous filter

2.5.1 Oxidation/chemical oxidation process

It is well known fact that iron surfaces have a strong affinity to adsorb arsenic. The adsorption and co-precipitation of As(III) and As(V) on iron oxide surfaces have

been investigated extensively by different researchers. Hoffman et al. (2006) suggested that in general, arsenic in groundwater containing both arsenic and iron will exist in the reduced form, As(III). To optimize arsenic removal, neutrally charged As(III) needs to be oxidized to As(V). As(V) exists as a negatively charged ion and can be adsorbed onto positively charged surfaces of ferric hydroxide particles. Consequently, if the arsenic in the source water is predominately As(III), oxidizing As(III) to As(V) using a strong oxidant will result in a higher rate of arsenic removal by an iron removal process.

Iron bearing waters are often deferrized by oxidizing the ferrous iron with dissolved oxygen and then removing the resulting ferric oxide flocs by sedimentation or filtration (Hoffman, 2006). The reaction of Fe(II) with oxygen generally leads directly to ferric oxides or hydroxides. The stoichiometric relationship is expressed as:

$$Fe(II) + \tfrac{1}{4}O_2 + 2OH^+ \longrightarrow \tfrac{1}{2}H_2O + Fe(OH)_3(s) \qquad (2.6)$$

However, in reality oxygen reacts with dissolved iron present in water very slowly and accelerated oxidation is being practiced in filters for iron removal. Cascade aeration, multiple orifice spray aeration are some of the means of conversion of dissolved ferrous iron to its precipitated form ferric iron, followed by sand filtration Removal of iron from water subsequently help removal of arsenic (mainly pentavalent arsenic) also. Whenever As(III) is the predominant species in groundwater simple oxidation is not effectively removed with iron removal process. Kim (2000) suggested that the oxidation of As (III) by pure oxygen was much more sluggish compared to ozone. Holm and Wilson (2006) mentioned that in contrast to air oxidation, As(III) oxidation by $KMnO_4$ and NaOCl are two common water treatment chemicals which acts very rapidly. Hydrogen peroxide in combination with Fe^{2+} found in As-containing groundwater also rapidly oxidizes As(III). Chlorination improved arsenic removal by oxidizing As(III). It is further observed that arsenic removal was better when NaOCl was added to anoxic water than adding NaOCl to water that had already been aerated. Ghurye and Clifford (2004) used chlorine, monochloramine (NH_2Cl), chlorine dioxide and ozone effectively for oxidation of As(III) to As(V). The further noted Hoffman et al. (2006) also used either chlorine or potassium permanganate or ozone for oxidation. This is followed by filtration through variety of filter media like anthracite/sand, pyrolusite, Brim (a patent material), manganese greensand etc.

2.5.2 Coagulation/filtration/Precipitation process

In this method, the physical or chemical properties of dissolved species (natural organic matter, inorganic matter) changed by addition of metal salt coagulants. This process has traditionally been used to remove solids from drinking water supplies.

Removal by ferric salts/alum: Conventional coagulation/filtration is a common water treatment methodology used to remove suspended and dissolved solids from source water. In arsenic contaminated water a coagulant is added to develop floc formation Alum and iron (III) salts, such as ferric chloride, are the most common coagulants used for drinking water treatment Removal mechanisms for dissolved inorganic consist of two primary mechanisms: adsorption and occlusion (Fields et al., 2000). Scott et al. (1995) however opined that alum is less effective than ferric chloride at removing arsenic. McNeill and Edwards (1997) stated that during coagulation As(V) removal efficiencies were limited by particulate aluminum formation and removal, because much of the added coagulant was not removed by 0.45 μm pore size filter. Removal increases on reducing coagulation pH from 7.4 to 6.8 (at constant alum dose).

Lime softening: Lime softening commonly is used to reduce hardness in source waters but a few studies have been conducted to evaluate arsenic removal during lime softening. McNeill and Edwards (1995) stated that removal of arsenic during softening can be mediated by calcite or Mg(OH)2 formation. The experiments showed that As(V) removal approaches 100% and As(III) removal approaches 75% at pH greater than 10.5.Coprecipitation of As(V) with Mg(OH)2 appears to be the primary arsenic removal mechanism for As(V) during lime softening (Fields et al., 2000).

Iron/manganese oxidation: The oxidation process used to remove iron and manganese leads to the formation of hydroxides that remove soluble arsenic by precipitation or adsorption reactions. The oxidation filtration technology mainly uses manganese greensand as the media which is used for arsenic removal from water. The active material in "greensand" is glauconite, a green, iron-rich, clay-like mineral that has ion exchange properties. Different researchers had shown that effectiveness will rise with Fe: As ratio increase (Fields et al., 2000).

2.5.3 Membrane filtration process

Membranes are a selective barrier, allowing some constituents to pass while blocking the passage of others. The movement of constituents across a membrane requires a driving force (i.e. a potential difference between the two sides of the membrane). Membrane processes are often classified by the type of driving force, including pressure, concentration, electrical potential, and temperature. The processes discussed here include only pressure-driven and electrical potential driven types.

Pressure-driven membrane processes are often classified by pore size into four categories: microfiltration (MF), ultrafiltration (UF), nanofiltration (NF), and reverse osmosis (RO). High-pressure processes (NF and RO) have a relatively small pore size compared to low-pressure processes (MF and UF). Typical pressure ranges for these processes are given in Table 2.3. NF and RO primarily remove constituents through chemical diffusion (USEPA, 2000). MF and UF primarily remove constituents through physical sieving (Aptel and Buckley, 1996). An advantage of high-pressure processes is that they tend to remove a broader range of constituents than low-pressure processes (USEPA, 2000). In recent years, a variety of new-generation RO and NF have been developed. These membranes have been vastly improved with respect to water flux, salt rejection and specially their ability to maintain high performance levels at substantially lower operating pressures than their predecessors (Yoon et al., 2009).

Table 2.3. Typical Pressure Ranges for Membrane process (Fields et al., 2000).

Membrane Process	Process Range (psi)
MF	5 - 45
UF	7 - 100
NF	50 - 150
RO	100 – 150

2.5.4 Electro-coagulation process

Electro-coagulation (EC) has been practiced for along period for treatment of water/wastewater in many countries for removal of turbidity, metal and organic chemical

removal. EC treatment seems to be a promising treatment method due to its high effectiveness, its lower maintenance cost, less need for labor and rapid achievement of results (Parga et al., 2005) In the EC process, coagulation is generated in situ by electrolytic oxidation of an appropriate anode material. During this process, charged ionic species are removed from wastewater by allowing it to react with an ion having opposite charge, or with floc metallic hydroxides generated within the effluent (Parga et al., 2009). The effect of DC electric fields in the EC treatment method, soluble electrodes (such as Fe or Al) must be selected as anode material. Iron in an electrolytic system produces ferrous and ferric hydroxide upon oxidation. When iron electrodes are used, the reactions occurring during the electrochemical treatment process are as follows (Arslan-Alaton et al., 2009):

Reactions in a cathode environment:

$$2H_2O + 2e^- \rightarrow H_2\,(g) + 2OH^-\,(aq) \quad (2.7)$$

$$8H^+\,(aq) + 8e^- + 4H_2\,(g) \quad (2.8)$$

Reactions in an anode environment:

$$2H_2O \rightarrow O_2\,(g) + 4H^+\,(aq) \quad (2.9)$$

$$Fe\,(s) \rightarrow Fe^{2+}\,(aq) + 2e^- \quad (2.10)$$

The anode melts and dissolves ferrous ions into solution & subsequently reacts with hydroxyl ion (OH^-) to form ferrous hydroxides shown in the following equations:

$$Fe^{2+}\,(aq) + 2\,OH^-(aq) \rightarrow Fe\,(OH)_2(s) \quad (2.11)$$

$$2Fe^{2+}(aq) + \tfrac{1}{2}O_2(g) + 5H_2O(l) \rightarrow 2Fe(OH)_3(s) + 4H^+(aq) \quad (2.12)$$

At or near neutral pH, $Fe(OH)_3$ has a tendency to remain in insoluble phase whatever the iron content remain in the solution (water in this case).

2.5.5 Ion exchange process

It is a physical/chemical processes by which ions on the solid phase (solid resin) is exchanged for an ion in the feed water. The solid resin is typically an elastic three-dimensional hydrocarbon network containing a large number of ionizable groups electrostatically bound to the resin. Important considerations in the applicability of the resin based process for removal of a contaminant include water quality parameters such

as pH, competing ions, resin type, alkalinity, and influent arsenic concentration (Cheremisinoff, 2002). Four types of ion exchange media have been used:

- Strong acid
- Weak acid
- Strong base
- Weak base

Because dissolved arsenic is usually in an anionic form, and weak base resins tend to be effective over a smaller pH. Strong base anion exchange resins are used for arsenic removal from water (Kim, 2004). Since these resins tend to be more effective over a larger range of pH than weak-base resins. The order of exchange for most strong-base resins is given below, with the adsorption preference being greatest for the constituents on the far left.

$$HCrO_4^- > CrO_4^{2-} > ClO_4^- > SeO_4^{2-} > SO_4^{2-} > NO_3^- > (HPO_4^{2-}, HAsO_4^{2-}, SeO_3^{2-}, CO_3^{2-}) >$$
$$CN^- > NO_2^- > Cl^- > (H_2PO^{4-}, H_2AsO_4^-, HCO_3^-) > OH^- > CH_3COO^- > F^-$$

Ion exchange resin has certain limitation that when TDS content and sulphate level is high arsenic removal is affected (Fields, 2000). Sarkar et al., 2007 have successfully used a hybrid anion resin for arsenic removal from groundwater in some parts of West Bengal. The effectiveness of ion exchange is reduced by common ions such sulphate (SO_4^{2-}), which the resin sites prefer to As. Clifford et al. (1999) also experienced similar effect of SO_4^{2-}), while worked with two different type of strong base resins Isonac ASB-2 and Dowex-11. Exhausted resins which losses its exchange capacity to lower arsenic concentration below desired level are regenerated. Regeneration is made through flowing brine solution to clear the occupied exchange sites for further use. Regenerated media is rinsed for a couple of times before it is fed in filter for water treatment. It was indicated by them that ion exchange capacity of virgin resin and regenerated resin might differ. The exchange capacity of regenerated resin is always less than virgin one.

2.5.6 Adsorption process

Adsorption is the process in which matter is extracted from one phase and concentrated at the surface of a second phase. It is a physical/chemical process by which ions (adsorbate) in the feed water are sorbed to the surface of a solid substrate (adsorbent)

primarily by Van der Waals forces, although chemical or electrical attraction may also be important. Adsorbents must have a very high specific surface area and include activated alumina, activated carbon, clay colloids, hydroxides and adsorbent resins.

. In the case of oxyanions, such as arsenate and arsenite, adsorption occurs on the oxide water interface by forming a complex with surface sites that may be positively charged, such as a protonated surface hydroxyl group. In other instances, the reaction may involve a ligand exchange mechanism in which the surface hydroxyl group is displaced by the adsorbing ions. Adsorption takes arsenic out of water and putting it onto a solid adsorbent with micro and macro pores. Under comparable conditions, better removal observed for As(V) than As(III) in adsorption experiments (Hering et al.1996).

The adsorption reaction mechanism of arsenic species onto solid surfaces may be generically represented by the following reaction:

$$A + S \rightleftarrows A{\cdot}S \qquad (2.13)$$

Some low-cost adsorbents are superior including treated slag, carbons developed from agricultural waste (char carbons and coconut husk carbons), bio-sorbents (immobilized biomass, orange juice residue), goethite and some commercial adsorbents, which include resins, gels, silica, treated silica tested for arsenic removal come out to be superior. Immobilized biomass adsorbents offered outstanding performances (Mohan and Pitman Jr., 2007). They mentioned that zirconium-loaded activated carbon iron oxide coated sand (IOCS), fly ash, manganese green sand and granular titanium dioxide are works successfully for arsenic removal. Fly ash from coal-fired power plants has also reported to work successfully in Bangladesh (Mathieu, 2010). Ferruginous manganese ore (FMO) is an efficient adsorbent for both As(III) and As(V) in the pH range of 2–8. The adsorbed arsenic does not become desorbed from the filter sludge even at pH 2, under laboratory conditions. The FMO has been successfully used for the removal of arsenic in six real life (in North 24 Parganas, West Bengal) arsenic contaminated water samples (Chakravarty et al., 2002). Manganese dioxide coated sand showed promise as a medium for use in small systems or home-treatment units in developing areas of the world, for removing As(III) and As(V) from ground water (Bajpai and Chaudhuri, 1999). EPA (2002) stated that types of sorbent used in adsorption to treat arsenic are: activated alumina (AA), activated carbon (AC), copper-zinc granules, granular ferric hydroxide,

ferric hydroxide coated newspaper pulp, iron oxide coated sand, iron filings mixed with sand, greensand filtration ($KMnO_4$ coated glauconite), proprietary media, surfactant-modified Zeolite.

The adsorption media requires periodic regeneration or disposal and replacement with new media. Some of the exhausted media like AA could be regenerated. The regeneration process for other regenerable media is similar to that used for AA It consists of desorption arsenic ions from the media surface at high pH with NaOH solution, flushing with water, and neutralizing with a strong acid, such as sulfuric acid, hydrochloric acid for surface protonation (Mohan and Pittman Jr., 2007). Factors affecting on adsorption performance are identified as:

- Fouling: The presence of suspended solids, organics, solids, silica, or mica, can cause fouling of adsorption media.
- Arsenic oxidation state: Adsorption is more effective in removing of As(V) than As(III).
- Flow rate: Increasing the rate of flow through the adsorption unit can decrease the adsorption of contaminants.
- Wastewater pH: The optimal pH to maximize adsorption of arsenic by activated alumina is acidic (pH 6). Therefore, pretreatment and post-treatment of the water could be required.

Adsorptive media that have been most widely used are activated alumina, ion exchange resin, elemental iron or iron compounds, organic polymers, chars, coal, red mud, blast furnace slag (BFS), kaolin clay and silica sand, etc. Sometimes a combination of the media mentioned above is used together to maximize the adsorption of arsenic compounds. Adsorption media may also be used in combination with oxidants such as manganese compounds to pre-oxidize any arsenites present to arsenates which are more efficiently adsorbed from the contaminated water (Malik et al., 2009).

2.5.7 Indigenous filters

There are several filters available in Bangladesh and India that use indigenous material as arsenic adsorbent. Red soil rich in oxidized iron, clay minerals, iron ore, iron

scrap or fillings and processed cellulose materials are known to have capacity for arsenic adsorption. The arsenic removal methodologies of some of the filters are discussed in Table 2.4.

Table 2.4. Arsenic removal unit with their operation principles and investments (Ahmed, 2001).

Technology (manufacturer)	Treatment process	Type	Capacity	Cost (US$)
AMAL	Adsorption by activated alumina	Household	7,000–8,000 L	50
RPM Marketing Pvt. Ltd.	Activated alumina + AAFS-50 (patented)	Community	200,000/cycle	1,200
All India Institute of Hygiene & Public Health	Oxidation followed by co-precipitation/ filtration	Household	30 L/d	5
PHED, India	Adsorption on red hematite, sand, and activated alumina	Community	600–1,000 L/h	1,000
Pal Trockner Ltd., India	Adsorption by ferric hydroxide	Household	20 L/d	8
Ion Exchange India) Ltd.	Adsorption by ion exchange resin	Community	30,000 L/cycle	2,000
Sono 45-25	Adsorption by oxidized iron chips and sand	Household	-	13
Shapla filter	Adsorption of iron- coated brick chips	Household	-	4
SAFI filter	Adsorption	Household	-	40
Bucket treatment unit	Oxidation and coagulation/ sedimentation/ filtration	Household	-	6-8

The effectiveness all of these filter in arsenic removal is not known. The Shafi and Adarsh filters use clay material as filter media in the form of candle. The Shafi filter was reported to have good arsenic removal capacity but suffered from clogging of filter media. The Adarsha filter participated in the rapid assessment program but failed to meet the technical criterion of reducing arsenic to acceptable level (BAMWSP, 2001). Bijoypur clay and treated cellulose were also found to adsorb arsenic from water (Khan et al., 2000). Comparisons of main arsenic removal technologies are shown in below (Table2.5).

Table 2.5. Comparison of main arsenic removal technologies (Ahmed, 2001).

Technologies	Advantages	Disadvantages	% of As Removal
Oxidation/ precipitation	Relatively simple, low-cost but slow process	Mainly removes arsenic (V) and accelerate the oxidation process	80
Air oxidation	Also oxidizes other inorganic and organic constituents in water		
Chemical oxidation	Oxidizes other impurities and kills microbes	Efficient control of the pH and oxidation step is needed	90
	Relatively simple and rapid process		
	Minimum residual mass		
Coagulation/co-precipitation	Durable powder chemicals are available	Produces toxic sludge	90
	Relatively low capital cost and simple in operation	Low removal of arsenic	
Alum coagulation		Pre-oxidation may be required	
	Effective over a wider range of pH.		
Iron coagulation	Common chemicals are available	Medium removal of As(III)	94.5
	More efficient than alum coagulation on weigh basis	Sedimentation and filtration needed	
Lime softening	Most common chemicals are available commercially	Readjustment of pH is required	91
Sorption techniques AA	Relatively well known and commercially available	Needs replacement after four to five regeneration	88
Iron coated sand	Expected to be cheap	Yet to be standardized	93
	No regeneration is required	Produces toxic solid waste	
	Remove both As(III) and As(V)		
Ion exchange resin	Well-defined medium and capacity	High cost medium	87
	The process is less dependent on pH of water	Requires high-tech operation and maintenance	
	Exclusive ion specific resin to remove arsenic	Regeneration creates a sludge disposal problem	
		As(III) is difficult to remove	
		Life of resins	
Membrane techniques	Well-defined and high-removal efficiency	Very high-capital cost	95
		Pre-conditioning	
Nanofiltration		High water rejection	
Reverse osmosis	No toxic solid waste is produced	High tech operation and maintenance	96
Electrodialysis	Capable of removal of other contaminants	Toxic wastewater produced	95

Among other cheap adsorbents bone-char is considered to be very effective adsorbing agent for As(V) in the pH range of 2–5. Red mud is a waste material generated during the production of alumina in Bayer process. Arsenic adsorption onto virgin activated carbon was minimal and regeneration was difficult, so it cannot be directly applied for arsenic treatment. Some iron compounds were impregnated into activated carbon, resulting in enhanced arsenic sorption (Mohan and Pittman Jr., 2007). Enhanced arsenic adsorption was similarly observed with copper-treated and zirconium-treated activated carbon. Iron oxide coated sands are found to be effective in removal of arsenic

from water. Low cost of operation for iron oxide coated sands beds and after it is adapted to the small equipment, found good for family usage (Mandal et al., 2011).

2.5.8 Role of iron compounds in arsenic adsorption

The strong affinity for As by Fe oxide surfaces has also been widely used in the water purification processes. Iron-based adsorbents, e.g., granular ferric hydroxides (GFH), Bayoxide Sorb33 (E33), zero-valent iron (ZVI), sulfur-modified iron (SMI), iron modified activated alumina (FS-50), modified Zeolite (Z33), iron-oxide impregnated activated carbon, have been investigated for arsenic removal efficiency and found to be good adsorbent for arsenic. Zero-valent iron, Z33, and SMI are less porous and rely upon external surfaces for arsenic adsorption, or rely upon reactive surfaces (iron dissolution and re-precipitation) for arsenic removal (Mohan and Pittman Jr., 2007).

It is well-established that hydrated Fe(III) oxides (HFOs) exhibit amphoteric sorption behaviors; i.e., they can selectively bind Lewis acids or transition-metal cations as well as Lewis bases or anionic ligands (e.g., arsenates and phosphates) through the formation of inner sphere complexes (Puttamraju and SenGupta, 2006). Elemental iron on the other hand, in the presence of aqueous solution, can be oxidized both aerobically and anaerobically providing electrons for the reduction of other redox sensitive chemical species such as arsenate and sulfate. This invention presents a new method for the immobilization of inorganic arsenic species, such as arsenates and arsenites, by iron filings. The method uses iron filings (zero valent iron) and sand to reduce inorganic arsenic species to iron co-precipitates, mixed precipitates and, in conjunction with sulfates, to arsenopyrites. Other constituents may be added to the mixture to control porosity or chemistry. The method may be employed, for ex-situ as part of groundwater extraction and treatment system (pump and treat). Inorganic arsenic contaminated water, spiked with equivalent sulfate concentrations passes through an iron filings/sand filter. This results in removing most of the arsenic from the solution.

The surface chemistry of an oxide surface in contact with an aqueous solution is determined to a large extent by the dissociation of the hydroxyl groups. The equilibria may conveniently be expressed as:

$$\underset{\text{Decreasing pH}}{\longleftarrow} \quad M\text{—}OH_2 \leftrightarrows M\text{—}OH \leftrightarrows M\text{—}O^- + H^+ \quad \underset{\text{Increasing pH}}{\longrightarrow} \qquad (2.14)$$

This indicates that by appropriate adjustment of pH, the surface may carry either a positive or a negative charge, while at an intermediate value, the hydroxyl groups are undissociated, and the surface has zero charge. This "point of zero charge" (pzc) more correctly defines the situation when there is net zero charge on the surface, which is readily determined by potentiometric titrations (Parfitt, 1976). As(III) and As(V) can associate with iron surfaces either by forming inner-sphere or outer-sphere complexes (Goldberg et al., 1998, 2003, 2007; Kookana et al., 1998). Surface chemistry is important in arsenic removal by metal oxides. The surfaces of metal oxides are collections of unfilled metal-oxygen bonds that hydrate in water. Electrostatic attraction of anionic species is favored onto positively charged surface sites. At the pH of zero point of charge (pH_{ZPC}), an equal number of positively and negatively charged surface sites exist, and proportionally more positively charged surface sites at pH levels below pH_{ZPC}. Therefore, pH_{ZPC} is one indicator for the potential of removing anionic arsenic species. Iron (hydr)oxides have pK_{a1} and pK_{a2} values of ~7.3 and 8.9, respectively, resulting in a pH_{ZPC} on the order of 8.0. Columbic forces favor association of anionic arsenate with positively charged sites on metal oxides. In addition to electrostatic bonding, arsenic also forms with some surfaces covalent bonds including monomolecular monodentate and bidentate. Whereas electrostatic bonds form rapidly (in seconds) and depend largely on the charge difference between arsenate and the media surface, covalent bonds form less rapidly and depend on their respective molecular structure. Covalent bonds are irreversible and stronger than electrostatic attractions. As covalent bonds form, surface sites can become available for electrostatic bonding again. The kinetics of bond formation may affect the optimal contact time required for a specific media in a column operation.

Iron fillings are susceptible for formation of rust when encounters moisture or directly exposed to water. The rusting of iron is an electrochemical process that begins with the transfer of electrons from iron to oxygen. The key reaction is the reduction of oxygen:

$O_2 + 4\ e^- + 2\ H_2O \rightarrow 4\ OH^-$ (2.15)

Because it forms hydroxide ions, this process is strongly affected by the presence of acid. The corrosion of most metals by oxygen is accelerated at low pH. Providing the electrons for the above reaction is the oxidation of iron that may be described as follows:

$Fe \rightarrow Fe^{2+} + 2\ e^-$ (2.16)

The following redox reaction also occurs in the presence of water and is crucial to the formation of rust:

$4\ Fe^{2+} + O_2 \rightarrow 4\ Fe^{3+} + 2\ O^{2-}$ (2.17)

Additionally, the following multistep acid-base reactions affect the course of rust formation:

$Fe^{2+} + 2\ H_2O \rightleftharpoons Fe(OH)_2 + 2\ H^+$ (2.18)

$Fe^{3+} + 3\ H_2O \rightleftharpoons Fe(OH)_3 + 3\ H^+$ (2.19)

As do the following dehydration equilibria:

$Fe(OH)_2 \rightleftharpoons FeO + H_2O$ (2.20)

$Fe(OH)_3 \rightleftharpoons FeO(OH) + H_2O$ (2.21)

$2\ FeO(OH) \rightleftharpoons Fe_2O_3 + H_2O$ (2.22)

Mohan et al. (2007) described the possible mechanism of arsenic from water in any iron media filters in two ways.

(i) Adsorption to corrosion product

$\equiv FeOH + HSO_4^{2-} + H^+ \leftrightarrow \equiv FeHAsO_4^{2-} + H_2O$ $K = 10^{12}$ (2.23)

$\equiv 2(FeOH) + HSO_4^{2-} + H^+ \leftrightarrow \equiv Fe_2HAsO_4^{2-} + H_2O$ $K = 10^{26.2}$ (2.24)

Where, K is the Langmuir equilibrium constant

(ii) Mineral formation

$Fe(OH)_3 + H_2AsO_4^- + H^+ \rightarrow FeAsO_4 \cdot 2H_2O + H_2O$ (2.25)

Awuah et al. (2009), in their experiment with cut pieces of iron rod in sand, removed the arsenic from influent water by iron species via precipitation and adsorption in aerobic atmosphere. The removal efficiency is related to the surface area or the type of iron used and improves over time, possibly due to pitting of the iron surface and increased surface area for sorption due to iron corrosion and ferrous iron adsorption or precipitation. Therefore, both As(III) and As(V) can be removed from aqueous using

zero-valent iron (Junyapoon, 2005, Anita, 2010). Iron plays an important role in contaminant mobility, sorption and breakdown due to its role as an electron donor (i.e. during the oxidation of Fe^{2+} to Fe^{3+}), and, in its various mineral forms, as a precipitant/sorbent substrate. Freshly precipitated, amorphous Fe oxyhydroxides (hydrous ferric oxides or HFO) are known to be particularly effective adsorbents of a range of contaminants. Sorbed metals can either be surface adsorbed, co-precipitated or incorporated into the (Fe) oxide structure (Cundy et al., 2008). Gottinger (2010) opined that in some groundwater, the iron concentration is insufficient to adsorb and co-precipitate with the arsenic. In these instances, iron may be added through such media as ZVI filings, to improve arsenic removal. ZVI filings are a proven and effective media for arsenic removal in permeable reactive barriers, in ZVI iron filings columns or in a mixture with filtration sand in columns. Iron filings are readily available and inexpensive and, therefore, have significant potential as an arsenic removal medium for small-scale potable water systems. Lien and Wilkin (2005) carried out experiments on removal of arsenite from groundwater by zero-valent iron. Analyzing HCl-extractable arsenic from iron samples, they found that approximately 28% of arsenic was in the form of arsenate which suggesting that a surface oxidation process was involved in the arsenic removal with zero-valent iron. Effective removal of inorganic As(V) and As(III) from groundwater by zero-valent iron has been demonstrated for practical use with flow-through cartridge systems as well as permeable reactive barrier systems. It is able to remove organic arsenic also from groundwater. The batch and column experiments consistently indicate a decrease in affinity of As species for Fe filings in the following order: inorganic As(III) > inorganic As(V) > MMA > DMA (Cheng et al., 2009). It was found that repeated contact of aerated water with zero-valent iron lead to continued release of Fe(II) and to complete oxidation of As(III) in parallel to the oxidation of Fe(II) with dissolved oxygen and without an added oxidant (Leupin, 2004). Arsenic appears to be removed mainly by precipitation in anaerobic condition, while the adsorption of arsenic to iron and iron corrosion products is very important in aerobic condition. Oxidation of arsenite to arsenate can be promoted by iron species in aerobic environment. Low pH is propitious to remove arsenic compounds in aerobic condition, while in relative

anaerobic condition, acidic and alkaline condition seems to be favorable for arsenate and arsenite removal, respectively (Sun et al., 2004).

2.5.9 Role of sand in arsenic adsorption

Sand is being used as a filtration bed media all over the world since long. Sand bed filters work by providing the particulate solids with many opportunities to be captured on the surface of a sand grain. As fluid flows through the porous sand along a tortuous route, the particulates come close to sand grains. Sand itself does not function as an adsorbent for arsenic removal from water; however, it is found straining of iron flocs, which combined with arsenic, embedded within it. Aerobic environment will help the reaction to removal of iron with arsenic too. Thus, arsenic contaminated in groundwater can be reduced to a level below MCL. Berg et al. (2006) developed a sand filter and used in Vietnam at household level. The filter comprise of two containers. The upper container is filled with locally available sand and the lower one serves to store the filtered water. It is suggested that advantage of presence of high iron groundwater oxidizes to form flocs of iron hydroxide and filtered within sand bed. In arsenic removal techniques involved the precipitation of iron and immobilization of the arsenic by sorption onto the Fe(III) precipitates have received much attention. During aeration and filtration, which are key treatment processes in many centralized water treatment facilities, part of the Fe(III) precipitate adheres to or nucleates on the surfaces of filter sand grains. Thus, the filter sand slowly is transformed into grains consisting of a center of the original sand grains (dominantly quartz) now covered with voluminous Fe(III)-dominated precipitates. The precipitate constitutes a significant part of the solids in the sand filter at any time and contributes both a high specific surface area of high reactivity and a large micro porosity. Poorly ordered ferrihydrite has been observed to constitute a substantial part of the precipitates formed in such treatment processes and in other places where groundwater containing ferrous iron is aerated (Jessen et al., 2005). In an early stage of the precipitation of pure ferrihydrite, the precipitate consists of nanometer-sized ferrihydrite crystallites. The ferrihydrite crystals subsequently grow as the crystallites aggregate by Van der Waal forces and as Fe-O-Fe bonds form between the iron octahedra of the

aggregated crystallites (Fuller et al., 1993; Waychunas, et al., 1993). During ferrihydrite precipitation, solutes in the water that sorb strongly to ferrihydrite surfaces (*e.g.* SiO_2) can decrease further the Fe-O-Fe polymerization by blocking up the ferrihydrite crystallite surfaces (Jessen et al., 2005), thereby maintaining a high specific surface area and reactivity of the precipitate. Both As(III) and As(V) form inner-sphere surface complexes on ferrihydrite (Goldberg and Johnston, 2001). As(V) sorption decreases gradually with increasing pH from 6 to 9 (Goldberg and Johnston, 2001; Raven et al., 1998; Dixit and Hering, 2003). In many studies it has been observed that, in the presence of competitive solutes, As(III) sorption increases with increasing pH from 4 to 8 (Dixit and Hering, 1997, Hering et al., 1997). It is also indicated that As(V) is removed more efficiently than As(III). In agreement with this, competition by co-occurring solutes such as SiO_4, PO_4^{3-}, SO_4^{2-}, HCO_3^-, or Cl^-, which are all present in the water, has been observed to inhibit sorption of As(III) to ferrihydrite more than As(V).

2.5.10 Role of laterite soil in arsenic adsorption

Laterites are soil types rich in iron and aluminium, formed in hot and wet tropical areas. Nearly all laterites are rusty-red because of iron oxides. They develop by intensive and long-lasting weathering of the underlying parent rock. Tropical weathering (laterization) is a prolonged process of chemical weathering that produces a wide variety in the thickness, grade, chemistry and ore mineralogy of the resulting soils. The lateritic soils (or red soil) in Assam extensively occurs almost entirely over the N.C. Hills district covering some parts of southern Karbi Plateau while few patches are confined to eastern margin of the Hamren sub-division of Karbe Anglong district, southern boarder of Golaghat district and the northern part of the Barak plain along the foothills of the Barail range. These soils are dark and finely texture with heavy loams and deficient in nitrogen, potash, phosphoric acid and lime (http://www.envisassam.nic.in/soiltype.asp). Laterite has been tested as an adsorbent and proved to be a promising low-cost remedial technique to safeguard high-As drinking water. Laterite occurs as a red-colored, vesicular, clayey residuum abundantly in tropical regions. Laterite is an acidic soil with a typical pH between 4 and 6. The major components of laterite are hydrous oxides of iron and

aluminum, with minor proportions of manganese and titanium. Both hydrous iron and aluminum oxide components in laterite have a pHzpc (zero point of charge) at 8.5–8.6.

Partey (2008) stated that 'lateritization' is the removal of silicon through hydrolysis and oxidation that results in the formation of laterites and lateritic soils. The degree of lateritization is estimated by the silica-sesquioxide (S-S) ratio ($SiO_2/(Fe_2O_3 + Al_2O_3)$) calculated as the weight percent of the minerals. Soils are classified by the S-S ratios into the following categories:

- An S-S ratio of 1.33 or less = laterite.
- An S-S ratio of 1.33 to 2.00 = lateritic soil.

Laterite could either be used in a filter column or directly mixed with water in the water vessel where the soil particles would act as adsorbent during sedimentation. Laterite can be used to develop an effective and inexpensive water purification system for communities that costs little, are easy to maintain, and produces high quality drinking water. Chakravarty et al. (2002) establish the role of laterite (ferralite) enriched with natural HFO as an arsenic scavenger through batch studies and demonstrated the better competency of the material over the natural/commonly used chemical coagulants generally used for water treatment. The pHzpc (point of zero charge) of latérite based on acid-base titration is found to be 8.5. Maji et al. (2007) performed fixed bed column study with As(V). The adsorption of As(V) in the fixed bed was strongly dependent on the flow rate, initial As(V) concentration and the bed height. They further pointed out that an aqueous 1M NaOH solution could be used for the regeneration of the adsorbent material after As(V) adsorption. Maji et al. (2007a) found out that arsenic removal is governed by the pH of the aqueous medium. It was further found that the removal efficiency of arsenic was suppressed with increase in temperature. The adsorption isotherm follows Langmuir, Freundlich and D-R (Dubinin- Radushkevich) isotherms well. Laterite soil shows a good potential to be used as an adsorbent for arsenic removal from aqueous media. It has been found that 98% and 95% of As(III) and As(V) (C_0= 0.5 mg L^{-1}) in the presence of 10 and 20 g L^{-1} dose of that adsorbent was possible (Maji et al., 2007b). Rahaman et al. (2008) stated that arsenic removal by heat-treated laterite was experimentally investigated and it was explored that laterite can be effectively used for the removal of arsenic from contaminated groundwater. The removal rate was found dependent on the initial arsenic

concentrations and adsorption equilibrium data indicates favorable adsorption of arsenic onto laterite. It can also be concluded that change in natural weather temperature may not have any significant effect on the arsenic adsorption efficiency of the laterite. Since laterite is a natural-substance, so, use of laterite for removal of arsenic from contaminated water is expected to be economical and feasible.

Maji et al. (2008) conducted column study with As(III) spiked water. The adsorption of As(III) in the fixed bed of laterite soil was strongly dependent on the flow rate, initial As(III) concentration and the bed height. It is found that the breakthrough time decreases with the increase in both flow rate and initial concentration. Maiti et al., (2009, 2010) opined that both Langmuir and Freundlich isotherms fit the adsorption data adequately.

2.5.11 Basic criteria for development of household level arsenic removal filter

Design of an appropriate and suitable technology is dependent on many factors. The factors are considered in the developing process with the primary considerations listed in Table 2.6.

Table 2.6. Major decision factors considered in the filter design process.

Decision Factors	Issues
Effluent characteristics	Safe arsenic and iron free water.
Filtration rate	The filtration rate should be enough so that it can fulfill the water requirement of an average family throughout the day
Preparation of filter	The filter will be simple; that can be made by rural people locally.
Capital Cost of the filter	The filter should be affordable for rural people.
Operation cost	The operation and maintenance cost should be nominal.
Complexity of System Operation	The operation mechanism will be very simple. It should be easy to maintain and easy to clean.
Filter life	The filter should serve arsenic free water for a reasonably long period of time.
Residuals Disposal	The disposal method should not be risky.
Adoptability	If the filter will be similar to the existed iron removal filter than it will be easily adoptable.

2.6 Summary

Literature survey corroborate that the many parts of the world including India are suffering due to arsenic contamination problem in groundwater. The Brahmaputra floodplain is one of the major affected areas in India. Arsenic is highly toxic and very dangerous to human health. Several technologies are already implemented to reduce the arsenic consumption, some of them removing arsenic successfully. From the literature survey it is clear that arsenic removal technology need to implement in Brahmaputra floodplains immediately. Madhupur block is chosen as study area to represent the groundwater quality parameters of Brahmaputra floodplains. Role of sand, iron oxides sand laterite soil in arsenic adsorptions are discussed in tabular form (Table 2.7).

Table 2.7. Role of sand, laterite soil and iron oxides in arsenic adsorption.

Adsorbent	Role in arsenic adsorption	References
Sand	Adsorption capacity of sand is poor. To enhance the adsorption capacity, the sand particles are coated using different oxides. Sand is a good filtration media, effective to arrest the arsenic which co-precipitates along with ferric flocs by adsorption and co-precipitation technique.	Gupta et al., 2005; Mohan and Pittman, 2007; Berg et al., 2006.
Laterite Soil	Laterite soils are rich in iron and aluminium. Laterite soil shows a good potential to be used as an adsorbent for arsenic removal from aqueous media. Arsenic removal efficiency was found 98% for As(III) and 95% for As(V) in past literature.	Maji et al., 2008; Rahaman et al., 2008.
Iron Oxides	Iron oxides, hydroxides, and oxy-hydroxides including amorphous hydrous ferric oxide (FeO-OH), hematite (α -Fe_2O_3) and goethite (α-FeO-OH) are promising adsorbents for removing both As(III) and As(V) from water Some popular iron-based adsorbents are granular ferric hydroxides (GFH), Bayoxide Sorb33 (E33), zero-valent iron (ZVI), sulfur-modified iron (SMI), iron modified activated alumina (FS-50), modified Zeolite (Z33) and iron-oxide impregnated activated carbon etc.	Badruzzaman et al., 2004; Raven et al., 1998; Mohan and Pittman, 2007.

In the present research, naturally oxidized iron scrap, sand, red soil and murum are selected as adsorbents for arsenic remediation. The proper justification of the thesis work is discussed in this chapter. This chapter indicated the urge of development of a new arsenic removal technology which will be affordable, sustainable and cheap and that can be made by local people using locally available materials.

Chapter 3

MATERIALS AND METHODS

3.1 Introduction

The objective of this chapter is to elaborately discuss on the materials and methods for the development of an arsenic removal filter. To achieve the goal, the chapter objective is divided into three subparts. First part consists of selection of study area, locating groundwater sampling points, collection of groundwater samples and methodology discussion to analysis the collected samples. The second part aims at the preparation of the selected materials (NOIS, sand, red soil and murum) as adsorbents and to determine of the physicochemical characteristics of them. In this part, the methodologies for preparations of standard solutions and reagents are elaborately discussed. The batch and column experimental methodologies are also narrated in this part. The objective of the last part is to discuss the preparation and testing methodologies for development and optimization of a porous media for arsenic removal filter preparation. The preparation, development and testing procedure of the arsenic removal filter is elaborately discussed at the end of this chapter.

3.2 Delineation of unsafe aquifer in the study area

3.2.1 Study area

Madhupur block is situated in the middle of the Nalbari district and nearer to the NH 31. Nalbari district is bounded by the Darrang and Kamrup districts in the east, Barpeta district in the west, Bhutan in the north and Brahmaputra in the south and is situated in between 26°-27°N latitude and 91°-97°E longitude. Nalbari is 60 km. away from Guwahati city. Most of the people rely on groundwater source for drinking and

cooking purpose. In the present study, the groundwater samples were collected at different seasons from the 48 no. of different tubewells, which were installed by Public Health Engineering Department (PHED), Assam. The groundwater sampling location is presented in Fig. 3.1.

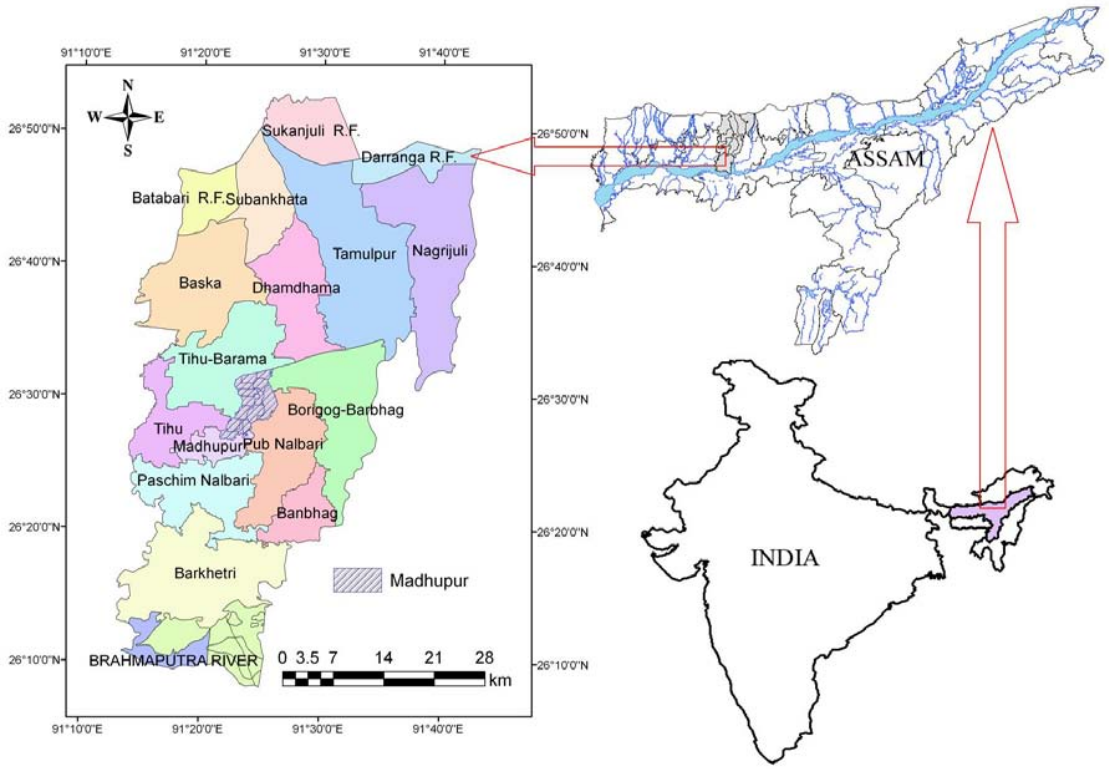

Fig. 3.1. Water samples and soil samples collection station in study area (Madhupur block of Nalbari district in Assam, India).

3.2.2 Field parameters estimation and water sampling procedure

Water samples were collected from the tube wells which are installed by PHED department of Assam. During sample collection name of the owner of the tube well, date of installation and GPS data were also noted. The selected tube wells (hand pump type) are in regular use. The samples were collected after minutes of pumping before collection of water samples until the electrical conductivity stabilized. From each well, two water samples were collected in 500 ml plastic bottle. The collected water Samples were

acidified in the field with HCl to lowering the pH value below 2 to analysis cations and arsenic. Measurements of temperature, pH, TDS, ORP and electrical conductivity were made in the field for each tube well.

3.2.3 Seasonal variation of arsenic concentration

The groundwater samples of the study area were collected in different season over the year. To collect the water sample the year was divided in four seasons. These are pre-monsoon, monsoon, post monsoon and winter season. The sample collection dates are showing in the given table (Table 3.1).

Table 3.1. Groundwater samples collection period from the study area.

Water Sampling	Sampling Date
1st Sampling	20/06/2008
2nd Sampling	18/09/2008
3rd Sampling	16/12/2008
4th Sampling	06/03/2009
5th Sampling	11/06/2009
6th Sampling	06/09/2009

3.2.4 Groundwater quality parameters estimation methods

Major anions: The major anions like chloride (Cl^-), sulphate (SO_4^{2-}), nitrate (NO_3^-), fluoride (F^-) and bicarbonate (HCO_3^-), other anion were analyzed in un-acidified water samples. All the samples were analyzed according to Standard Methods for the Examination of Water and Wastewater (20th edition, 1998).

Major cations & arsenic: The major cations like calcium (Ca^{2+}), potassium (K^+), sodium (Na^+), total iron (Fe) and other cations were analyzed in acidified water samples. All cations of the water samples were analyzed by Varian Atomic Absorption Spectrometry (AAS). Arsenic of the water sample was analyzed by AAS with vapor generation accessory (VGA-77) in the form of As (III).

The instruments/methods which were generally used to estimate the groundwater quality parameters in the laboratory have been summarized in tabular form (Table 3.2).

Table 3.2. Instrument/method used to determine the water quality parameters.

Parameters	**Instruments / Methods**	**References**
Temperature	Thermometer	Standard method (APHA, 1998)
E.C.	Conductivity Meter	Standard method (APHA, 1998)
pH	pH meter	Standard method (APHA, 1998)
Alkalinity	Titration Method	Standard method (APHA, 1998)
Magnesium	AAS in flame mode	EPA 7000B; Standard method
Calcium	AAS in flame mode	EPA 7000B; Standard method
Arsenic	AAS in VGA mode	Hung et al., 2004; Standard method
Sodium	AAS in flame mode	EPA 7000B; Standard method
Potassium	AAS in flame mode	EPA 7000B; Standard method
D.O.	Electrode meter	Standard method (APHA, 1998)
Hardness	Titration method	Standard method (APHA, 1998)
Nitrate	UV Visible Spectrophotometer	Standard method (APHA, 1998)
Ammonia	Colorimetric method	Standard method (APHA, 1998)
Phosphate	Spectrophotometer	Standard method (APHA, 1998)
Sulphate	Turbidimetric Method	Standard method (APHA, 1998)
Turbidity	Turbidimeter	Standard method (APHA, 1998)
Chloride	Argentometric Method	Standard method (APHA, 1998)
Iron	AAS in flame mode	EPA 7000B; Standard method
Lead	AAS in flame mode	EPA 7000B; Standard method
Fluoride	UV Visible Spectrophotometer	Standard method (APHA, 1998)
Chromium	AAS in flame mode	EPA 7000B; Standard method
Cadmium	AAS in flame mode	EPA 7000B; Standard method
Mercury	AAS in flame mode	EPA 7000B; Standard method
Other Anoins	Standard Method	Standard method, APHA, 1998
Other Cations	AAS in flame mode	EPA 7000B; Standard method

The preparation of reagents and arsenic determination methods were discussed in the section 3.3.3 of within this chapter.

3.3 Comparative evaluation of arsenic adsorption potential of the locally available materials

3.3.1 Adsorbents materials

Sand, naturally oxidized iron scrap (NOIS), red soil and murum were collected from different local sources. Each individual item was processed in the laboratory for use as adsorbent in arsenic remediation. Material descriptions, process mechanism and physicochemical characteristics materials are also explained in this part of thesis work.

3.3.1.1 Sand

Locally available river sand that generally used for building constructions was tested for adsorption capacity of arsenic. The rural and semi urban people of Assam have been using sand from few decades ago to treat the ground water for drinking and cooking purpose without knowing its removal mechanism. So, the sand is used as adsorbent to evaluate its arsenic removal mechanism, capacity and field applicability. The local building material suppliers supplied the necessary amount of river sand which is collected from Kulsi River, around 40 km away from Guwahati city in India. The collected sand was processed to remove the impurities and silt. Initially the sand particles were properly washed with tap water till clay and suspended particles were totally removed. Thereafter, the sand particles were washed with distilled water to ensure that there are no impurities remain on the external surfaces of the sand particles. The washed sand dried in hot oven at 105 ± 2^{0}C for 24 hours and then allowed to cool in the room temperature. Sand particles were then allowed to pass through 2 mm sieve and retain in 425 µm sieve to prepare sand particles homogeneous and silt free for experimental purpose. To observe the effect of surface area on arsenic sorption the processed sand particles were filtered through 600 µm and 1mm sieve. From the sieving test, the sand particles were distributed into three groups to determine the relation of sorption mechanism with the particle size of the sand. The sand particles were classified in the groups according to the particle size in the following order: 425 µm-600 µm, 600 µm-1 mm and 1 mm-2 mm. Fig. 3.2 represented the comparison of color and texture of the sand particles before and after processing.

Fig. 3.2. Color comparison of the sand particles before and after processing.

3.3.1.2 Naturally Oxidized Iron Scraps (NOIS)

Iron scraps were collected from mechanical workshop of IIT Guwahati where iron scraps were produced by various cutting and filing operations. These scraps were disposed in an open container where this scraps was naturally oxidized on exposure to the atmosphere. The iron scraps were collected about after 3 months of deposition and it was highly corroded in this course of time. Scraps were of reddish brown in color and were irregular in structure. These naturally oxidized scarps were collected in an airtight bag and properly washed with tap and distilled water respectively to remove the foreign suspended and dissolved particles. The iron scraps were dried to remove moisture in hot oven at 105±2ºC for 24 hours. The scraps were filtered through 2 mm sieve and retained particles were used for the experimental purpose. A sieve analysis was conducted of the processed NOIS particles using 1mm, 600µm and 300µm sieve to categorize the particles in different size ranges to estimate the effect of surface area on arsenic sorption mechanism. The particles were categorized as less than 300 µm, 300µm-600µm, 600µm-1mm and 1mm-2mm size of particle. Batch studies were carried out with four different particle sizes (particle size less than 300µm, 300µm-600µm, 600µm-1mm and 1mm-2mm) to ensure sorption kinetic behavior with specific surface area of oxidized iron scraps. From the Fig. 3.3, the different particle size of NOIS images can be seen.

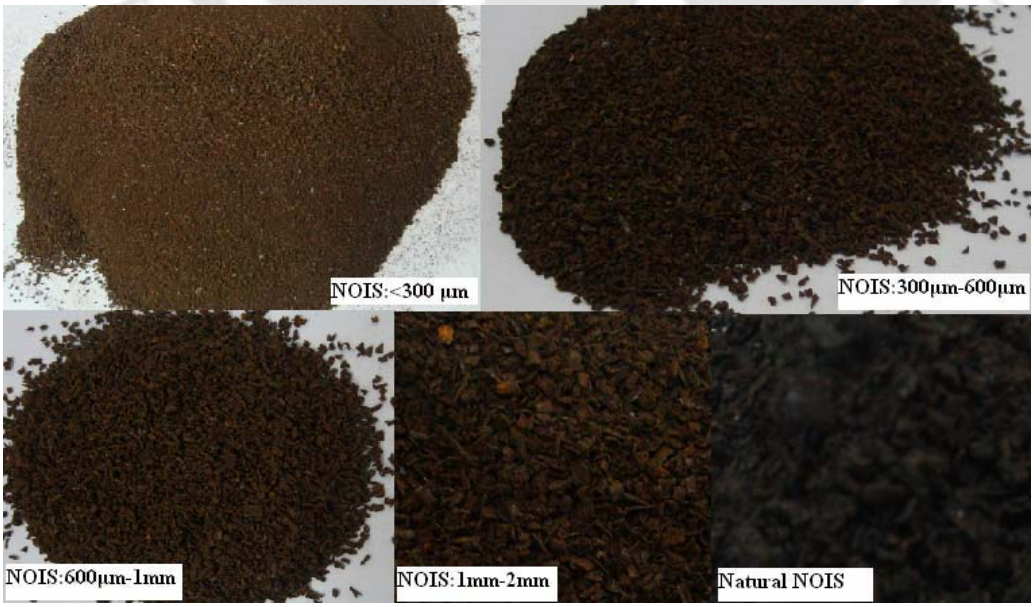

Fig. 3.3. Image of the different size of the processed NOIS particle.

3.3.1.3 Red Soil

Red soil is easily available everywhere in Assam, India. For the experimental purpose, this soil was collected from the Hilltop of IITG Campus. Collected samples were allowed to be dried in room temperature. The dried up soils were crushed using rubber hammer and allowed to pass through 425 μm sieve. Sorption studies were carried out with this prepared red soil. Fig. 3.4 is showing the image of processed red soil.

Fig. 3.4. Image of the processed red soil.

3.3.1.4 Murum

Murum is the laterite soil, elsewhere available in Rarh region of West Bengal, India. Rarh region is located between and the Ganges Delta. Bankura, Purulia, Birbhum, Burdwan, Howrah, Hooghly and Midnapore districts are covered within Rarh region of West Bengal. Sticky, red color of this soil is a combination of finer particles and coarser particles. This soil is generally used for local road construction purpose due to its good binding property. The soil contains aluminum silicates, aluminum hydro-silicates and high amount of iron oxides and iron hydroxides (Maji, 2007). Arsenic adsorption capacity of the murum is checked for its possible use as effective adsorbent for arsenic remediation in Assam, India. To prepare the murum as adsorbent, the fine particles and other impurities were washed out using tap water. The coarse particles were allowed to dry in room temperature for approximate 7 days. Soft natures of coarse particles were broken into small pieces and washed with distilled water to remove dust. Thereafter, the

materials were dried in hot oven at 105±2^{0}C for 48 hours to ensure the materials were moisture free. Then particles were sieved through 2 mm and 4 mm sieve. The 0-2 mm and 2-4 mm size of particles were tested for arsenic sorption from aqueous medium. The processed murum is shown in Fig. 3.5.

Fig. 3.5. Image of the processed murum.

3.3.2 Characterization of the adsorbents

To characterize the adsorbents i.e. sand, red soil, NOIS and murum, several experimental studies were carried out. To analyze the surface morphology and structural characteristics of the sand and red soil particles before and after adsorption, scanning electron microscope (Model: LEO, 1430 VP, Carl Zeiss, Germany) and field emission scanning electron microscopy (FESEM, Sigma, Zeiss) images are investigated. The pore shape and sizes of the circular porous disk (CPD) were also examined using FESEM. The energy dispersive X-ray (EDX) analyses of sand and red soil were done simultaneously with the scanning electron microscope (SEM) to determine the chemical and mineralogical composition of the prepared adsorbent. While the exact elemental composition cannot be determined accurately from EDX spectra, the presence and absence of elements in the surface of the particle can be verified. The major oxides composition of the sand, red soil and NOIS were determined by X-ray fluorescence (XRF) spectrometry (Model: AXIOS, PANalytical, Make: Philips) analysis. The major and minor mineralogical composition of the adsorbents were identified using X-ray

powder diffraction (XRD) system (Model: XRD 3003TT, SEIFFRT, Make: Rich Seifert & Co., Ahrensburg, Germany) with CuKα radiation (λ=1.54 Å), a Cu filter on secondary optics, 45 kV voltage and 20mA current. The XRD profile of the samples were measured from 10-95^0 with the step size of 0.05^0/sec. Fourier transform infrared spectroscopy (FTIR) was used to identify the chemical bonds in the molecules by producing an infrared absorption spectrum that is like a molecular "fingerprint". By interpreting the infrared absorption spectrum, the chemical bonds present in the adsorbents were determined. The FTIR spectra were analyzed in KBr pellets using Perkin-Elmer 281 IR spectrophotometer. The spectra were determined in the range of 4000-450 cm^{-1}, and the band intensities were expressed in terms of transmittance (%). To understand the arsenic sorption mechanism, the FESEM, XRD and FTIR analysis were accomplished with the powder NOIS for both before and after adsorption. To conduct FESEM, XRD, XRF and FTIR analysis, the adsorbents were ground to produce fine powder and dried at 105±2^{0}C in the hot oven.

3.3.3 Reagents and analytical methods

All the chemicals were analytical grade and used without further purification. HPLC grade ultra pure water prepared using Chemiton water purification system was used for preparation of regents and aqueous solutions. 1000 mgL^{-1} of arsenic stock solutions were prepared using arsenic trioxide (As_2O_3; AR) for As(III) solutions and sodium arsenate ($Na_2HAsO_4.7H_2O$; AR) for the As(V) solutions. The stock solutions were preserved with 1% trace metal grade nitric acid. Necessary standard solutions were prepared from stock solution using serial dilution method for the experiments and arsenic determination purpose. Necessary arsenic spiked solutions [As(III) and As(V)] were prepared just prior to conducting the experiments. Distilled water as well as tap water of the Environmental Engineering Laboratory (IIT Guwahati) is used for preparation of arsenic spiked water for other studies. The parameters of tap water were measured according to Standard Methods for the Examination of Water and Wastewater (APHA, 1995). Aqueous samples were analyzed for total arsenic by atomic absorption spectrometry (AAS) with vapor generation accessory (VGA-77) in the form of As(III)

with an electrode less discharge lamp (EDL) as the radiation source at a wavelength of 193.7nm. Before estimation of the arsenic concentrations in the samples, both the standard and samples were treated with at least 1(M) HCl and ensured that any analyte present as As(V) is reduced to As(III) by the action of potassium iodide at a concentration of 1% w/v. The reduction takes about 50 minutes at room temperature. Necessary amount of distilled water was added to the standards and the samples to produce appropriate dilution and arsenic concentrations of the solutions were quantified using AAS. Arsenic concentrations of the solutions were estimated according to guideline of AAS user manual. Separation of As(III) and As(V) species were obtained using an ion exchange column using Indion GS 300 strong base type-1 anion exchange resin, containing quaternary ammonium groups (Manufactured by Ion Exchange, India). As(V) species is adsorbed within resin column allowed passing of As(III) species along with aqueous portion.

The inlet and outlet arsenic concentrations were estimated which gives the value of As_{total} and As(III) repectively. The concentration of As(V) was calculated from the difference of As_{total} and As(III). Arsenic species concentrations in the column inlet solution were verified at the beginning and at the end of each experiment. All cations present in aqueous solutions were analyzed by Varian atomic absorption spectrometry (AAS) in flame mode.

Effects of co-ions were also observed in the stock solutions, prepared using analytical reagents. Salts of sodium phosphate monohydrate (NaH_2PO_4), anhydrous sodium sulfate (Na_2SO_4), sodium bicarbonate ($NaHCO_3$), and calcium carbonate ($CaCO_3$) were used to prepare 1000 mg L^{-1} stock solutions. These were diluted prior to every experiment to meet desire concentration. Magnesium stock solution was prepared by dissolving 1g magnesium metal dust in 1:4 nitric acid (HNO_3) and diluted to 1 L using distilled water to give 1000 mg L^{-1} Mg. 1g of iron metal powder was dissolved in 20 ml of 6N H_2SO_4 and diluted to 1 L using distilled water to make 1000 mg L^{-1} ferrous iron (Fe^{2+}) stock solution. Ferric iron (Fe^{3+}) stock solution was prepared from ferric chloride ($FeCl_3$). In order to conduct the experiments and to detect the required parameter of the adsorbents as also of aqueous solution some instruments were used. Table 3.3 shows the list of equipments (along with their manufacturing detail) used in the current work.

Table 3.3. Details of analytical instruments used in the present work.

Instrument	Manufacturer & Model	Purpose
Digital pH Meter	Model: µpH system 361, Systronics India Ltd.	To determine pH of water sample in Lab
Digital conductivity Meter	Model: VSI 04, VSI, India	To determine conductivity of water sample in Lab
Digital Nephelo-Turbidity Meter	Model-132, Systronics, Ahmedabad, India	To determine turbidity of water sample in Lab
Digital Spectrophotometer	Model:166, Systronics, Ahmedabad, India	To determine the concentration of elements in a sample
UV Visible Spectrophotometer	Varian, The Natherlands Cary 50 Bio	To determine the concentration of elements in a sample
High Speed Research Centrifuge	Model: R24, Remi, Mumbai, India	For high speed centrifuging
Analytical Balance	Model:AB304S, Metteler Instrument AG, Switzerland	For accurate weighing, Accuracy level upto four decimal
Hot Plate	JSGW, India	For heating volatile materials
Drying Oven	Model: PSI, M/S Mahindra Scientific Instrument Co., India	To dry the glassware and reagents
Muffle Furnace	ICI, International Commercial Traders, Kolkata	To burn solid samples at desire temperature
Membrane Filter Assembly	ICT- SINCO, Millipore	To produce Milipore water
Magnetic Stirrer (1/8 HP)	Model: LS 104BELTEK, Mumbai, India	To dissolved soild perticles
Water Purification System	Model: QRP-380 BC, CHEMITON SL, Spain	To produce RO and Ultrapure water
Mechanical Stirrer	Model: LS04BELTEK, Mumbai, India	To mix the solution
Horizontal shaker	REICO, Calcutta	To shake the solution
Incubator Shaker	Model: LSI-1005R, Make is M/s Daihan Labtech Co. Ltd., Korea	To shake the solution at desire temperature and shaking speed
End over end rotary shaker	Wagner's shaking machine, Reico Pvt. Ltd., Kolkata	To shake the solution
Atomic Absorption Spectrophotometer	Model: Spectra Duo, Varian BV, The Netherlands	For determining the concentration of a particular metal element in a sample
Microwave Digester	Microwave digestion system, Model: 7295, OI Analytical, Texas	Digestion soil, sludge, waste to make it in dissolved form
Peristaltic pump	Model: PA-SF Control, IKA-WERKE, Germany	For pumping liquids
Particle size analyzer	Model: PP-10 EX, Miclins India Model: AWM 2000, Malvern instruments, Worcestershire	To determine particle size distribution using either dry or wet dispersion module
Scanning Electron Microscopy (SEM)	Model: LEO, 1430 VP, Carl Zeiss, Germany	To take picture at micro level
Field Emission Scanning Electron Microscopy (FESEM)	Model: Sigma, Zeiss Make: Germany	To take picture at micro level
X-ray Fluorescence Spectrometer (XRF)	Model: AXIOS, Make: Philips (Now PANalytical)	To determine oxide composition of samples
X-ray powder diffraction (XRD)	Model: XRD 3003TT, SEIFFRT, Make: Rich Seifert & Co., Ahrensburg, Germany	To determine the mineralogical composition of the powdered samples

3.4 Experimental methods

Adsorption studies with arsenic species by the selected adsorbents (NOIS, sand, red soil and murum) have been conducted in two manners: batch mode and continuous column mode adsorption. The kinetics of the co-precipitation technique and the effect of ionic strength of iron on co-precipitation have been investigated. The desorption and regeneration experiments have been conducted in the present study. The details of the methodologies of these experiments are described in this present chapter.

3.4.1 Determination of pH_{zpc} (Point of zero charge)

Point of zero charge (pH_{ZPC}) is a fundamental property of adsorption process. pH_{ZPC} of the adsorbents (sand, NOIS, red soil and murum) were determined to investigate the surface behavior of the adsorbents. The determination of the pH_{ZPC} of the samples was carried out as described by Srivastava et al. (2011), Namdeo and Bajpai (2008) and Nomanbhay and Palanisamy (2005). In brief, 50 ml of 0.01 M NaCl solution was placed in a closed 100 ml volume of specimen tube. The pH was adjusted to a value between 1 and 13 by adding HCl 0.1 M or NaOH 0.1 M solutions. Then, 0.2 g of sand sample was added and the final pH measured after 48 hrs under agitation at room temperature. The pH_{ZPC} is the point where the curve pH_{final} vs. $pH_{initial}$ crosses the line $pH_{initial} = pH_{final}$. Similarly, the pH_{ZPC} was also determined for NOIS, red soil and murum samples using the above method (Nomanbhay and Palanisamy, 2005).

3.4.2 Batch experimental procedures

Batch experiments of the adsorbents were conducted to optimize the adsorption capacity of the selected adsorbents and to study the behavior of the materials at different operating conditions. Synthetic arsenic spiked solutions prepared by diluting arsenic stock solution in distilled water were used for carrying out experiments. Details of batch experimental procedures of the adsorbents are described below.

3.4.2.1 Effect of agitation speed on arsenic sorption

Effect of agitation speed on arsenic sorption on the red soil, sand, NOIS and murum, a series of experiments were conducted using different agitation speed at equilibrium. 1g red soil, 2g sand, 0.5 g of NOIS and 2 g of murum were used as adsorbent dose for conducting experiments. Adsorbent doses were applied to the 100 ml of 200 μgL^{-1} arsenic [As(III) and As(V)] spiked solutions in 250 ml conical flask. Separate conical flasks were used for each adsorbent dose with each arsenic species and with each agitation speed. Conical flasks were placed in incubator shaker at different agitation speed (50, 100, 125, 150, 175, 200, 225 and 250 rpm) at 25^0C temperature for 180 min to reach equilibrium concentration. Thereafter the solution and adsorbents were separated using Whatman filter paper no. 42. Treatment, collection and storage of the effluent were accomplished as discussed in batch sorption study. The experimental data were plotted in excel spreadsheet to assess the effect of agitation speed on arsenic sorption.

3.4.2.2 Effect of pH on arsenic sorption

Adsorption capacity of red soil, sand, oxidized iron scrap & murum were analyzed at different pH in the range of 0.94 to 12.37. Effect of pH on these adsorbent (red soil, sand, NOIS and murum) were carried out at an initial arsenic concentration [both As(III) and As(V)] of 200 μgL^{-1} with specific adsorbent mass at 25ºC for 180 min equilibrium time. The dose of NOIS, sand, red and murum are 5, 20, 10 and $20gL^{-1}$ respectively. Desired pH of the arsenic spiked solution were adjusted using 1N NaOH and 1N HCl as per requirement. Arsenic spiked solutions were taken in 250 ml conical flasks and appropriate amount of adsorbent was added to the solution and placed in incubator shaker. Thereafter, 50 ml supernatant were filtered with Whatman filter paper no. 42 and preserved with 1ml 1:1 HCl for arsenic analysis.

3.4.2.3 Batch sorption studies

Batch sorption studies were carried out using fixed amount of adsorbent in appropriate amount of arsenic spiked solution at constant strength and temperature for both type of arsenic species [As(III) and As(V)]. In order to observe the effect of surface area on adsorption, different size of sand NOIS and murum were used for batch sorption study.

Batch sorption studies were performed at 25ºC in an incubator shaker at an agitation speed of 200 rpm., Fixed amount of adsorbent (1 g red soil, 0.5 g NOIS, 2 g sand and 2 g murum) was added to each of the 100 ml of 200 μgL^{-1} of arsenic spiked solution in 250 ml conical flask to find out the effect of contact time. Each of the flasks was covered with aluminum foil to avoid any possible reaction due to exposure. Before starting of the experiments, pH of the arsenic spiked solutions [both As(III) and As(V)] were adjusted to 7 using 0.1N NaOH and 0.1N HCl. Strength of the arsenic was measured for each of the experiments. Conical flasks where placed in incubator shaker for the desire contact time of 1, 2.5, 5, 10, 15, 20, 30, 45, 60, 90, 120, 150, 360, 480 and 720 minutes. Subsequently the supernatant was immediately filtered through Whatman filter paper no. 42 using high pressure filtration device. 50 ml of filtered sample were preserved with 1ml of 1:1 HCl to assess arsenic concentration in the solution. Separate conical flasks were used for each individual contact time. Arsenic concentrations of the filtered samples were assayed for arsenic after completion of the experiments. For sand, batch sorption studies were carried out in same manner excepting that dose was taken as 2 g since its adsorption capacity is lower in rate than that with other materials.

3.4.2.4 Effect of temperature

Sorption kinetics of arsenic [As(III) and As(V)] onto the selected adsorbents (red soil, NOIS, sand and murum) were investigated as a function of temperature. The experiments were conducted at different temperatures of 10, 25, 40 and 55ºC at constant adsorbent dose (sand: 2g, NOIS: 0.5g, red soil: 1g and murum: 2g) with an initial concentration of 200 $\mu g\ g^{-1}$. Initially 100 ml of arsenic spiked solutions were kept in 250

ml of conical flasks and placed in the incubator shaker for 1h so as to reach desired constant temperature. Thereafter, constant dose of adsorbents were added to the arsenic solutions and the sorption kinetic experiments were performed. Data obtained from experiments plotted in excel spreadsheet to analyze the effect of the temperature on arsenic sorption.

3.4.2.5 Effect of adsorption dose

Effect of adsorption dose on arsenic sorption was carried out for four different type of adsorbent (for red soil, sand, NOIS and murum). These experiments were conducted in the same conditions as mentioned in the earlier part in kinetic sorption study. This study was conducted at 25ºC using 100 ml arsenic content (200 µg L^{-1}) water and different amount adsorbent (0, 0.5, 1, 1.5, 2, 3, 4 and 5 g) in 250 ml conical flasks. Conical flasks were placed in incubator shaker at 200 rpm for 180 minutes to reach equilibrium time. Supernatants were filtered through Whatman filter paper no. 42 and preserved in a similar manner as in the case of batch sorption study. Arsenic concentrations of the all generated samples were analyzed in AAS after experiments were completed.

3.4.2.6 Effect of initial arsenic concentration

Effects of initial arsenic concentration were investigated for NOIS, sand, red soil and murum by varying the initial arsenic strength (100, 200, 300 and 500 µg L^{-1}) for both As(III) and As(V) species at ambient temperature (25^0C) and 7 pH. 100 ml appropriate strength of arsenic spiked solution was taken in a 250 ml conical flask and then desired amount of adsorbent (red soil:1g, NOIS: 0.5g, sand: 2g and murum: 2g) was applied to that solution. The mixed solutions were placed in an incubator shaker for 3 h to reach the equilibrium. Thereafter the supernatant were separated using Whatman filter paper no. 42 and stored in proper way to assess the arsenic content in the solution. Detailed batch experimental conditions used for arsenic sorption onto the surface of the adsorbents are presented in Table 3.4.

Table 3.4. Experimental design of batch studies for removal of As(III) and As(V) by NOIS, sand, red soil and murum.

Experiments	Variable parameters	Arsenic species	Adsorbent	Control parameters						
				Adsorbent dose (g L^{-1})	Agitation speed (rpm)	Initial pH	Initial As conc. (µg L^{-1})	Volume (ml)	Temp (^{0}C)	Contact time (min)
Variable agitation speed	Agitation Speed: 50, 100, 125, 150, 175, 200, 225 and 250 rpm	As(III)	NOIS	5	-	7	200	100	25±1	180
			Sand	20						
		As(V)	Red soil	10						
			Murum	20						
Variable of pH	pH: 0.94, 2.07, 3.57, 5.05, 6.47, 7.11, 8.6, 10.14, 1.45 and 12.3	As(III)	NOIS	5	200	-	200	100	25±1	180
			Sand	20						
		As(V)	red soil	10						
			Murum	20						
Variable contact time	Contact time: 1, 2.5, 5, 10, 15, 20, 30, 45, 60, 90, 120, 150, 360, 480 and 720 min	As(III)	NOIS	5	200	7	200	100	25±1	-
			Sand	20						
		As(V)	red soil	10						
			Murum	20						
Variable temperature	Temperature: 10, 25, 40 and 550C	As(III)	NOIS	5	200	7	200	100	-	0-720
			Sand	20						
		As(V)	red soil	10						
			Murum	20						
Variable adsorbent dose	Adsorbent dose: 0, 5, 10, 15, 20, 30, 40 and 50	As(III)	NOIS	-	200	7	200	100	25±1	180
			Sand	-						
		As(V)	red soil	-						
			Murum	-						
Variable initial arsenic concentration	Initial As conc.: 100, 200, 300 and 500 µg L-1	As(III)	NOIS	5	200	7	-	100	25±1	180
			Sand	20						
		As(V)	red soil	10						
			Murum	20						

3.4.2.7 Effects of coexisting ions

Common ion effects *i.e.* calcium (Ca^{2+}), magnesium (Mg^{2+}), ferrous iron (Fe^{2+}), phosphate (PO_4^{3-}), sulfate (SO_4^{2-}) and alkalinity (HCO_3^-) during As(III) and As(V) adsorption onto the adsorbents (sand, NOIS, red soil and murum) were investigated. The experimental protocol of co-existing ion effects are illustrated in Table3.5.

Table 3.5. Experimental protocol for estimation the effect of co-existing ions on arsenic sorption onto NOIS, sand, red soil and murum.

Co-existing Ions	Ionic Strength	Arsenic species	Arsenic Strength (µM)	Adsorbent	Adsorbent dose ($g\ L^{-1}$)
Calcium	0, 0.5, 1, 2, 3, 4 and 5 mM	As(III)	10	NOIS	5
				Sand	20
		As(V)		Red soil	10
				Murum	20
Magnesium	0, 1, 2, 3, 4, 6, 8 and 10 mM	As(III)	10	NOIS	5
				Sand	20
		As(V)		red soil	10
				Murum	20
Ferrous iron	0, 20, 50, 100, 150, 200, 250, 300, 400, 500, 600 and 800 µM	As(III)	10	NOIS	5
				Sand	20
		As(V)		red soil	10
				Murum	20
Phosphate	0, 1, 5, 10, 25, 50, 100, 150, 200 and 500µM	As(III)	10	NOIS	5
				Sand	20
		As(V)		red soil	10
				Murum	20
Sulfate	0, 10, 20, 50, 100, 150 and 200 µM	As(III)	10	NOIS	5
				Sand	20
		As(V)		red soil	10
				Murum	20
Alkalinity	0, 1, 2, 4, 6, 8, 10, 12, 14 and 16 mM	As(III)	10	NOIS	5
				Sand	20
		As(V)		red soil	10
				Murum	20

Note: Equilibrium contact time = 180 min, temperature= 25±1^{0}C, agitation speed = 200 rpm, volume of arsenic spiked solution = 100 ml.

These experiments were performed in 250 ml conical flask containing 50 ml As(III) or As(V) solution and 1 g adsorbent each case. 10 µM arsenic [As(III) or As(V)] concentrated solution was used with different molar ratio of added ion. The experiments

were conducted with different molar concentration to estimate the effects of coexisting ions. For each molar solution separate conical flask were used. pH level of the solutions was adjusted at neutral except for ferrous iron. pH value of the solutions containing ferrous iron was kept below 2 to avoid the conversion of Fe^{2+} to Fe^{3+}. Conical flasks were placed in incubator shaker at 200 rpm at 25ºC for 3hrs to reach at equilibrium. Supernatants were filtered through Whatman filter paper no. 42 and duly preserved for analysis.

To verify the results of all the batch experiments, duplicate experiments of each set were conducted. The mean values of the experimental data were used to interpret the experimental results. The initial and final pH of the samples had been recorded whenever required.

3.4.3 Continuous mode laboratory scale column experimental procedures

Although batch experimental adsorption studies provide useful data and parameters on the application of adsorbents for the removal of arsenic, column experiments are also necessary to provide practical operational information with respect to the adsorption of constituents with the use of a particular adsorbent (Eckenfelder, 2000).

In order to evaluate the behavior of NOIS, sand, red soil and murum for adsorption of arsenic in continuous mode, a series of column studies were performed. The experiments were carried out to investigate impact of bed depths (or heights), flow rates and initial arsenic concentrations on arsenic uptake in continuous mode column adsorption studies. All of the columns were operated in down-flow mode. In small-scale column tests, influent and effluent concentrations, column bed depths, amount of adsorbent, column diameters, influent flow rates, time to adsorbent exhaustion are all important parameters which can be selected or monitored, and subsequently applied in the determination of suitable influent concentrations and flow rates for the columns, and to estimate scale-up requirements (Chenxi, 2008). Column diameter, height and flow rate should be select in such a way that channelization, wall and axial dispersion effects can be minimize. LeVan and Vermeulen (1984) reported that to avoid channeling, the ratio of

bed diameter to the mean particle diameter should me greater than 20. On the other hand, Carberry (1976) suggested that in order to avoid radial temperature gradients, the ratio of bed diameter to particle diameter should be less than 5 or 6. To minimize possible wall and axial dispersion effects in fixed-bed columns, Zhou et al. (2004) recommended that the bed length to particle diameter ratio be greater than 20. The influent hydraulic loading or flow rate is one of the most important parameters in continuous mode study. If the flow rate is too high, useful breakthrough curves can be difficult to obtain. The lower the influent flow rate, the longer the adsorbent bed service time. Crittenden (1991) recommended selecting lower velocity in the small column so that the effect of dispersion can not dominate over other mass transport processes.

In the present study, a 2.5 cm ID column is used, so that the volume of water required for the experiments can be reduced significantly. The ratio of internal diameter of column to the mean particles diameter for NOIS, sand, murum and red soil are 31, 38, 15 and 1200 respectively, thus channelization, wall and axial dispersion effects for all adsorbents are negligible. All of column experiments were performed in a transparent perspex tube with an internal diameter (ID) of 2.5 cm and length of 55 cm. One funnel was fitted in the bottom of the column using sealing paste and silicon pipe was connected at the end of the funnel for easy drainage of the effluent. Using pinchcock the effluent flow was controlled. The column was made airtight using rubber cork at the top of the tube. The inlet pipe was connected with the column through the rubber cork that will allow passing the influent without any air passing through it. A twenty liters volume of aspirator bottle was used as storage reservoir for the arsenic spiked solution to conduct the column experiments. One silicon pipe was used to carry the influent to the column from the bottom of the container through the peristaltic pump at a desired flow rate. Optimum quantity of glass wool was packed at the bottom of the column to prevent escaping out of the adsorbent media from the column and on the top to distribute the feed water uniformly. A schematic diagram of the column setup is shown in Fig. 3.6. Fig. 3.7 is showing the complete setup of a column for NOIS adsorbent. All columns were initially filled with distilled water before packing adsorbent media to prevent the entrapment of air during column preparation. Wet adsorbent media was the transferred within the column slowly and allowed to settle down at the bottom.

.

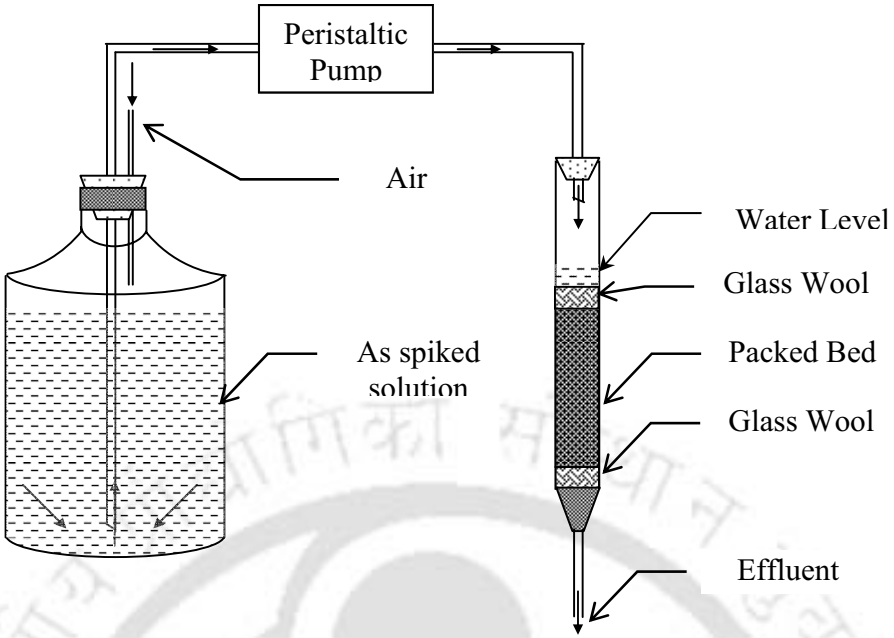

Fig. 3.6. Schematic diagram of the column experimental setup.

Fig. 3.7. Column experimental setup for NOIS adsorbent (Flow rate: 10 ml min^{-1}, Bed depth: 45 cm).

The process was continued until the desire depth was achieved. The mass of the added adsorbent media was estimated from the bulk density and the volume of adsorbent applied to the column. Distilled water was allowed to pass through the column until such time all the adsorbent particles settled down. Meanwhile final depth of the packed bed was also measured. Constant water depth of 5 cm was maintained above the packed bed. Thereafter, the rubber cork was fixed at top of the column to make the column air tight. The flow rate of the peristaltic pump was calibrated using distilled water prior to attaching the columns. After connecting the pump to the column, distilled water was passed through the packed bed for 30 minutes to ensure the flow rate as well as to allow additional settlement of adsorbent media. The volume of the distilled water present in the pipe and the column was deducted from the estimated effluent quantity.

The column experiments were performed for different flow rates and also with different bed depths for the selected adsorbents. 200 µg L^{-1} concentration of As(III) as well as As(V) spiked solutions were prepared with distilled water. The detailed experimental operating conditions applied in the continuous mode laboratory scale column studies are summarized in Table 3.6.

Table 3.6. Experimental conditions applied to the continuous mode laboratory scale columns for As(III) and As(V) species sorption onto NOIS, sand, red soil and murum.

Experiments	Adsorbent	Arsenic species	Bed depth (cm)	Flow rate (ml min^{-1})	Initial As conc. (µg L^{-1})
Effect of bed depth	NOIS Sand Red soil Murum	As(III) As(V)	7.5, 15, 30, 45	5	200
Effect of flow rate	NOIS Sand Red soil Murum	As(III) As(V)	45	5, 10, 15	200
Effect of initial As conc.	NOIS Sand Red soil Murum	As(III) As(V)	30	5	100, 200, 300

3.4.4 Co-precipitation test methodology

Co-precipitation of arsenic along with ferric iron was estimated in the laboratory conditions in a 2 L volume of plastic beaker (made of Borosil).Experiments were conducted with three different molar ratios (1:50, 1:100 and 1:200) of arsenic and iron. The kinetic of arsenic co-precipitation was evaluated using 1:100 ratio (molar ratio) of arsenic and iron. Initially the beaker was filled with some quantity of distilled water and required amount of arsenic stock solution to produce 4 µM As solution. Stock ferrous iron solution was added in the solution already present in the beaker and final volume was adjusted to 1 L using distilled water. pH of the solution was adjusted to 7 using 0.1N HNO_3 acid. The solution was continuously mixed using mechanical stirrer. Initially the mixing was rapid for proper mixing then the mixing was made gentle to form the ferric flocs and adsorb arsenic onto the same. At different time interval (1, 5, 15, 30, 45, 60, 90, 120 and 150 min) 25 ml of sample was drawn from the surface of the solution and immediately filtered through Whatman filter paper no 42. All the samples were acidified to pH below 2 and stored to assess arsenic and iron concentration. During the experiment, pH of the solution was monitored. Co-precipitation tests were conducted for both As(III) and As(V) species and for different molar ratio of arsenic and iron. The batch studies for 1:50 and 1:200 ratios of iron and arsenic were conducted at 120 minutes of equilibrium time. Before conducting the experiment, the dissolve oxygen level was maximized using aeration technique.

3.4.5 Desorption and regeneration studies

To recover the adsorbed arsenic and regenerate the adsorbents, desorption and regeneration experiments were carried out. Batch experiments were conducted to recover both As(III) and As(V) ions from the adsorbents (NOIS, sand, red soil and murum) using different desorbing agents such as NaOH, HCl, HNO_3 and $NaHCO_3$. To perform desorption test, first the adsorbate [both As(III) and As(V)] was allowed to adsorb onto the adsorbents at predetermined conditions and then desorption test was carried out. The spent adsorbents were used for desorption and regeneration test. To conduct batch

adsorption study, 1 g of adsorbent was applied into 100 ml of 200 µg L^{-1} arsenic [As(III) or As(V)] spiked solution in 100 ml beaker. The beaker was placed in an incubator shaker in 200 rpm shaking speed at 25^0C temperature for 4 hours to attain equilibrium. The mixer was placed in centrifuge at 8000 rpm for 5 min to separate the adsorbent from the solution. Filtered sample was stored to assess arsenic remains in the solution. Spent adsorbent was washed with distilled water for 15 min. 2 bed volume of desorbing agent with predetermined strength was applied to the spent adsorbent in beaker and placed it in shaker at 200 rpm for 1 hour. One blank sample was also taken as a control measure to experiment. Supernatant was filtered through Whatman filter paper no. 42 and assayed for arsenic. To observe the effect and optimize the strength, different dose (0.1N, 0.5N, 1N and 6N) of desorbing agent were examined. Kinetics of As(III) and As(V) desorption were performed for the desire contact time of 5, 10, 15, 20, 30, 45, 60, 90, 120 min using 0.5N NaOH solution. Desorption experiments also conducted for column spent adsorbents. 1 g air dried spent and saturated adsorbents of the selected column (45 cm height and 10 ml min^{-1} flow rate) were used for desorption study. Desorption experiments for column were simply opposite to that of adsorption experiments. The elution tests for column (45 cm height and 5 ml min^{-1} flow rate) were performed using 0.5N NaOH solution at 18 ml min^{-1} in reverse direction than that carried in the adsorption test. The arsenic concentrations in effluent were recorded with time. The adsorbents after desorption were regenerated using 0.5N HCl and washed with distilled water until the pH 7 is achieved in the solution. Adsorbents were allowed to dry at room temperature and kept for reuse in arsenic contaminated water treatment.

3.5 Development of porous media

The removal efficiency of the adsorbents is dependent on the flow rate of the filter. Since groundwater of Assam contains lots of iron that make the water turbid. For removal of turbidity from groundwater it is necessary to develop one suitable filtration unit. Apart from turbidity control the filtration unit should be capable to maintain steady flow rate without any hindrance during its operation. The concept of the preparation of the porous device and its preparation procedure is discussed below.

3.5.1 Preparation methodology of circular porous disk (CPD)

Before developing porous filter an attempt was made to develop circular porous disk (CPD) in the laboratory scale. Porous disks were developed on the basic concept that wheat husk is a good burning material. If it is added with a binder fired, the end product will generate enough voids/pores within it due to burning of husks. Circular disks were prepared using a mixture of wheat husk and red soil. The disks were burned at high temperature to complete burning of wheat husk. The development mechanism of the porous disk as well as porous media is discussed in the present chapter.

Wheat husk, which is readily available in the local market, was used for preparation of this porous media. Wheat husk passing through 2 mm sieve was used for the experimental purpose. Wheat husks with different quantities were mixed with fixed volume of 200 ml red soil and appropriate quantity of water is added to the mixer to prepare workable paste. This paste was moulded within a circular ring of 4.5 cm ϕ x 1 cm thick. Circular disks were allowed to dry in normal room temperature for 7 days. It was found that the disk shrank during air-drying when diameter reduced to 4.2 cm from 4.5 cm. The air-dried disks were burned in muffle furnace at 540^0 C for 6 hours. It was found that 4 hour burning time is sufficient to burn the disks completely. The wheat husk burned completely at 540^0 C temperature and left voids (pores) inside the disk. These voids inside the disk made the disk porous. These porous disks were ready for batch and column study to optimize its arsenic removal efficiency, turbidity removal efficiency and loading rate. Fig. 3.8 is showing the picture of circular porous disk.

Fig. 3.8. Circular porous disk (CPD) made of red soil with 1 cm depth and approx 4.2cm diameter.

3.5.2 Batch experiments procedures of CPD

To optimize the porosity and arsenic sorption capacity, the disks were prepared using different quantity (0, 5, 10, 15, 20, 30, 40, 50, 60, 70, 80, 90, 100, 110, 120, 130 and 140 ml) of wheat husk with fixed volume of red soil (200 ml). The prepared disks were used for experimental purpose.

Batch sorption studies were conducted using 200 µg L^{-1} of 100 ml arsenic [both As(III) and As(V)] spiked solution for 6 hours at 25^0 C. Each of the disks was placed in 250 ml of Borosil beaker separately with 100 ml of arsenic spiked solution was added onto the same. The beakers were placed in incubator shaker for 6 hours to reach at equilibrium. Supernatants filtered through Whatman filter paper no. 42, duly preserved with Conc. HCl at pH<2 and stored for arsenic analysis.

Batch kinetic and equilibrium studies were conducted using the optimized CPD. The ratio of wheat husk and red soil was maintained 0.55: 1 in optimized CPD. To conduct the batch experiments, the CPDs were crashed into small pieces to meet needed quantity of adsorbent. 475 µm -2mm size of crushed particle is used in the present study.

The effect of pH on arsenic sorption was conducted at different pH (0.78, 1.97, 3.54, 5.13, 6.86, 7.52, 8.92, 10.16 and 12.08) with both As(III) and As(V) arsenic species. 100 ml of 200 µg L^{-1} arsenic spiked solutions with 2.5 g adsorbent were placed in incubator shaker at 200 rpm and 25^0C for 120 minute equilibrium time. pH of the solution was adjusted using 0.1N HCl and 0.1N NaOH solution. Adsorbents were allowed to adsorbed arsenic at adjusted pH for the equilibrium time. Effluents were separated from the mixtures using Whatman filter paper no. 42 and stored it (lowering the pH below 2 using 1:1HCl solution) for arsenic analysis.

Kinetic study was conducted at different time interval (0, 2.5, 5, 10, 20, 30, 60, 90 and 120 min) at 200 rpm and 25^0C temperature. 100 ml of 200 µg L^{-1} arsenic [As(III) or As(V)] spiked solutions were taken in 250 ml beaker. 2.5 g of adsorbents were applied to the solution and placed in the shaker for the desired time interval. Supernatants were separated using Whatman filter paper no. 42 preserving in the same manner as stated earlier and stored for arsenic analysis.

Equilibrium studies were conducted for both arsenic [As(III) and As(V)] species using 100 ml of arsenic spiked solution at 200 rpm and at 25^0C temperature. Variable dose of adsorbent (5, 15, 20, 25, 30, 50 and 100 g L^{-1}) were applied to the fixed strength of (200 µg L^{-1}) of arsenic spiked solution for 120 min to reach equilibrium concentration. Samples were filtered, preserved and stored as done in case earlier studies for arsenic analysis.

3.5.3 Column experiments procedures of CPD

To optimize the arsenic removal efficiency, filtration rate and loading rate column studies were carried out. To conduct the column studies one mechanical device was designed using Teflon tube. The device consists of two chambers as shown in Fig. 3.9.

Fig. 3.9. Performance testing of the circular porous disk (water head= 40 cm).

CPD was placed inside the lower chamber followed by fixing the upper chamber above the lower chamber. In both the chambers, 3.5 cm diameter of free passage was available.

The circular disk placed inside the device and this provides the only passage of water. Constant 40 cm of water head was maintained for the estimation of loading rate. For each disk, the water was allowed to pass for 1 hour and the effluent volume is measured. The effective area is calculated using area of the pathway (3.5 cm diameter) of the device. 100 NTU standard solutions were used to estimate the turbidity removal efficiency of different disks. Turbid solution was passed through the porous media with a constant 40 cm water head. Nephelometric Turbidity Unit was used to estimate the turbidity present in the effluents. Effluents generated from the experiments were analyzed using AAS in VGA mode and experimental data were plotted in Excel spreadsheet.

3.5.4 Porous pot preparation procedures

After optimization of the CPD, an attempt was made to design porous filter with the help of local potter. Initially two porous pots were made to check the practical applicability at field level. The optimum red soil and wheat husk proportion was maintained during the preparation of the pots (1 cm thick and 7.5 cm height). Pots were dried in normal atmospheric temperature and thereafter placed in potter's kiln to burn for two days. Fig. 3.10 is showing the photograph of the prepared porous pot. Burnt pots were examined for loading rate and arsenic adsorption capacity using 200 µg L^{-1} of arsenic spiked solution. Total volume of the effluent was measured and assayed for arsenic concentration.

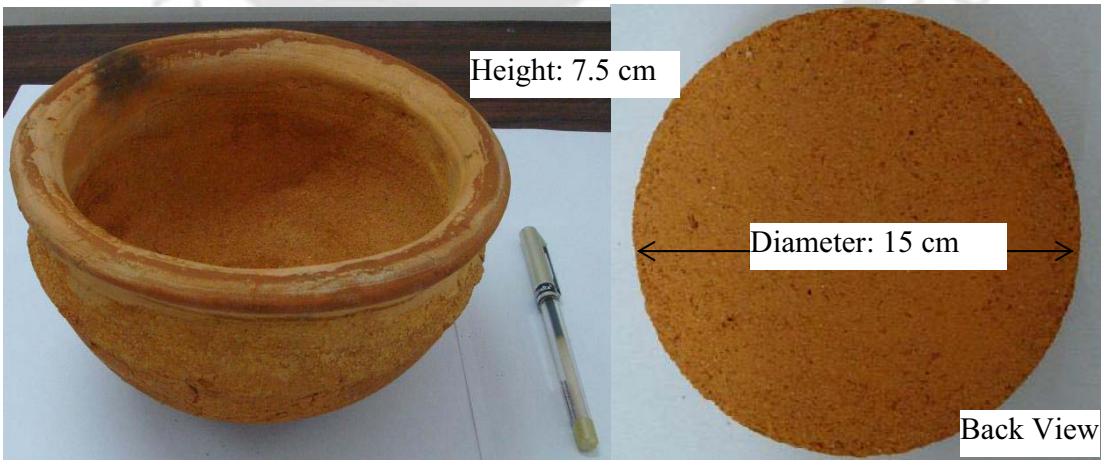

Fig. 3.10. Photograph of prepared porous pot.

Discharge through the porous media is strictly dependent on the water head; the filtration rate decreases with the decrease in water head. So, the discharge was measured at initial stage of the filtration. Initially, the pot was filled with 1 L water and allowed to pass for 30 minutes. Volume of the collected water was measured and discharge rate was calculated. Repetition of the procedure was made for couple of times to get average discharge rate. Inner surface area was measured assuming the pot is spherical in shape.

3.5.5 Porous filter preparation procedure

The arsenic removal porous filter was prepared by the same local potter who prepared the porous pot. Before preparation of the filter, the potter was properly trained. Fig. 3.11 is showing the photographs of the designed filter. This arsenic removal porous filter consists of two chambers. Lower chamber was made of normal white clay to retain the treated arsenic free water. Upper chamber plays the major role on removing arsenic as well as suspend particles from the influent. The porous portion of the filter was made with a thickness of 1 cm, 8 cm height and 29 cm diameter at the top of the porous portion. The upper chamber was made in such a way that the chamber can retain the adsorbent as well as sufficient quantity of water.

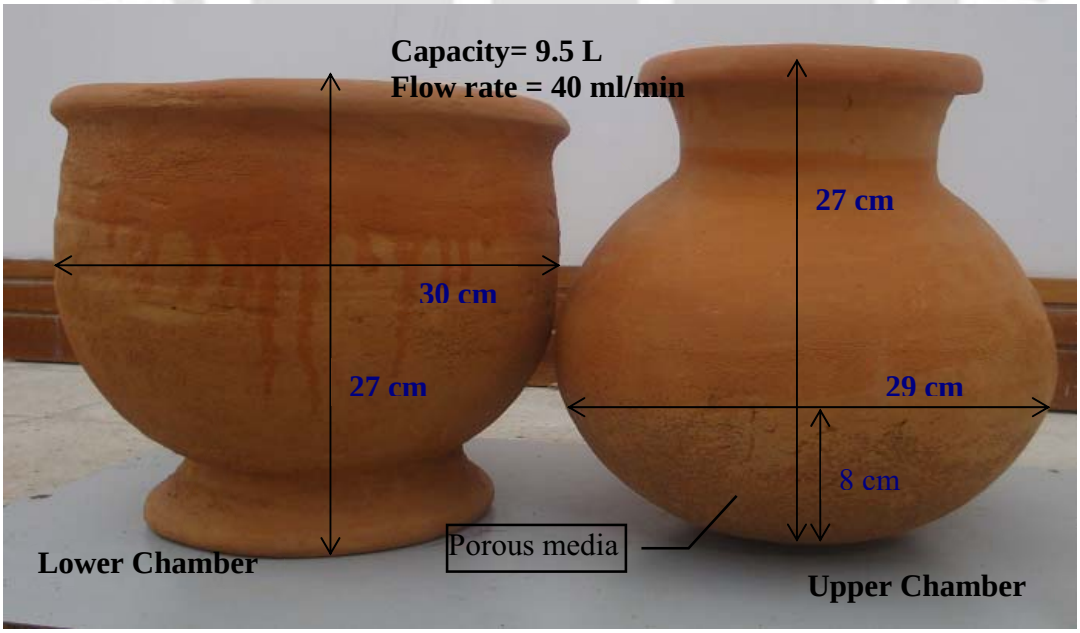

Fig. 3.11. Photograph of arsenic removal filter.

Thus, upper portion of the upper chamber was made non-porous using white clay to increase water retaining capacity. Lower portion of the chamber was made porous using appropriate composition of red soil and wheat husk (1:0.55) so that, loading rate, turbidity removal efficiency and arsenic uptake capacity keep up at optimum level. Both the chamber can contain 9.5 liters of water. The filter was tested for arsenic removal efficiency using synthetic arsenic spiked solution.

3.5.6 Arsenic removal filter (ARF) test procedure

Before estimating arsenic sorption capacity, loading of the filter was examined. Prior to actual experiment upper chamber was completely filled up with distilled water and allowed to empty in natural course. The time interval was noted and volume of the water was measured for both before and after filtration. The procedure was repeated several times so that average loading rate can be calculated. Thereafter, appropriate quantities of adsorbents were placed in the filter. This was repeated to examine loading rate of the filter. No significant deviation in loading rate of the filter was found.

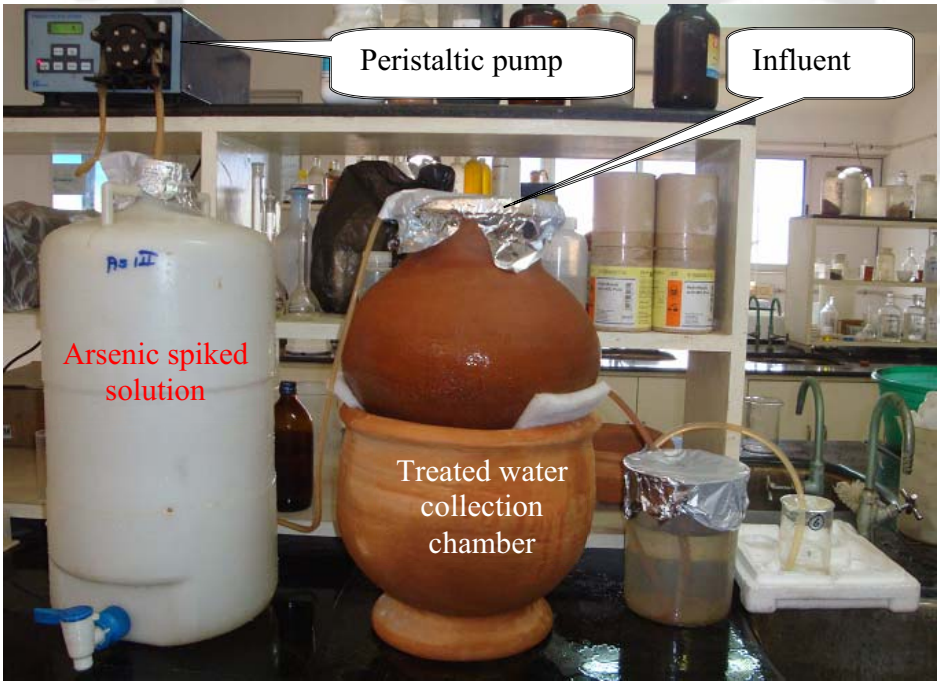

Fig. 3.12. Complete setup of testing of arsenic removal filter (ARF).

Arsenic removal efficiency of the adsorbent (NOIS) along with the filtration media (sand) was examined. Fig. 3.12 is showing the complete setup of testing in arsenic removal filter. The influent flow rate was kept little lower than the filtration rate of the filter. Before placing adsorbents in the upper chamber, both the chambers were duly washed using distilled water. The adsorbent (NOIS) and filtration media (sand) were placed inside the chamber as discussed in chapter 7, prior the testing of arsenic removal capacity of the filter. With constant loading rate arsenic challenged water (200 μg L^{-1}) was allowed to pass through the adsorbents and the filter. The effluent was collected in the lower chamber. The effluent was drained out from the lower chamber to prevent the overflow as shown in Fig. 3.12. The effluent was collected at a fixed time interval and stored it to quantify the arsenic concentration present in effluent.

3.6 Summary

The complete methodology of the present research is discussed in this chapter. This chapter talks about the groundwater sampling location, procedure and analysis technique. The process mechanisms of adsorbents and the experimental methodologies are also discussed in this chapter. The process mechanisms of the materials to prepare as adsorbents are very simple. Initially the collected materials were resized except for sand to achieve homogeneous size and then they were washed thoroughly using tap water and distilled water to remove the impurities. The dried processed materials were used as adsorbents. The batch and column experimental methodologies, co-precipitation test procedure, desorption and regeneration test procedures are illustrated in the present chapter. The preparation methodology of the porous filter is ensuring that it can be easily made by the local potter itself. The main thesis objective is to develop an arsenic removal filter which can be made by the local people. The methodology is ensuring that the arsenic removal filter can be made using locally available materials by the consumers of Brahmaputra floodplains. The outcomes of the experiments are elaborately discussed in the latter chapters.

Chapter 4

Delineation of Unsafe Aquifers in a Major Arsenic Contaminated Area of Madhupur Block in Nalbari District, Assam

4.1 Introduction

The major objective of this chapter is to delineate the unsafe aquifers of the study area (Madhupur block) and to check the severity of arsenic contamination. To meet the goal, the chapter objective aims at preparing of spatial arsenic distribution database and identify the unsafe aquifer zones. The objective of this chapter is also to estimate the correlations of arsenic with other coexisting ions and to determine the seasonal variation of arsenic.

4.2 Spatial distribution of arsenic

To identify the unsafe aquifers in the study area, from 48 different discrete locations, the groundwater samples were collected and analyzed for arsenic determination along with the other water quality parameters. The groundwater collected locations are shows in Fig. 4.1. The groundwater sampling stations of the study area were classified into 5 different groups i.e. less than 10 µg L^{-1}, 10.01-50 µg L^{-1}, 50.01-100 µg L^{-1}, 100.01-200 µgL^{-1}, and greater than 200.01 µg L^{-1} of arsenic concentration. From the Fig. 4.1 it can be seen that in the whole study area is severely affected with arsenic contamination. The arsenic contamination in Baranagar Banekuchi was found within the range of 100µgL^{-1} whereas the groundwaters of other villages contain more than 100 µg L^{-1} arsenic concentration in maximum tubewells. The results indicate that the aquifer of the Madhupur block is highly contaminated with arsenic and unsafe for drinking and cooking purpose.

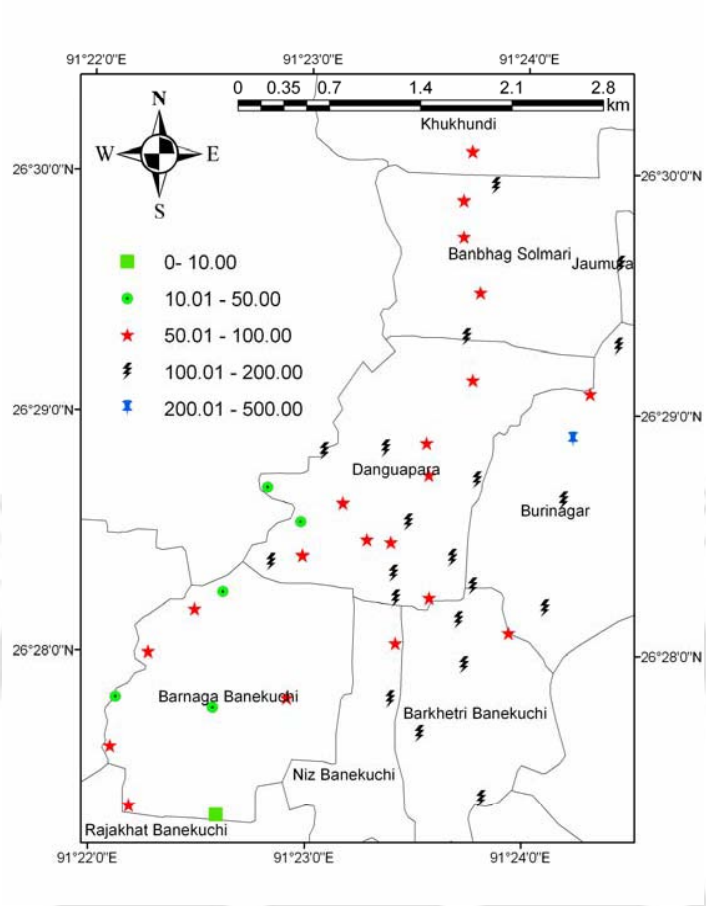

Fig. 4.1. Groundwater sampling stations in the study area (Madhupur block).

4.3 Field parameters variations

The groundwater pH value was found slightly acidic 6.0-7.0 in all sampling. The field measured redox potential (Eh) value ranges from -160 mV to -242 mV indicated moderate to higher reducing condition in the aquifer. Observed EC value (110 – 320 µSc m^{-1}) indicated low to moderate level of dissolve particles present in the groundwaters. Moderate EC value also indicates the presence of saline groundwater.

4.4 Geochemistry and distribution of arsenic in groundwater

The geo-chemical characteristics of the groundwater in the study area were estimated and presented in Table A.2. The results of statistical analysis of the

groundwater quality parameters were depicted in Table 4.1. The pH values of groundwater samples varied from 6.18 to 7.40 with alkalinity values ranging from 110 to 220 mg L^{-1}. The groundwater samples exhibited electrical conductivity (ranging from 140 to 380 µS cm^{-1}); iron (ranging from 3.3 to 19.3 mg L^{-1}); calcium (ranging from 10.4 to 40.8 mg L^{-1}); sodium (ranging from 11.0 to 37.0 mg L^{-1}) and manganese (ranging from 0.1 to 1.2 mg L^{-1}). Relatively low concentrations of nitrate (ranging from 0.4 to 1.4 mg L^{-1}); sulphate (ranging from BDL to 1.8 mg L^{-1}); phosphate (ranging from 0.3 to 1.8 mg L^{-1}) and fluoride (ranging from BDL to 0.5 mg L^{-1}) were found in the groundwater samples. The geochemical parameters and negative ORP (-232 to -135 mV) values indicated that the groundwater of the study area is in reducing condition. As the groundwater is used to be in reducing condition, the observed geochemical data is comparable with the earlier data on the BDP (PHED 1993; BGS and DPHE 2001; Bandyopadhyay 2002; McArthur et al. 2001, 2004; Nath et al., 2008). The arsenic concentration in the study area of Nalbari district is found very high (5.7 to 235.2 ppb) in few samples. In the study area total forty eight numbers of samples was tested, among of them 98% of samples exceeding the permissible limit (10 µg L^{-1}) according to World Health Organization (WHO) guideline, 88% of samples contained arsenic beyond the permissible limit (50 µg L^{-1}) set by Bureau of Indian Standards (IS 10500:1991) and 46% samples contain more than 100 µg L^{-1} of arsenic. Fig. 4.1 is showing the arsenic distribution of the study area. From the study, it is observed that maximum number of tube wells contain higher arsenic contamination. To serve arsenic free water to the common people alternate drinking water source need to be set; otherwise arsenic removal facility need to be installed.

Table 4.1. Statistical analysis of the groundwater quality parameters.

Statistical Parameters	Temp	pH	EC	TDS	As	Fe	Ca	Na	K	Mg	Mn	HCO_3	Cl	F	PO_4	SO_4	NO_3
Minimum	22.2	6.2	140.0	120.0	5.7	3.3	10.4	11.0	1.1	2.1	0.1	80.0	2.5	0.0	0.3	0.0	0.4
Maximum	29.8	7.4	380.0	280.0	235.2	19.3	40.8	37.0	2.2	8.2	1.2	284.0	17.0	0.5	1.8	1.8	1.4
Mean	27.5	6.7	199.9	171.9	101.8	11.4	25.2	24.1	1.5	4.6	0.6	170.3	8.9	0.1	1.1	0.4	1.0
Standard Deviation	1.2	0.2	53.5	37.4	45.9	3.8	8.3	6.5	0.2	1.7	0.3	46.6	4.0	0.1	0.4	0.3	0.3

Note: pH is unit less, the unit of As is µg L^{-1}, Temperature is degree centigrade (^{0}C), EC is µS cm^{-1} and the unit of the other water quality parameters are mg L^{-1}.

4.5 Groundwater geochemistry

The piper diagram, along with the linear diagrams, allows for both the anions as well as the cations compositions to be represented on a single graph. The major ion concentrations of the study area were plotted as percent milliequivalent/L in piper diagram (Chadha, 1999). The plot is used to classify water types and to identify trends in major ion chemistry down-gradient (Pe-Piper, 1982). From Fig.4.2, it can be observed that all of ground water samples are Ca-Na-HCO_3 type. In these, samples the Ca^{2+} and Na^{+} concentrations are relatively higher. Higher concentration of Na^{+} can be attributed to the stronger impact of cation exchange for the monovalent ions in the clayey formation.

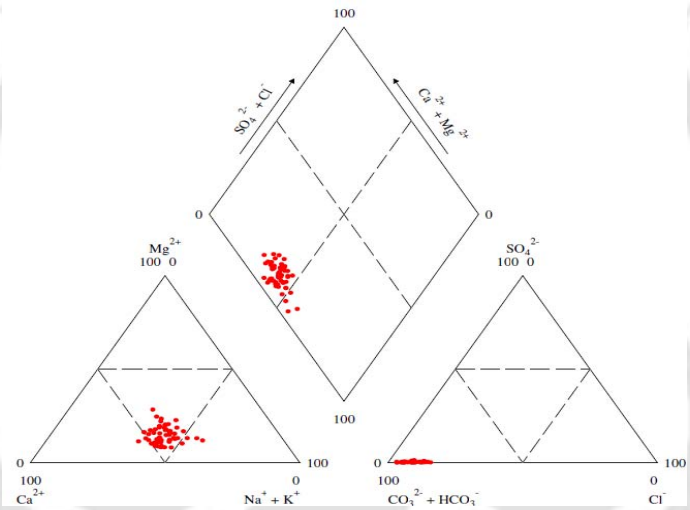

Fig. 4.2. Piper plot with representation of major ions in groundwater samples.

4.6 Correlation of arsenic with co-existing ions

Presence and mobilization of arsenic in the groundwater system is controlled by several co-existing ions. Presence of Ca, Na, K, Fe, PO_4, HCO_3 and SO_4 ions at higher level may elevate the arsenic concentration in the groundwaters. An attempt was made to estimate the correlations of arsenic with other water quality parameters so that the arsenic contamination in the groundwaters of the study area can be understood. In this study, linear regression analysis was applied to develop relationships between arsenic and different water quality parameters (Ca, Na, K, Fe, PO_4, HCO_3 and SO_4). Another value,

the p-value, was estimated to check the correlation between the variables was significant or not (Joarder et al., 2008; Roychowdhury et al., 2002). A p-value > 0.05 is insignificant, a p-value < 0.01 is significant; and a p-value < 0.001 is strongly significant.

4.6.1 Arsenic versus calcium and sodium

From Fig. 4.3, it is observed that the arsenic concentration varies with changes of both calcium (R^2 = 0.4705; p = 7.45E-8) and sodium (R^2 = 0.4119; p = 8.82E-8) concentrations. It can be predicted that leaching of more cations increase the arsenic concentration in groundwater.

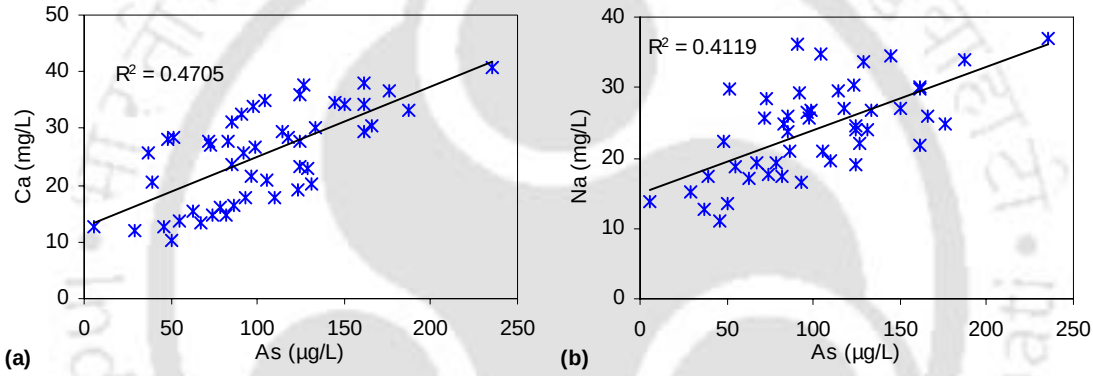

Fig. 4.3. Arsenic (As) versus Calcium (Ca) and Sodium (Na).

4.6.2 Arsenic versus manganese and iron

In Fig. 4.4(a), it is observed that low concentration of manganese is correlating with high levels of arsenic (R^2 = 0.551; p = 1.56E-9). The samples are distributed in linear proportion. Since the water chemistry indicates high reducing conditions, it may be possible that arsenic concentration increase due to buffering of manganese at higher level of redox stages. The results (Fig.4.4(b)) shows a moderate co-relation (R^2 = 0.4402; p = 2.75E-7) of iron with arsenic, which can occur in reducing groundwaters with high CO_3^{2-} and PO_4^{3-} levels, where Fe^{2+} may precipitate as siderite ($FeCO_3$) and vivianite ($Fe_3(PO_4)_2 \cdot 8H_2O$) according to Ahmed et al. (2004).

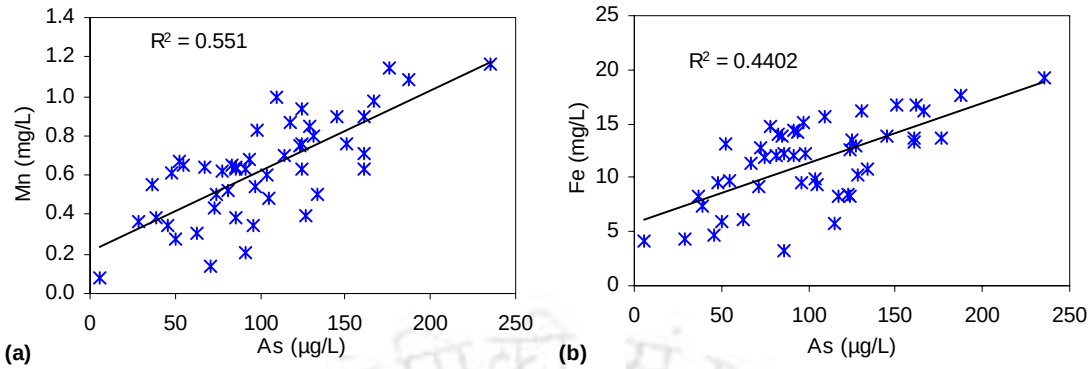

Fig. 4.4. Arsenic (As) versus Manganese (Mn) and Iron (Fe).

4.6.3 Arsenic verses pH

Several studies have shown that desorption of arsenic from sediment could be induced by increasing pH which is indicated in the plot below (Fig.4.5). According to McArthur et al (2004), pH does not contribute significantly to the release of arsenic. It is the reducing conditions in the sediments that lead to the release of arsenic from iron oxy-hydroxides. The reason for lower pH in these soils is probably due to acidic nature of soil.

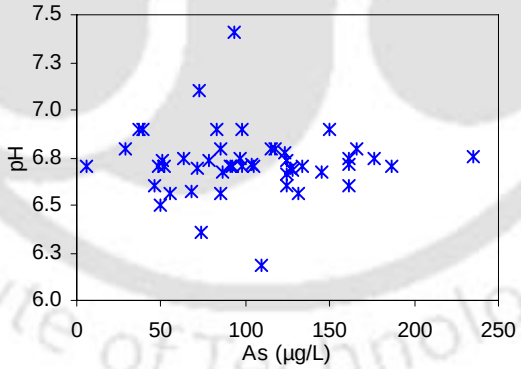

Fig. 4.5. Arsenic (As) versus pH.

4.6.4 Arsenic versus phosphate and bicarbonate

A positive correlation (R^2=0.6245; p = 2.4E-11) between arsenic and bicarbonate (HCO_3) can be seen in the groundwater samples [Fig. 4.6(a)]. The co-relation (R^2=0.4282; p = 4.54E-7) of arsenic and phosphate is shown in Fig. 4.6(b). Phosphate

easily adsorbs arsenic in oxy-anions forms in the presence of Fe, Al and Mn oxides. In reducing conditions, the arsenic and the phosphate desorbs from the oxides, when these ions are dissolve, which might be one reason for higher levels in the soil. As the arsenic and phosphate have similarities in adsorption sites, arsenic could also be replaced by phosphate when higher levels of phosphate are present (Sracek et al., 2002).

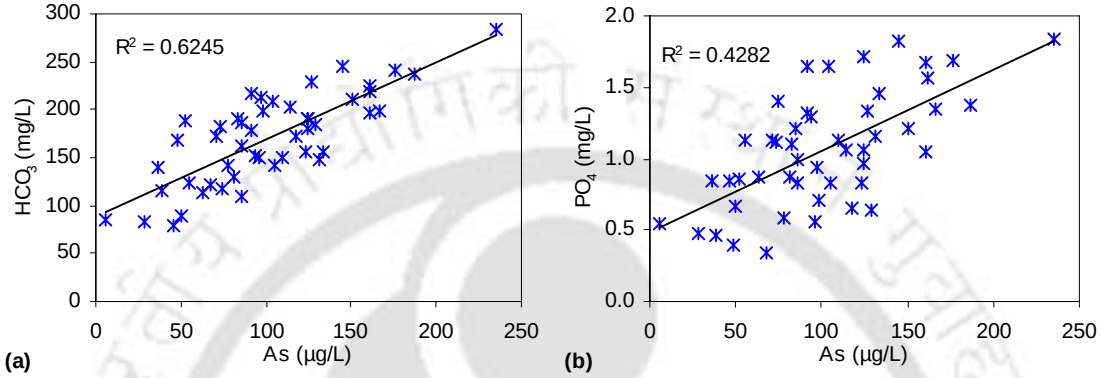

Fig. 4.6. Arsenic (As) versus phosphate (PO_4) and bicarbonate (HCO_3).

From Fig. 4.3-6, it can be seen that Ca, Na, K, As and HCO_3 have good correlations values with each other. TDS values linearly increase with conductivity (correlation value above 0.98). From regression analysis it is found that phosphate has low correlation with other ions. Finally from the geochemical parameters analysis data it is observed that low sulfate concentration with higher level of bicarbonate, which indicates sulfate reduction in the aquifer zone. The high amounts of arsenic and iron in the water also point out towards this redox process. Sulphate reduction usually generates H_2S, some bad smell (smell like rotten egg) was detected during sampling. High amounts of iron can contribute to the formation of FeS, which might reduce the amount of H_2S and therefore also the smell.

4.7 Groundwater characteristics over the different seasons

The groundwater quality parameters along with arsenic were monitors for 18 months at the interval of approximate 3 months. The groundwater samples collections dates were 20/06/2008 for 1st sampling, 18/09/2008 for 2nd sampling, 16/12/2008 for 3rd sampling,

06/03/2009 for 4th sampling, 11/06/2009 for 5th sampling and 06/09/2009 for 6th sampling. Variations of major ion concentrations in groundwater samples of six different phases are plotted in Piper diagram (Fig. 4.7). Plots of major ions on Piper diagram show that all samples from different sampling are cluster near of the centre of the central diamond in every case, which is the region of water of temporary hardness. The graphs also indicate that the groundwaters are Ca^{2+}, Na^{+}, K and HCO_3^{2-} type. Higher concentration of sodium (Na) can be attributed to the stronger impact of cation exchange for the monovalent ions in the clayey formation. The Na^{+} & K concentrations are slightly increased over the time in the groundwaters otherwise; there is no wide variation in major ion concentration during seasonal variation of the study area.

Variations of the all measured ion concentrations in groundwater samples from the six different sampling time are presented in Box and Whisker plots (Fig. 4.8). The box and whisker plot is a convenient way of graphically depicting groups of numerical data through their five-number summaries: the smallest observation (sample minimum), lower quartile (Q1), median (Q2), upper quartile (Q3), and largest observation (sample maximum). The bottom and top portion of the box are always the 25th and 75th percentile (Q1 and Q2) respectively and the band near the middle of the box is always the 50th percentile (the median). And the ends of the plots are representing minimum and maximum value of the dataset (http://en.wikipedia.org). From the graphs it is observed that the groundwaters are containing both Ca^{2+} and Na^{+} ions in same level. The groundwater samples are HCO^{3-} type and the NO_3^{-} ion concentration is low which indicate the reducing environment in the aquifer zone. Mg^{2+} and Mn^{2+} concentration is slightly higher, where as Cl^{-} ion concentration is in the moderate level (mean value $10mgL^{-1}$ approx). Elevated level of SO_4^{2-} and PO_4^{3-} due to microbial degradation of organic matter (BGS and DPHE 2001; Bhattacharya et al. 2006) which indicate dissolution of arsenic in groundwater. Arsenic which was earlier associated with ferric oxides forming a complex goes into the dissolved state which is enhanced in the reducing environment. F^{-} ion concentration is very low which is may be due to dissolution of ions from minerals to the groundwaters.

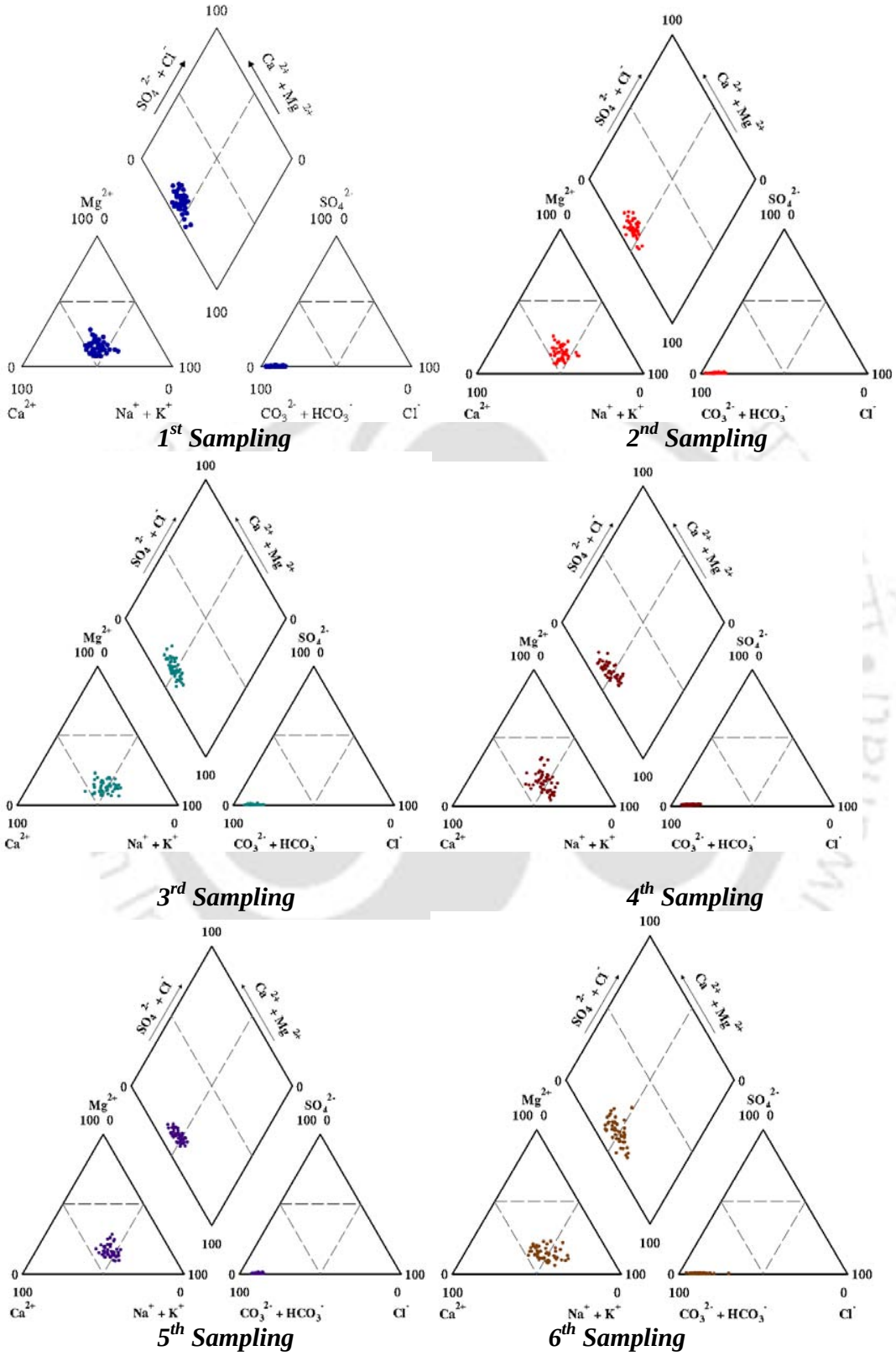

Fig. 4.7. Major ion composition of the groundwater samples plotted in piper diagram.

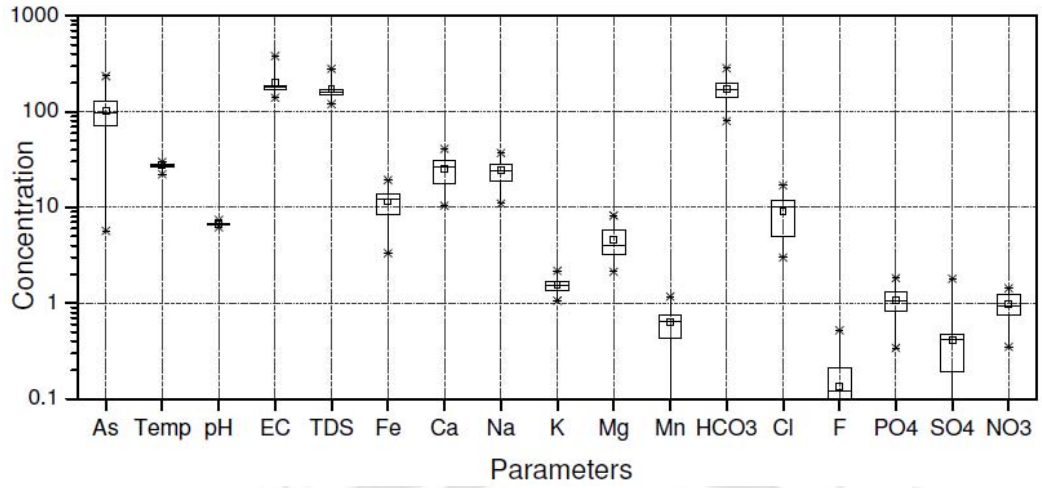

1st Sampling

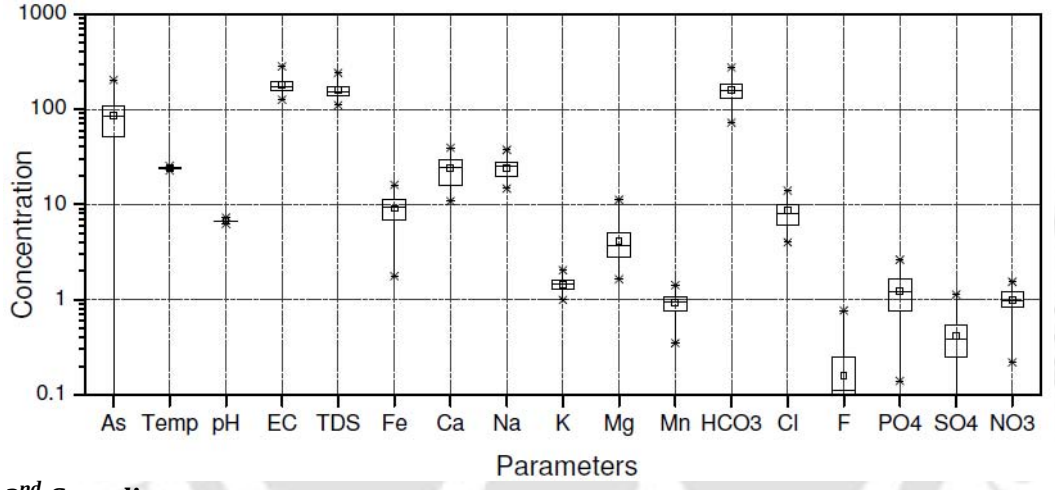

2nd Sampling

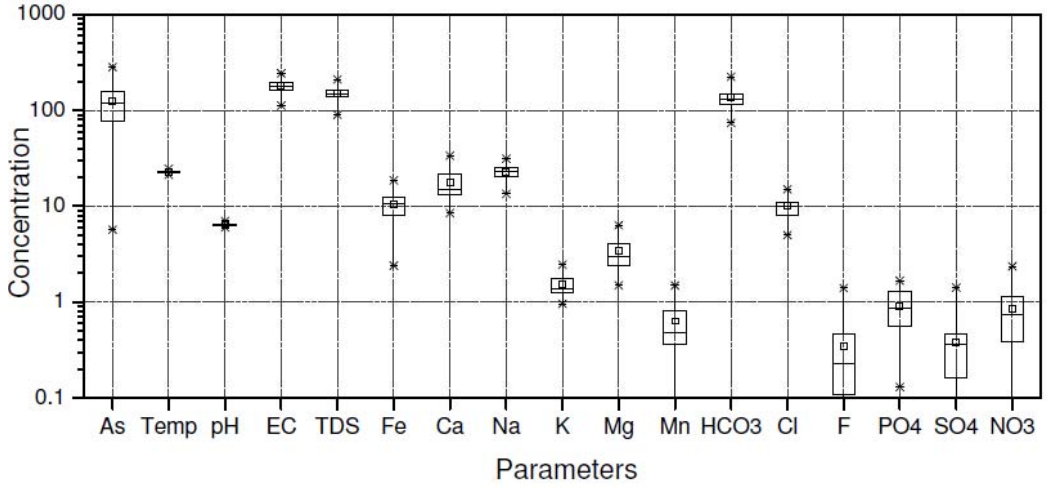

3rd Sampling

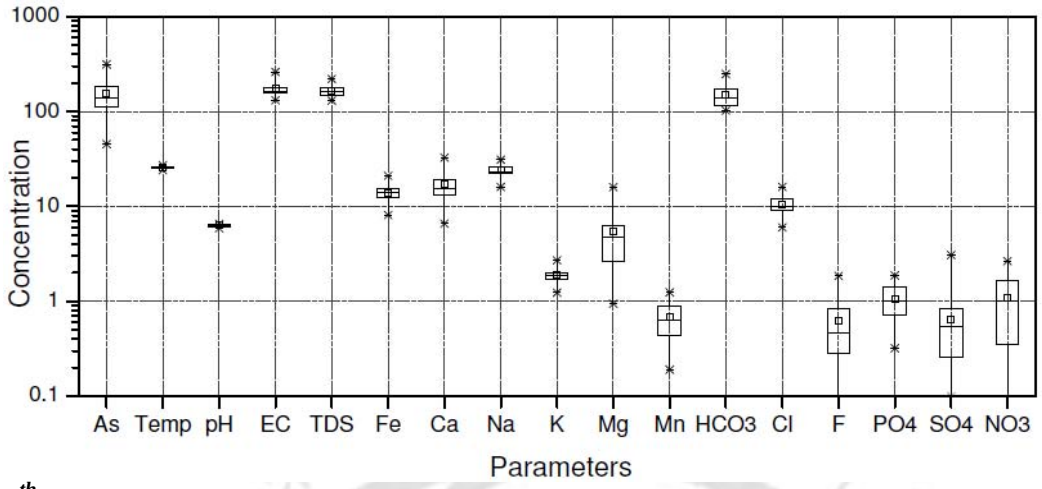

4th Sampling

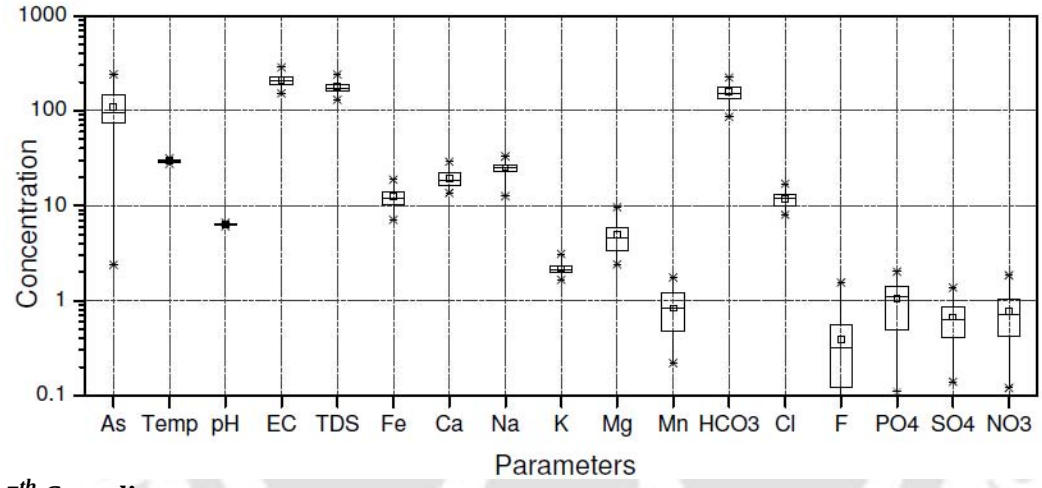

5th Sampling

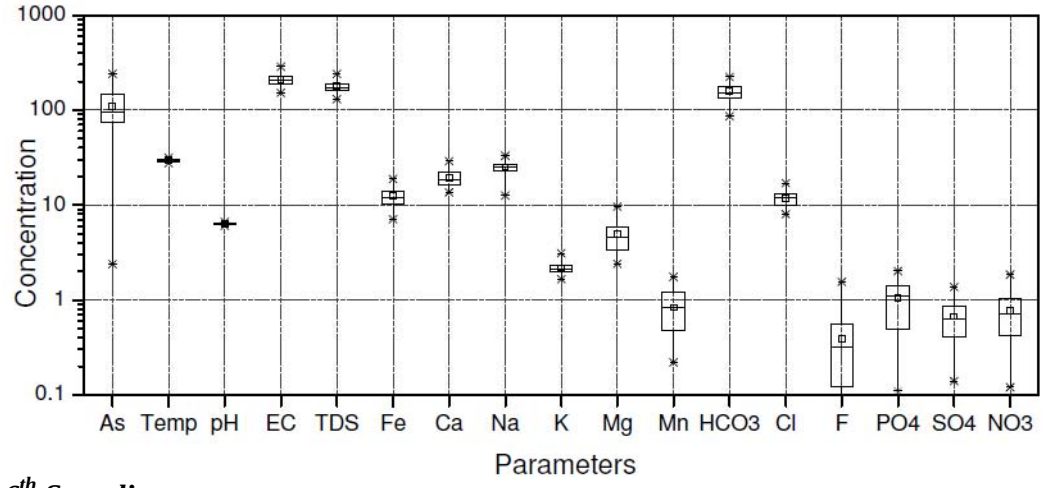

6th Sampling

Fig. 4.8. Box and Whisker plots showing variations of major ion concentrations in the shallow groundwater of the study area.

4.8 Seasonal variation of arsenic

From the plot (Fig. 4.9), we can observe that arsenic concentration in the first sampling ranges from 5.70 to 235.16 µg L^{-1}, while arsenic concentration increases up to 303.36 µg L^{-1} in sixth water sampling. From Table 4.2 and Fig. 4.9, it can be seen that the arsenic concentration of post monsoon is decreased in most of the sampling station. Whereas during winter season the arsenic concentration is quite high and maximum concentration is reached in the month of the March. In the second year sampling the arsenic concentration is increased over the time. The decrease of arsenic in groundwater in the post monsoon period decreases may be due the percolation of the surface water to the groundwater layer as the tube wells are in shallow depth.

Table 4.2. Variations of arsenic concentrations in different sampling.

Well No	Depth (m)	First Sampling	Second Sampling	Third Sampling	Fourth Sampling	Fifth Sampling	Sixth Sampling
		Arsenic (µg L^{-1})					
1	31	81.40	66.77	89.60	132.37	92.35	111.72
2	22	50.27	60.23	96.30	45.26	52.23	68.25
3	26	74.22	91.78	160.50	170.28	98.25	148.13
4	21	124.52	104.88	145.60	166.16	45.30	43.84
5	32	71.30	98.21	204.57	213.54	164.91	214.10
6	39	38.80	48.84	120.90	125.30	81.49	134.00
7	39	91.60	107.13	230.30	240.81	145.08	195.28
8	29	91.30	98.11	155.37	165.00	75.29	165.00
9	21	46.20	26.39	47.84	71.17	44.91	56.25
10	39	105.10	108.83	148.65	312.86	224.16	276.36
11	29	114.70	110.25	145.60	257.11	215.09	243.27
12	21	98.30	80.6	118.19	231.00	149.72	175.06
13	29	72.96	63.04	100.60	103.66	76.56	87.38
14	29	133.40	116.15	165.32	166.68	94.82	131.88
15	29	85.14	69.31	96.36	175.68	143.46	161.25
16	29	117.30	55.92	77.95	85.88	79.36	146.35
17	29	51.97	42.81	65.28	121.68	65.89	115.74
18	31	166.25	143.03	198.65	202.80	176.48	191.97
19	31	150.30	137.9	180.36	183.08	163.84	173.25
20	29	124.22	105.19	143.26	150.63	129.37	135.26
21	39	85.43	70.45	98.45	163.07	91.28	123.88
22	21	235.16	201.95	282.42	288.26	241.26	303.36
23	39	161.00	111.67	148.26	83.19	42.39	47.51
24	29	145.12	119.49	167.28	250.63	154.39	164.11
25	39	126.68	100.33	134.70	135.25	137.09	151.46
26	37	161.44	140.98	201.02	224.56	159.78	160.58
27	29	67.43	52.11	75.50	85.69	34.26	50.19

Well No	Depth (m)	First Sampling	Second Sampling	Third Sampling	Fourth Sampling	Fifth Sampling	Sixth Sampling
		Arsenic (µg L^{-1})					
28	31	128.43	101.49	128.00	146.66	134.05	142.34
29	39	124.11	99.99	134.48	135.84	94.33	146.45
30	30	176.00	140.25	196.35	208.86	186.52	207.62
31	39	96.43	75.19	118.10	127.24	106.38	124.05
32	39	123.23	115.5	174.33	186.54	135.26	165.70
33	39	62.87	49.46	73.10	133.21	55.27	60.16
34	39	130.86	102.26	139.81	142.14	127.37	130.86
35	21	109.74	84.45	115.80	122.24	78.37	106.36
36	42	55.16	40.81	59.36	87.41	75.69	136.63
37	29	78.03	118.26	228.36	237.33	224.62	267.84
38	39	86.00	58.39	76.32	77.44	46.39	56.73
39	39	93.50	42.38	65.60	76.36	67.65	74.99
40	39	97.40	83.88	112.03	138.61	96.26	106.80
41	30	48.10	36.05	56.32	173.56	112.36	156.76
42	29	28.80	25.22	45.38	174.98	156.38	170.01
43	30	36.50	26.44	46.78	135.77	87.37	123.12
44	39	161.00	106.43	105.70	118.23	87.49	102.38
45	29	187.00	125.47	105.70	84.68	71.36	91.18
46	29	104.00	42.25	67.90	111.23	91.74	108.21
47	29	83.10	66.35	100.00	113.56	76.52	81.86
48	29	5.70	0	5.70	82.77	2.38	8.05

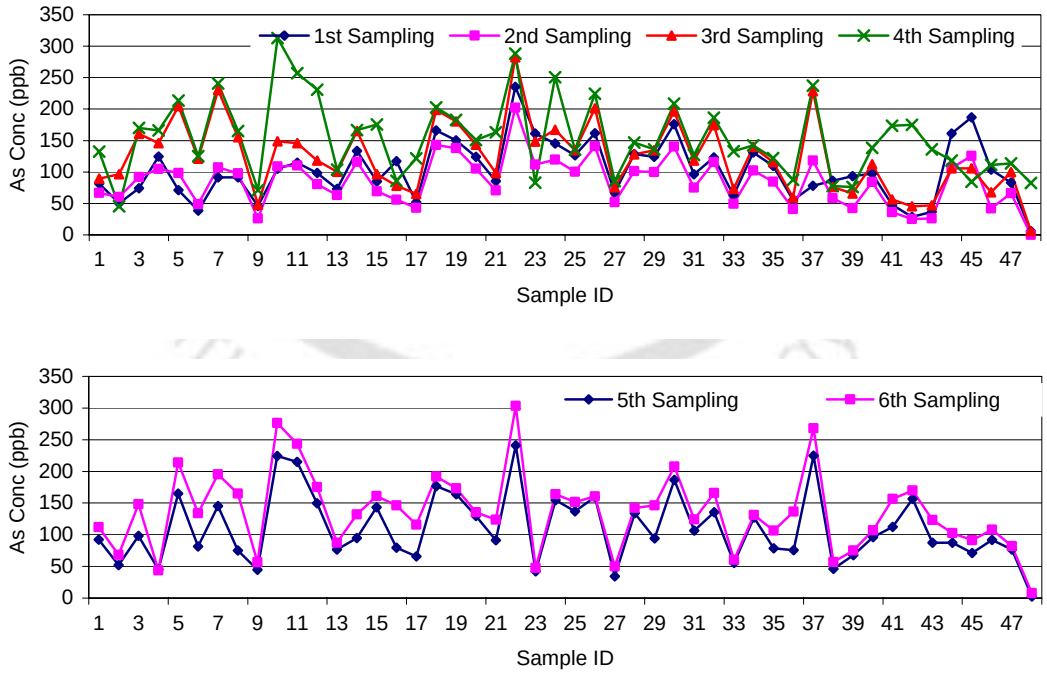

Fig. 4.9. Seasonal variations of arsenic of different locations.

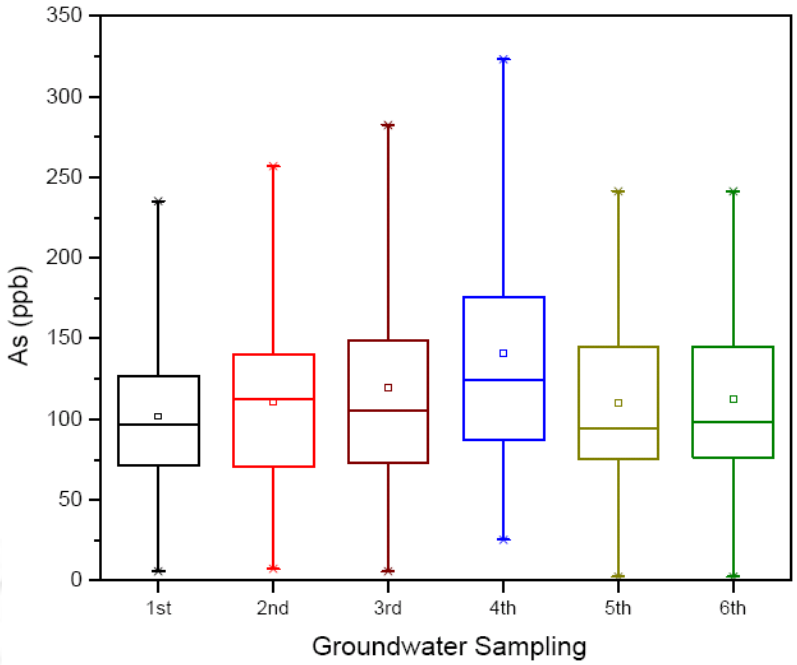

Fig. 4.10. Box and Whisker plots showing variations of arsenic concentrations during different groundwater sampling period.

All of tube wells are within the shallow aquifer zone (depth 21 to 39 m). So, at the monsoon period there is high possibilities of passing of the contaminant of surface water to groundwater. The statistical parameters of arsenic concentration variations over the seasons were shown in Table 4.3 as tabular form and depicted in Fig. 4.10. The mean value of arsenic concentration in the month of September (Fig. 4.10 and Table 4.3) is lower than the other time period of the year. It may be due to dilution of groundwater. From the plots (Fig.4.9-10) is can be concluded that there is some tendency of increase in arsenic concentration during remaining period. This is may be due to excessive use of groundwater which increases pyrite oxidation enhancing the arsenic leaching mechanism.

Table 4.3. Statistical analysis of arsenic concentration variations in different sampling.

Water Sampling	Date	Mean	Median	Standard Deviation	Range	Minimum	Maximum
First	20/06/2008	101.82	96.92	45.87	229.46	5.70	235.16
Second	18/09/2008	84.85	88.12	39.13	201.95	0.00	201.95
Third	16/12/2008	124.04	118.15	56.61	276.72	5.70	282.42
Fourth	06/03/2009	153.46	140.38	60.84	267.60	45.26	312.86
Fifth	11/06/2009	110.27	94.57	54.56	238.88	2.38	241.26
Sixth	06/09/2009	136.32	134.63	62.33	295.31	8.05	303.36

4.9 Summary

The groundwater of the study area (Madhupur block) was severely affected with arsenic contamination. More than 98% of samples contained arsenic above permissible limit according to WHO guideline and 88% of samples contained arsenic beyond the BIS standard (50 µg L^{-1}). Higher concentration level of arsenic indicated the requirement of immediate switching to alternate safe drinking water source. Again spatial distribution database indicated that the groundwater is not safe for drinking as the whole area is affected with arsenic contamination. Thereby, it is necessary to implement arsenic removal technology so that arsenic contaminated water can be treated for drinking purpose. The geochemistry indicated that the groundwaters of study area are Na-Ca-HCO_3 type and contain higher amount of iron which is also need to treat. The arsenic correlating with major cations, iron and anions which indicated that at reducing environment arsenic released in the groundwater system due dissolution of the minerals and oxides present in soil. Seasonal variations of major ions were not significant. During winter season the arsenic concentration was quite high and maximum concentration was reached in the month of the March. There was no significant depression (<10 µg L^{-1}) of arsenic concentration in the groundwater samples observed throughout the year; which underlined the requirement of immediate implementation of arsenic removal technology as a mitigation measure all round the year.

Chapter 5

Comparative Evaluation of Arsenic Adsorption Potential of the Locally Available Materials

(Batch Experiments)

5.1 Introduction

Main aim of this chapter is to determine the physicochemical properties and adsorption characteristics of NOIS, sand, read soil and murum. Surface morphology, mineralogical characteristics, elemental analysis and physicochemical prosperities of the selected adsorbents are also estimated in the current chapter. The chapter also aims at determination of arsenic adsorption capacities of the individual adsorbents at different operating conditions. In this chapter elaborate discussion has been made about the arsenic adsorption behavior with respect to (1) agitation speed of the incubator shaker, (2) pH of the arsenic spiked solution, (3) contact time between solute adsorbate and the adsorbents, (4) initial arsenic concentration and (5) different dose of adsorbent on the strengthen arsenic spiked solution. The results of the arsenic sorption onto the studied adsorbents under different operating conditions are also elaborately discussed. Interpretation of the same is accomplished to optimize the adsorbents for arsenic sorption at the predetermined operating conditions.

5.2 Characterization of adsorbent

The physicochemical properties of the selected adsorbents i.e. sand, red soil, murum and NOIS were investigated using SEM, EDX, XRD, FTIR and laboratory analysis method. pH of the adsorbents were determined according to EPA 9045D method. Mean particle sizes of the adsorbents were analyzed using Particle size analyzer instrument (Model: AWM 2000, Malvern instruments). Basic properties of adsorbents are depicted in tabular form (Table 5.1).

Table 5.1. Basic properties of the selected adsorbents.

Properties	NOIS	Red Soil	Sand	Murum
Particle size range (mm)	0-2	0-0.425	0.425–2	0.425-2
Mean particle size diameter (μm)	801	20	653	1722
Density (g/cm^3)	5.03	2.54	2.65	2.80
Bulk density (g/cm^3)	2.74	1.31	1.51	1.64
pH (1:1 ratio of adsorbent and water)	8.46	6.02	6.96	6.47
pH_{zpc}	8.44	5.82	6.93	6.80
Surface area (m^2/g)	-	4.38	0.38	-

5.2.1 Point of zero charge (pH_{ZPC})

The point of zero charge (zpc) is a concept related to the phenomenon of adsorption and it describes the condition when the electrical charge density on the surface of the adsorbent is zero. Usually, zpc is the pH value at which a solid submerged in an electrolyte exhibits zero net electrical charge on the surface of the adsorbent. The value of pH is used to describe zpc only for systems in which H^+/OH^- are the potential determining ions. If the measured pH of the adsorbent is lower than the zpc, the surface is net positively charged which attracted anions; conversely, above zpc the surface is negatively charged and attracted cations. Generally, arsenic is found in the groundwater system in anionic forms (arsenite and arsenate). Therefore, arsenic can be removed efficiently at pH below pH_{ZPC}. The pH of zero point charge (pH_{ZPC}) were determined and depicted in Fig. 5.1. From the figure (Fig. 5.1), the pH_{ZPC} values of sand, NOIS, red soil and murum were found to be 6.93, 8.44, 5.82 and 6.80 respectively. Hence, the adsorbents will remove arsenic effectively below the respective pH_{ZPC} value.

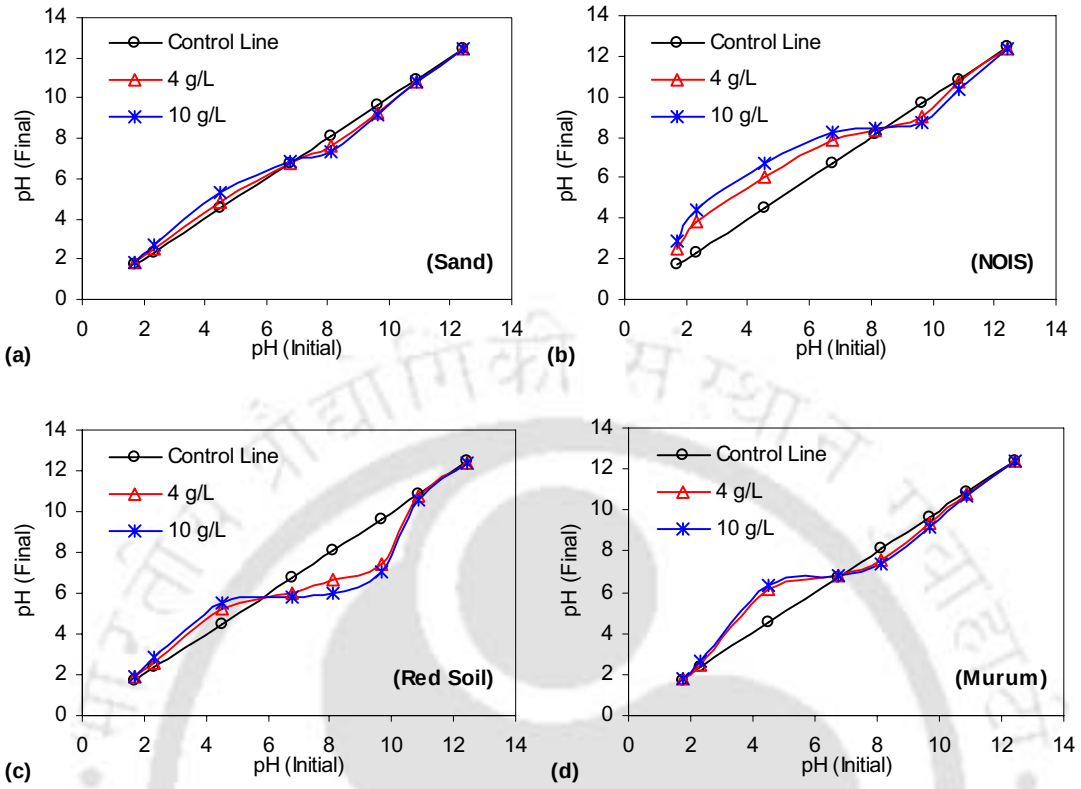

Fig. 5.1. pH of zero point charge of the selected adsorbents: (a) sand, (b) NOIS, (c) red soil and (d) murum.

5.2.2 SEM and XRF analysis of adsorbents

To analyze the surface morphology and structural characteristics of the sand and red soil particles before adsorption, scanning electron microscope (SEM) images were investigated (Figs. 5.2-5.3). Sand and red soil particles are irregular in shape with sharp edges and in amorphous type (Figs. 5.2-5.3). The energy dispersive X-ray (EDX) analyses of sand and red soil were done simultaneously with the SEM to determine the chemical and mineralogical composition of the prepared adsorbent. While the exact elemental composition cannot be determined accurately from EDX spectra, the presence and absence of elements in the surface of the particle were verified. The EDX spectra of the sand and red soil (Fig. 5.2-3 and Table 5.2) indicate that Si, and O_2 are the major elements for both whereas red soil contained 25.5% of C and 4.5% of Fe. It may be possible that the presence of Fe in the surface facilitate arsenic adsorption. The surface

morphology of murum and NOIS were investigated using field emission scanning electron microscopy (FESEM). At 33.68 KX magnification, it can be observed that several minerals are present in the surface of murum (Fig. 5.4). At higher magnification of 99.84 KX, it was confirmed that the minerals are irregular in shape and size, the edges of the surface of the minerals are not sharp and distinct, and they are heterogeneous and amorphous in nature (Fig. 5.4). FESEM images showed the surface morphology and the mineralogical structure of NOIS (Fig. 5.5). NOIS particles are combination of different forms of different compounds. They are irregular in shape and size and highly amorphous in nature. Highly amorphous in nature of the particles may be elevated arsenic adsorption capacity of NOIS.

Table 5.2. EDX analysis of sand and red soil.

Element	Red soil		Sand	
	Weight (%)	Atomic (%)	Weight (%)	Atomic (%)
C	25.53	35.90	-	-
O	45.29	47.82	40.86	56.46
Mg	0.93	0.64	-	-
Al	9.51	5.96	10.26	8.41
Si	12.40	7.46	33.84	26.64
Cl	1.76	0.84	-	-
Fe	4.58	1.39	-	-
K	-	-	15.03	8.50

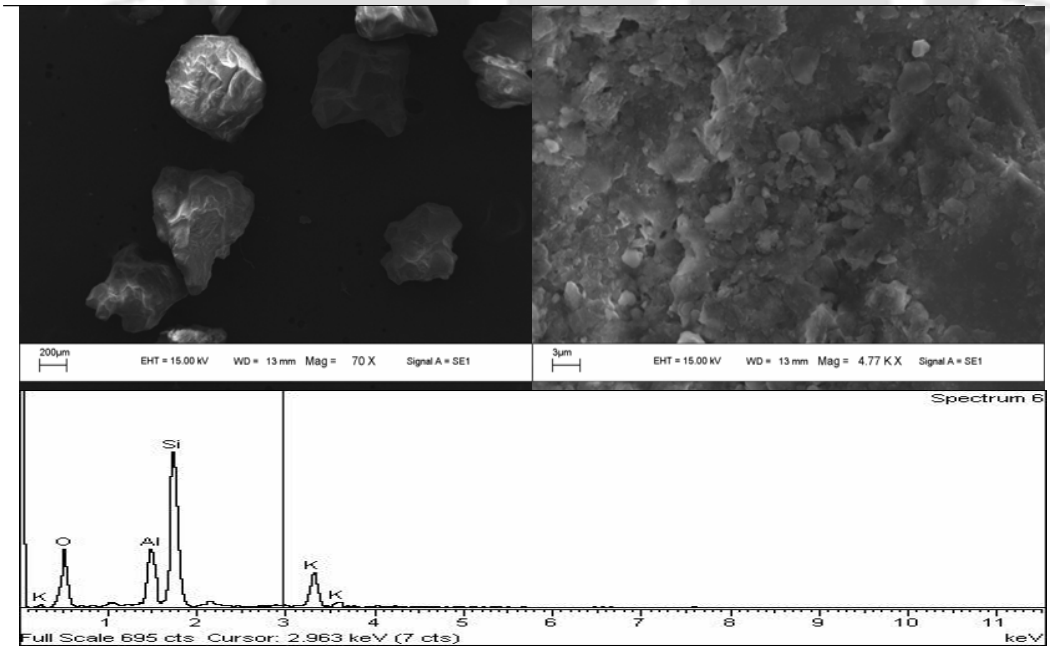

Fig. 5.2. SEM images and EDX spectrum of sand particles.

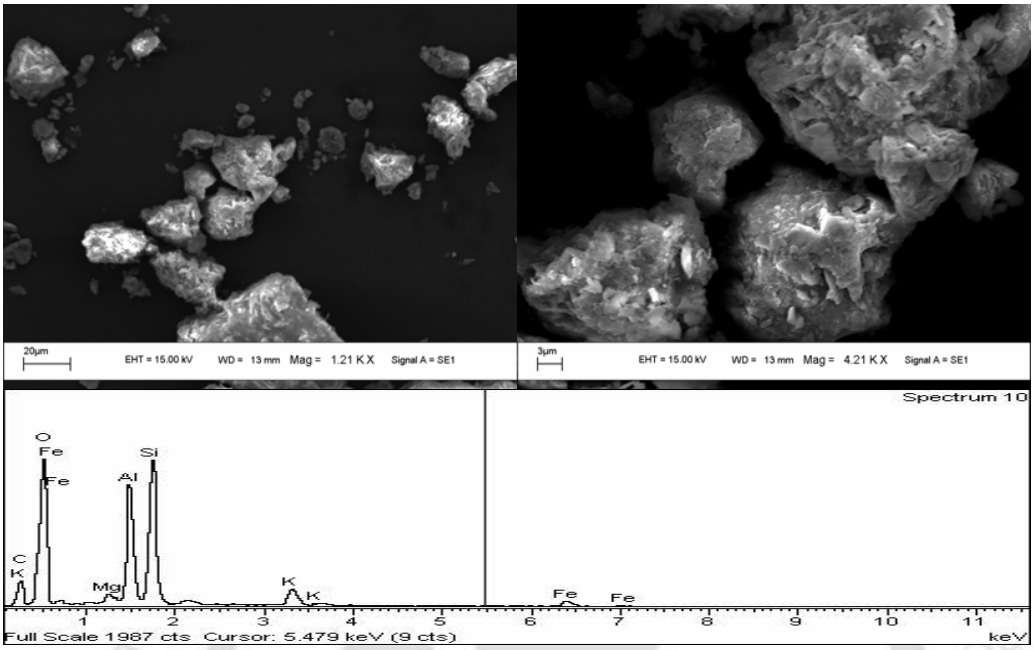

Fig. 5.3. SEM images and EDX spectrum of red soil.

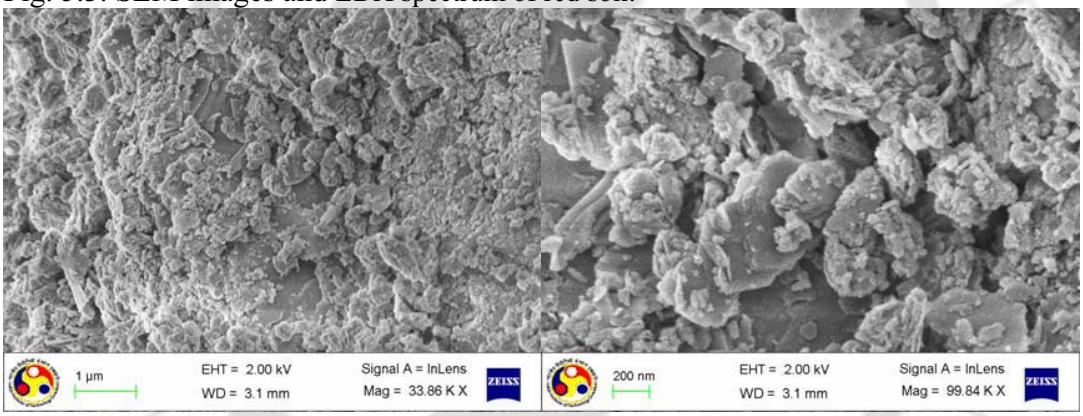

Fig. 5.4. SEM images of murum.

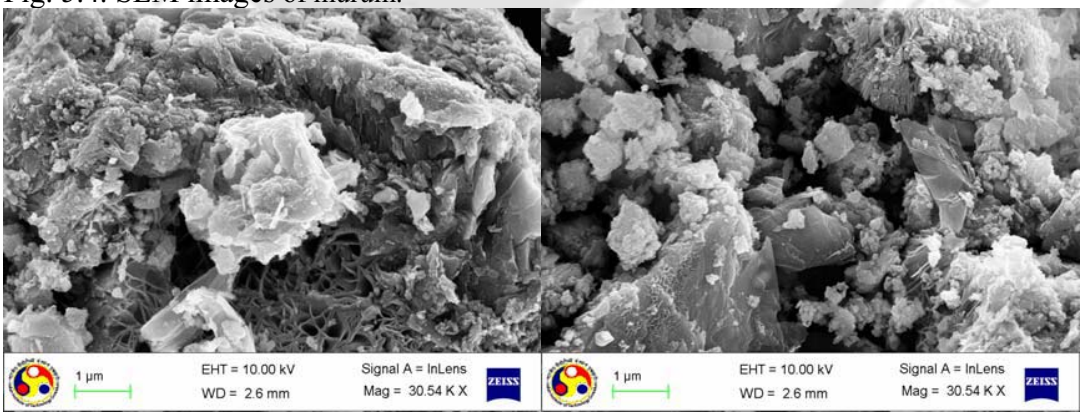

Fig. 5.5. SEM images of NOIS.

The major oxides composition of the sand, red soil and NOIS were determined by X-ray fluorescence (XRF) spectrometry. The results confirm that (Table 5.3) iron oxide was the major composition (52.3%) of NOIS. Red soil also contained 8.2% of iron oxide that may play major role on adsorbing arsenic from aqueous solution. The major oxides of red soil, murum and iron oxides are SiO_2, Al_2O_3 and Fe_2O_3. The degree of lateritization for the red soil is estimated from the silica-sesquioxide (S-S) ratio ($SiO_2/(Fe_2O_3 + Al_2O_3)$). The soil type can be characterized from the obtained value of degree of lateritization using following relation:

<1.33: Laterite Soil

1.33 to 2: Lateritic Soil

>2: Non Lateritic, Tropical Soil

Degree of lateritization for red soil is 1.77, indicating that the soil is lateritic soil.

Table 5.3. Major oxide compositions of the adsorbents (all the values in weight percent).

Adsorbent	SiO_2	Al_2O_3	Fe_2O_3 (Total)	MnO	MgO	CaO	Na_2O	K_2O	TiO_2	P_2O_5
Red soil	57.61	24.31	8.23	0.16	1.10	0.58	2.25	4.09	1.36	0.20
Sand	70.08	14.46	4.40	0.15	0.58	1.22	3.06	3.37	0.42	0.12
NOIS	23.14	9.53	52.29	0.48	0.14	0.07	2.18	0.28	0.14	0.53

5.2.3 XRD analysis of adsorbents

The X-ray diffraction (XRD) patterns of the adsorbents i.e. NOIS, sand, red soil and murum are presented in Fig. 5.6. The important XRD references and their corresponding annotated patterns are presented in Table 5.4. The obtained characteristics strong peaks of sand [Fig. 5.6 (a)] at 2θ values of 20.85, 26.65, 36.55, 39.5, 40.13, 42.45, 45.8, 50.15, 54.95, 60, 64.1, 67.75 and 68.4 are related to quartz (JCPD file no. 05-490). Absence of other prominent peak in the XRD pattern confirms that quartz is the major composition of sand. The characteristic peaks related to quartz are identified at 2θ values of 20.85, 26.65, 36.55, 39.45, 42.5, 45.95 and 50 for red soil [Fig. 5.6 (b)] and 21.0, 24.4, 26.8, 35.05, 39.7, 42.5, 50.3, 54.4, 60.1, 67.9 and 81.7 for murum [Fig. 5.6 (c)]. The predominant diffraction peak correspond to maghemite (γ-Fe_2O_3) and are obtained at 2θ= 30.27, 35.65, 37.29, 43.33, 53.77, 57.32 and 62.95 (JPCD file no. 89-5892). The

corresponding peaks are recorded at 2θ= 30.16, 35.65 and 42.8 for red soil and 2θ= 29.65, 35.8, 37.05, 42.5, 53.8 and 62.92 for murum [Figs. 5.6 (b) and (c)]. The peaks corresponding to goethite arise in the XRD pattern at 2θ values of 24.78, 38.87, 42.78, 46.73 and 62.18 (JCPD file no. 03-249). The related peaks appeared at 2θ= 24.8, 38.40, 42.8 and 46.7 for red soil and 2θ= 24.6, 38.1, 42.5, 45.95 and 61.93 for murum [Figs. 5.6 (b) and (c)]. The peaks of XRD spectra at 2θ= 21.0, 35.95 and 38.1 for murum and 12.3, 19.9, 36.0 for red soil indicated the presence of kaolinite in the samples. The XRD patterns [Figs. 5.6 (b) and (c)] indicated that red soil and murum both contained quartz, maghemite, goethite and kaolinite which agree with the FTIR spectra. Due to its highly amorphous nature, no prominent peak is obtained in case of NOIS [Fig. 5.6 (d)]. The FESEM images confirmed that the NOIS particles were amorphous in nature, which may facilitate better arsenic removal.

Table 5.4. XRD references and corresponding annotate patterns.

Elements	Symbol	JCPDF	References
Quartz, SiO_2	Q	05-490	Maiti et al., 2010; Fernandez-Jimenez et al., 2005; Hajjaji et al., 2009; Chen et al., 2011; Haiying et al., 2011
Maghemite, γ- Fe_2O_3	M	89-5892	Nishide et al., 1995; Liu et al., 2006;
Hematite, α- Fe_2O_3	H	33-0664	Liu et al., 2006; Mohapatra et al., 2011
Goethite, FeO(OH)	G	03-249	Maiti et al., 2010; Mohapatra et al., 2011
Kaolinite, $Al_2Si_2O_5(OH)_4$	K	14-164	Haiying et al., 2011

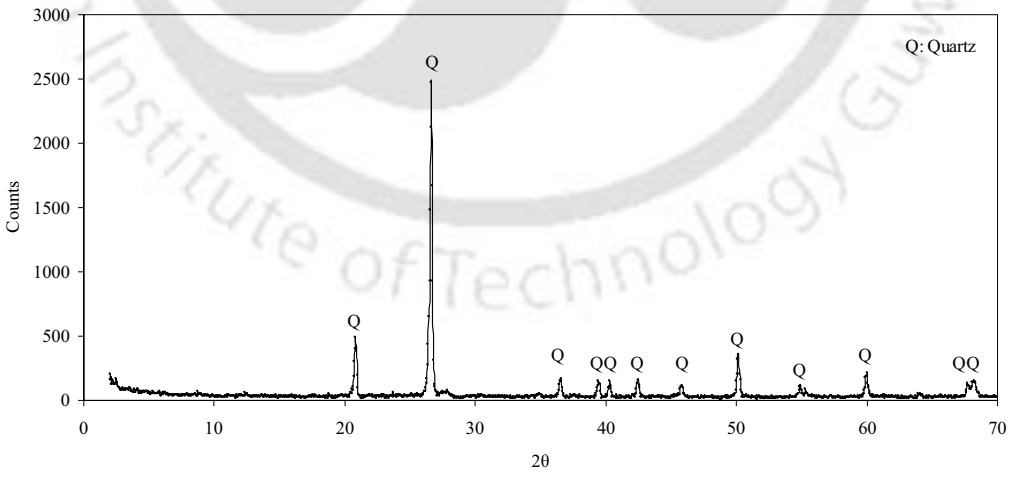

(a)

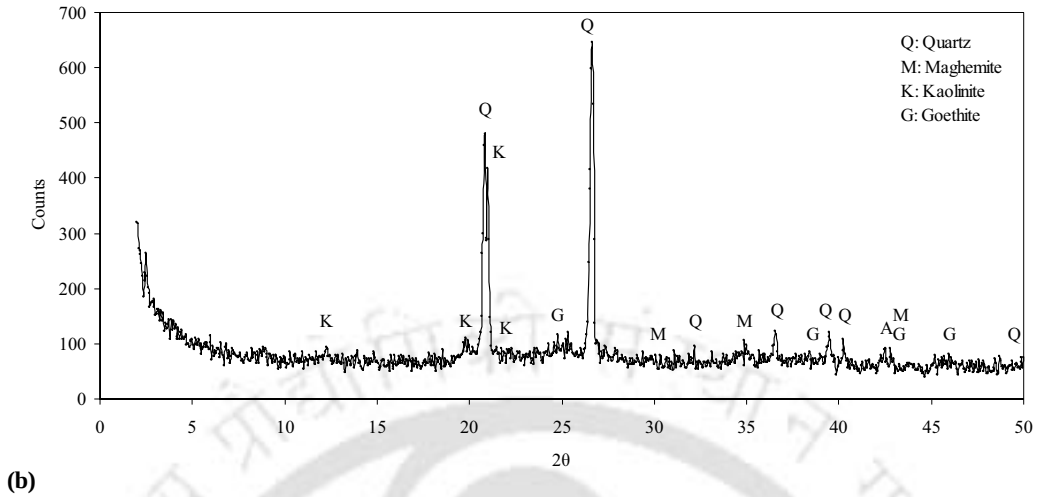

(b)

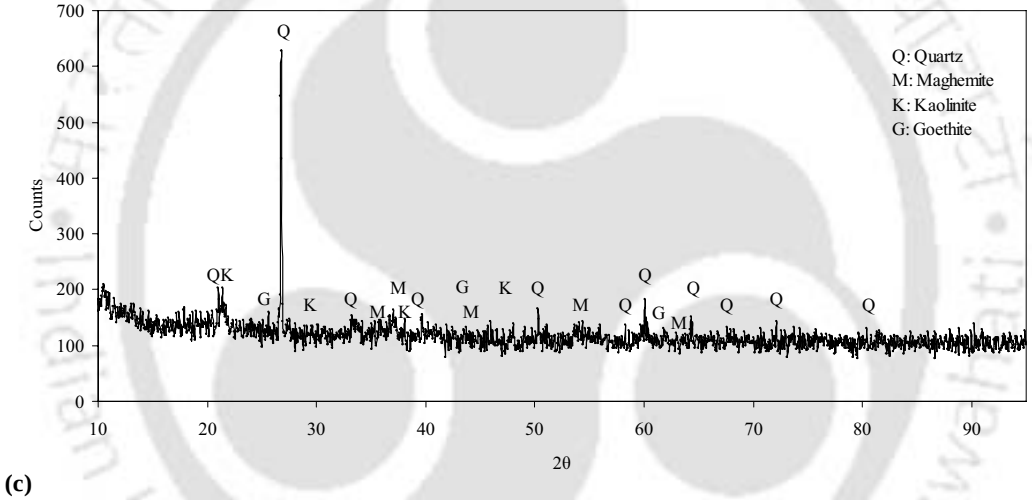

(c)

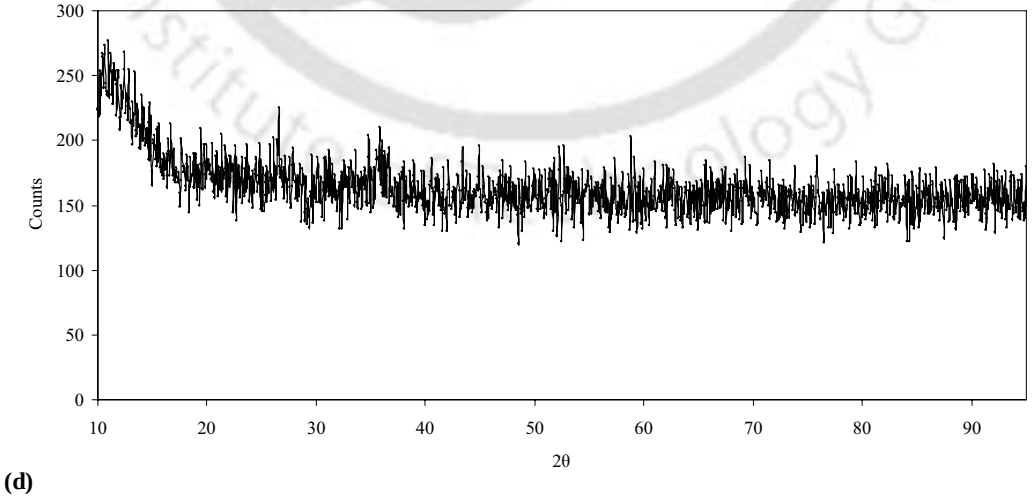

(d)

Fig. 5.6. XRD patterns of (a) sand, (b) red soil, (c) murum and (d) NOIS.

5.2.4 FTIR analysis of adsorbents

The FTIR spectra of NOIS, sand, red soil and murum were recorded in the region of 4000-450 cm^{-1} (Fig. 5.7) and the related peaks are presented in Table 5.5.

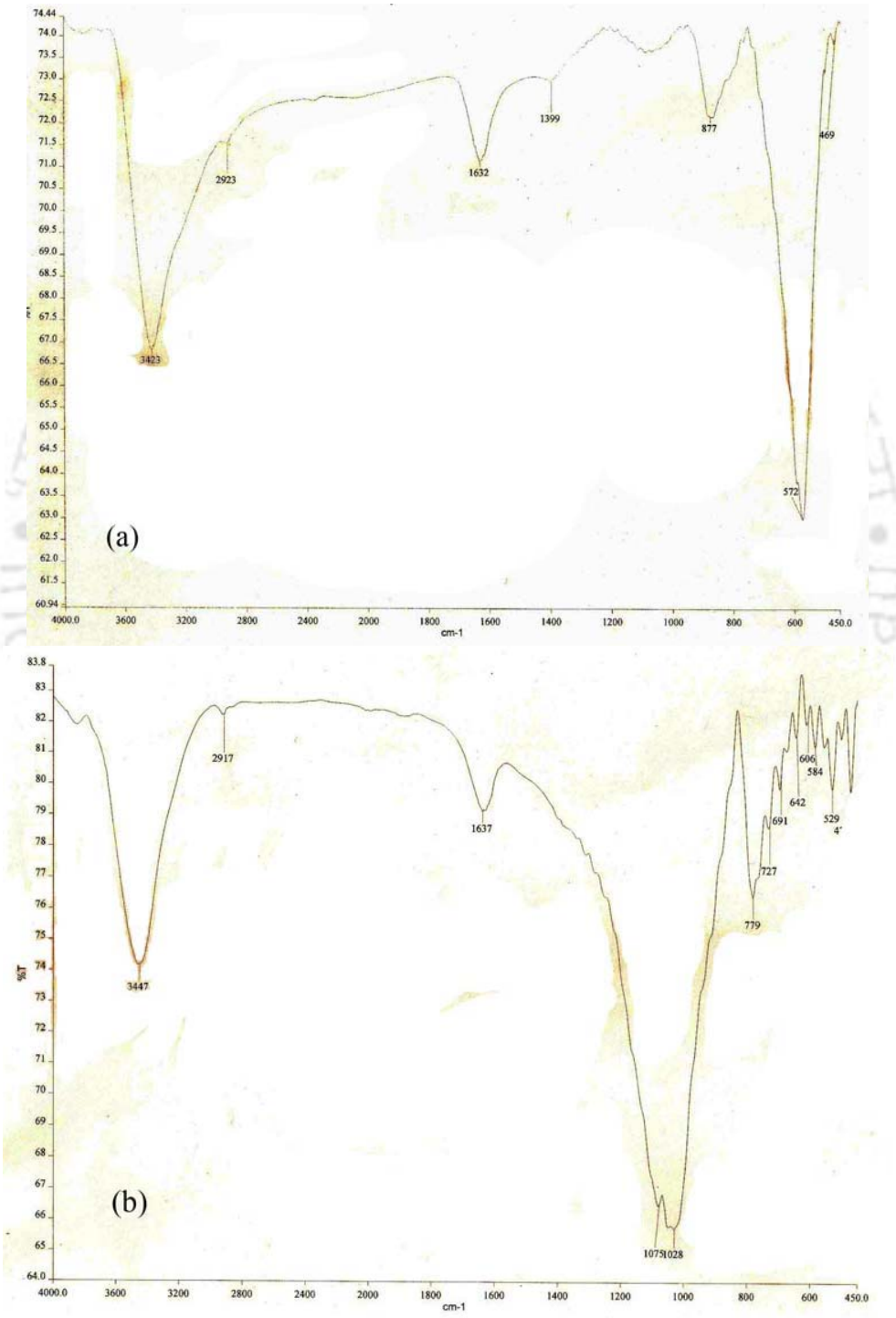

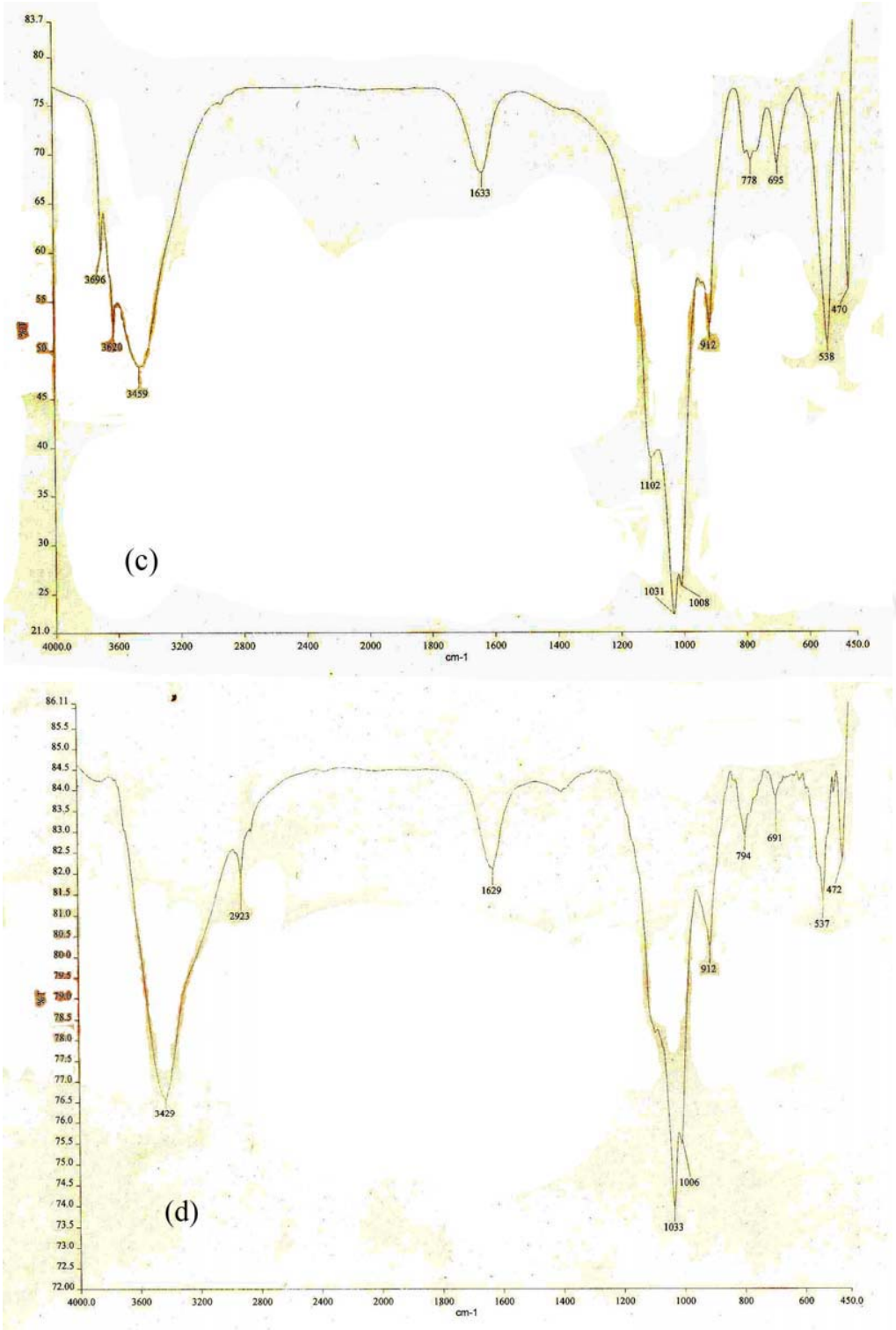

Fig. 5.7. FTIR spectra of (a) NOIS, (b) sand, (c) red soil and (d) murum.

Table 5.5. Observed FTIR spectra peak positions of the adsorbents.

Adsorbents	Band (cm^{-1})
NOIS	3423, 2923, 1632, 1399, 877, 572 and 469
Sand	3447, 2917, 1637, 1075, 1028, 779, 727, 691, 642, 606, 584 and 529
Red soil	3696, 3620, 3459, 1633, 1102, 1031, 1008, 912, 778, 695, 538 and 470
Murum	3429, 2923, 1629, 1033, 1006, 912, 794, 691, 537 and 472

The broad absorption peaks in the range of 3150 to 3100 cm^{-1} correspond to hydroxyl (-OH) stretching vibration of water group, indicating existence of the hydroxyl groups in the materials (Mohapatra et al., 2011; Gupta et al., 2011). The IR bands at 1635, and 1161 cm^{-1} are assigned to the hydroxyl bending mode of water and the bending vibration of the surface hydroxyl group respectively (Mohapatra et al., 2011; Ruan et al, 2002). The two peaks at 2920 and 2854 cm^{-1} are assigned to the C-H stretching vibrations of aliphatic CH_2 and CH_3 groups respectively (Gupta et al., 2011; Guin and Manorama, 2008). Predoi (2007) described that the 2925 cm^{-1} peak is related to C-H of -CH_2 asymmetrical stretching vibration mode and C-C group exists in the range of 800-1200 cm^{-1}. The two IR bands at 799 cm^{-1} and 898 cm^{-1} are related to the Fe–O–H bending vibration of goethite and the intensity of bands are dependent on the shape of the goethite particles (Mohapatra et al., 2011; Parida, 1996). Some important IR bands related to the present study are summarized in Table 5.6.

Table 5.6. Important FTIR spectra bands along with their assignments.

Band (cm^{-1})	Assignment	References
3435	-O-H stretching vibration	Anbalagan et al., 2010
2925	C-H of –CH_2 asymmetrical stretching vibration	Predoi, 2007
1632	-O-H bending	Anbalagan et al., 2010
1082	Si-O, SiO symmetrical stretching vibration	Anbalagan et al., 2010
797	Si-O symmetrical stretching	Anbalagan et al., 2010
778	Si-O symmetrical stretching	Anbalagan et al., 2010
694	Si-O symmetrical bend	Anbalagan et al., 2010
516	Si-O-Al or Fe asymmetrical bend	Anbalagan et al., 2010
475	Si-O-Si asymmetrical bend	Anbalagan et al., 2010
800-1200	C-C	Predoi, 2007

The presence of the minerals and their corresponding bonds in the samples can be identified from the peaks of the IR spectra. The FTIR bands at 3423 cm^{-1} (NOIS), 3447

cm^{-1} (sand), 3459 cm^{-1} (red soil) and 3429 cm^{-1} (murum) are corresponding to the –OH (hydroxyl) stretching vibration of water molecules. The IR peaks at 2923 cm^{-1}, 2917 cm^{-1} and 2923 cm^{-1} corresponding to NOIS, sand and murum respectively, indicated the presence of C-H group in the adsorbents. Paluszkiewicz et al. (2008) described that the FTIR peak appears for quartz at 1165, 1083, 1014, 797, and 778 cm^{-1} and for montmorillonite at 1118, 1050, 917, 875, 840 cm^{-1}. The IR band at 795 and 777 cm^{-1} assigned to Si-O symmetrical stretching vibrations, 460 cm^{-1} relates to Si-O asymmetrical bending vibration and 692 cm^{-1} corresponds to symmetrical bending vibration which is in agreement with the presence of quartz. The bands at 1080 and 1172 cm^{-1} arise from Si-O asymmetrical stretching vibrations due to low Al for Si substitution (Anbalagan et al., 2010). Sharp intense bands at 692, 513, and 460 cm^{-1} are attributed to O-Si-O, Si-O-Al, and Si-O-Si bending modes. Liu et al. (2010) observed the FTIR spectra display bands at 1080 cm^{-1}, 1011 cm^{-1} and 959 cm^{-1} originated by stretching vibrations of the Si-O-Si bonds. The FTIR spectra (Fig 5.7) confirm that all the adsorbents i.e. sand (1075, 1028, 779 and 691 cm^{-1}), red soil (1102, 1031, 912, 778 and 695 cm^{-1}) and murum (1033, 1006, 912, 794 and 691 cm^{-1}) contain Si-O group at different mineral forms. Pure hematite (α-Fe_2O_3) had vibration adsorption peaks at around 3419, 1624, 1400, 546 and 458 cm^{-1} and maghemite (γ-Fe_2O_3) had strong adsorption peak at around 3450, 1630, 546 and 458 cm^{-1} (Suresh et al., 2009). From the literature (Ruan et al., 2002; Guin et al., 2008; Anbalagan et al., 2010,) it is evident that sand (1075, 1028 and 779 cm^{-1}) red soil (1031, 1008 and 778 cm^{-1}) and murum (1006 and 794 cm^{-1}) contain quartz in different forms. All of these adsorbents i.e. NOIS (3423, 1632 and 469 cm^{-1}), sand (3447 and 1637 cm^{-1}), red soil (3459 and 1633 cm^{-1}) and murum (3429 and 1629 cm^{-1}) contained variable amount of maghemite (Fig 5.7). The kaolinite clay vibrates at 3696 cm^{-1}, 3624 cm^{-1} and 695 cm^{-1} band in the IR spectra. The Al(OH) vibrated at 912 cm^{-1} (Pozo et al., 2007). The characteristics of sharp bands at 876 and 712 cm^{-1} can be assigned to the bending vibration of calcite ($CaCO_3$). The characteristics bands at 3140, 894 and 790cm^{-1} can be assigned to the –OH and 637, 455, 405, 397, 375 and 268 cm^{-1} related to the Fe-O stretching vibration of goethite (Mendelovici et al., 1979). FTIR spectra at 3423 cm^{-1} (or 3419 cm^{-1}), 1632 cm^{-1} (or 1624 cm^{-1}) and 1399 cm^{-1} (or 1400 cm^{-1}) indicate that hematite may be one of the major constituents of NOIS. The Al(OH) vibration peaks was

attributed in the red soil to the kaolinite clay at 3696 cm^{-1}, 3620 cm^{-1} and 912 cm^{-1}. IR spectrum at 691 cm^{-1} indicated the presence of kaolinite along with the quartz minerals in murum and sand (Pozo et al., 2007).

5.3 Theory of batch study

5.3.1 Adsorption capacity

The amount of arsenic species adsorbed at time *t*, which is known as adsorption capacity, q_t, (µg g^{-1}), was calculated from the mass balance equation below (Crini, 2008; Hamdaoui, 2006):

$$q_t = \frac{(C_0 - C_t)V}{m} \quad (5.1)$$

Where, C_0 is the initial concentration (µg L^{-1}), C_t the concentration of the arsenic spiked solution at time *t* (µg L^{-1}), *V* the volume of sample (L), and *m* the mass of adsorbent (g). The amount of arsenic species adsorbed at the equilibrium, q_e, is calculated from Equation (5.1), when *t* is the equal to the equilibrium contact time, $C_t = C_e$, $q_e = q_t$.

5.3.2 Kinetic modeling

Adsorption is a time dependent process and it is very important to find out the equilibrium contact time and rate of adsorption to design and evaluate the adsorbent for removal of arsenic species from water. It is also important to know the rate of sorption mechanism at which the solute is removed from the aqueous solution in order to apply adsorption by solid particles to remove the arsenic species. The essential stages in the adsorption processes are (Hamdaoui, 2006):

1. Transport of the adsorbate from the bulk solution to the exterior surface of the adsorbent across the boundary layer (film diffusion).
2. Adsorption of the solute within the pore of the adsorbate (particle diffusion).
3. Adsorption of adsorbate with the surface itself through either pore diffusion or solid-phase diffusion model (Intraparticle diffusion) (Ranjan et al., 2009).

In order to investigate the arsenic adsorption rate and sorption mechanism onto the adsorbents (red soil, sand, NOIS & murum), first order reaction model, pseudo first order reaction model, second order reaction model, pseudo second order reaction model, intraparticle diffusion model, film diffusion model, liquid film mass transfer model, Richenberg model and Bangham's model were analyzed (Maji et al., 2008).

5.3.2.1 First order reaction model

The first order reaction model is based on reversible reactions where equilibrium is established between liquid and solid phases (Liu et al., 2009) and that can be expressed as:

$$\frac{dC_t}{dt} = -k_1 C_t \qquad (5.2)$$

Where, k_1 is the first order rate constant (min^{-1}). Integrating the Equation (5.2) for the boundary condition $t = 0$ to $t = t$ and $C_t = 0$ to $C_t = C_0$ gives:

$$\ln C_t = \ln C_0 - k_1 t \qquad (5.3)$$

The plot of $\ln C_t$ versus t will give a straight line and k_1 value can be obtained from the slope of the graph.

5.3.2.2 Pseudo first order reaction model

Pseudo first order reaction model or Lagergren expression is the first equation for the adsorption of liquid/solid system based on solid capacity. The expression can be represented by (Lagergren, 1898):

$$\frac{dq}{dt} = k_{s1}(q_e - q_t) \qquad (5.4)$$

Where, k_{s1} is the pseudo first order adsorption rate constant (min^{-1}). Integrating the equation (4) for the boundary condition $t = 0$ to $t = t$ (use another symbol) and $q_t = 0$ to $q_t = q_e$ gives:

$$\ln[(q_e - q_t)/q_e] = -k_{s1} t \qquad (5.5)$$

If the plot of $\ln[(q_e - q_t)/q_e]$ versus t follows a straight line, k_{s1} can be obtained from the slope of the graph.

5.3.2.3 *Second order reaction model*

The second order reaction model can be described as the rate of a second order adsorption proportional to the product of concentrations of two reactants or to the concentration of a reactant squared. It can be written as (Nacèra and Aicha, 2006; Pillewan et al., 2011):

$$\frac{dC_t}{dt} = -k_2 C_t^2 \qquad (5.6)$$

Where, k_2 is the second order adsorption rate constant (min^{-1}). Integrating and rearranging the Equation (5.6) for the boundary condition t=0 to t=t and C_t = 0 to $C_t = C_0$ gives:

$$\frac{1}{C_t} - \frac{1}{C_0} = k_2 t \qquad (5.7)$$

This model will be valid for liner plot of $\frac{1}{C_t}$ versus t and k_2 can be obtained from the slope of the graph.

5.3.2.4 Pseudo second order reaction model

The pseudo second order reaction model, proposed by Ho, is based on the adsorption capacity of adsorbent that may be expressed in the form below (Hamdaoui, 2006; Fan et al., 2011):

$$\frac{dq}{dt} = k_{s2}(q_e - q_t)^2 \qquad (5.8)$$

Where, k_{s2} is the rate constant of pseudo second order adsorption (g μg^{-1} min^{-1}). Integration the Equation (5.8) for boundary condition t=0 to t=t and q_t = 0 to $q_t = q_e$ gives:

$$\frac{t}{q_t} = \frac{1}{k_{s2} q_e^{\,2}} + \frac{t}{q_e} \qquad (5.9)$$

The validity of the model can be checked by liner plot of $\frac{t}{q_t}$ versus t. The q_e and k_{s2} can be obtained from the slope and intercept and slope of the linear plot. The advantage of this model is that the adsorption capacity at equilibrium is directly calculated from Equation (5.9) (Hamdaoui, 2006).

5.3.2.5 Intraparticle diffusion model

Intraparticle diffusion model (ID) or parabolic diffusion model developed by Weber and Morris (1963) is also frequently used to describe the adsorption kinetics. This model is also used for describing adsorption processes on the adsorbents. The model can be expressed as (Wu et al., 2009; Weber, 1963):

$$q_t = k_i t^{1/2} + C_i \qquad (5.10)$$

Where, k_i is the intraparticle diffusion rate constant (μg g^{-1} $min^{-1/2}$) and C_i (μg g^{-1}) the constant that gives idea about the thickness of the boundary layer (Cabal et al., 2009). k_i and C_i can be calculated from the slope and intercept of linier plot of q_t versus $t^{1/2}$.

5.3.2.6 Film diffusion model

Boyd, Adamson and Myers derived an equation based on the assumptions that (a) the radius of the particle is greater compared to the film thickness, (b) the process is totally controlled by film diffusion and no other mechanism is involved and (c) the concentration gradient inside the adsorbent is negligible. The equation can be expressed as (Reichenberg, 1953):

$$\ln(1-F) = K_1 t \qquad (5.11)$$

Where, F is the fraction of the solute and K_1 is the adsorption rate constant (min^{-1}). The constant value can be obtained from the plot of $\ln(1-F)$ vs. t. The initial adsorption rate constant can be evaluated from the given expression as the initial rapid adsorption of solute is controlled by the film diffusion (Hamdaoui, 2006).

5.3.2.7 Adam-Bohart-Thomas relation

Initially the adsorption process is rapid and controlled by film diffusion mechanism. Initial adsorption kinetic coefficient can be determined by Adam-Bohart-Thomas equation (Djeribi, 2008) that can be expressed as:

$$\frac{dq}{dt} = K_{sorp} C_t (q_m - q) - K_{des} q_t \tag{5.12}$$

Where, K_{sorp} (L μg^{-1} min^{-1}) is the adsorption kinetic constant and K_{des} (min^{-1}) the desorption kinetic constant. At the initial stage of the sorption process, when $t \to 0$, $q \to 0$ and $C \to C_0$ the Equation (5.12) can be modified as:

$$\left(\frac{dq}{dt}\right)_{t\to 0} = \left(\frac{d(C_0 - C_t)}{dt}\right)_{t\to 0} \frac{V}{m} = K_{sorp} q_m C_0 \tag{5.13}$$

Initial adsorption kinetic coefficient, γ ($L\mu g^{-1}m^{-1}$), was calculated from the following expression:

$$\gamma = K_{sorp} q_m = -\frac{V}{C_0 m}\left(\frac{dC_t}{dt}\right)_{t\to 0} \tag{5.14}$$

The values of the kinetic coefficient were determined using the initial slope of the plots of the solute concentration (C_e) vs. time (t).

5.3.2.8 Liquid film mass transfer model

Mathews and Weber proposed the initial estimation of liquid film mass transfer model that can be expressed as (Mathews and Weber 1976):

$$V\frac{dC}{dt} = k_f A_s (C - C_s) \tag{5.15}$$

Where, V is the volume of arsenic spiked solution (L), k_f the liquid film mass transfer coefficient (m^2s^{-1}), C_s the liquid-phase concentration at external sorbent surface ($\mu g\ L^{-1}$) and A_s the surface area of adsorbent. Integrating the equation (5.15) at t→0, $C_s \to 0$ we get (Choy et al., 2004):

$$-\ln\left(\frac{C}{C_0}\right) = k_f \frac{A_s}{V} t \tag{5.16}$$

The value of $k_f A_s$, which is known as global external transport coefficient ($m^3 s^{-1}$), can be calculated from the slope of the linear plot of $-\ln\left(\frac{C}{C_0}\right)$ versus time (t).

5.3.2.9 Richenberg model

The Richenberg model (1953) was developed by Richenberg to check if the sorption process is based on film diffusion or intraparticle diffusion mechanism. It can be written in the following form:

$$\frac{q_t}{q_e} = \left(1 - \frac{6}{\pi^2}\right)\exp(Bt) \tag{5.17}$$

B_t can be calculated for each value of q_t as:

$$Bt = -0.4977 \ln\left(1 - \frac{q_t}{q_e}\right) \tag{5.18}$$

The intraparticle diffusion will be the sole rate-controlling step if linear plots of *Bt* versus *t* pass through the origin (Ranjan et al., 2009).

5.3.2.10 Bangham's equation

Bangham's equation is used to check whether the pore diffusion is the rate-controlling step or not (Aharoni et al., 1979). The equation can be expressed as (Malana et al., 2011; Manna and Ghosh, 2007; Mall et al., 2006; Mane et al., 2007):

$$\ln\ln\left(\frac{C_0}{C_0 - q_t m}\right) = \ln\left(\frac{k_0 m}{V}\right) + \alpha \ln(t) \tag{5.19}$$

Where, V is the Volume of solution (ml), m the adsorbent concentration (g L^{-1}), C_0 is the initial arsenic concentration (µg L^{-1}), q_t is the amount of adsorbate adsorbed (µg g^{-1}), k_0 is the constant of proportionality and α (<1) is the Bangham constant. If a straight line obtained from the plot of $\ln\ln\left(\frac{C_0}{C_0 - q_t m}\right)$ vs. $\ln(t)$, then it can be conclude that pore diffusion is the rate-controlling step. The constants α and k_0 can be calculated from the slope and intercept of the plot.

5.3.3 Statistical measure

The batch sorption data of the adsorbents were fitted to the various theoretical models to evaluate appropriate kinetic and arsenic uptake rate. The coefficient of determination (R^2) and standard error were used to evaluate the adequateness of the different models to fit the adsorption process. The coefficient of determination was calculated using the following notation (Anirudhan and Radhakrishnan, 2009; Foo and Hameed, 2010; Kundu and Gupta, 2006; Chang et al., 2004):

$$R^2 = \frac{\sum (y_c - y_a)^2}{\sum (y_c - y_a)^2 + (y_c - y_e)^2} \tag{5.20}$$

Where, y_e, y_c and y_a are the experimental value, calculated value and average of the experimental values, respectively.

The standard error (SE) of the estimate can be expressed as (Jalali, 2008; Banerjee et al., 2008; Maiti et al., 2011):

$$SE = \left[\frac{\sum (y_e - y_c)^2}{(n-2)} \right]^{1/2} \tag{5.21}$$

Residual root mean square error (RMSE) can be expressed as (Rostamian et al., 2011):

$$RMSE = \sqrt{\frac{1}{n-2} \sum_{i=1}^{n} (y_e - y_c)^2}$$

Where, y_e and y_p represented the measured and predicted values and n the data point evaluated.

5.3.4 Thermodynamic study

The thermodynamic equilibrium constant (K_c) can be evaluated from the following expression (Pandey et al., 2009):

$$K_c = \frac{C_a}{Ce} \tag{5.22}$$

Where, C_e (μg L^{-1}) is the equilibrium concentration of arsenic in solution and C_a (μg L^{-1}) is the concentration of arsenic on the adsorbent at equilibrium.

The thermodynamic parameters can be evaluated from the following equations (Ranjan, 2009; Senthil Kumar et al., 2010; Pandey, 2009; Maiti, 2009):

$$\Delta G^0 = -RT \ln K_C \quad (5.23)$$

$$\Delta G^0 = \Delta H^0 - T\Delta S^0 \quad (5.24)$$

Where, ΔG^o, ΔH^o and ΔS^o are the Gibb's free energy of arsenic sorption (kJ mol^{-1}), enthalpy (kJ mol^{-1}) and entropy (J $mol^{-1}K^{-1}$) change of adsorption (Ranjan, 2009). T is the adsorption temperature (K) and R is the universal gas constant (8.314J$mol^{-1}K^{-1}$). The K_c may be expressed as a function of temperature using the following expression (Ranjan, 2009):

$$\ln K_c = -\frac{\Delta H^0}{RT} + \frac{\Delta S^0}{R} \quad (5.25)$$

The values of ΔH^o and ΔS^o can be evaluated from the slope and intercept of the plot of K_c vs. 1/T (van't Hoff plot).

5.3.5 Equilibrium study

Equilibrium study is important to describe the adsorption system of adsorbents and optimize the design adsorption mechanism of adsorbate. Thus, it is important to establish the most appropriate correlation of equilibrium data with theoretical or empirical equation. Several isotherm models have been used to describe the equilibrium characteristics of adsorption. (Mall et al., 2005). In this study, Langmuir (Gupta et al., 2005), Freundlich (Kundu and Gupta 2006; Voice and Weber, 1983), Redlich-Peterson (Örnek et al., 2007; Redlich and Peterson 1959), Dubinin-Radushkevich (Dubinin, 1947) and Temkin (Maiti et al., 2010; Manna and Ghosh, 2007; Temkin, 1940) methods were used to interpret the obtained equilibrium values.

5.3.5.1 Langmuir isotherm

The basic assumptions of Langmuir Isotherm are based on (Mane et al., 2007; Ruthven, 1984):

1. Fixed numbers of well-defined one molecular thick localized sites are available for adsorbate.
2. All sites are energetically equivalent and there is no interaction between adsorbed molecules of neighboring sites.

The Langmuir isotherm can be represented as:

$$\frac{q_e}{q_m} = \frac{bC_e}{1+bC_e} \tag{5.26}$$

Where, C_e is the solute concentration of adsorbate at equilibrium (μg L^{-1}), q_e the amount of adsorbate adsorbed at equilibrium (μg g^{-1}), q_m the maximum adsorption capacity of adsorbent, b the Langmuir constant which is directly related to Henry constant ($K^{'} = bq_m$). The Equation (5.26) can be rewritten as (Hamdaoui, 2006; Weber, 1972):

$$\frac{C_e}{q_e} = \frac{1}{bq_m} + \frac{C_e}{q_m} \tag{5.27}$$

The above model is known as type1 Langmuir isotherm. Plot of C_e/q_e vs. C_e gives good fit over wide concentration ranges and represents qualitative type1 isotherm form. Weber and Chakraborti expressed the favorable nature and the essential characteristics of adsorption isotherm in terms of a dimensionless separation factor that is defined by (Pandey et al., 2009; Weber, 1974):

$$R_L = \frac{1}{1+bC_0} \tag{5.28}$$

Where b is the Langmuir constant and C_0 is the initial adsorbate concentration (μg L^{-1}).

The value of R_L indicates the type of isotherm which can be expressed as irreversible adsorption ($R_L = 0$), favorable adsorption ($0 < R_L < 1$), linear ($R_L = 1$) and unfavorable adsorption ($R_L > 1$) (Hamdaoui, 2006).

5.3.5.2 Freundlich isotherm

Freundlich (Freundlich, 1906) developed an empirical equation applicable to adsorption onto heterogeneous surface composed of different classes of adsorption sites

with adsorption in each class following the Langmuir isotherm. The isotherm is defined as follows (Chen et al., 2010):

$$q_e = K_F C_e^{1/n} \tag{5.29}$$

Where, K_F is constant related to adsorption capacity of the adsorbent ($\mu g^{1-(1/n)} L^{1/n} g^{-1}$) and n is the Freundlich empirical constant depending on heterogeneity properties of adsorbent (Mall et al., 2005; Hamdaoui, 2006).

The Freundlich equation can be linearized as follows:

$$\ln q_e = \ln K_F + (1/n) \ln C_e \tag{5.30}$$

K_F and n values can be evaluated from the linear plot of $\ln q_e$ vs. $\ln C_e$, if the sorption technique obeys Freundlich model.

The maximum adsorption capacity (q_m) of the sorbent can be evaluated from Halsey equation using constant initial concentration C_0 and variable weight of the adsorbent. The equation is defined as (Hamdaoui, 2006; Halsey, 1952).

$$K_F = \frac{q_m}{C_0^{1/n}} \tag{5.31}$$

5.3.5.3 The Redlich-Peterson (R-P) isotherm

The Redlich-Peterson (R-P) isotherm is a combined form of Langmuir and Freundlich isotherm. It approaches the Freundlich isotherm at high concentrations and is in accord with the low concentration limit of the Langmuir isotherm (Mall et al., 2005; Senthil Kumar et al., 2010; Redlich and Peterson, 1959). The R-P isotherm can be expressed as:

$$q_e = \frac{K_R C_e}{1 + \alpha_R C_e^{\beta}} \tag{5.32}$$

Where K_R (L g^{-1}) and α_R (L μg^{-1}) are the isotherm constants and β is the constant, the value lies between 0 and 1. For $\beta = 1$, the equation will be performed as Langmuir and for $\beta = 0$, it will reduce to Henry equation.

The linear form of the Equation (5.32) can be written as:

$$\ln(K_R \frac{C_e}{q_e} - 1) = \ln \alpha_R + \beta \ln C_e \quad (5.33)$$

K_R, α_R and β can be determined using non-linear regression method.

5.3.5.4 Dubinin-Radushkevich (D-R) isotherm

D-R isotherm can be described as below (Senthil Kumar et al., 2010; Dubinin, 1947):

$$q_e = q_m e^{-\beta \varepsilon^2} \quad (5.34)$$

Where q_m is the D-R monolayer adsorption capacity, ε the Polanyi potential related to equilibrium concentration, which can be evaluated from the following expression (Chabani, 2006):

$$\varepsilon = RT \ln(1 + \frac{1}{C_e}) \quad (5.35)$$

Where, T is the absolute temperature, R is the gas constant (8.314 J mol K^{-1}) and β is the constant related to the free energy (E) of sorption. The free energy (E) of sorption (kJ/mol) can be computed using the following equation: (Senthil Kumar et al., 2010):

$$E = \frac{1}{\sqrt{2\beta}} \quad (5.36)$$

The D-R isotherm can be expressed in its linear form as:

$$\ln q_e = \ln q_m - \beta \varepsilon^2 \quad (5.37)$$

q_m, β and corresponding E value will be evaluated using the liner plot of $\ln q_e$ vs. ε^2.

5.3.5.5 Temkin isotherm

The Temkin isotherm (Temkin, 1940) is based on the following assumptions (Mall et al., 2005):

i. The heat of adsorption of all the molecules in the layer decreases linearly with coverage due to adsorbent–adsorbate interactions.

ii. The sorption is characterized by a uniform distribution of the binding energies, up to some maximum binding energy (Mall et al., 2005; Kim et al., 2004; Temkin, 1940).

The equation of the Temkin isotherm can be written as follows (Hamdaoui, 2006):

$$\frac{q_e}{q_m} = \frac{RT}{\Delta Q}\ln(K_0 C_e) \tag{4.38}$$

The equation can be expressed as

$$\frac{q_e}{q_m} = \frac{RT}{\Delta Q}\ln K_0 + \frac{RT}{\Delta Q}\ln C_e \tag{4.39}$$

Where, R is the universal gas constant (8.314J $mol^{-1}K^{-1}$), T the absolute temperature (K), ΔQ the energy transmission during sorption of the sorbate (k J mol^{-1}) and K_0 the Temkin constant (L μg^{-1}). Values of ΔQ and K_0 can be calculated from linear plot of q_e/q_m vs. $\ln C_e$.

5.4 Batch experimental results and discussions

5.4.1 Effect of agitation speed on arsenic sorption

The effect of agitation speed on arsenic sorption was investigated for the both As(III) and As(V) species onto the selected adsorbents i.e. NOIS, sand, red soil and murum. Experiments were conducted using 200 µg L^{-1} of arsenic spiked solution along with specific adsorbent dose at different speed of the incubator shaker. The results (Fig. 5.8) shows the effects of agitation speed of the shaker on sorption from aqueous medium on the surface of the studied adsorbents.

From the Fig. 5.8, it can be observed that the maximum uptake of arsenic increases with increase of agitation speed of the shaker. The As(III) uptake capacity of NOIS was gradually increased with the increase of shaker speed and it became constant after 175 rpm. Similar observation had also been made for the both arsenic species sorption by red soil, sand and NOIS [Figs. 5.8 (a), (b) and (c)]. Whereas murum achieved constant arsenic uptake rater at 200 rpm [Fig. 5.8 (d)] of the shaker speed. It may be

possible that increasing of shaker speed, the boundary layer resistant decreases and film diffusion enhancing the mass transfer from solution to the surface of the adsorbents (Mamisahebei, 2007).

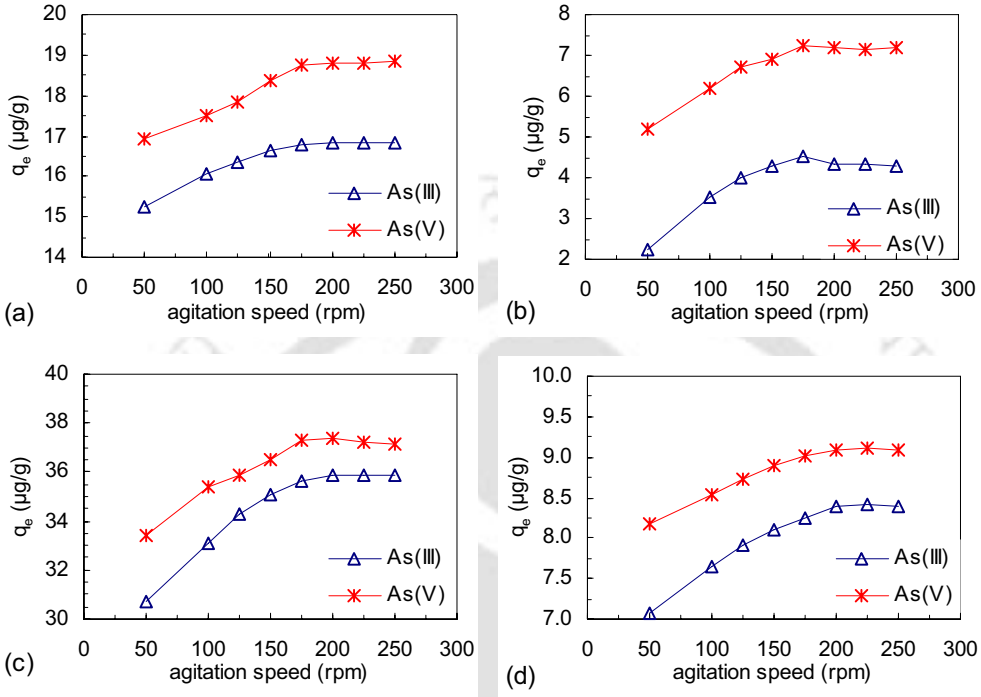

Fig. 5.8. Effect of agitation speed on arsenic adsorption onto different adsorbent: (a) red soil, (b) sand, (c) NOIS and (d) murum. [Matrix: Initial As(III) & As(V) concentration = 200 µg L^{-1}; contact time = 180 min; dose of red soil =1g, sand= 2g, NOIS = 0.5 g & murum = 2 g; volume of solution = 100 ml; temperature = 25±1ºC and pH = 7].

5.4.2 Effect of pH on arsenic sorption

Arsenic sorption from aqueous medium onto adsorbent is governed by pH level of the solution. One set of batch experiments were conducted to observe the effect of pH on arsenic [either As(III) or As(V)] sorption onto the characterized adsorbents (NOIS, sand, red soil and murum). To analysis the effect of pH on adsorption process, the experimental data were depicted in Figs. 5.9-5.12 and Fig. B5. The plots (Figs. 5.9-5.12) show that, arsenic adsorption capacities do much not differ much in the acidic media. Generally it is found that, As(III) remains in the solution in neutral state as H_3AsO_3 at the pH range of 3 to 8.5 (Maji et al., 2007). A positive surface charge of the sorbent acts as driving force for the adsorption process at this pH range (Alshaebi et al., 2010; Bhakat et al., 2006;

Debasish et al., 2008). In Fig. 5.10 and Fig. 5.12, increase of pH of the solution, a little decrement in As(III) sorption on sand and murum is observed. From the Fig. 5.9 and Fig. 5.11, it can be assured that As(III) sorption rates of NOIS and red soil are almost constant in acidic media but at higher pH, it decreases with increasing the pH of the solution. Similar results were observed for the arsenic sorption onto laterite iron (Partey et al., 2008), ferric hydroxides (Valencia-Trejo et al., 2010) and titanium dioxide nanoparticles (Meng et al., 2000). They argued that arsenate [As(V)] sorption mechanism is influenced by the pH of the solution in greater extent. Neutral arsenite (H_3AsO_4) existed in the aqueous medium below pH 2 at oxidizing condition. Whereas, arsenate presence in the solution in the form of $HAsO_4^-$ and $HAsO_4^{2-}$ (Alshaebi et al., 2010) even at normal condition. From the Figs. 5.9-5.12, it is confirmed that the arsenate sorption decreases with increasing pH of the solution. In the acidic condition, lowering the pH of the solution, a minute increment of arsenate adsorption capacity can observed. On the contrary, the arsenate uptake capacity rapidly decreases with raising the pH of the solution in alkaline condition. Similar observations were observed on As(V) sorption by ferric hydroxides and titanium dioxide nanoparticles (Valencia-Trejo et al., 2010; Meng, 2000). From the observations, it can be interpreted that the adsorbents effectively removed arsenic in acidic media and they are also efficient on removing arsenic at normal pH level of the drinking water.

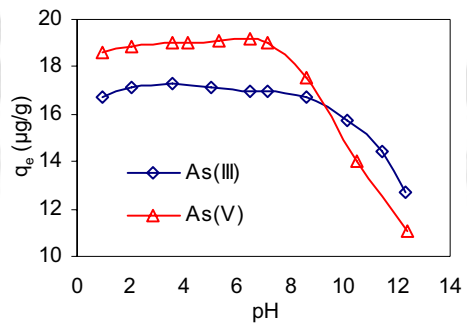

Fig. 5.9. Effect of pH on arsenic sorption using red soil. [Matrix: Initial As(III) & As(V) conc. = 200 µg L^{-1}; contact time = 180 min; agitation speed= 200 rpm; volume of solution = 100 ml; adsorbent dose= 1g and temperature = 25±1ºC].

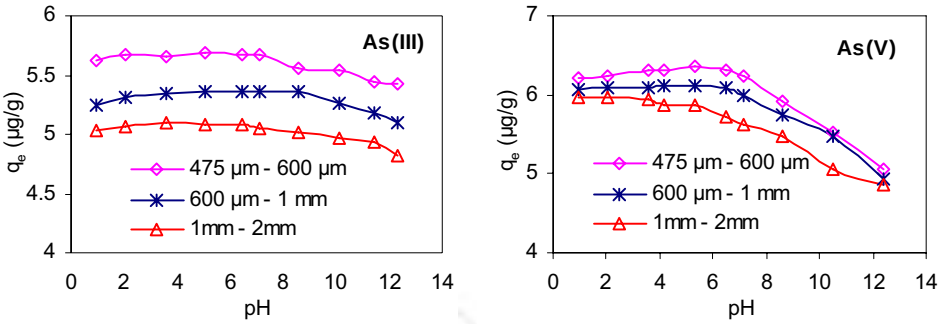

Fig. 5.10. Effect of pH on arsenic sorption using different size of sand. [Matrix: Initial As(III) & As(V) conc. = 200 µg L^{-1}; contact time = 180 min; agitation speed= 200 rpm; adsorbent dose= 2g; volume of solution = 100 ml and temperature = 25±1ºC].

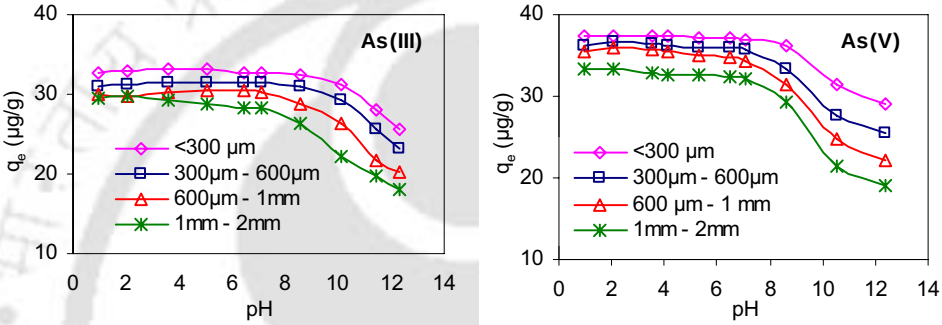

Fig. 5.11. Effect of pH on arsenic sorption using different size of NOIS. [Matrix: Initial As(III) & As(V) conc. = 200 µg L^{-1}; contact time = 180 min; agitation speed= 200 rpm; adsorbent dose= 0.5g; volume of solution = 100 ml and temperature = 25±1ºC].

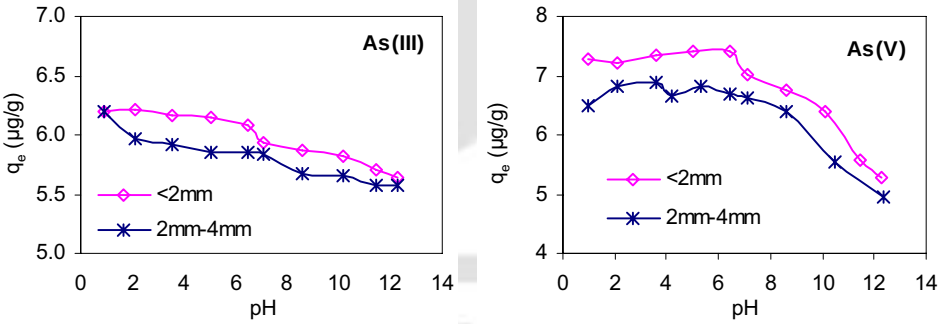

Fig. 5.12. Effect of pH on arsenic sorption using different size of murum. [Matrix: Initial As(III) & As(V) conc. = 200 µg L^{-1}; contact time = 180 min; agitation speed= 200 rpm; adsorbent dose= 2g; volume of solution = 100 ml and temperature = 25±1ºC].

5.4.3 Effect of contact time

The contact time between sorbate and the sorbent is significant in the water treatment by adsorption. In physiochemical sorption process, most of the adsorbents adsorbed adsorbate within a short interval of contact time. Available literature corroborate that uptake capacity of sorbate is faster at the initial stage of sorption process, thereafter, it decreases as the solute concentration reach to equilibrium (Chen et al., 2011; Islam et al., 2011; Choksi et al., 2007). It may possible that initially too large number of vacant sites are available for the sorbate; but as the time elapse, remaining vacant sites are difficult to access for the sorbate due to repulsive force between the solute molecules presence in solid and bulk phase (Mall, 2006). The effect of contact time for the adsorption of As(III) and As(V) on various adsorbents i.e. NOIS, red soil sand and murum were depicted in Fig. 5.13 and Fig. 5.14. The experiments were carried out for the time interval of 0-720 minutes using 200 μg L^{-1} arsenic [either As(III) or As(V)] spike solution at 25ºC. From the Fig. 5.13 and Fig. 5.14, it is clear that the both As(III) and As(V) species reached the equilibrium concentration within 120 minutes of the sorption process for the all adsorbents Results indicate that the sorption rate is faster at initial stage and the rate is retarded as time elapses. It is also found that As(V) is better removed than As(III) by the all the adsorbents. Within 120 minutes of the adsorption process, maximum quantities of arsenic were adsorbed by all adsorbents. The initial uptake rate of NOIS was higher compared to the other adsorbents. To achieve 80% removal efficiency, NOIS took only 15 min for As(V) and 30 min for As(III) species. Based on performance, the materials can be arranged in the following order: NOIS> red soil> murum>sand. Fig. 5.14 shows that better performance is achieved for smaller size of particle than larger size because of small size of particles have larger surface area that can adsorb larger number of ions.

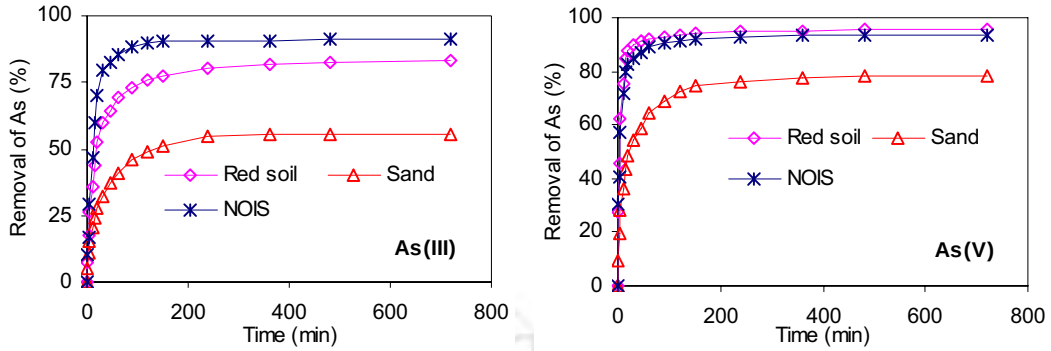

Fig. 5.13. Dynamics of arsenic adsorption onto red soil, sand and NOIS.

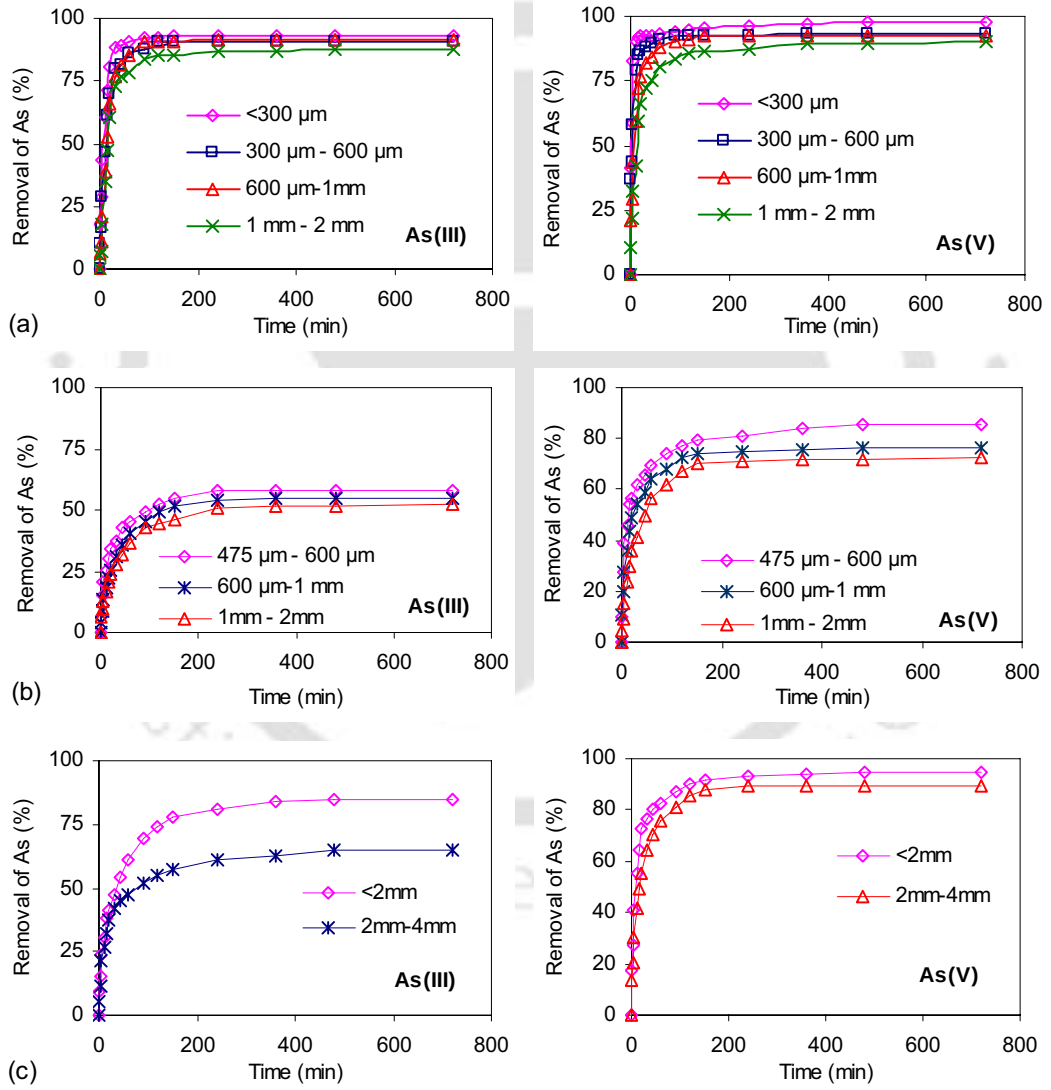

Fig. 5.14. Dynamics of arsenic species adsorption onto different size of adsorbent: (a) NOIS, (b) sand and (c) murum. [Matrix: Initial As(III) & As(V) concentration = 200 µg L^{-1}; dose of adsorbent: red soil =1g, sand= 2g, NOIS = 0.5 g & murum = 2 g; volume of solution = 100 ml; agitation speed = 200 rpm; temperature = 25±1ºC and pH = 7].

5.4.4 Kinetic modeling

The sorption of sorbate from aqueous solution by sorbent is a complex mechanism, influenced by several parameters related to physicochemical properties of sorbate and sorbent, interaction period of solute with sorbent, affinity of the sorbate towards sorbent, available free energy for sorption, strength of the sorbate, and the condition applied to the sorption process etc (Hamdaoui et al., 2008). In order to investigate the arsenic adsorption rate and sorption mechanism onto the adsorbents (red soil, sand, murum and NOIS) first order, second order, surface diffusion, pore-film diffusion and intraparticle diffusion models were employed to the kinetic data to describe the transport mechanism and to define kinetic rate of sorption (Ornek, 2007).

5.4.4.1 First, Second Order and Pseudo First Order Reaction Model

To describe the kinetics of arsenic sorption, initially relatively simple reaction models were used to the kinetic data. Thus, the first order, second order and pseudo first order reaction models are applied to determine the reaction rate of arsenic sorption by the adsorbents. The related results are depicted in graphical form as shown in the Fig. 5.15 to Fig.5.20. Non-linear plots (Fig.5.15 to Fig.5.16) of $\ln C_t$ vs. t indicate that first order kinetic reaction model can not evident the experiments data of arsenic sorption by the selected adsorbents. Second order reaction model (Fig. 5.15 to Fig.5.16) also fails to derive kinetic rate of arsenic sorption as non-linear plot of $1/C_t$ vs. t obtained from batch experiment data of the adsorbents.

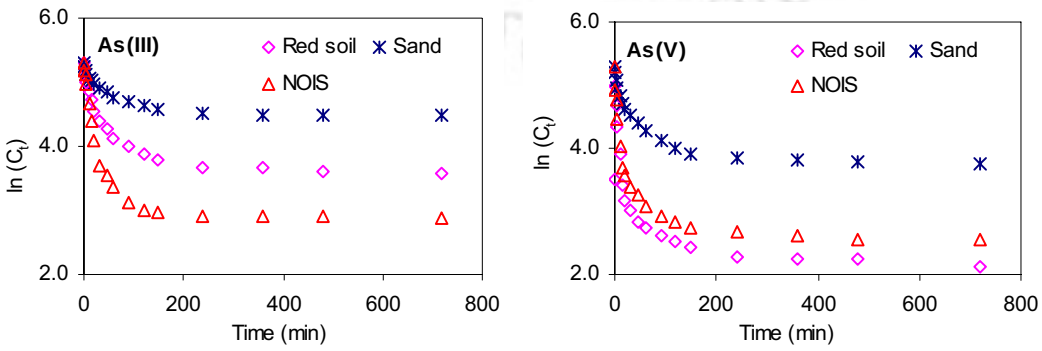

Fig. 5.15. First order kinetic plot of arsenic adsorption onto three different adsorbent.

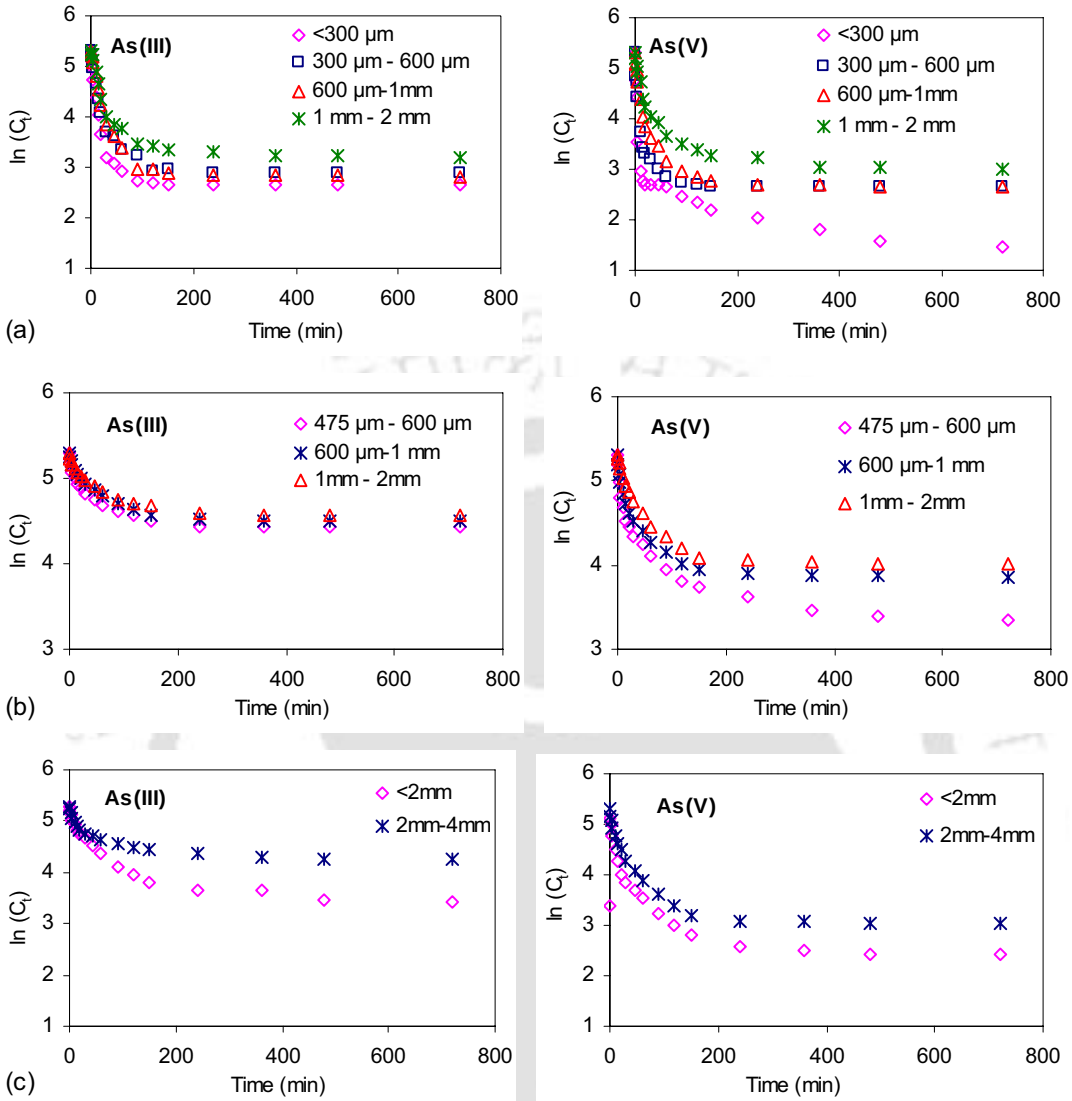

Fig. 5.16. First order kinetic plot of arsenic adsorption onto different size of adsorbent: (a) NOIS, (b) sand and (c) murum.

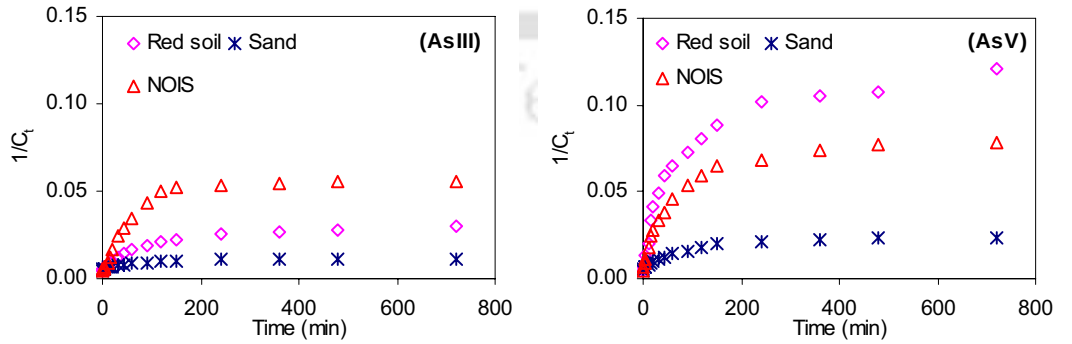

Fig. 5.17. Second order kinetic plot of arsenic adsorption onto various adsorbents.

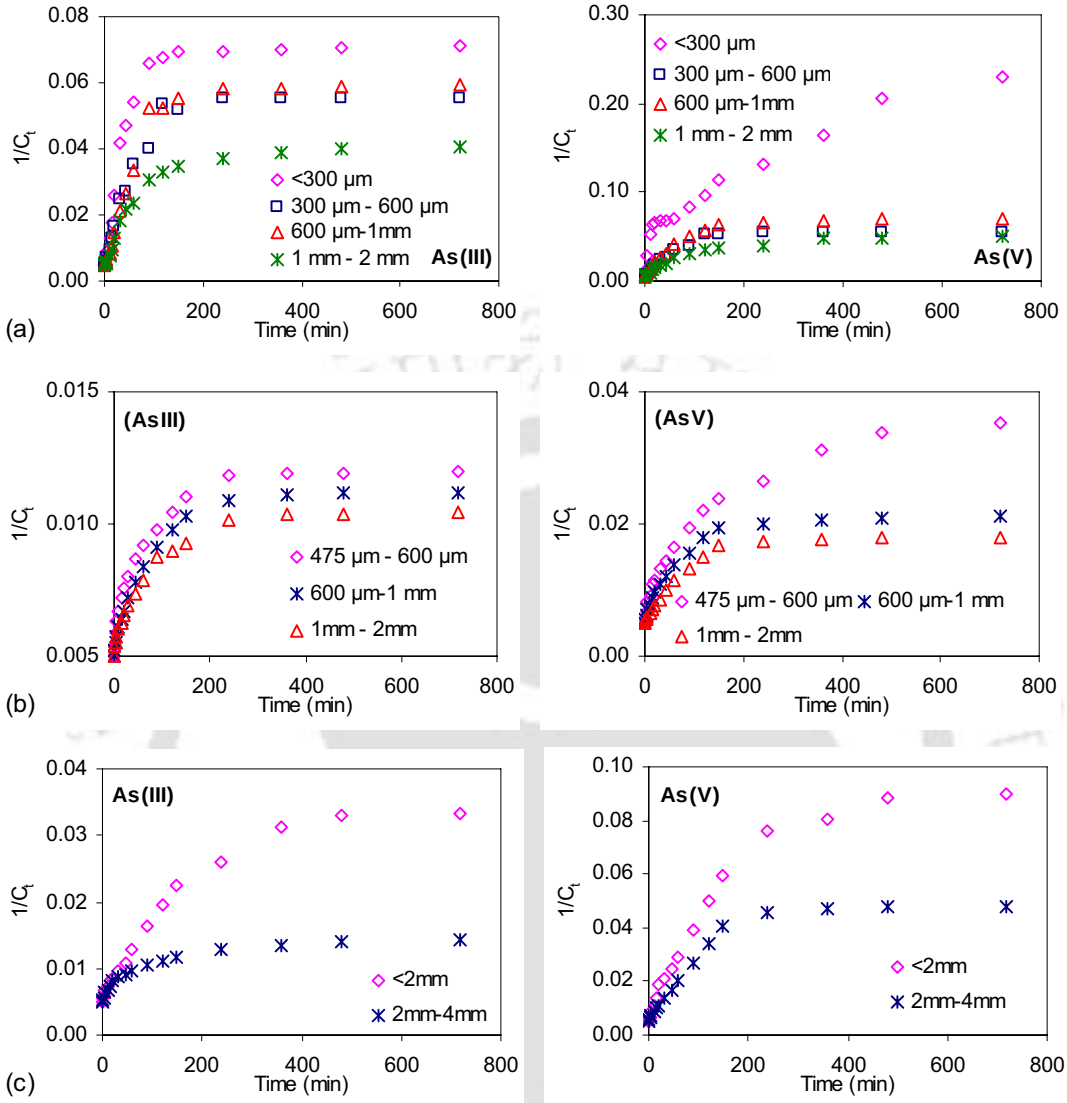

Fig. 5.18. Second order kinetic plot of arsenic sorption [As(III) and As(V)] adsorption onto various adsorbents: (a) NOIS, (b) sand and (c) murum.

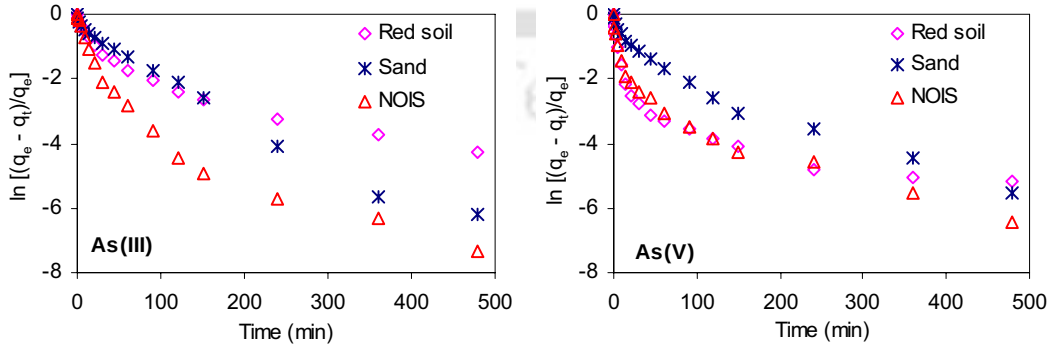

Fig. 5.19. Pseudo first order kinetic plot of arsenic adsorption onto red soil, sand and NOIS.

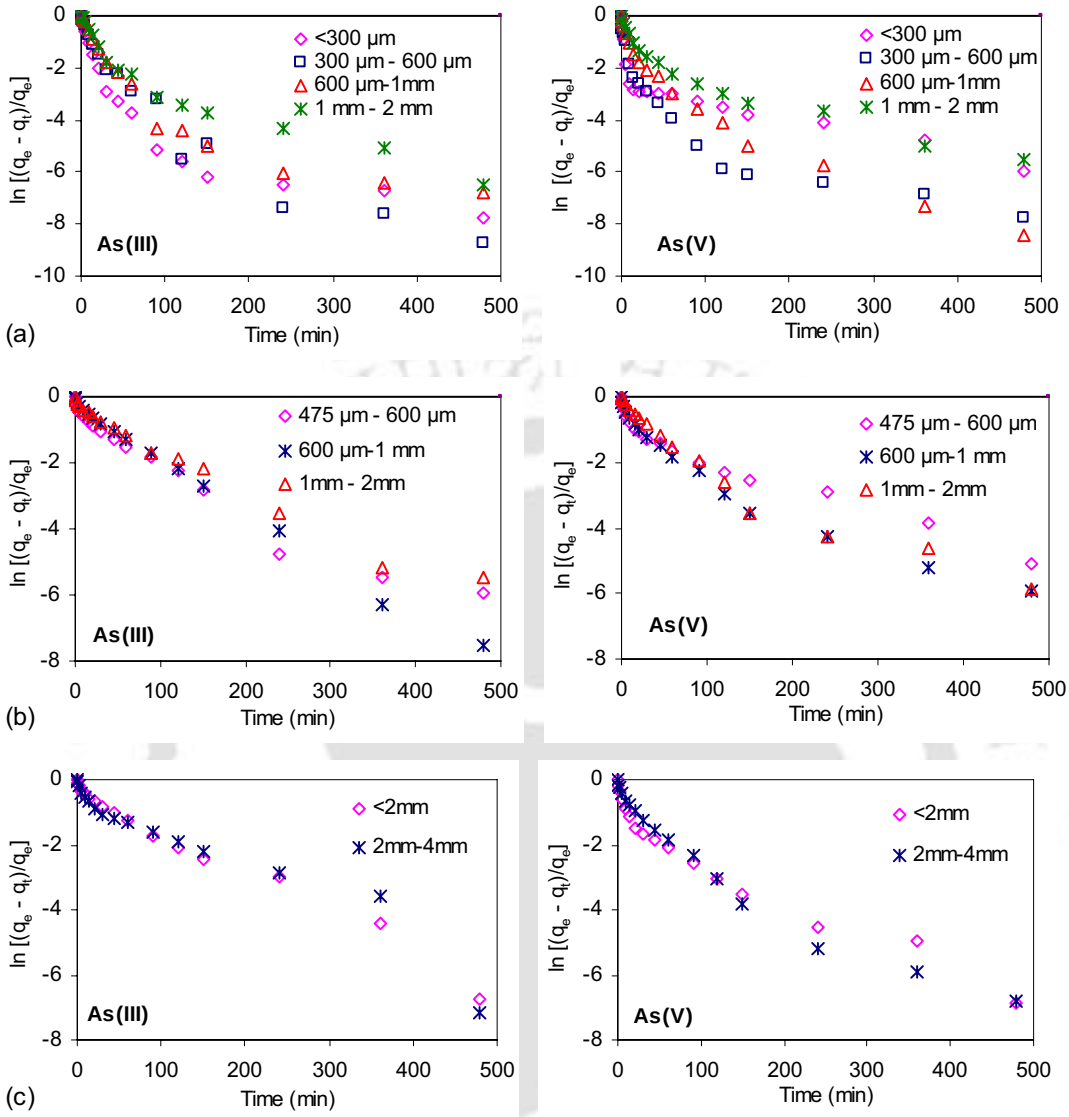

Fig. 5.20. Pseudo first order kinetic plot of arsenic [As(III) and As(V)] adsorption onto various size of different adsorbents: (a) NOIS, (b) sand and (c) murum.

In Fig. 5.19 and Fig. 5.20, plot of $\ln[(q_e - q_t)/q_e]$ versus t is represented the Lagergren first order kinetic equation. Initial portion of the plots were found to be liner due to rapid sorption of arsenic. Later, non-linear portion indicates that other diffusion mechanism is also involved on arsenic sorption. Hamdaoui (2006) reported the similar results for methylene sorption by sawdust and crushed brick. Ho and McKay (1998) had similar findings for dye sorption using sphagnum moss peat. In case of sand, the coefficient of determination values are higher than compared with the other materials but

sorption mechanism could not be justified properly. It may be possible that the adsorption process is mainly controlled by film diffusion.

5.4.4.2 Pseudo second order reaction model

To investigate the arsenic sorption mechanism, pseudo second order reaction model was applied to the batch As(III) and As(V) sorption kinetic data of the studied adsorbents (NOIS, sand, murum and red soil). In the Figs. 5.21-5.22, straight-line plots of t/q_t vs. t represented pseudo second order reaction model that was obtained from the experimental data. Table 5.8 and Table 5.9 confirm that the coefficients of determination values (R^2) of the studied adsorbents are found to be very close to 1 or 1 itself. R^2 values above 0.95 indicate that this model can interpret the sorption mechanism. To check the certainty of this method, standard error (*SE*) of the experimental data were calculated.

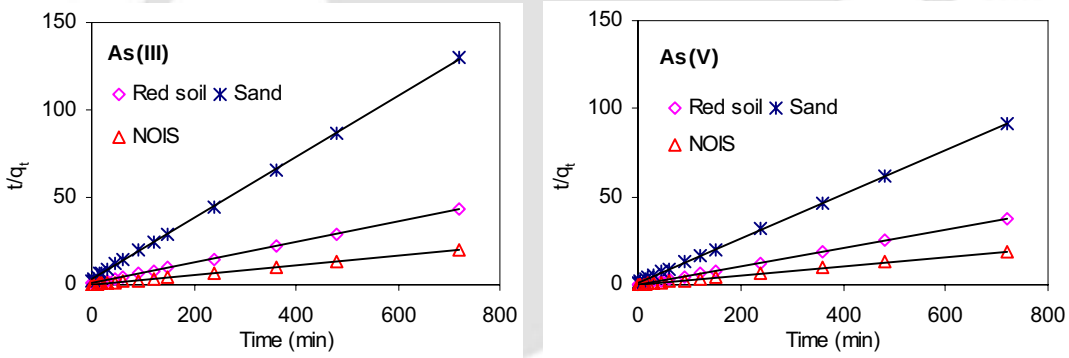

Fig. 5.21. Test of pseudo second order reaction model for arsenic [As(III) and As(V)] adsorption onto different material.

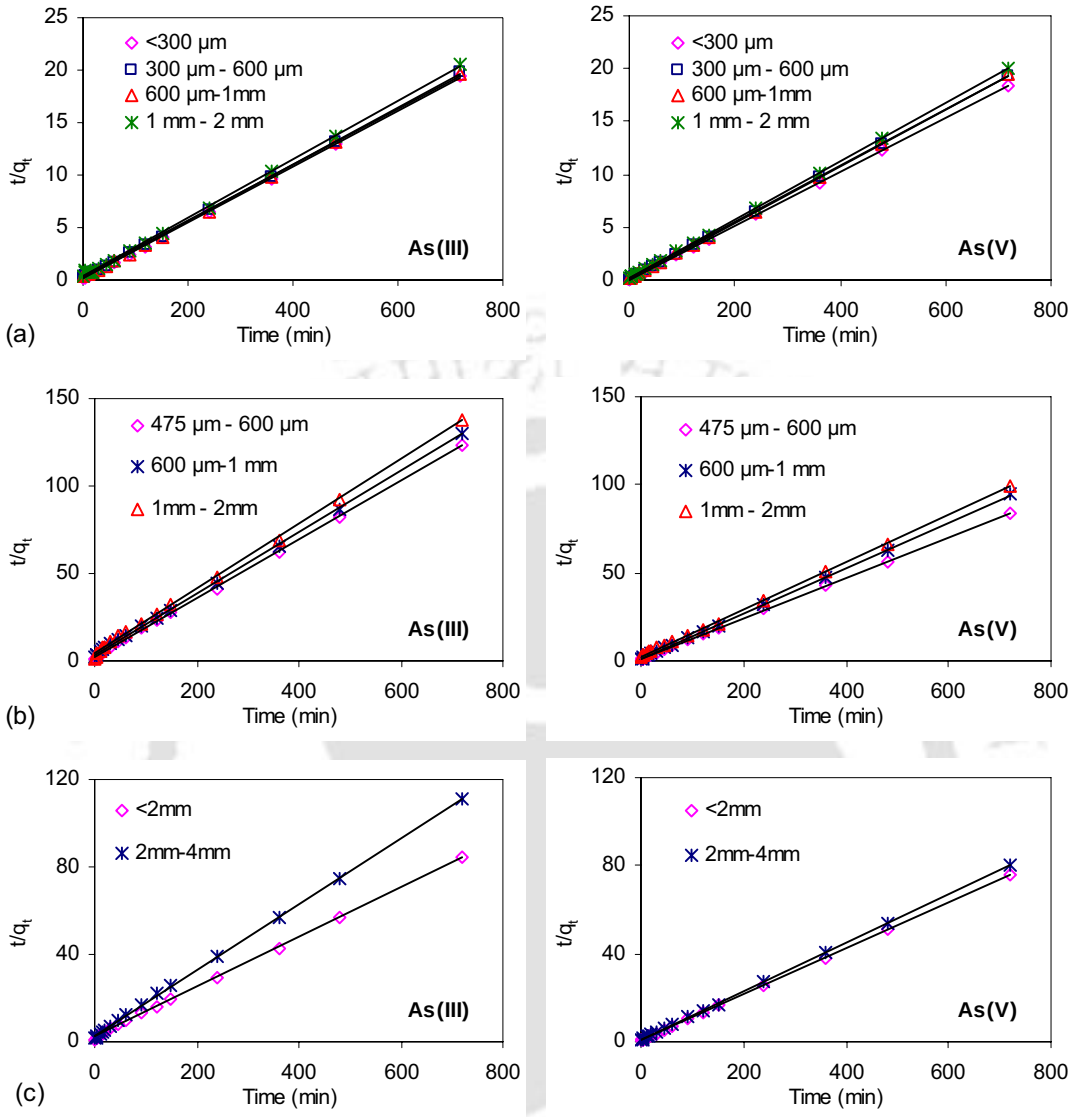

Fig. 5.22. Test of pseudo second order kinetic plot of arsenic [As(III) and As(V)] adsorption onto different size of adsorbents.: (a) NOIS, (b) sand and (c) murum.

Standard error (*SE*) is the standard deviation of the experimental data distribution associated with the predicted data. Low values of *SE* (0.209-2.569) confirm that the kinetic of the arsenic sorption by the selected materials are following pseudo second order reaction model. Maji (2008) got some what similar results for arsenic sorption onto laterite soil. The comparison plots of experimental data and predicted equation for the all selected materials were depicted in Fig. 5.23 to Fig.5.26. It can be noticed that the experimental and predicted data are in the same path that proves the best fit of this model.

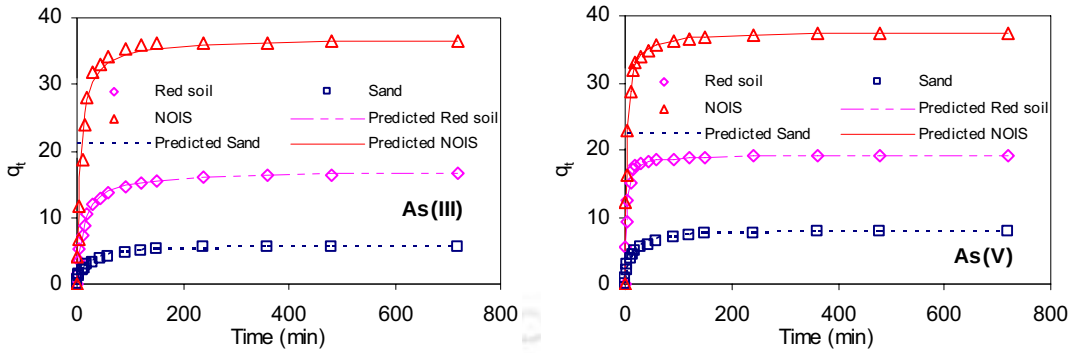

Fig. 5.23. Comparison plots of predicted model using pseudo second order reaction model and experimental data of arsenic sorption onto three different materials.

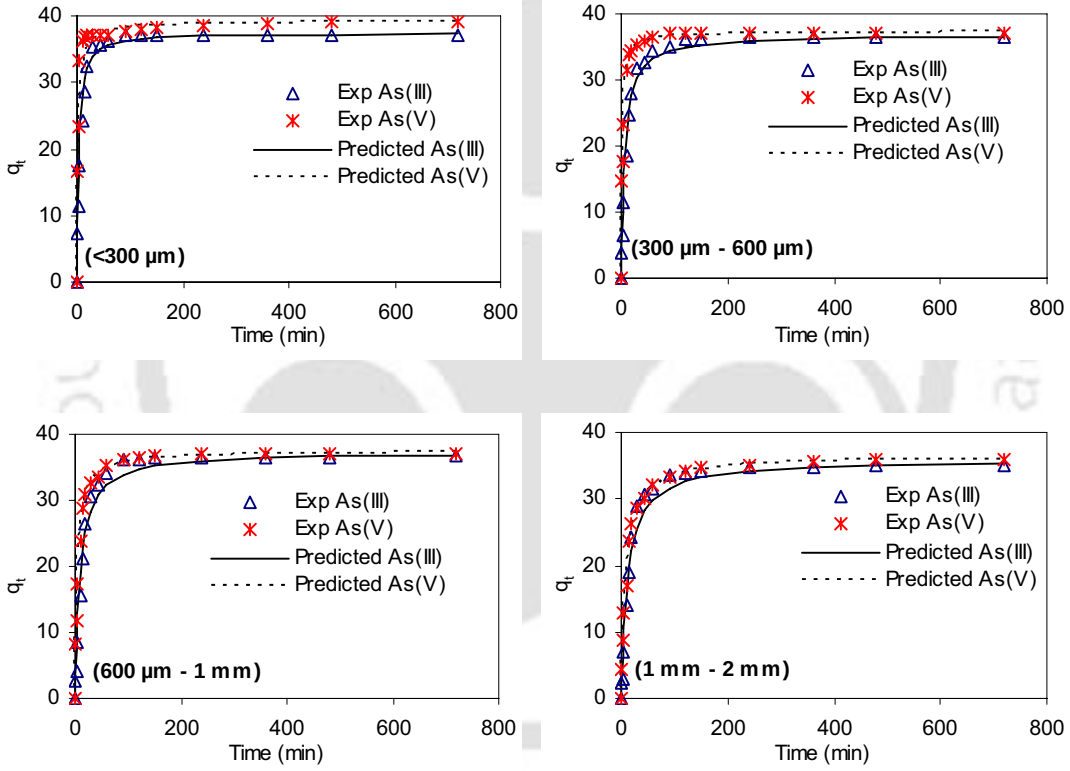

Fig. 5.24. Comparison plots of predicted model using pseudo second order reaction model and experimental data of arsenic sorption onto different size of NOIS.

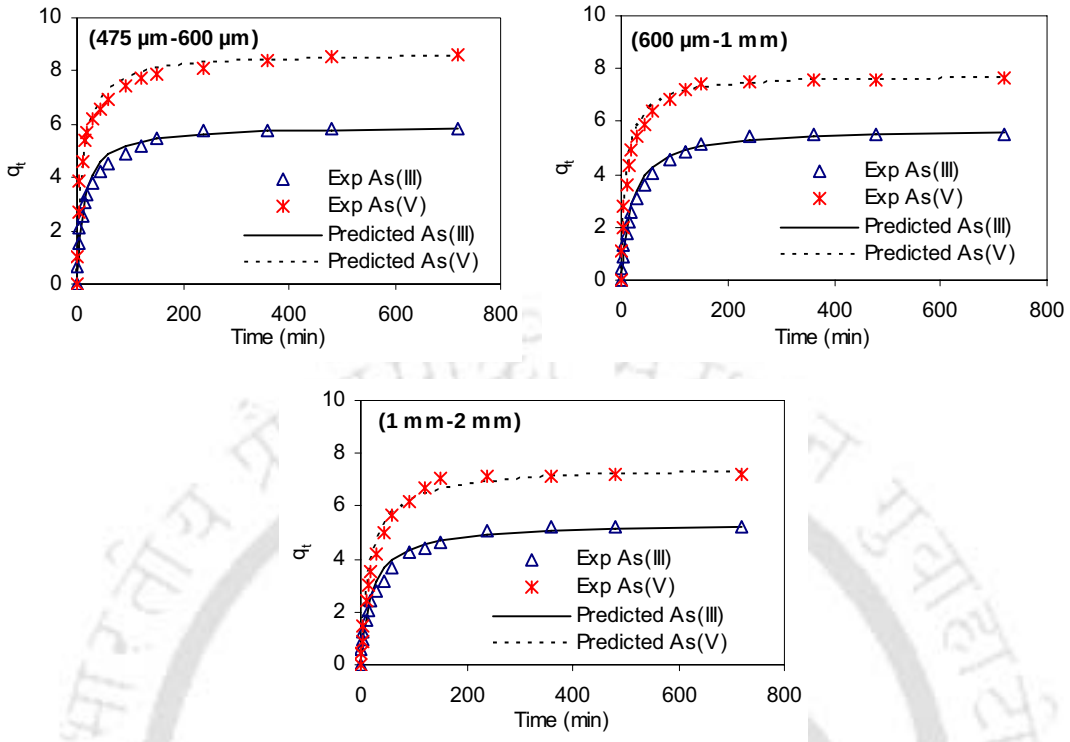

Fig. 5.25. Comparison plots of predicted model using pseudo second order reaction model and experimental data of arsenic sorption onto different size of sand particles.

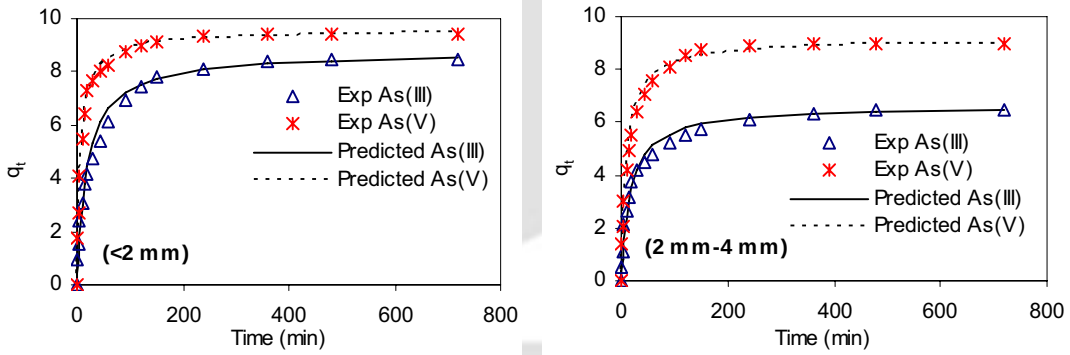

Fig. 5.26. Comparison plots of predicted model using pseudo second order reaction model and experimental data of arsenic sorption onto different size of murum.

Pseudo second order reaction model kinetic parameters for the individual adsorbents are summarized in Table 5.7 and Table 5.8 and a comparative plot of the selected adsorbent is shown Fig. B.6. Results indicate that maximum adsorption capacity (q_e) was more in the case of As(V) than As(III) and smaller particles are adsorbing larger amount of arsenic due to higher surface area. Similar trend was obtained for the variation

of k_{s2} values with the particle size and arsenic species. The k_{s2} values vary within 0.0023-0.0206 g μg^{-1} min^{-1}. The q_e values were found maximum for NOIS [36.887 μg g^{-1} for As(III) and 37.613 μg g^{-1} for As(V)] and then for red soil [As(III): 16.946 μg g^{-1} & As(V): 19.214 μg g^{-1}]. The q_e values for murum (particle size less than 2 mm) are 8.756 and 9.551μg g^{-1} for As(III) and As(V) respectively whereas for the sand, the q_e values are 5.720 and 7.992 μg g^{-1} respectively.

Table 5.7. Comparison of pseudo second order reaction model parameters for arsenic adsorption on different adsorbents.

Adsorbent	As Species	q_e (μg g^{-1})	K_{s2} (g μg^{-1} min^{-1})	R^2	*SE*
Red soil	As(III)	16.946	0.0046	0.9999	0.317
	As(V)	19.214	0.0206	1.0000	0.270
Sand	As(III)	5.720	0.0098	0.9994	0.246
	As(V)	7.992	0.0107	0.9999	0.282
NOIS	As(III)	36.887	0.0042	0.9998	2.019
	As(V)	37.613	0.0087	1.0000	0.849

Table 5.8. Pseudo second order reaction model parameters for adsorption kinetics of arsenic species on different size of adsorbents (*i.e.* NOIS, sand and murum).

Adsorbent	As Species	q_e (μg g^{-1})	K_{s2} (g μg^{-1} min^{-1})	R^2	*SE*
NOIS					
<300 μm	As(III)	37.434	0.0083	0.9999	2.4161
	As(V)	39.161	0.0115	1.0000	2.5692
300 μm - 600 μm	As(III)	36.912	0.0041	0.9998	1.9654
	As(V)	37.312	0.0163	1.0000	1.8997
600 μm-1mm	As(III)	37.381	0.0028	0.9994	2.2564
	As(V)	37.427	0.0064	1.0000	1.2939
1 mm - 2 mm	As(III)	35.919	0.0023	0.9991	2.0744
	As(V)	36.460	0.0032	1.0000	0.8371
Sand					
425 μm - 600 μm	As(III)	5.952	0.0124	0.9996	0.2791
	As(V)	8.681	0.0102	0.9997	0.5200
600 μm-1 mm	As(III)	5.716	0.0087	0.9993	0.2220
	As(V)	7.760	0.0125	0.9998	0.2723
1mm - 2mm	As(III)	5.399	0.0085	0.9989	0.2622
	As(V)	7.478	0.0072	0.9996	0.2413
Murum					
<2mm	As(III)	8.756	0.0059	0.9993	0.397
	As(V)	9.551	0.0150	1.0000	0.209
2mm-4mm	As(III)	6.619	0.0086	0.9995	0.279
	As(V)	9.128	0.0108	0.9998	0.332

5.4.4.3 Intraparticle diffusion model

To identify the sorption mechanisms in the sorption process several models have been used. Plot of q_t vs. t is analyzed for the kinetic data to ensure the control of intraparticle diffusion mechanism in the sorption process. The intraparticle diffusion plots and correlation parameters of arsenic sorption by the different grade of selected adsorbent are depicted in the Table 5.9 and Table 5.10 and the Fig. 5.27 to Fig. 5.30 to observe the behavior of the kinetic sorption process. In the Fig. 5.27 to Fig. 5.30, it can be noticed that multiple lines are presenting the sorption mechanism. Similar result was obtained for the adsorption of acid dye onto chitosan (Cheung et al., 2007). The first portion, started form the origin attributed to the external diffusion or boundary layer diffusion. Steepness of the line is the evidence of rapid sorption. The second portion, gradually increasing with the square root of time, indicates that the intraparticle diffusion is the rate limiting stage in this stage. Last portion of the curve is almost parallel to the x-axis which confirms the retardation of intraparticle diffusion and existence of low concentration of sorbate in the solute (Cheung et al., 2007; Ho and McKay, 1998). Plots of arsenic sorption onto different materials indicate that the sorption process is barely controlled by one mechanism; it also consists of intraparticle diffusion followed by film diffusion. On the other hand, it can be concluded that initially the sorption process is controlled by bulk phase to exterior surface, second portion relation to the diffusion into mesopores and third portion related to the micropores. The intraparticle diffusion parameters are calculated and showed in Table 5.9. C_{il} values were found to be zero as the plot passes through the origin.

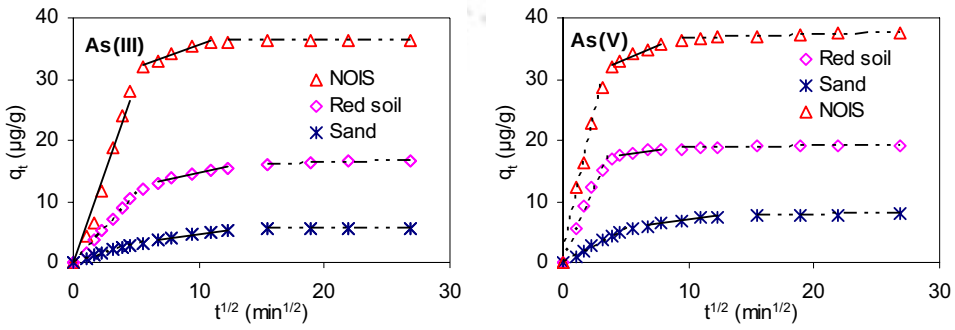

Fig. 5.27. Plots of intraparticle diffusion for arsenic [As(III) and As(V)] sorption onto NOIS, red soil and sand.

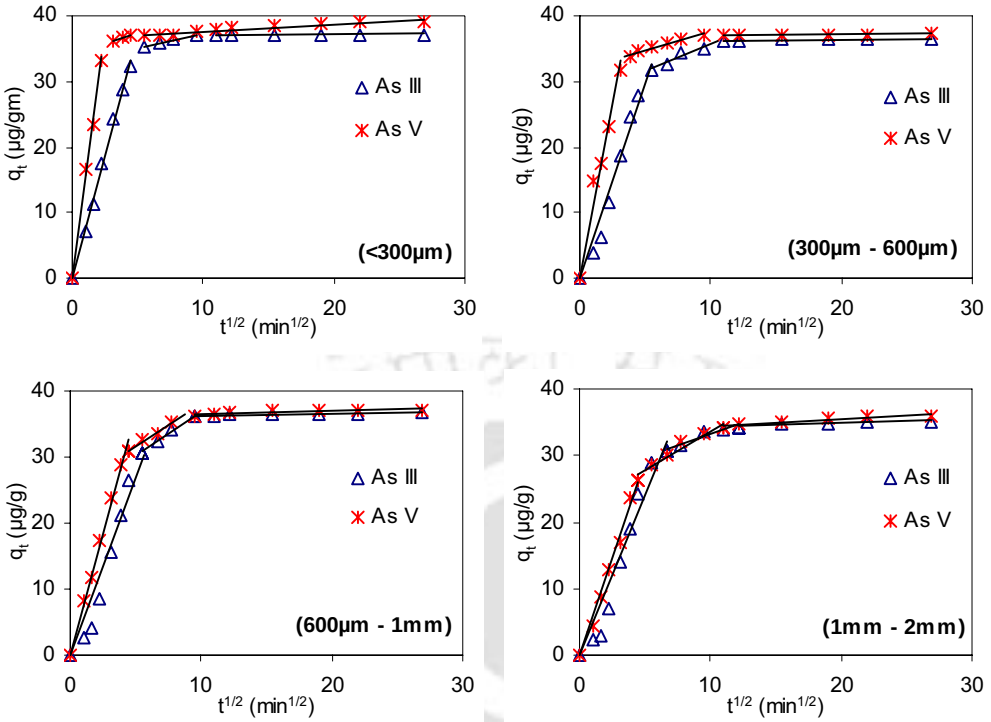

Fig. 5.28. Intraparticle diffusion plot for arsenic sorption onto the different graded NOIS.

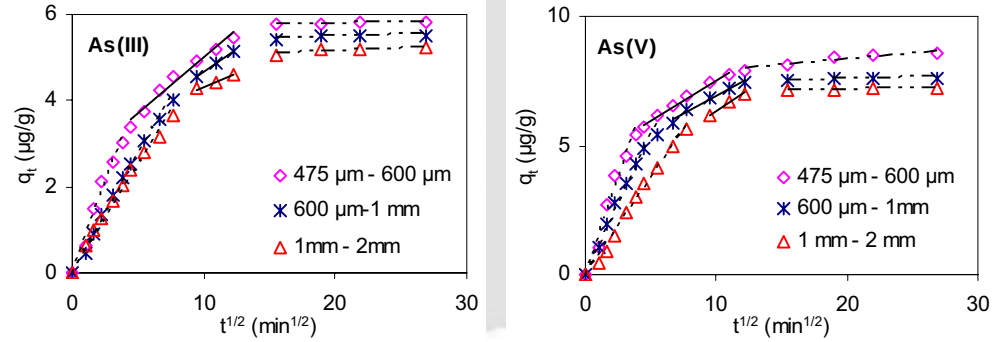

Fig. 5.29. Intraparticle diffusion plot for arsenic sorption onto different graded sand.

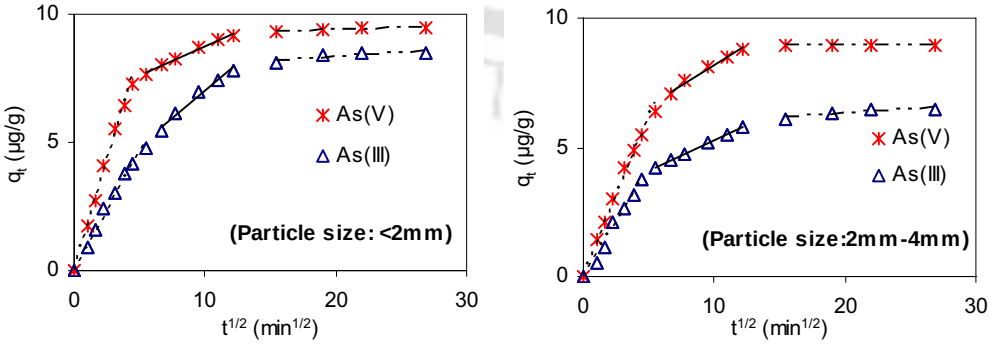

Fig. 5.30. Intraparticle diffusion plot for arsenic sorption onto different graded murum.

Table 5.9. Parameters of the intraparticle diffusion rate constant for the arsenic sorption onto red soil, sand and NOIS.

Adsorbent	As Species	K_{i1}	R_{i1}^2	C_{i2}	K_{i2}	R_{i2}^2	C_{i3}	K_{i3}	R_{i3}^2
Red soil	As(III)	2.25	0.992	10.03	0.46	0.963	15.20	0.057	0.988
	As(V)	4.81	0.959	6.50	0.26	0.965	18.46	0.029	0.851
Sand	As(III)	0.62	0.990	2.10	0.25	0.982	5.37	0.007	0.725
	As(V)	1.08	0.975	4.13	0.28	0.971	7.37	0.019	0.859
NOIS	As(III)	5.95	0.975	28.07	0.75	0.969	35.98	0.017	0.841
	As(V)	9.71	0.974	28.67	0.91	0.963	36.01	0.061	0.827

Table 5.10. Parameters of the intraparticle diffusion rate constant for the arsenic sorption onto different size of specific adsorbents.

Adsorbent	As Species	K_{i1}	R_{i1}^2	C_{i2}	K_{i2}	R_{i2}^2	C_{i3}	K_{i3}	R_{i3}^2
NOIS									
<0.3mm	As(III)	7.40	0.998	32.79	0.44	0.995	37.00	0.007	0.825
	As(V)	15.05	0.995	34.23	0.63	0.944	36.58	0.109	0.919
300 - 600µm	As(III)	5.96	0.969	27.30	0.84	0.925	36.09	0.013	0.577
	As(V)	10.49	0.959	32.09	0.54	0.961	37.03	0.006	0.964
600µm - 1mm	As(III)	5.34	0.948	23.22	1.37	0.998	35.99	0.028	0.776
	As(V)	7.28	0.991	25.06	1.31	0.974	36.00	0.050	0.629
1 - 2mm	As(III)	4.78	0.946	26.45	0.67	0.922	33.70	0.056	0.876
	As(V)	5.80	0.989	21.96	1.18	0.942	33.23	0.114	0.868
Sand									
425 - 600µm	As(III)	0.82	0.976	2.38	0.26	0.977	5.71	0.004	0.947
	As(V)	1.47	0.963	4.42	0.31	0.983	7.38	0.048	0.902
600µm -1mm	As(III)	0.54	0.994	2.46	0.22	0.997	5.33	0.008	0.628
	As(V)	1.08	0.981	4.16	0.27	0.965	7.39	0.009	0.859
1- 2mm	As(III)	0.50	0.983	3.04	0.13	0.984	4.92	0.012	0.723
	As(V)	0.74	0.992	3.29	0.31	0.993	6.99	0.009	0.935
Murum									
<2mm	As(III)	0.93	0.985	2.77	0.42	0.975	7.64	0.035	0.718
	As(V)	1.69	0.995	6.47	0.23	0.986	9.21	0.009	0.885
2 - 4mm	As(III)	0.83	0.984	2.98	0.23	0.998	5.64	0.033	0.820
	As(V)	1.24	0.990	5.11	0.31	0.978	8.85	0.004	0.918

5.4.4.4 Liquid film mass transfer model

Intraparticle diffusion model and rapid adsorption of arsenic indicates that film diffusion is playing major role in adsorption process. Boyd-Adamson-Myers Equation (5.11) was employed to the kinetic data to determine the role of film diffusion in arsenic adsorption by the described adsorbents and their kinetic rate constant. The model was employed to the initial straight portion of the plot of $\ln(1-F)$ vs. t. The values obtained from the plots of $\ln(1-F)$ vs. t, (Figs. 5.31-5.32) were tabulated in Table 5.11 and 5.12. Good coefficient of determination values supports the applicability of this model. From

the figures (Figs. 5.31-5.32), it can be observed that the initial portion of the plots is linear, which is the evidence of film diffusion. Remaining portion of the plot is confirming that film diffusion is not the rate-limiting step; some other diffusion processes are involved in sorption process. In Table 5.11 and 5.12, it can be seen that the film diffusion rate constants (K_1) are greater for As(V) sorption from aqueous medium than As(III). The K_1 values for NOIS and red soil are higher than that of sand which is an indication of higher affinity of arsenic towards the sorbent. It may be possible that red soil and NOIS contain iron oxides which are freely available for the arsenic adsorption and enhances the uptake capacity. High K_1 values are found for smaller size of particles due to lager surface area. Initial kinetic coefficients (γ) are determined for the selected adsorbents. The γ values are approximately 2 times higher for As(V) than compared to As(III). For the As(V) sorption, maximum value 41.46 x10^{-3} L$\mu g^{-1}m^{-1}$ is found for NOIS (particle size: <300µm) whereas minimum value 3.16 x10^{-3} L$\mu g^{-1}m^{-1}$ obtained for the sand (particle size: 1-2mm).

Liquid film mass transfer model (k_f) is applied to the kinetic data when t tends towards zero. Global mass transfer coefficients (k_fA_s) are determined instead of k_f to standardize the material adsorption properties. Global mass transfer coefficients (k_fA_s) are determined for all of the adsorbents. The obtained results are depicted in Tables 5.11-5.12 and Figs. 5.33-5.34. Maximum k_fA_s value was obtained as 35.96 x10^{-4} for less than 300µm size of NOIS particles. Better results were found with NOIS and red soil rather than murum and sand.

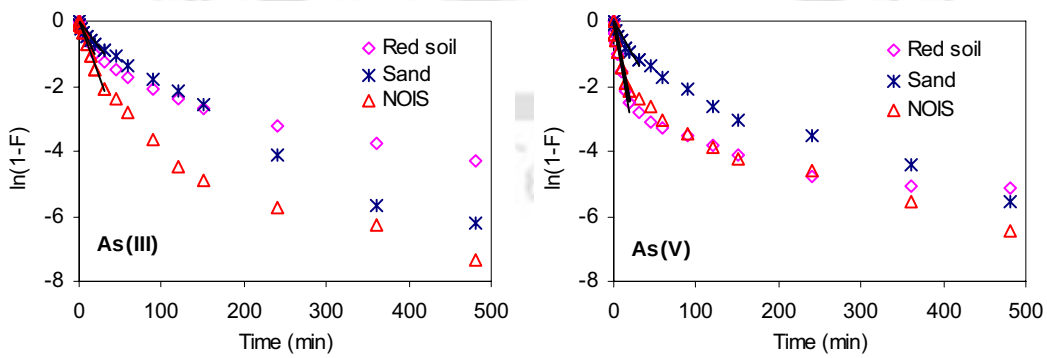

Fig. 5.31. Plots of ln(1-F) vs. t for arsenic adsorption onto different adsorbent.

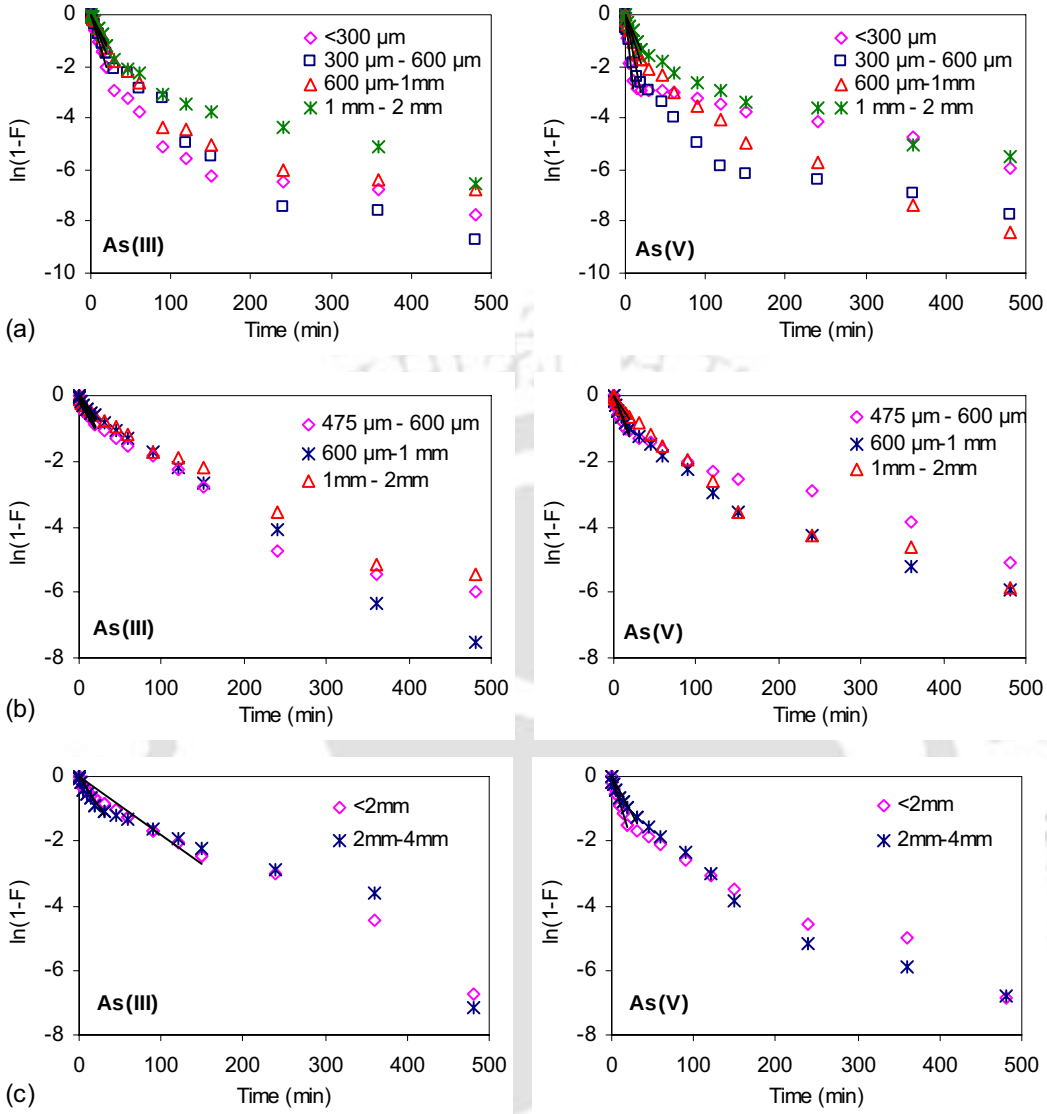

Fig. 5.32. Plots of ln(1-F) vs. *t* for arsenic adsorption onto different size of adsorbent: (a) NOIS, (b) sand and (c) murum.

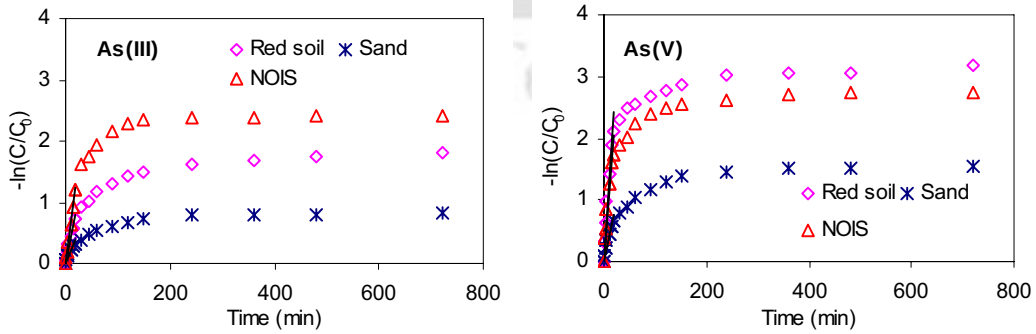

Fig. 5.33. Estimation of global external transport coefficients for the adsorption of arsenic [As(III) and As(V)] onto different adsorbent.

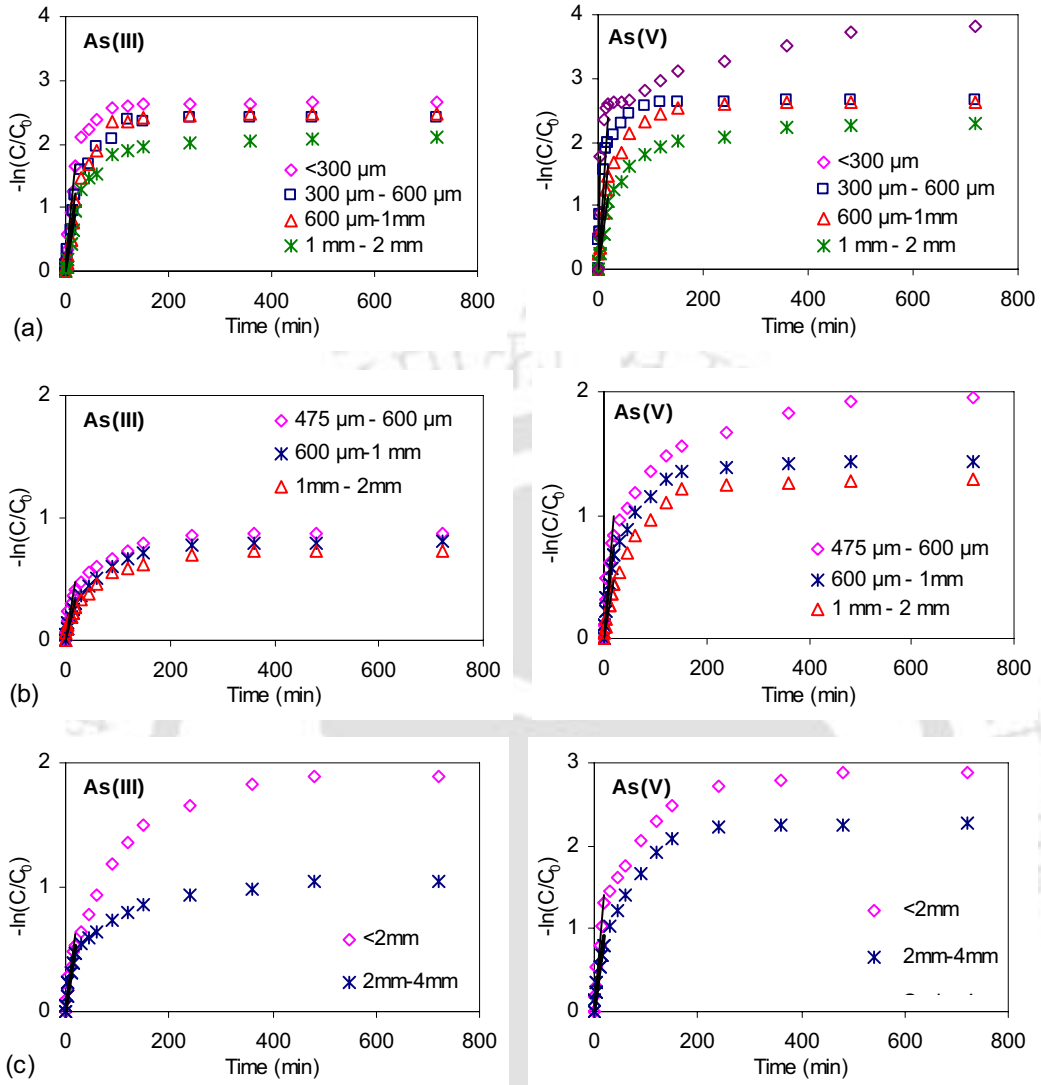

Fig. 5.34. Estimation of global external transport coefficients for the adsorption of arsenic [As(III) and As(V)] onto different size of adsorbent: (a) NOIS, (b) sand and (c) murum.

Table 5.11. Adsorption kinetics and mass transfer coefficients of arsenic sorption onto different adsorbent.

Adsorbent	Arsenic Species	K_1 (min^{-1})	R^2	γ ($L\mu g^{-1}m^{-1}$) x10^{-3}	$k_f A_s$ (m^3s^{-1}) x10^{-4}	R^2
Red Soil	As(III)	0.0517	0.9451	7.11	3.97	0.9377
	As(V)	0.1391	0.9315	17.91	12.10	0.8948
Sand	As(III)	0.0168	0.9715	2.20	1.87	0.8096
	As(V)	0.0230	0.8700	3.95	3.81	0.8497
NOIS	As(III)	0.0715	0.9978	12.79	6.15	0.9961
	As(V)	0.1216	0.8932	31.19	10.19	0.8425

Table 5.12. Adsorption kinetics and mass transfer coefficients of arsenic sorption onto different size of adsorbent.

Adsorbent	Arsenic Species	K_1 (min^{-1})	R^2	γ ($L\mu g^{-1}m^{-1}$) x10^{-3}	$k_f A_s$ (m^3s^{-1}) x10^{-4}	R^2
NOIS						
<300µm	As(III)	0.1022	0.9860	18.00	8.58	0.9729
	As(V)	0.2882	0.9088	41.68	35.96	0.9799
300µm - 600µm	As(III)	0.0738	0.9987	9.75	6.19	0.9963
	As(V)	0.1518	0.9117	37.00	11.86	0.8413
600µm - 1mm	As(III)	0.0605	0.9908	3.99	5.21	0.9954
	As(V)	0.0952	0.9623	20.88	8.09	0.9407
1mm - 2mm	As(III)	0.0551	0.9853	3.47	4.47	0.9922
	As(V)	0.0636	0.8205	10.72	5.70	0.9672
Sand						
425µm - 600µm	As(III)	0.0202	0.9401	6.07	2.42	0.7613
	As(V)	0.0636	0.8205	10.83	5.00	0.7793
600µm -1mm	As(III)	0.0167	0.9872	4.35	1.66	0.8610
	As(V)	0.0564	0.9081	8.27	3.79	0.8593
1mm - 2mm	As(III)	0.0149	0.9734	2.90	1.55	0.7815
	As(V)	0.0358	0.9757	3.16	2.37	0.9612
Murum						
<2mm	As(III)	0.0181	0.9187	3.03	3.10	0.8424
	As(V)	0.0786	0.9515	5.22	7.04	0.9375
2mm-4mm	As(III)	0.0406	0.9065	2.24	2.62	0.8964
	As(V)	0.0472	0.9028	4.00	4.52	0.8770

5.4.4.5 Richenberg model

The plots of *Bt* vs. time for arsenic sorption by different grade of sorbent are shown in Figs. 5.35-5.36. The non-linear plots of the kinetic data are the evidence of intraparticle diffusion and it is not a rate-limiting step. An attempt has been made to determine the coefficient of determinations of the linear portions, starting from the origin but poor results are obtained (not shown here).

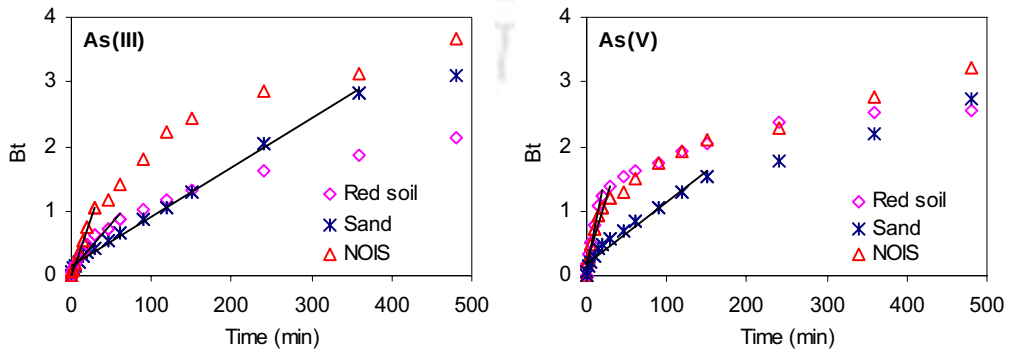

Fig. 5.35. Plots of *Bt* vs. time for sorption of arsenic onto different adsorbent.

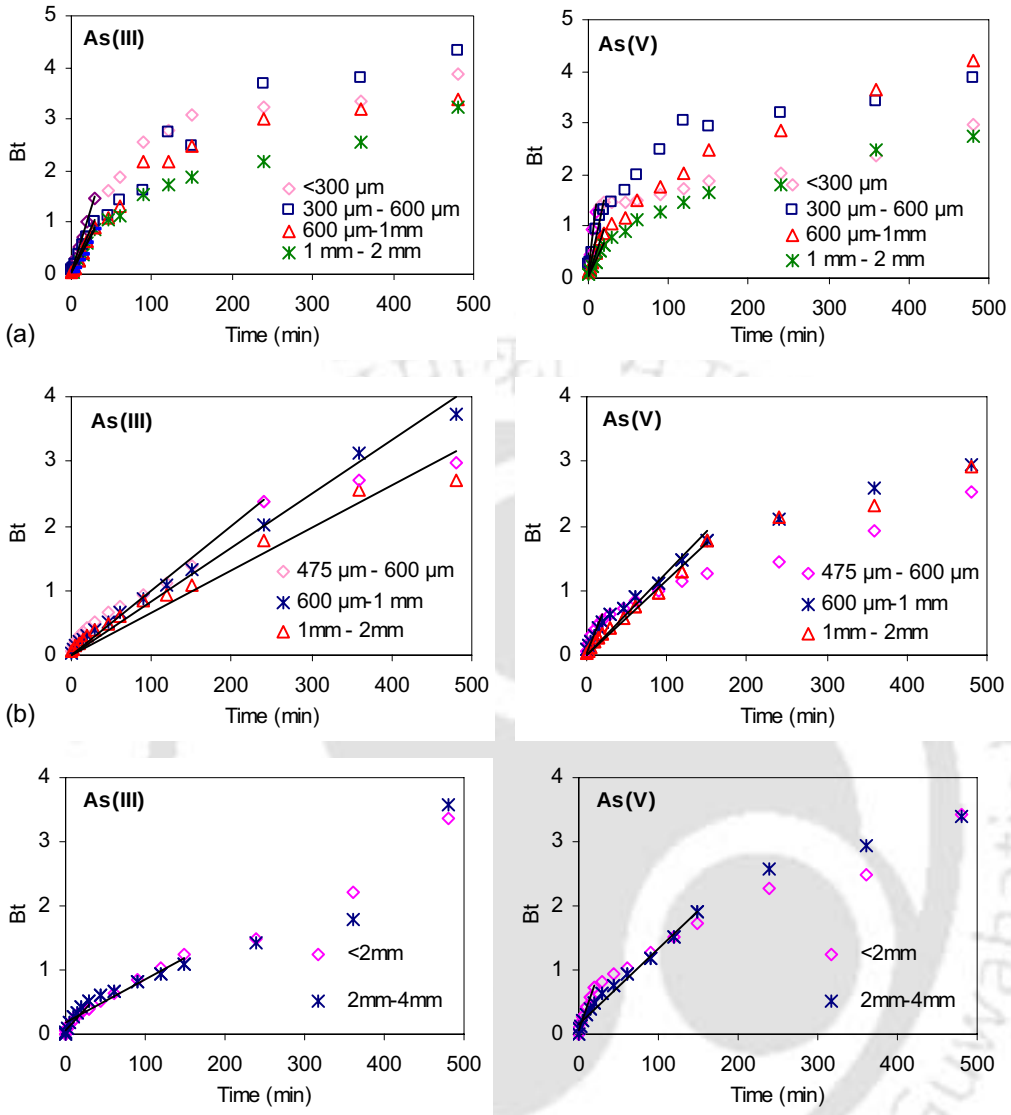

Fig. 5.36. Plots of *Bt* vs. time for sorption of arsenic onto different size of adsorbents: (a) NOIS, (b) sand and (c) murum.

5.4.4.6 Bangham's equation

Bangham's equation is applied to kinetic data to know about the slow step occurring in the adsorption process. Plots of $\ln\ln\left(\frac{C_0}{C_0 - q_t m}\right)$ vs. $\ln(t)$ for the arsenic sorption using different graded adsorbents are delineated in Tables 5.7-5.8 and Figs. 5.37-5.38. In the figures (Figs. 5.37-5.38), it can be noticed that two different straight lines

represent the total adsorption process. From the other models, it is already established that film diffusion is the rate limiting step for initial rapid adsorption process. In the relatively slow phase, the sorbate molecules are adsorbed within the pores and reach to equilibrium. The first line of the Bangham's plot is representing the film diffusion process, whereas the second straight line is confirming the pore diffusion mechanism. From the aforesaid figures it can be observed that film diffusion is playing major role for the arsenic sorption for sand, whereas for other materials both pore and film diffusion have significant contribution. The Bangham's constants with their coefficient of determinations for the both straight lines are summarized in Tables 5.13 and 5.14.

Table 5.13. Bangham's equation parameters for arsenic sorption by different adsorbent.

Adsorbent	As Species	α_1	k_{01} (ml/(g/L))	R_1^2	α_2	k_{02} (ml/(g/L))	R_2^2
Red Soil	As(III)	0.603	0.089	0.9725	0.076	0.539	0.9239
	As(V)	0.426	0.298	0.9764	0.023	0.875	0.9042
Sand	As(III)	0.429	0.036	0.9721	0.015	0.259	0.7935
	As(V)	0.429	0.062	0.9451	0.042	0.313	0.9112
NOIS	As(III)	0.668	0.199	0.9951	0.040	1.509	0.7499
	As(V)	0.376	0.615	0.9937	0.042	1.540	0.8637

Table 5.14. Bangham's equation parameters for the different graded adsorbent

Adsorbent	As Species	α_1	k_{01} (ml/(g/L))	R_1^2	α_2	k_{02} (ml/(g/L))	R_2^2
Red Soil	As(III)	0.705	0.009	0.9857	0.195	0.054	0.9049
	As(V)	0.648	0.033	0.9973	0.110	0.161	0.9464
NOIS							
<300µm	As(III)	0.519	0.368	0.9972	0.037	1.775	0.6973
	As(V)	0.282	0.931	0.9071	0.021	1.803	0.9713
300µm - 600µm	As(III)	0.696	0.187	0.9953	0.043	0.149	0.7398
	As(V)	0.322	0.723	0.9744	0.015	1.785	0.6736
600µm - 1mm	As(III)	0.815	0.118	0.9907	0.051	1.426	0.6807
	As(V)	0.465	0.411	0.9944	0.040	1.544	0.7489
1mm - 2mm	As(III)	0.863	0.091	0.9655	0.059	1.295	0.8143
	As(V)	0.601	0.233	0.9894	0.072	1.222	0.8551
Sand							
425µm - 600µm	As(III)	0.385	0.048	0.9339	0.008	0.285	0.9774
	As(V)	0.657	0.061	0.9139	0.129	0.207	0.9406
600µm -1mm	As(III)	0.479	0.028	0.9779	0.016	0.257	0.7050
	As(V)	0.409	0.066	0.9644	0.028	0.032	0.8393
1mm - 2mm	As(III)	0.411	0.033	0.9945	0.026	0.227	0.7892
	As(V)	0.570	0.028	0.9742	0.019	0.333	0.9402
Murum							
<2mm	As(III)	0.422	0.055	0.9815	0.048	0.328	0.7891
	As(V)	0.491	0.090	0.9964	0.071	0.325	0.8706
1mm-2mm	As(III)	0.650	0.030	0.9714	0.148	0.135	0.9509
	As(V)	0.394	0.079	0.9752	0.014	0.431	0.7759

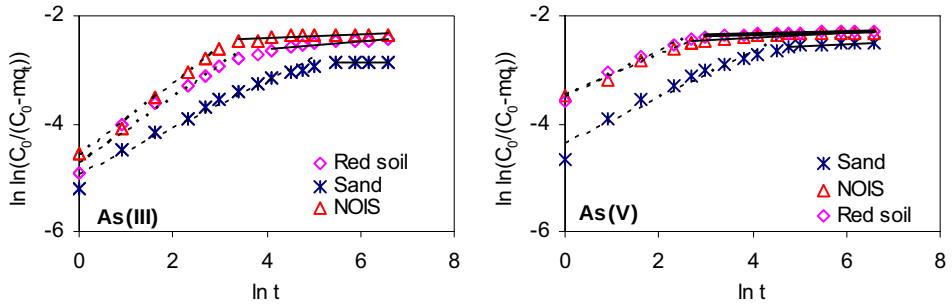

Fig. 5.37. Bangham plot for removal of arsenic by different adsorbents.

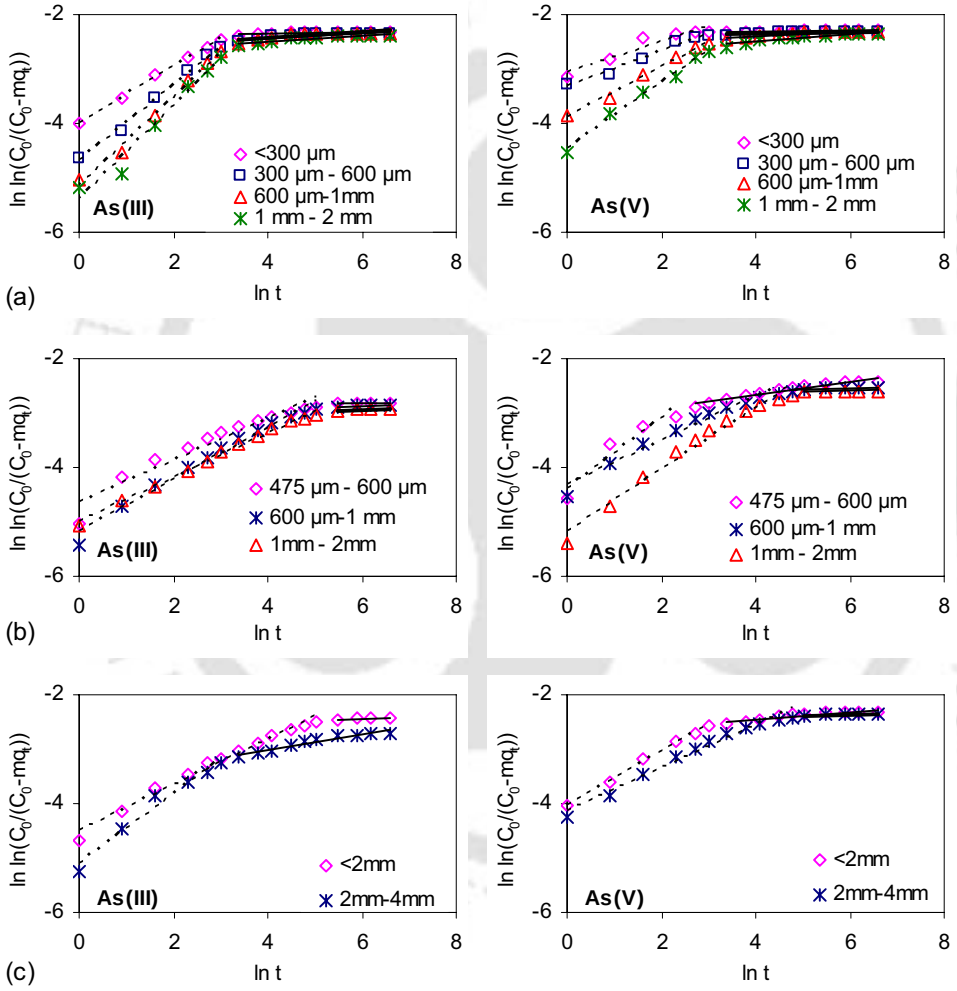

Fig. 5.38. Bangham plot for removal of arsenic by different size of adsorbents: (a) NOIS, (b) sand and (c) murum.

5.4.5 Effect of temperature

The adsorption kinetics of arsenic [As(III) and As(V)] onto red soil, sand, NOIS, murum at different temperature are shown in Fig. 5.39. The plots of arsenic adsorption capacity (q_t) vs. time (Fig. 5.39) indicate that uptake capacity of the arsenic is decreased with increasing temperature of the solution. Further these data show that temperature does affect on the nature of adsorption kinetic but it influences the overall reaction rate. Maximum uptake capacity can be observed at the lower temperature and it decreases with the increment of temperature. The plots also indicate that the both As(III) and As(V) sorption is exothermic in nature. Similar result can be observed on biosorption of arsenic using agricultural residue 'rice polish' (Ranjan et al., 2009).

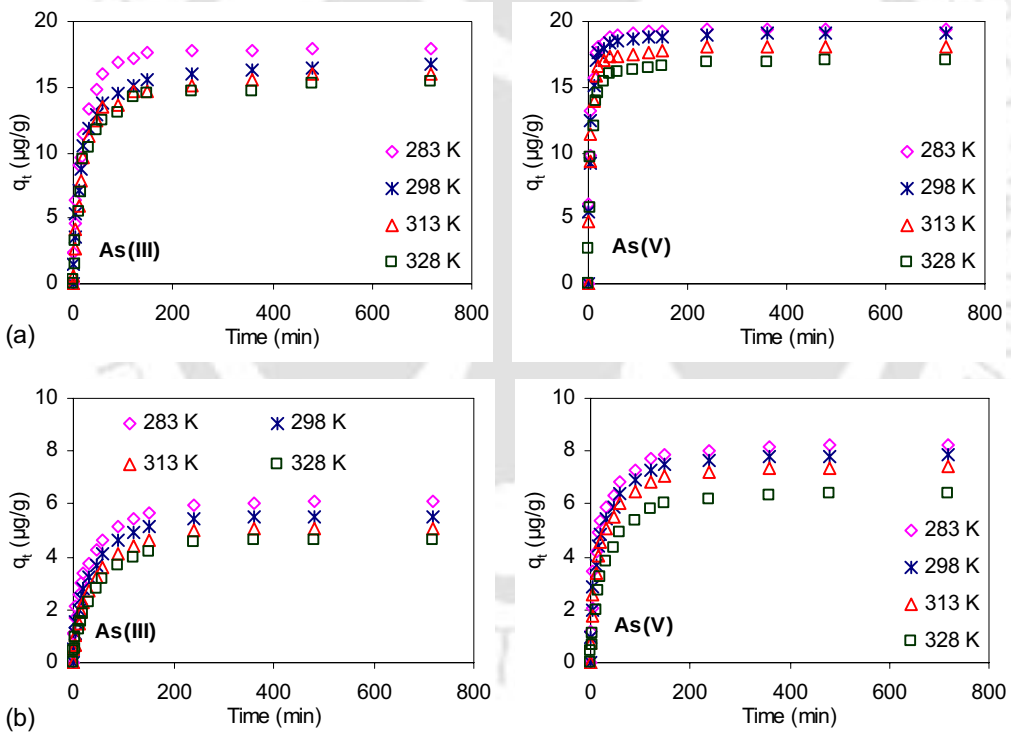

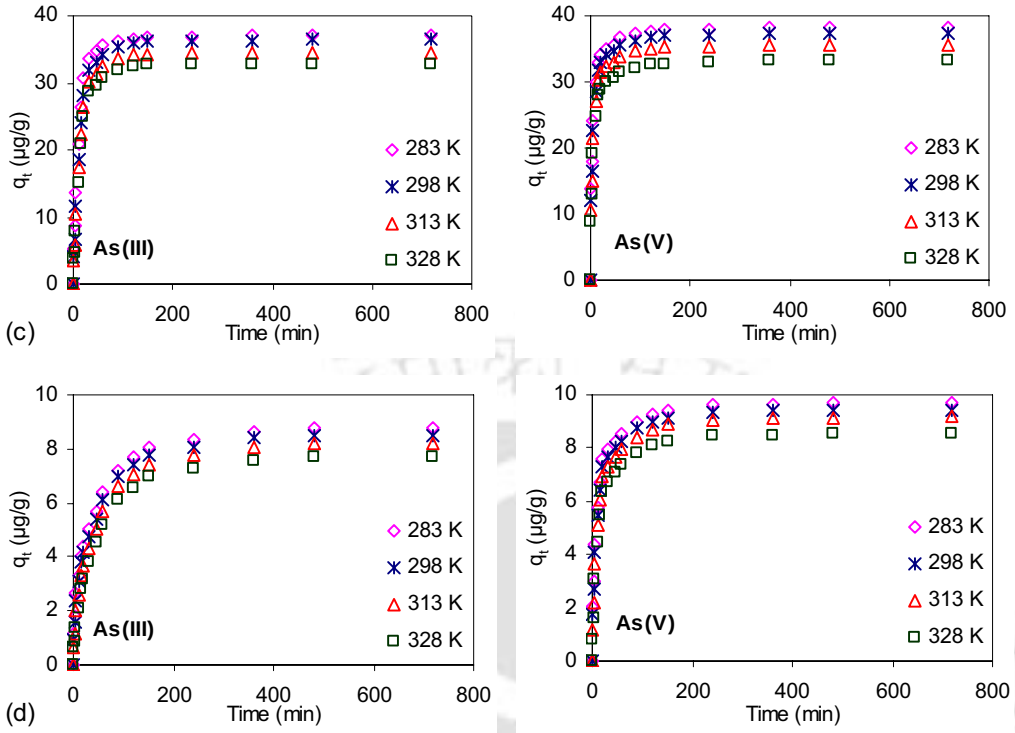

Fig. 5.39. Effect of temperature for the adsorption of arsenic [As(III) and As(V)] onto different adsorbents: (a) red soil, (b) sand, (c) NOIS and (d) murum [Matrix: Initial As(III) & As(V) concentration = 200 µg L^{-1}; adsorbent dose: red soil= 1g, NOIS = 0.5 g, sand = 2 g and murum = 2 g; volume of solution = 100 ml; agitation speed = 200 rpm and pH = 7].

5.4.6 Thermodynamics evaluation of arsenic sorption

The van't Hoff plots ($\ln K_c$ vs. 1/T) for the arsenic [As(III) and As(V)] sorption onto red soil, sand, NOIS and morum shown in Fig. 5.40. The evaluated thermodynamic parameters using the Equations (5.23) and (5.24) are summarized in Fig. 5.40 and Table 5.14. From the van't Hoff plots, negative values of change in enthalpy (H^o) and entropy (ΔS^o) are obtained. From the Table 5.14, it can be seen that Gibb's free energy of arsenic sorption (ΔG^o) values are negative except for As(III) sorption using sand at 328K. Negative ΔG^o values confirm that the adsorption process is feasible and spontaneous in nature (Sarkar et al., 2007). Increasing ΔG^o values with temperature indicate that the adsorption process is not favourable at higher temperature. The negative values of change in enthalpy (H^o) for both As(III) and As(V) sorption confirm that the adsorption process is exothermic in nature. Further negative values of entropy change (ΔS^o) in both cases

indicate that the degree of freedom of solute molecules decreases as the adsorbate adsorbed onto the surface of the adsorbent (Maji et al., 2007; Ranjan et al., 2009).

Table 5.14. Thermodynamic parameters of both As(III) and As(V) sorption.

Adsorbent	Temp-erature (K)	As(III)			As(V)		
		ΔG^o (kJmol^{-1})	ΔH^o (kJmol^{-1})	ΔS^o (Jmol^{-1}K^{-1})	ΔG^o (kJmol^{-1})	ΔH^o (kJmol^{-1})	ΔS^o (Jmol^{-1}K^{-1})
Red Soil	283	-4.95	-16.65	-41.35	-8.70	-33.43	-87.37
	298	-4.33			-7.39		
	313	-3.71			-6.08		
	328	-3.09			-4.77		
Sand	283	-1.04	-10.09	-31.98	-3.78	-16.09	-43.49
	298	-0.56			-3.13		
	313	-0.08			-2.48		
	328	0.40			-1.82		
NOIS	283	-6.15	-18.39	-43.23	-7.53	-26.99	-68.75
	298	-5.51			-6.50		
	313	-4.86			-5.47		
	328	-4.21			-4.44		
Murum	283	-4.67	-12.81	-28.74	-8.29	-29.30	-74.25
	298	-4.24			-7.17		
	313	-3.81			-6.06		
	328	-3.38			-4.95		

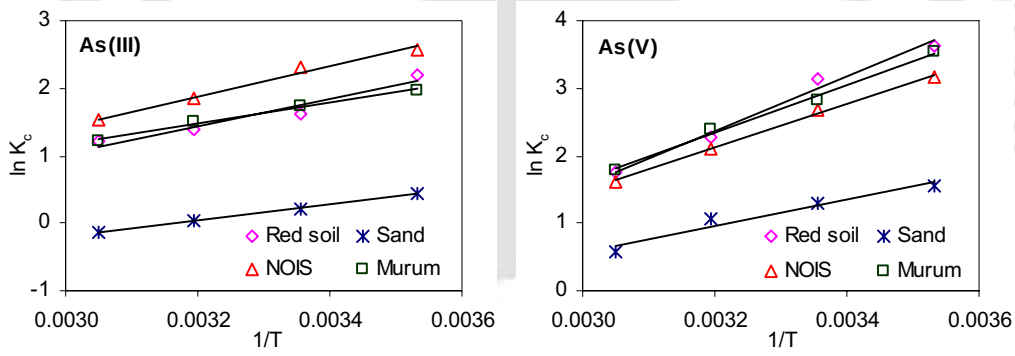

Fig. 5.40. Thermodynamic study of arsenic sorption onto several adsorbents.

5.4.7 Effect of adsorbent dose

A spreadsheet program was developed to process the experimental data of the sorption equilibrium studies. The effect of arsenic removal efficiency on different adsorbent, arsenic uptake capacity with varying adsorption dose is summarized in Table 5.16 and Table 5.17. The results confirm that all the adsorbents are more efficient on As(V) removal rather than As(III). The effect of adsorption dose on arsenic removal was

delineated in Fig. 5.41 and Fig. 5.42, which corroborate that smaller sizes of adsorbent particles (sand, NOIS and murum) adsorbs higher quantity of arsenic as they contributed more surface area for adsorption. From the Fig. 5.41 and Fig. 5.42, it can be observed that arsenic removal efficiency asymptotically increases with the increase of adsorption dose except for NOIS. At low concentration of adsorbent, the removal capacity of As(III) and As(V) is found almost same for both red soil and murum. However, at higher concentration, As(V) sorption is more. The possible reason is that at low concentration of adsorbent, approximately all the available sites used to filled up due to high competition of sorbate anions. But at low concentration of sorbate, sorption is controlled by the surface activity of sorbent and adsorption affinity towards arsenic.

Table 5.16. Comparison of arsenic removal efficiencies of different adsorbents (red soil, sand and NOIS).

Adsorbent dose (g/L)	Arsenic removal efficiency (%)					
	Red soil		Sand		NOIS	
	As(III)	As(V)	As(III)	As(V)	As(III)	As(V)
1	8.00	16.00	4.78	8.68	35.76	46.79
5	34.50	57.00	21.98	37.63	78.73	84.55
10	58.00	79.00	38.37	60.09	89.11	92.25
15	69.00	86.00	51.00	72.77	93.14	95.00
20	79.00	90.50	59.50	80.78	95.01	96.40
30	87.00	94.00	71.32	88.31	96.73	97.70
40	91.00	95.55	78.01	91.87	97.57	98.26
50	93.00	96.40	82.02	93.76	98.07	98.62

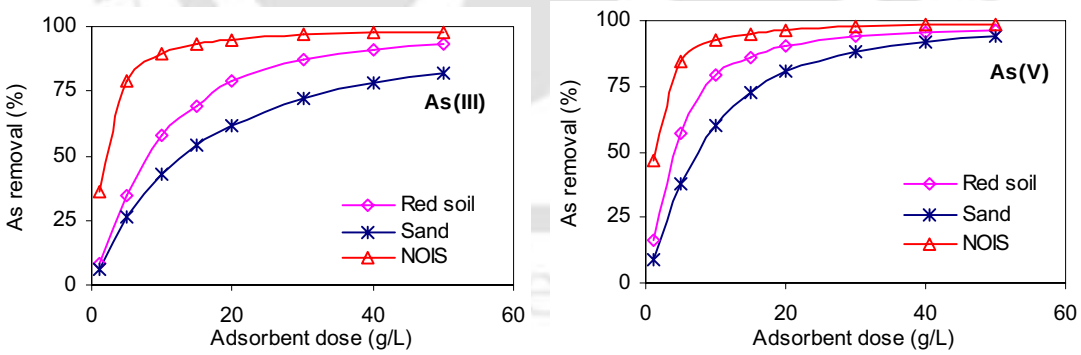

Fig. 5.41. Effect of adsorbent dose on arsenic [As(III) and As (V)] sorption by different adsorbents. [Matrix: Initial As(III) & As(V) concentration = 200 µg L^{-1}; contact time = 180 min; volume of solution = 100 ml; agitation speed = 200 rpm and pH = 7].

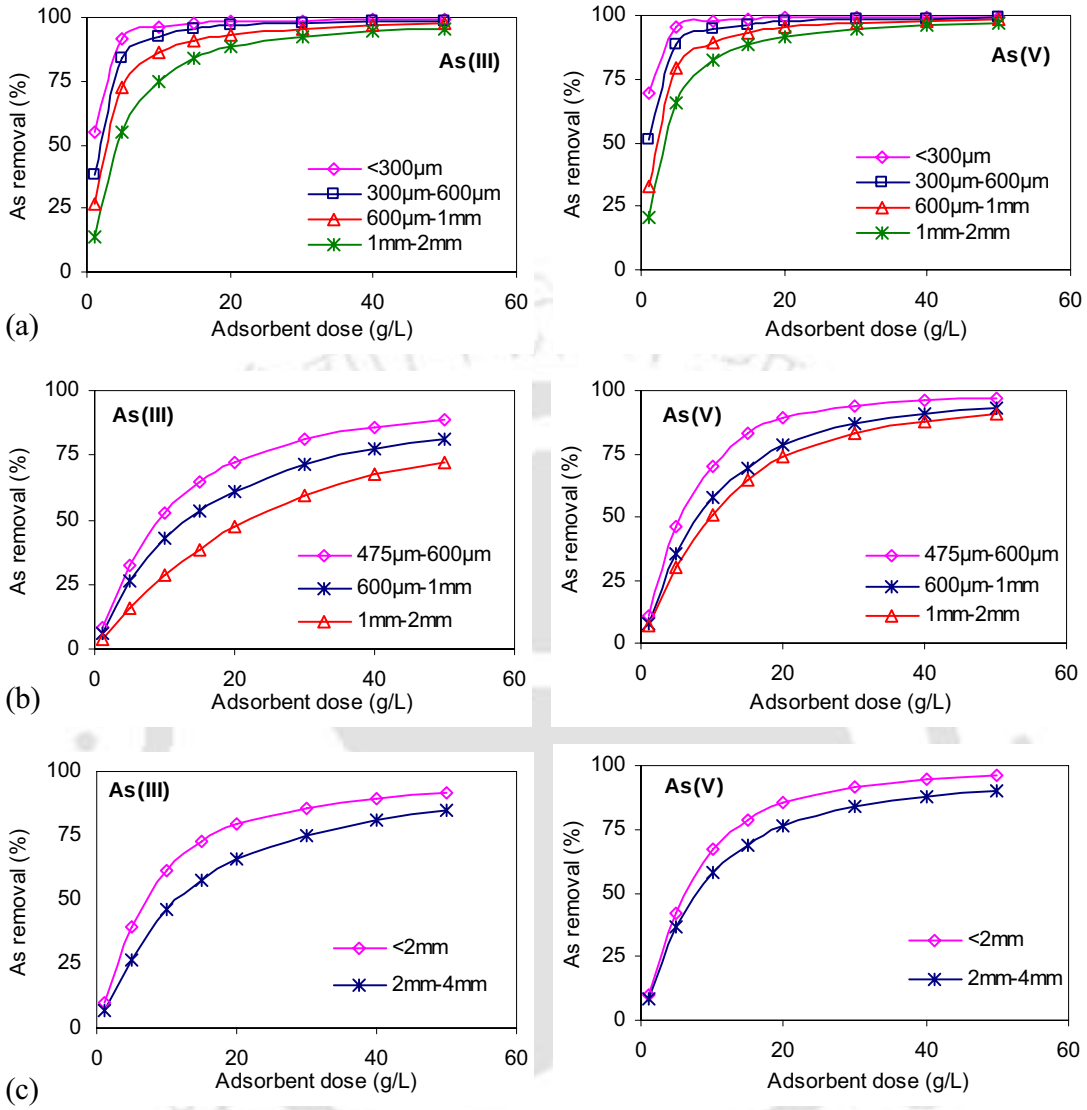

Fig. 5.42. Effects of adsorbent dose on arsenic (As(III) & As (V)) sorption by different adsorbents with their different sizes: (a) NOIS, (b) sand and (c) murum. [Matrix: Initial As(III) & As(V) concentration = 200 µg L^{-1}; contact time = 180 min; volume of solution = 100 ml; agitation speed = 200 rpm and pH = 7].

Fig. 5.42 (a) shows that the removal efficiency increases rapidly with an increase in adsorbent dose from 1 to 10 g L^{-1}; on increasing further adsorbent dose a marginal increase in sorption is observed. Initially smaller sized particles adsorb more quantity of arsenic but with the increment of adsorbent dose, the adsorption capacity started depleted [Fig. 5.42 (a)]. As iron oxides have high affinity towards arsenic, arsenic sorption is depends on the available surface area. So, deficient smaller size NOIS sorbent will adsorb

more amounts of arsenic than that with bigger size. At 20 g L^{-1} dose of red soil, 79% and 90.50% removal efficiency were observed for As(III) and As(V) respectively. To achieve 80% removal efficiency approximately more than 30 g L^{-1} of murum and sand is required for both As(III) and As(V), whereas, NOIS can accomplish with minimum 10 g L^{-1} dose with almost all graded particles.

Table 5.17. Comparison of arsenic uptake capacities of different size of adsorbents (*i.e.* NOIS, sand and murum).

As species	Adsor-bent dose (gL^{-1})	Arsenic removal efficiency (%)								
		NOIS				Sand			Murum	
		<300µm	300-600µm	600µm-1mm	1-2mm	425-600µm	600µm-1mm	1-2mm	<2mm	2-4mm
As(III)	1	55.13	37.82	26.36	13.88	8.00	6.18	3.48	10.00	6.50
	5	91.65	84.28	72.87	54.77	32.50	26.21	15.97	39.60	26.77
	10	96.15	92.66	85.93	74.88	53.00	42.81	28.83	61.70	46.00
	15	97.55	95.53	91.09	83.93	65.00	53.74	38.25	72.60	57.75
	20	98.20	96.77	93.37	88.44	72.50	61.19	47.37	79.20	66.00
	30	98.80	97.77	95.64	92.73	81.50	71.40	59.62	85.80	75.30
	40	99.10	98.26	96.78	94.73	86.00	77.29	67.36	89.10	81.15
	50	99.30	98.65	97.43	95.77	89.00	81.47	72.56	91.40	85.00
As(V)	1	69.40	50.77	32.88	20.88	11.00	7.83	6.98	10.00	8.29
	5	95.40	88.73	79.10	66.00	46.00	35.27	29.91	41.85	36.73
	10	97.80	94.60	89.48	82.28	70.00	57.32	50.84	67.25	58.38
	15	98.75	96.43	93.37	88.38	83.00	69.41	64.30	78.25	68.84
	20	99.10	97.43	95.23	91.61	89.00	78.30	73.53	85.80	76.36
	30	99.35	98.29	96.90	94.93	94.00	86.76	82.91	91.40	84.00
	40	99.50	98.77	97.71	95.99	96.00	90.88	87.69	94.50	87.81
	50	99.60	99.01	98.23	96.78	97.00	92.83	90.81	95.90	90.38

5.4.8 Equilibrium study

The equilibrium study of adsorption of arsenic species [As(III) and As(V)] for different locally available soils (i.e. red soil, sand, murum) and naturally oxidized iron scraps (NOIS) were carried out at laboratory in controlled environment. To observe the effect of particle size on arsenic adsorption, various sizes of sand (425-600 µm, 600 µm-1 mm and 1-2 mm) and NOIS (0-300 µm, 300-600 µm, 600µm-1 mm and 1-2 mm) were used for equilibrium study. The adsorption isotherms of arsenic species [As(III) and As(V)] on the selected material were shown in Fig. 5.43 and Fig. 5.44. From the Fig. 5.43 and Fig. 5.44 it can be concluded that arsenic [As(III) and As(V)] uptake capacity on

NOIS is higher than other variety of adsorbents. Moreover, particles with smaller sizes adsorb higher amount of arsenic, as they have higher surface area.

5.4.8.1 Langmuir isotherm

Langmuir isotherm constants for arsenic sorption onto different adsorbents were determined by linear regression method by plotting C_e/q_e vs. C_e (Figs. 5.43-5.44 and Table 5.18-5.19). The R^2 values of red soil and sand are above 0.99 that suggest the adsorption isotherm follows the Langmuir model. The R^2 values of NOIS are 0.96 for As(III) and 0.92 for As(V) respectively, indicating Langmuir isotherm may not be a good model for arsenic sorption. From the R^2 values of comparative fit of equilibrium data for different particle sizes of adsorbents (Table 5.19), the Langmuir model may be considered as a best fit model. From Tables 5.18 and 5.19, it can be seen that the dimensionless R_L values (0.17 to 0.69) lie within favourable limit. From the Tables 5.18 and 5.19, it can be conclude that the arsenic sorption capacity increases with decreasing particle sizes and the maximum sorption capacity is found 245.10 µg g^{-1} for As(V) sorption on NOIS.

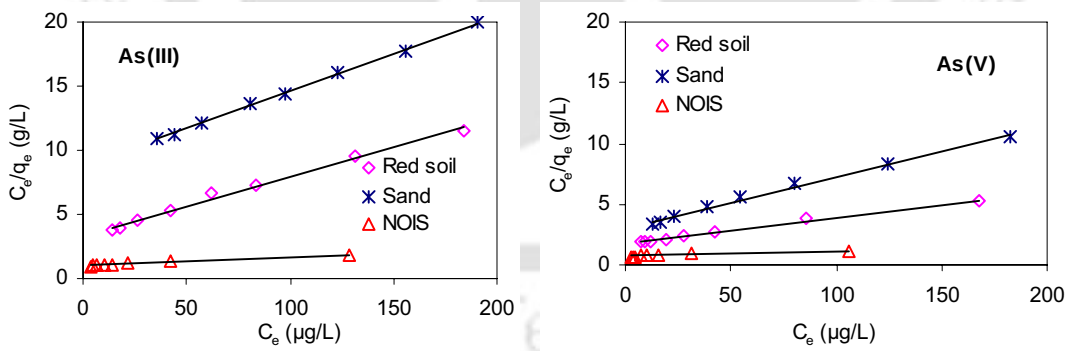

Fig. 5.43. Langmuir plots of arsenic species [As(III) and As(V)] adsorption onto different adsorbents.

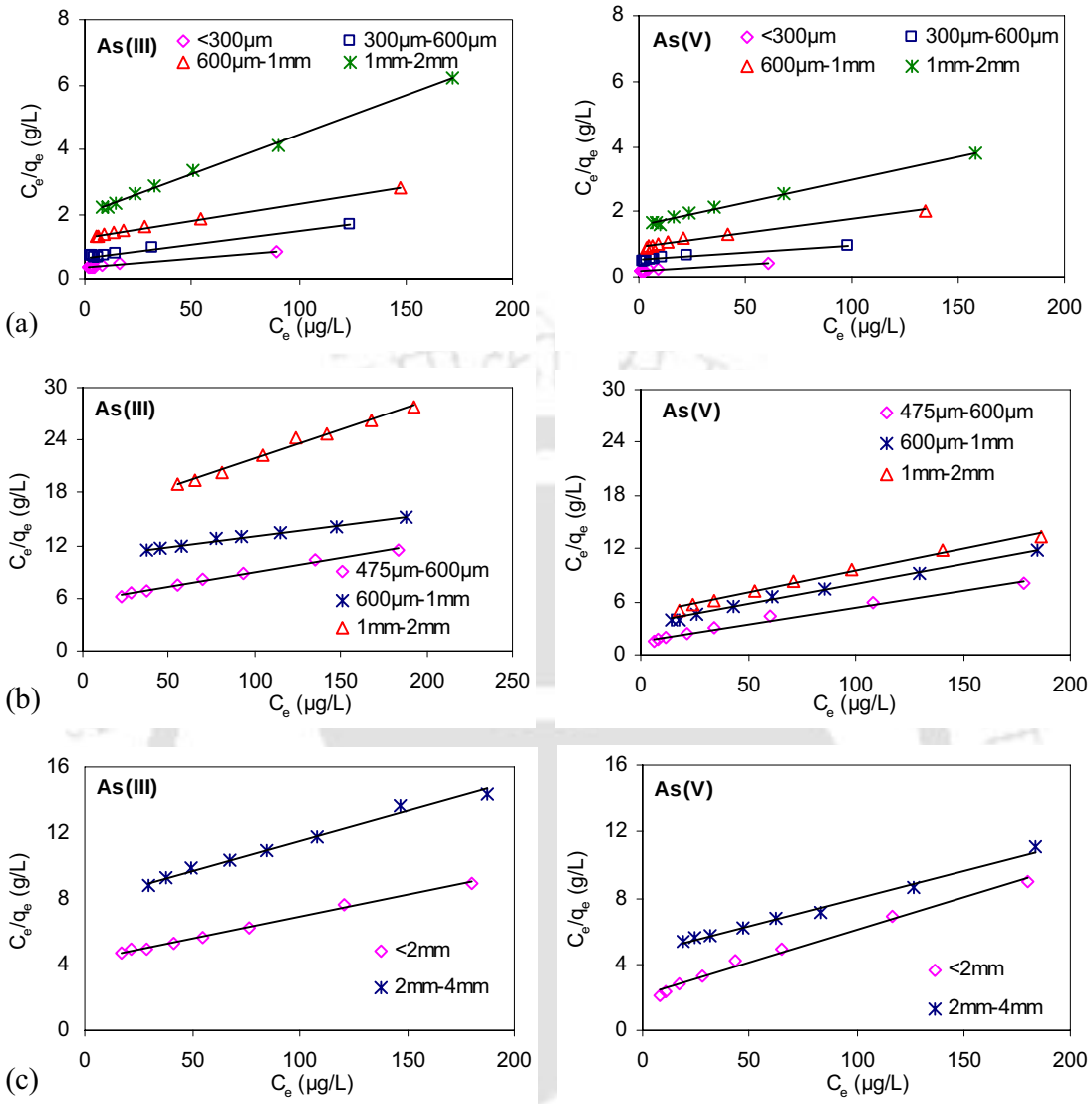

Fig. 5.44. Langmuir plots of arsenic [As(III) and As(V)] adsorption onto different size adsorbents: (a) NOIS, (b) sand and (c) murum.

Table 5.18. Langmuir isotherm parameters of various adsorbents.

Adsorbent	As Species	q_m (µg g^{-1})	b (L µg^{-1})	R^2	R_L	Remarks
Red soil	As(III)	21.86	0.0136	0.9906	0.27	Favourable
	As(V)	46.44	0.0124	0.9932	0.29	Favourable
Sand	As(III)	17.16	0.0066	0.9991	0.43	Favourable
	As(V)	23.81	0.0138	0.9937	0.27	Favourable
NOIS	As(III)	155.60	0.0064	0.9670	0.44	Favourable
	As(V)	245.10	0.0056	0.9289	0.47	Favourable

Table 5.19. Langmuir isotherm parameters of different size of adsorbents.

Adsorbent	As Species	q_m (µg g^{-1})	b (L $µg^{-1}$)	R^2	R_L	Remarks
NOIS						
<300µm	As(III)	193.92	0.0146	0.9976	0.26	Favourable
	As(V)	244.76	0.0212	0.9829	0.19	Favourable
300µm-600µm	As(III)	125.15	0.0122	0.9949	0.29	Favourable
	As(V)	210.16	0.0094	0.9913	0.35	Favourable
600µm-1mm	As(III)	96.97	0.0080	0.9972	0.38	Favourable
	As(V)	118.22	0.0091	0.9878	0.35	Favourable
1mm-2mm	As(III)	96.97	0.0080	0.9972	0.38	Favourable
	As(V)	118.22	0.0091	0.9878	0.35	Favourable
Sand						
425µm-600µm	As(III)	30.02	0.0059	0.9916	0.46	Favourable
	As(V)	26.23	0.0242	0.9881	0.17	Favourable
600µm-1mm	As(III)	41.50	0.0023	0.9935	0.69	Favourable
	As(V)	21.80	0.0135	0.9940	0.27	Favourable
1mm-2mm	As(III)	15.13	0.0043	0.9889	0.54	Favourable
	As(V)	20.12	0.0110	0.9913	0.31	Favourable
Murum						
<2mm	As(III)	37.23	0.0064	0.9969	0.44	Favourable
	As(V)	25.20	0.0188	0.9904	0.21	Favourable
2mm-4mm	As(III)	27.57	0.0046	0.9871	0.52	Favourable
	As(V)	29.60	0.0073	0.9905	0.41	Favourable

5.4.8.2 Freundlich isotherm

Freundlich isotherms for the arsenic sorption on various adsorbents are depicted in Fig. 5.45 and Fig. 5.46. The corresponding Freundlich parameters are presented in Table 5.20 and Table 5.21. The maximum adsorption capacity determined by Freundlich model, are found to be almost same or lower than Langmuir model except for the sorption of arsenic by 0-300µm and 300-600µm size of NOIS sorbent. The coefficient of determination values (R^2) show that the Freundlich model delineates the sorption isotherm better than the Langmuir model. The values of n varying from 1.16 to 1.97 indicate the favourable adsorption of arsenic on the sorbent.

Table 5.20. Freundlich parameters for arsenic removal by various adsorbents.

Adsorbent	As Species	K_F ($µg^{1-(1/n)}L^{1/ng-1}$)	n	q_m (µg g^{-1})	R^2
Red soil	As(III)	0.899	1.77	17.82	0.9911
	As(V)	1.156	1.49	40.26	0.9866
Sand	As(III)	0.345	1.56	10.35	0.9928
	As(V)	0.941	1.74	19.69	0.9924
NOIS	As(III)	1.352	1.21	109.73	0.9981
	As(V)	1.700	1.16	166.95	0.9994

Table 5.21. Comparison of Freundlich parameters for arsenic removal by different size adsorbents.

Adsorbent	As Species	K_F ($\mu g^{1-(1/n)}L^{1/ng-1}$)	n	q_m ($\mu g\ g^{-1}$)	R^2
NOIS					
0-300µm	As(III)	3.335	1.24	241.97	0.9921
	As(V)	5.509	1.22	417.90	0.9903
300µm-600µm	As(III)	2.064	1.28	128.33	0.9866
	As(V)	2.393	1.19	202.92	0.9963
600µm-1mm	As(III)	1.166	1.27	75.61	0.9929
	As(V)	1.549	1.27	99.94	0.9952
1mm-2mm	As(III)	1.166	1.27	75.61	0.9929
	As(V)	1.549	1.27	99.94	0.9952
Sand					
425µm-600µm	As(III)	0.416	1.42	17.56	0.9967
	As(V)	1.712	1.97	25.31	0.9896
600µm-1mm	As(III)	0.163	1.20	13.41	0.9990
	As(V)	0.874	1.76	17.80	0.9912
1mm-2mm	As(III)	0.192	1.46	7.21	0.9968
	As(V)	0.699	1.72	15.08	0.9948
Murum					
0-2mm	As(III)	0.492	1.37	23.33	0.9904
	As(V)	1.319	1.86	22.86	0.9911
2mm-4mm	As(III)	0.290	1.37	13.98	0.9957
	As(V)	0.490	1.43	19.80	0.9853

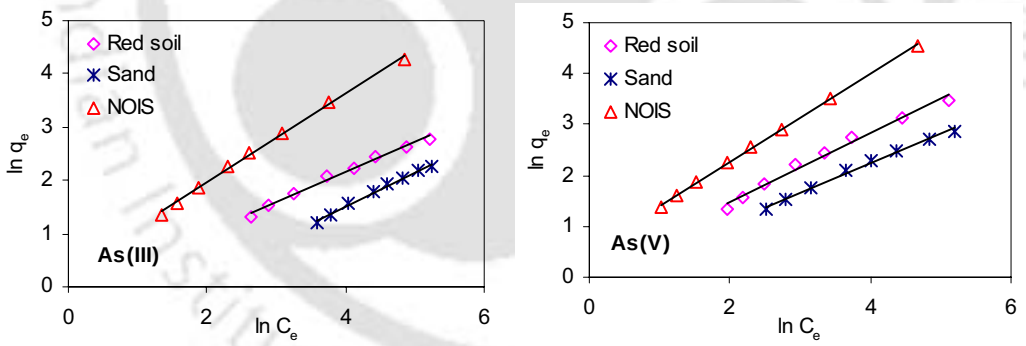

Fig. 5.45. Freundlich plots of arsenic [As(III) and As(V)] adsorption on different adsorbent.

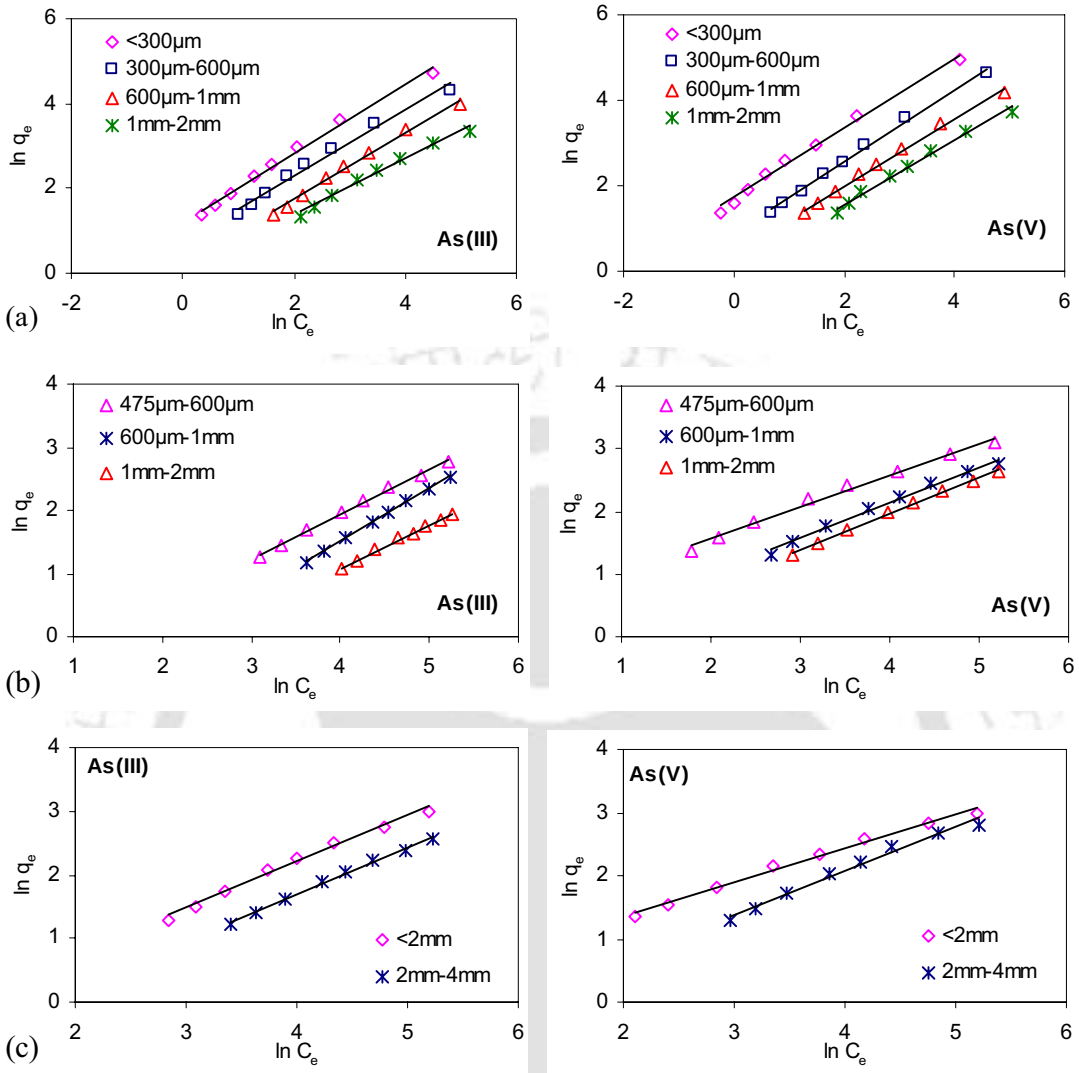

Fig. 5.46. Freundlich plots of arsenic species [As(III) and As(V)] adsorption on different size of adsorbents: (a) NOIS, (b) sand and (c) murum.

5.4.8.3 Redlich-Peterson (R-P) isotherm

The R-P equation was solved by minimizing the root mean square errors (RMSE) & maximizing the coefficient of determination (R^2) between predicted data for q_e and the experimental equilibrium data, using the solver add-in function in MS excel spreadsheet. The R-P isotherm constants for arsenic sorption were summarized in Table 5.22 and Table 5.23. Low RMSE value and high coefficient of determination (R^2) confirmed the best fit of experimental data in the R-P model.

Table 5.22. Comparison of R-P isotherm parameters for arsenic sorption by different adsorbents.

Adsorbent	As Species	α_R (L μg^{-1})	β	K_R (L g^{-1})	R^2	RMSE
Red soil	As(III)	0.0639	0.7742	0.3998	0.9971	0.0363
	As(V)	0.0227	0.9028	0.6194	0.9902	0.0935
Sand	As(III)	0.0100	0.8172	0.1072	0.9771	0.0701
	As(V)	0.0758	0.7483	0.4529	0.9997	0.0126
NOIS	As(III)	0.0815	0.5438	1.2000	0.9932	0.0499
	As(V)	0.1990	0.3690	1.8640	0.9883	0.0460

Table 5.23. Comparison of R-P isotherm parameters for arsenic sorption by different particle size of adsorbents.

Adsorbent	As Species	α_R (L μg^{-1})	β	K_R (L g^{-1})	R^2	RMSE
NOIS						
<300µm	As(III)	0.0362	0.8031	2.9602	0.9851	0.1264
	As(V)	1.3134	0.2592	12.5477	0.8398	0.1519
300µm-600µm	As(III)	0.0946	0.5787	1.7831	0.8940	0.2387
	As(V)	0.0550	0.6457	2.1781	0.9913	0.0733
600µm-1mm	As(III)	0.0163	0.8703	0.8101	0.9977	0.0448
	As(V)	0.0749	0.6195	1.2859	0.9956	0.0467
1mm-2mm	As(III)	0.0263	0.8626	0.5337	0.9969	0.0477
	As(V)	0.0854	0.6035	0.7926	0.9624	0.1235
Sand						
425µm-600µm	As(III)	0.0283	0.7498	0.2079	0.9987	0.0192
	As(V)	0.1632	0.7404	1.0511	0.9996	0.0164
600µm-1mm	As(III)	0.0159	0.6800	0.1038	0.9944	0.0271
	As(V)	0.0643	0.7678	0.3915	0.9978	0.0308
1mm-2mm	As(III)	0.0079	0.9075	0.0692	0.9913	0.0359
	As(V)	0.0773	0.7181	0.3194	0.9990	0.0172
Murum						
<2mm	As(III)	0.0062	1.0000	0.2351	0.9943	0.0588
	As(V)	0.1815	0.6840	0.8260	0.9984	0.0284
2mm-4mm	As(III)	0.0138	0.8199	0.1379	0.9923	0.0437
	As(V)	0.0068	1.0000	0.2121	0.9942	0.0566

5.4.8.4 Dubinin-Raduhkevich (D-R) isotherm

Tables 5.24 and 5.25 present the D-R isotherm constants determined by linear regression using a spreadsheet routine programme. The maximum adsorption capacity, q_m, of the all adsorbents determined by D-R isotherm model are found very low than other models. Determined free energy (E) values less than 8 $kJmol^{-1}$ indicate that the sorption process is of physical nature (Mall et al., 2005). The values of coefficient of

determinations, R^2, are the lowest, in comparison to the values of other three models (Langmuir, Freundlich and R-P model). Thus, it may be concluded that D-R isotherm does not interpreted the equilibrium data satisfactorily.

Table 5.24. Comparison of D-R isotherm parameters for arsenic sorption by various adsorbents.

Adsorbent	As Species	q_m (μg g^{-1})	E (kJ mol^{-1})	R^2
Red soil	As(III)	11.47	0.1064	0.8134
	As(V)	17.50	0.1716	0.7748
Sand	As(III)	9.91	0.0429	0.8676
	As(V)	12.07	0.1161	0.7981
NOIS	As(III)	23.90	0.2736	0.6695
	As(V)	26.54	0.3562	0.6481

Table 5.25. Comparison of D-R isotherm parameters for arsenic sorption by different particle size of adsorbents.

Adsorbent	As Species	q_m (μg g^{-1})	E (kJ mol^{-1})	R^2
NOIS				
<300μm	As(III)	29.75	0.6036	0.6571
	As(V)	36.39	0.8739	0.6981
300μm-600μm	As(III)	26.16	0.3631	0.6990
	As(V)	27.88	0.4677	0.6471
600μm-1mm	As(III)	21.60	0.2174	0.7072
	As(V)	23.02	0.2978	0.6673
1mm-2mm	As(III)	16.32	0.1505	0.7773
	As(V)	19.89	0.1821	0.7485
Sand				
425μm-600μm	As(III)	11.42	0.0670	0.8255
	As(V)	13.77	0.2222	0.7584
600μm-1mm	As(III)	9.94	0.0414	0.8645
	As(V)	11.47	0.1040	0.8174
1mm-2mm	As(III)	6.59	0.0336	0.9270
	As(V)	10.32	0.0843	0.8139
Murum				
<2mm	As(III)	13.48	0.0803	0.8227
	As(V)	12.87	0.1696	0.7524
2mm-4mm	As(III)	10.06	0.0515	0.8537
	As(V)	12.33	0.0745	0.8402

5.4.8.5 Temkin isotherm

To plot the Temkin equation, the maximum adsorption capacity (q_m) is derived from Freundlich equation. The Temkin isotherm plots and the parameters are depicted in Tables 5.26-5.27 and Figs. 5.47-5.48. Positive adsorption energy indicates that the adsorption reaction is exothermic. The correlations of determination values (R^2) of the arsenic sorption by different adsorbents reveal that the Temkin model can represent the equilibrium data satisfactory.

Table 5.26. Temkin isotherm parameters of red soil, sand and NOIS.

Adsorbents	As Species	K_0 (µg L^{-1})	ΔQ (kJ mol^{-1})	R^2
Red Soil	As(III)	0.1380	9.33	0.9850
	As(V)	0.1718	11.44	0.9685
Sand	As(III)	0.0628	6.76	0.9958
	As(V)	0.1439	9.59	0.9851
NOIS	As(III)	0.2055	15.08	0.8786
	As(V)	0.2587	18.26	0.8467

Table 5.27. Comparison of Temkin isotherm parameters of arsenic sorption by different size of adsorbents.

Adsorbents	As Species	K_0 (µg L^{-1})	ΔQ (kJ mol^{-1})	R^2
NOIS				
<300µm	As(III)	0.4894	24.36	0.8844
	As(V)	0.8342	34.83	0.8757
300µm-600µm	As(III)	0.3002	17.53	0.9200
	As(V)	0.3535	21.23	0.8701
600µm-1mm	As(III)	0.1776	13.31	0.9265
	As(V)	0.2298	15.21	0.9024
1mm-2mm	As(III)	0.1539	10.88	0.9749
	As(V)	0.1618	12.07	0.9441
Sand				
425µm-600µm	As(III)	0.0727	7.58	0.9758
	As(V)	0.2856	11.88	0.9817
600µm-1mm	As(III)	0.0427	5.94	0.9751
	As(V)	0.1346	9.28	0.9866
1mm-2mm	As(III)	0.0437	5.63	0.9907
	As(V)	0.1084	8.48	0.9860
Murum				
<2mm	As(III)	0.0840	8.37	0.9807
	As(V)	0.2077	10.83	0.9815
2mm-4mm	As(III)	0.0572	6.73	0.9804
	As(V)	0.0837	8.18	0.9880

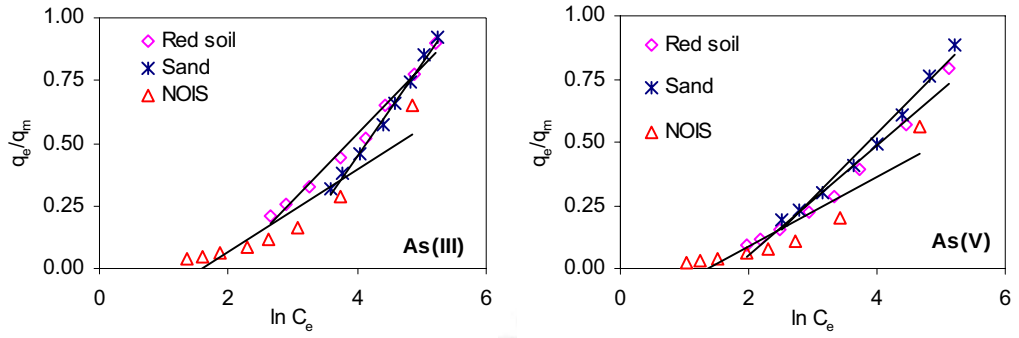

Fig. 5.47. Temkin plots of arsenic [As(III) and As(V)] sorption by various adsorbents.

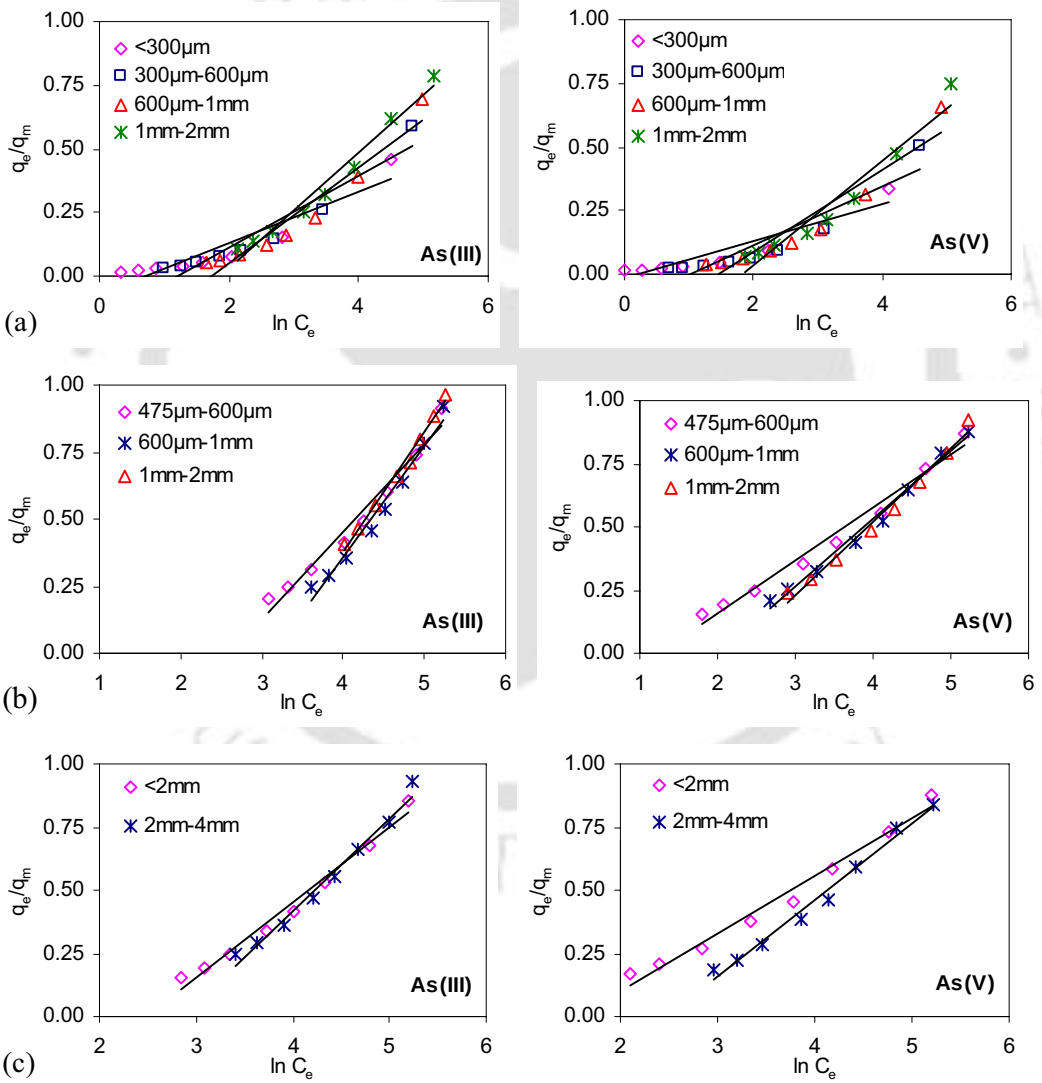

Fig. 5.48. Temkin plots of arsenic [As(III) and As(V)] adsorption by different size of adsorbents: (a) NOIS, (b) sand and (c) murum.

From all the results of the equilibrium study (Tables 5.16-5.27 and Figs. 5.41-5.48), it is clear that As(V) can be removed efficiently than As(III) by all of the adsorbents and arsenic removal capacity is more for lesser size of particles. Based on the coefficient of determination, it may be concluded that Freundlich model is the best fit model for the adsorption of arsenic. However, Langmuir and R-P model is also applicable for describing the equilibrium data. The isotherm models can be arranged in order of excellent fit of the equilibrium data as: Freiundlich > Redlich-Peterson >Langmuir >Temkin >Dubinin-Radushkevich. The experimental data confirm that NOIS can remove arsenic to a greater extent. Based on the adsorption capacity (Tables 5.16-5.27 and Table B.1) , the materials can be arranged in the following order: NOIS> red soil > murum> sand.

5.4.9 Effect of initial arsenic concentration

The adsorptions of arsenic [both As(III) and As(V)] onto the selected adsorbents were studied by varying initial arsenic concentration at ambient temperature (25 ± 1^0C) and contact time of 3 h. The results are represented in tabular (Table 5.28) form as percentage removal versus initial arsenic concentration. The initial As(III) concentration was increased from 100 µg L^{-1} to 500 µg L^{-1} and the corresponding removal efficiency gradually decreases from 98.65 % to 87.16% for NOIS. Similarly, As(V) removal efficiency by NOIS was decreased from 99.76% to 91.88%. For the other adsorbents (sand, red soil and murum) similar trend can also be observed. It is clear from the Table5.28 that there was appreciable decrease in percentage removal with increase in concentration of arsenic sample. This may because of the fact that for the lower adsorbate concentration sufficient amounts of free sites are available which results maximum removal of the adsorbate. Whereas for higher adsorbate concentration all the limited free sites of adsorbents are occupied by the competitive adsorbate and all the available sites of adsorbents are saturated. The excess amounts of adsorbate are remained in the solution (Mondal et al., 2008). From Fig. 5.49 it can be noticed that the decreasing rate of adsorption with the increase in initial arsenic concentration is higher for sand than that with red soil and murum. In both As(III) and As(V) removal efficiencies of NOIS were

slightly decreased whenever the initial arsenic concentration was increased to a greater extent. This is because of the fact that the adsorption capacity of the NOIS is higher and many free sites are available for arsenic adsorption. Although the arsenic concentration in the bulk solution was increased significantly vacant sites still available for adsorption. In case of other adsorbents, the numbers of free sites are less compared to the presence of adsorbate. The result is that the adsorbate molecules remain in the solution and affect on the removal efficiency of the adsorbents. From the Fig. 5.49 the adsorbents can be ordered according to decrease in removal efficiency of the initial arsenic concentration as NOIS, murum, red soil and sand.

Table 5.28. Effect of initial arsenic concentrations on arsenic sorption on NOIS, sand, red soil and murum.

Adsorbent	Arsenic species	Initial arsenic concentration (µg L^{-1})							
		100	200	300	500	100	200	300	500
		As removal efficiency (%)				As Adsorption Capacity (µg g^{-1})			
NOIS	As(III)	98.65	91.56	88.59	87.16	19.73	36.62	53.16	87.16
	A(V)	99.76	95.13	92.87	91.88	19.95	38.05	55.72	91.88
Sand	As(III)	66.53	55.50	46.88	24.70	3.33	5.55	7.03	6.18
	A(V)	89.41	77.90	54.57	37.95	4.47	7.79	8.19	9.49
Red soil	As(III)	95.61	83.80	71.37	44.72	9.56	16.76	21.41	22.36
	A(V)	96.63	95.19	89.54	57.95	9.66	19.04	26.86	28.97
Murum	As(III)	88.18	83.69	74.89	62.50	4.41	8.37	11.23	15.63
	A(V)	97.86	94.45	86.31	74.41	4.89	9.45	12.95	18.60

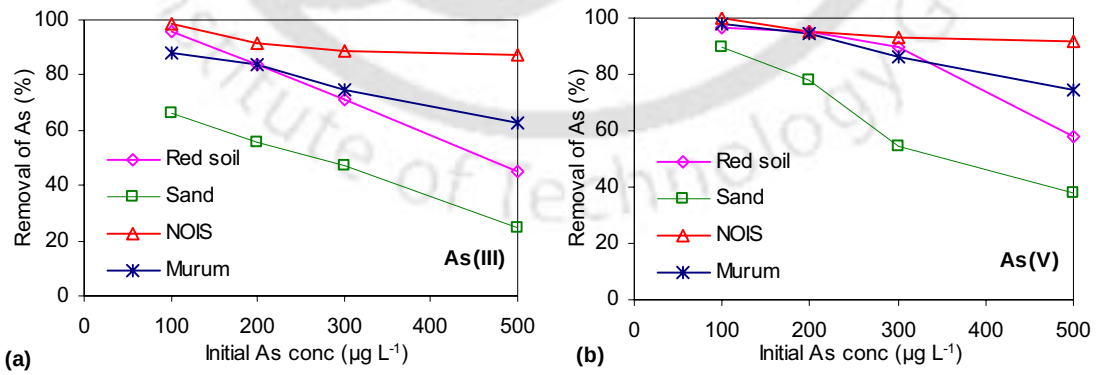

Fig. 5.49. Effect of initial arsenic concentrations for adsorption of (a) As(III) and (b) As(V) onto the surface of NOIS, sand, red soil and murum [Matrix: Volume of the solution= 100 ml; agitation speed= 200 rpm; contact time= 180 min; adsorbent dose: red soil= 1 g, NOIS= 0.5 g, sand= 2 g and murum= 2 g; temperature = 25±1ºC and pH = 7].

5.4.10 Effect of coexisting ions on arsenic removal

In rural area of Assam, groundwater is the major drinking water source. Some parts of Assam are highly polluted with arsenic contamination. Groundwater is composite of cations and anions that can play significant role on arsenic sorption by the adsorbents. To evaluate the effect of hardness on arsenic adsorption, Ca^{2+} and Mg^{2+} were utilized in the present study, as they are the major component of hardness. In reducing environment, the groundwater of Assam generally contain high concentration of ferrous iron that oxidizes to ferric iron when comes in contact with oxygen. The oxidation of Fe^{2+} to Fe^{3+} is a time dependent process and influenced by oxygenation rate, pH, quantity and oxidation/reduction potential. Hence, iron is the important parameter that can affect on arsenic adsorption process. The effects of both Fe^{2+} and Fe^{3+} ions on arsenic adsorption onto the selected adsorbents were estimated. The effect of phosphate (PO_4^{3-}), sulfate (SO_4^{2-}) and alkalinity (HCO_3^{2-}) were estimated as their presence in groundwater may influence the adsorption process.

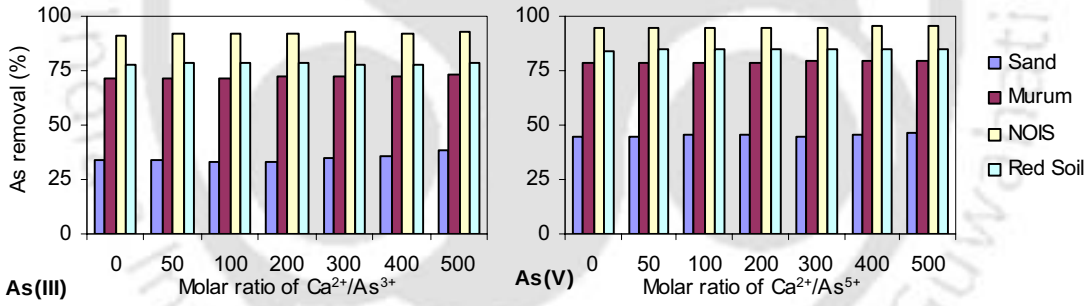

Fig. 5.50. Effects of Ca^{2+} on arsenic sorption from solution.

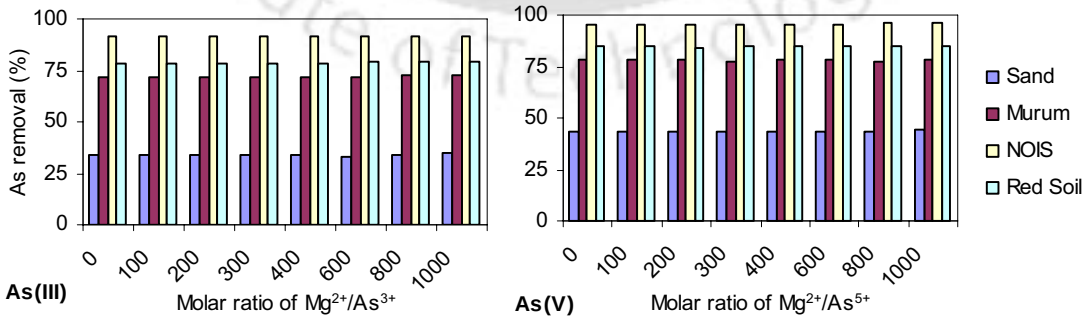

Fig. 5.51. Effects of Mg^{2+} on arsenic sorption from solution.

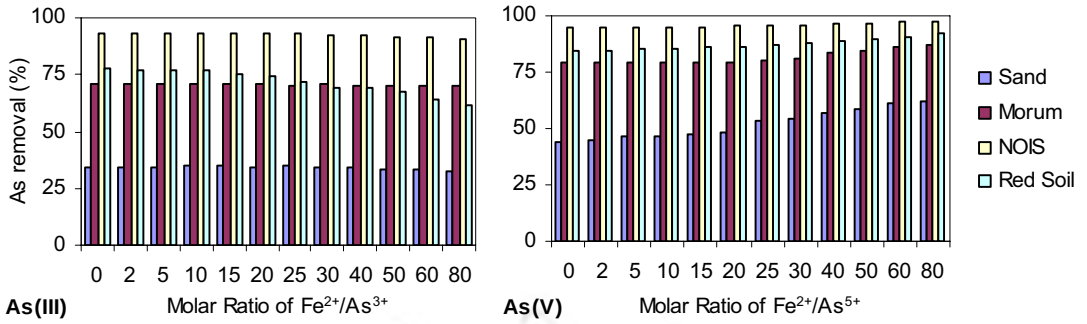

Fig. 5.52. Effects of Fe^{2+} on arsenic sorption from solution.

In the present study, the effects of the cations Ca^{2+} and Mg^{2+} on arsenic adsorption by sand, red soil, murum and NOIS were investigated. In Fig 5.50-5.52, presence of Ca^{2+}, Mg^{2+} and Fe^{2+} at low level, slight variations on arsenic adsorption were observed. Similar result can be noticed for the low level of anions i.e. HCO_3^{2-}, PO_4^{3-} and SO_4^{2-} also. Relatively higher concentrations of the cations Ca^{2+} and Mg^{2+} enhanced the both As(III) and As(V) adsorption capacity onto the adsorbents. At 500 molar ratio of Ca^{2+} to As (III), 4.54% maximum adsorption variation was observed for sand, whereas 1.55% increment in As(V) adsorption by sand can be noticed. At the same molar ratio, little increments for murum [1.85% for As(III) and 1.08% for As(V)], NOIS [1.73% for As(III) and 0.53% for As(V)] and red soil [0.55% for As(III) and 0.91% for As(V)] are observed. Increasing molar ratio of Mg^{2+} to arsenic (shown in Fig. 5.51) a little increment (less than 1%) on arsenic adsorption by the different adsorbents were estimated. Fe^{2+} was found (Fig. 5.52) to enhance the adsorption of arsenate significantly on sand (17.94%), murum (8.01%), NOIS (3.10%) and red soil (7.23%) at 800 µM of Fe^{2+} concentration. Arsenite sorption rates were dramatically decreased by 1.95% and 1.36%, 2.07% and 16.08% respectively for sand, murum, NOIS and red soil in the presence of 800 µM of Fe^{2+}. Adverse effect of Fe^{2+} on arsenite sorption is unknown. Zhu et al. (2009) observed similar result for arsenic adsorption on the supported nano zero-valent iron on activated carbon. They concluded that divalent metal cations such as Ca^{2+}, Mg^{2+} and Fe^{2+} significantly enhanced the adsorption of arsenate on the supported nano zero-valent iron on activated carbon but arsenite sorption capacity was reduced in the presence of Fe^{2+} (Zhu et al., 2009). It may be possible that the more positively charged cations were sifted from the solution to the surface of the adsorbent and they enhanced affinity of the

adsorbent for the arsenate anions (Zhu et al., 2009). Chen et al. (2008) reported that higher concentration of Ca^{2+} and Mg^{2+} slightly reduced As(III) removal efficiency onto molybdate-impregnated chitosan beads (MICB) but did not effect on As(V) adsorption. They also noticed that anion have no effect on arsenic sorption (Chen et al., 2008). Ramesh et al. (2004) evaluated that the presence of cations (Na^{+}, K^{+}, Ca^{2+} and Mg^{2+}) and anions (NO_3^{-}, SiO_3^{2-}, SO_4^{2-} and Cl^{-}) but found no significant effect on the removal of As(III) by polymeric Al/Fe modified montmorillonite, As(V) with the exception of PO_4^{3-} and Fe^{2+}.

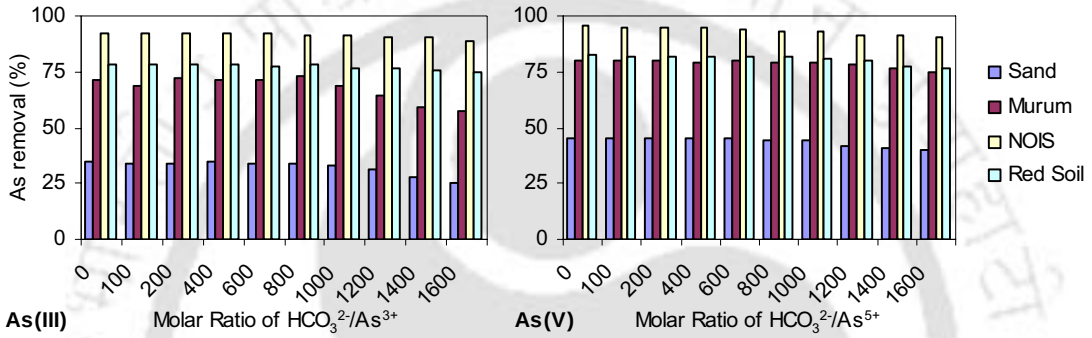

Fig. 5.53. Effects of HCO_3^{2-} on arsenic sorption from solution.

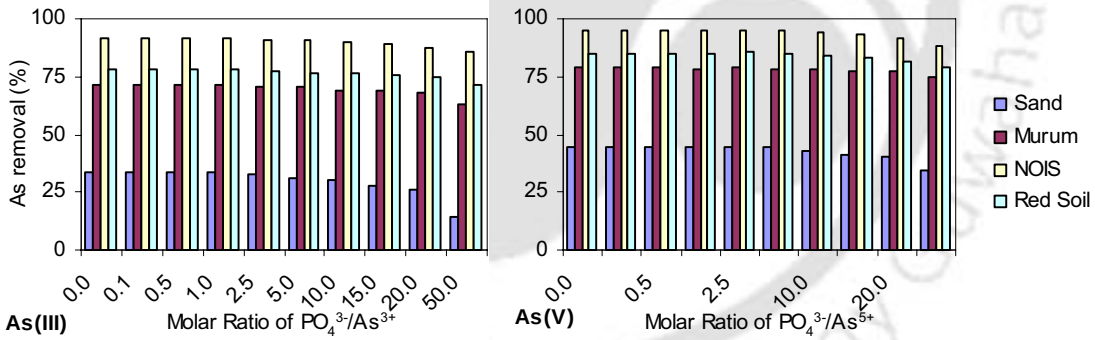

Fig. 5.54. Effects of PO_4^{3-} on arsenic sorption from solution.

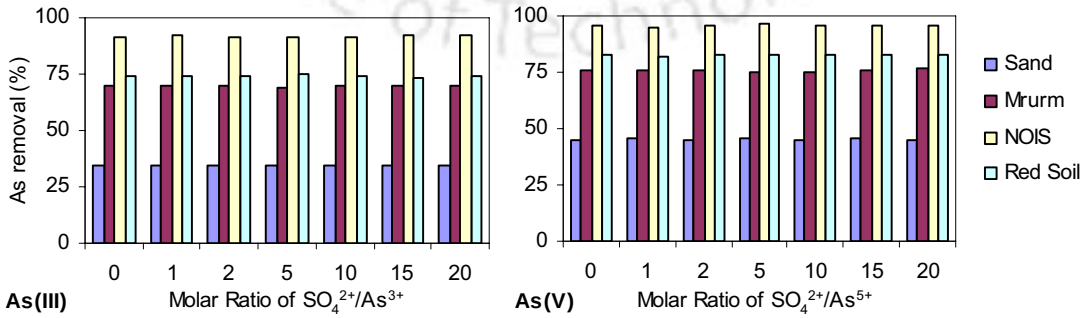

Fig. 5.55. Effects of SO_4^{2-} on arsenic sorption from solution.

In the present study, it can be observed (Fig. 5.53-5.55) that the removal of the both arsenate and arsenite are adversely affected by the presence of PO_4^{3-} and HCO_3^{2-} anions but no significant variation on arsenic sorption was observed for SO_4^{2-} ion. In the presence of 16mM HCO_3^{2-} ion in 10 µM arsenic spiked solution, significant reduction of arsenic adsorptions are recorded for the adsorbents i.e. for sand [As(III): 9.66%; As(V): 5.18%], murum [As(III): 13.45%; As(V): 4.57%], NOIS [As(III): 3.52%; As(V): 5.07%] and red soil [As(III): 3.38%; As(V): 5.71%]. In presence of 0.5 mM PO_4^{3-}, arsenite adsorptions are reduced 19.69% for sand, 8.04% for murum, 5.90% for NOIS and 7.22% for red soil whereas arsenate adsorptions are reduced 10.39% for sand, 4.50% for murum, 6.70% for NOIS and 6.11% for red soil. Zhang et al. (2003) reported that with the increase of molar ratio of PO_4^{3-} to As, the As(V) adsorption capacity of Ce(IV)-doped iron oxide adsorbent decreased significantly. Manna and Ghosh (2007) observed that sulfate, nitrate, chloride and fluoride ions had no interference in arsenic adsorption on synthetic hydrous stannic oxide while at higher phosphate concentration level arsenic adsorption rate was reduced from 88% to 79%. Kundu et al. (2004) concluded that presence of higher level Cl^-, NO_3^-, PO_4^{3-}, SO_4^{2-} anions in aqueous solution reduced arsenate adsorption capacity onto Portland cement. They also observed that presence of Fe^{2+} ion also affects on arsenate sorption (Kundu et al., 2004). In iron oxides surface, arsenate and phosphate can form inner-sphere complexes and they could compete for similar adsorption sites (Zhu et al., 2009) hence arsenate sorption decrease with the presence of PO_4^{3-}. Maiti et al. (2010) studied the effects of the co-ions on As(III) and As(V) removal efficiency on treated laterite. They reported that phosphate, silicate, bicarbonate and sulfate did not significantly affect the As(V) adsorption but at higher concentration phosphate, silicate and carbonate reduced the As(III) removal efficiency.

The results corroborate that presence of cations and anions at higher concentration level can affect arsenic adsorption efficiency but at lower level, interference on sorption process is negligible. In the groundwater of Assam 110 to 220 mg L^{-1} of alkalinity, 0.7 to 19.3 mg L^{-1} of iron, 10.4 to 39.3 mg L^{-1} of calcium, low level of nitrate (range 0.12 to 0.65 mg L^{-1}), phosphate (range 0.1 to 1.7 mg L^{-1}) and fluoride (range 0.0 to 0.9 mg L^{-1}) is detected. The concentration range of the coexisting ions found to having negligible interference on arsenic adsorption onto the examined adsorbent.

5.5 Summary

The adsorption characteristics of NOIS, sand, red and murum was estimated in this chapter. Total adsorption capacity and adsorption mechanism of the adsorbents, behavior of the adsorbents at different inlet concentration, pH and ionic strength was evaluated. The requirements of the minimum adsorbent dose for the individual adsorbents to reach desired effluent concentrations (10 and 50 μg L^{-1}) were evaluated. To decrease the boundary layer resistance of the adsorbents, the agitation rate of the incubator shaker was optimized. It was found that 200 rpm agitation speed of the incubator shaker was sufficient for all the adsorbents to overcome the boundary layer resistance. From the pH study, it was found that sorption rate of As(V) was more sensible to the pH of the aqueous medium than that with the As(III) sorption. The adsorbents were efficient on adsorbing arsenic in acidic media than in alkaline media. The obtained results ensured that the adsorbents were efficient on adsorbing arsenic from the solution at the normal pH (6.5-8) range of the drinking water. From the kinetic study it was found that the both arsenic species [As(III) and As(V)] for all adsorbents were reached the equilibrium concentration within 3 hours and maximum arsenic sorption was achieved by the adsorbents within 2 hours. NOIS was highly efficient on adsorbing arsenic. Within 30 minutes, 80% arsenic removal efficiency was achieved by NOIS. The kinetic experimental data of the arsenic sorption by the adsorbents were interpreted to determine the adsorption kinetic rate and adsorption mechanism. The results corroborate that pseudo second order reaction rate model is the best fit model and that could describe the both As(III) and As(V) sorption mechanisms for the each adsorbents. To define the sorption mechanism intraparticle diffusion model, liquid film mass transfer model, Richenberg model and Bangham's equation were applied to the kinetic data. The models confirm that at the sorption process was controlled by intraparticle diffusion followed by film diffusion. The thermodynamic study evaluated that the adsorbents adsorb more arsenic at lower temperature than at higher temperature and the arsenic sorption process is exothermic in nature. The equilibrium study for the both arsenic species was conducted to extrapolate the adsorption capacity and adsorption isotherm. From the interpretation of the equilibrium data, the isotherm models can be arranged in the order of excellent fit as:

Freundlich> Redlich-Peterson> Langmuir> Temkin> Dubinin-Radushkevich. Maximum adsorption capacity was found for NOIS and the adsorbents can be ordered according adsorption capacity as: NOIS>red soil>murum>sand. From the results, it can be concluded that NOIS can be used as promising adsorbent for removing arsenic from the solutions. The initial strength of the arsenic in the aqueous medium influences the sorption capacity of the adsorbents. Arsenic removal efficiency of the NOIS was not much influenced by the initial arsenic concentration due to higher adsorption capacity. However removal efficiencies were rapidly decreased with the increase in solution arsenic strength for murum, red soil and sand due to low adsorption capacity. The effects of major cations and anions on arsenic sorption were also examined. At higher concentration, Ca^{2+} and Mg^{2+} ions slightly enhance As(III) and As(V) adsorption capacity onto the adsorbents. Fe^{2+} helps to adsorb As(V) but resist on As(III) sorption. Both As(III) and As(V) adsorption onto the adsorbents are adversely affected by the presence of PO_4^{3-} and HCO_3^{2-} anions but no significant variation on arsenic sorption was observed for SO_4^{2-} ion. Moreover, the coexisting ions were found to have negligible interference on the arsenic adsorption within their normal range in ground water.

Chapter 6

Comparative Evaluation of Arsenic Adsorption Potential of the Locally Available Materials

(Column Experiments, Co-Precipitation, Desorption/Regeneration)

6.1 Introduction

The main objective of this chapter is to determine the arsenic removal efficiency in continuous mode fixed bed column run and to evaluate the breakthrough behavior of arsenic sorption onto the studied adsorbents (NOIS, sand and murum) at different bed depth, different inlet concentration and different flow rate. The breakthrough parameters of the column experiments for the all adsorbents are calculated in this chapter. Bed depth service time (BDST) model, Thomas model, Yoon-Nelson model and mass transfer models are applied to the column experimental data to describe column kinetics and design column dynamics. The evaluated model parameters are summarized to develop arsenic removal filter. This chapter also aims at the co-precipitation of arsenic along with iron at different operating conditions that will help to predict the life of the developed filter in the actual scenario. Desorption and regeneration studies are carried out for the all adsorbents in this chapter to facilitate the reuse of the adsorbents.

6.2 Continuous mode laboratory scale column studies

Column study is the procedure to separate the adsorbate form the solute in continuous mode. This study is conducted by scaling down of pilot scale filter study to examine the adsorption characteristic of the column material. Although in batch study the characterization of the adsorbents can be done easily, column study is necessary to evaluate run time of the filter at desire effluent concentration. Column studies ensure

about the amount of adsorbent requirement for the specific loading rate and run time for desired effluent concentration.

6.2.1 Theory of column performance

The column performance is usually defined by the concept of the breakthrough curve, which is obtained by the plotting of normalized arsenic concentration (C_t/C_0) versus throughput volume (V_t) at time t for a given bed depth (h) and flow rate (Q). Normalized arsenic concentration (C_t/C_0) is the ratio of effluent arsenic concentration (C_t) to inlet arsenic concentration (C_0). The throughput volume (V_t) can be calculated from the following equation (Kumar and Chakraborty, 2009):

$$V_t = \frac{Qt}{1000} \tag{6.1}$$

Where, Q is the volumetric flow rate (ml min^{-1}) of the column and t the run time (min) of the column respectively. Total quantity of arsenic adsorbed is estimated until the column exhausted. When the effluent concentration of the column remains same for longer period and very close to Influent concentration, then the column is assumed as exhausted (Kumar and Chakraborty, 2009). The total quantity of arsenic, which could not be adsorbed (M_{pass}) by the column, can be calculated from the area under the breakthrough curve and that can be expressed as (Kumar and Chakraborty, 2009):

$$M_{ads} = \frac{Q}{1000}\int_{t=0}^{t=total} C_{ads}\,dt = \frac{QA_{ads}}{1000} \tag{6.2}$$

Where, C_{ads} is the arsenic adsorbed (µg L^{-1}) at time t during the column run and A_{ads} is the area of arsenic adsorbed in the breakthrough curve. The total quantity of arsenic which could not adsorbed (M_{pass}) by the column can be calculated from the area under the breakthrough curve that can be expressed as (Kumar and Chakraborty, 2009):

$$M_{pass} = \sum\left[\frac{(V_{n+1} - V_n)(C_{n+1} + C_n)}{2}\right] \tag{6.3}$$

Where, V_n and V_{n+1} are the throughput volume (L) at n and $(n+1)$ reading respectively. C_n and C_{n+1} are the effluent arsenic concentrations (µg L^{-1}) at n^{th} and $(n+1)^{th}$ reading respectively. Arsenic applied to the column is determined from the given equation:

$$M_{total} = V_{total} C_0 \tag{6.4}$$

Therefore, total arsenic adsorbed (M_{ads}) by the column can be calculated by deducting the value of arsenic passed through the column (M_{pass}) from the total arsenic applied (M_{total}) that can be expressed mathematically as:

$$M_{ads} = M_{total} - M_{pass} \tag{6.5}$$

The total percentage of arsenic removal by the column, i.e. the column performance (CP) by the column bed can be calculated from the following relation (Kundu and Gupta, 2007):

$$CP = \left(\frac{M_{ads}}{M_{total}} \right) \times 100\% \tag{6.6}$$

The total arsenic uptake capacity (q_e) can be calculated from the following expression:

$$q_e = \frac{M_{ads}}{m} \tag{6.7}$$

Where, m is the mass of the column bed.

6.2.2 Breakthrough curve modeling

The performance of a fixed bed column can be evaluated through the interpretation of breakthrough curve. The run time of column and the shape of breakthrough are most important characteristics for the design of the operating criteria of the arsenic removal filter. Successful design of a column adsorption process is the predominant factor for prediction of shape and time of appearance of breakthrough curve. Several models have already been developed to describe column kinetics and design

column dynamics. In this study, continuous mode column experimental data of the adsorbents were validated using Bed Depth Service Time (BDST) model (Ayoob et al., 2006), Thomas model (Baral et al., 2009), Yoon-Nelson model (Baral et al., 2009) and Mass Transfer model (Ayoob et al., 2006).

6.2.2.1 Bed depth service time (BDST) model

Bohart and Adams (1920) presented Bed depth-service time (BDST) model based on surface reaction rate theory for design of activated carbon columns and that can be expressed as follows (Sankararamakrishnan et al., 2008):

$$\ln\left(\frac{C_0}{C_B}-1\right)=\ln\left(e^{KN_0(x/v)}-1\right)-K_aC_0t_s \qquad (6.8)$$

Where, C_0 is the initial arsenic concentration (µg L^{-1}), C_B the desire arsenic concentration at breakthrough (µg L^{-1}), K_a the rate constant (L $\mu g^{-1}h^{-1}$) of adsorbent, N_0 the adsorptive capacity of adsorbent (µg L^{-1}), x the bed depth of adsorbent (cm), v the linear flow velocity of feed or loading rate (cm h^{-1}) and t_s the service time of column under above conditions (h). The Equation (6.8) can be rearranged to yield an expression for service time, t_s considering the following:

$$e^{K_aN_0(x/v)} >> 1, \qquad t_s=\frac{N_0}{C_0v}x-\frac{1}{C_0K_a}\ln\left(\frac{C_0}{C_B}-1\right) \qquad (6.9)$$

That form of the Bohart-Adams equation (Equation 6.9) can be used to determine the service time (t_s) of a column of predicted bed depth (x) given the values of N_0, C_0 and K_a, which must be determined for laboratory columns operated over a range of velocity values (v).

Setting $t = 0$ and solving equation [6.9] for x yields

$$x_0=\frac{v}{K_aN_0}\ln\left(\frac{C_0}{C_B}-1\right) \qquad (6.10)$$

Where, x_0 is the minimum column height necessary to produce an effluent concentration C_B.

In bed depth / service time (BDST) approach, Hutchins presented the modified form of the Bohart – Adams equation as:

$$t_s = ax + b \tag{6.11}$$

Where, $a = \frac{N_0}{C_0 v}$ (6.12)

and $b = -\frac{1}{K_a C_0} \ln\left(\frac{C_0}{C_B} - 1\right)$ (6.13)

If a laboratory test is conducted at a solute concentration of C_1 and loading rate v_1, yields an equation of the form:

$$t_s = a_1 x + b_1 \tag{6.14}$$

It is possible to predict the equation for the inlet concentration C_2 and loading rate v_2 as follows:

$$t_s = a_2 x + b_2 \tag{6.15}$$

The new slope and intercept values can be determined as:

$$a_2 = a_1\left(\frac{C_1}{C_2}\right)\left(\frac{v_1}{v_2}\right) \tag{6.16}$$

$$b_2 = b_1\left(\frac{C_1}{C_2}\right)\frac{\ln(C_2/C_F - 1)}{\ln(C_1/C_B - 1)} \tag{6.17}$$

Where, a_1 and a_2 are the slopes at concentration C_1 and C_2 respectively whereas b_1 and b_2 are the intercept at concentration C_1 and C_2 respectively. The flow rate has little or no effect on the intercept as the intercept is independent of the flow rate in linearized BDST Equation (6.9). C_B and C_F are representing the breakthrough concentrations for C_1 and C_2 inlet arsenic concentrations respectively.

6.2.2.2 Thomas model

Thomas (1944) developed one of the most general and widely used models in the column performance theory (Baral et al., 2009). He developed the equation based on the three assumptions that the adsorption process follows Langmuir model with no axial dispersion, the rate of adsorption kinetic force obeys 2nd order reversible reaction and the model assume a separation factor which is applicable for both favorable and unfavorable isotherm. This linear form of the model can be written as:

$$\ln\left(\frac{C_0}{C_t}-1\right)=\left(\frac{k_{Th}q_0m}{Q}\right)-\left(\frac{k_{Th}C_0V_t}{Q}\right) \quad (6.18)$$

Where, k_{Th} is the Thomas rate constant (ml μg^{-1} min^{-1}), q_0 the maximum adsorption capacity ($\mu g\ g^{-1}$), V_t the throughput volume, m the mass of adsorbent (g) and Q the flow rate (ml min^{-1}). C_0 and C_t are the influent and effluent concentration of the column respectively. The Thomas rate constant (k_{Th}) and the maximum adsorption capacity (q_0) can be obtained from the plot of $ln((C_0/C_t)-1)$ against t ($=V_t/Q$) for a given flow rate (Q).

6.2.2.3 Yoon-Nelson model

Yoon and Nelson (1984) have developed a relatively simple model to describe the adsorption kinetic and breakthrough of adsorbate gases with the respect to activated charcoal (Baral, 2009). They developed the model based on the assumption that the rate of decrease in the probability of adsorption for each adsorbate molecule is proportional to the probability of adsorbate adsorption and the probability of adsorbate breakthrough on the adsorbent (Kundu and Gupta, 2007). Mathematically, the model can be expressed as follows:

$$\ln\frac{C_t}{C_0-C_t}=k_{YN}t-\tau k_{YN} \quad (6.19)$$

Where, k_{YN} is the rate constant (min^{-1}) and τ the time required for 50% adsorbate breakthrough (min). The theoretical breakthrough curve can be drawn using the Yoon-Nelson parameters i.e. k_{YN} and τ, which can be determined from the plot of $ln(C_t/(C_0-C_t))$ versus t.

6.2.2.4 Mass transfer model

Using batch isotherm data, it is possible to predict the theoretical breakthrough curve, which is well compared with the experimental data (Kundu and Gupta, 2007). Based on mass transfer equation, the theoretical breakthrough curve concept was presented by Michaels in 1952 (Kundu and Gupta, 2005). The procedure for preparation of theoretical breakthrough curve from the equilibrium batch study experimental data is given below:

1. Firstly, the equilibrium line is drawn assuming various C_e values and calculating corresponding q_e values using best fit isotherm model.
2. An operating line is passing through the origin and the point (C_0, q_e^*). q_e^* value is the correspondence C_0 value which can be obtained from the best fit isotherm model. So, it is obvious that the operating line and the best fit isotherm line will meet at (C_0, q_e^*) point. The significant of this operating line is that the data of the continuously mixed batch reactor and the data of the fixed bed reactor are identical at these two points, first at the initiation and other at the exhaustion of the reaction (Ayoob et al., 2007).
3. According to Weber (Weber, 1972), the rate of transfer solute from the solution over a differential depth, *dh*, of column is given by:

$$F_W dC = K_a \left(C - C^*\right) dh \tag{6.20}$$

Where, F_W is the flow rate, K_a the overall mass transfer coefficient and C^* the equilibrium concentration of solute in solution corresponding to an adsorbed concentration q_e^*. The term (C-C^*) is the driving force for adsorption and can be calculated from the distance between the operating line and isotherm best line for each q_e value (Ayoob et al., 2007).

4. Integrating the Equation (6.20), for the height, h_z, of adsorption zone, we have:

$$h_z = \frac{F_W}{K_a} \int_{C_B}^{C_E} \frac{dC}{C - C^*} \tag{6.21}$$

In the plot $(C\text{-}C^*)^{-1}$ versus C, area under the curve represents the integrated value of the above equation for any value of $h<h_z$. For any value of h

($<h_z$), corresponding to a concentration C ($C_B<C<C_E$), the Equation (21) can be written as:

$$h = \frac{F_W}{K_a}\int_{C_B}^{C}\frac{dC}{C-C^*} \tag{6.22}$$

Dividing the Equation (6.22) by Equation (6.21), we get:

$$\frac{h}{h_z} = \frac{\int_{C_B}^{C} dC/(C-C^*)}{\int_{C_B}^{C_E} dC/(C-C^*)} = \frac{(V-V_B)}{(V_E-V_B)} \tag{6.23}$$

Where, V_E and V_B are the volume of water treated at exhausted point and breakthrough point respectively. V is represented the treated water volume for the effluent concentration C ($C_B<C<C_E$). The value of $(V\text{-}V_B)/(V_E\text{-}V_B)$ can be evaluated by from the integration value of h and h_z.

5. Now the plot of C/C_0 versus $(V\text{-}V_B)/(V_E\text{-}V_B)$ represents the theoretical breakthrough curve.

6.2.3 Results and discussions of column studies

For fixed bed column study for arsenic removal, arsenic [As(III) or As(V)] spiked solution was passed through the fixed bed of selected adsorbent in down-flow mode. The down-flow mode was applied for all the adsorbents (NOIS, sand and murum). This mode is applied for the column study because the filter will be designed using gravitational movement of water, which is down-flow mode. The red soil is iron oxides rich clay with low permeability. Due to sticky in nature, red soil is used to develop a porous arsenic removal filter. Batch experimental study confirmed the potential of arsenic sorption capacity of red soil. Arsenic sorption capacity in continuous mode of red soil was not evaluated as it will be not used directly as adsorbent. Thus the column experiments of red soil were not performed. In continuous column mode, the effluent pH was found neutral for sand and murum, whereas the pH of the effluent for NOIS was alkaline in nature. Arsenic removal capacity and efficiency are strongly dependent on the adsorbent bed depth and the loading rate. So, the column studies were performed using different bed depth, different influent arsenic concentration as also variation in flow rate till it reaches

different breakthrough point. Observations were made at different breakthrough point and exhausting point. WHO (World Health Organization) recommended guideline value for the arsenic concentration in drinking water is 10 µg L^{-1} (desirable) with no relaxation in maximum permissible limit (WHO, 1993). BIS (Bureau of Indian Standard) set the permissible limit of arsenic in drinking water as 50µg L^{-1} (IS 10500:1991). Also in some developing countries 50 µg L^{-1} is the desirable permissible limit for drinking purpose. According to BIS old guideline, 50 µg L^{-1} is the desirable limit of drinking water. Thus, arsenic concentrations of 10 µg L^{-1} and 50 µg L^{-1} were considered as different breakthrough concentrations for the column study (Reza and Singh, 2010). Although two different breakthrough points (10 µg L^{-1} and 50 µg L^{-1}) were examined for experimental purpose, the arsenic removal filter was designed assuming arsenic concentration of the effluent will not exceed 10 µg L^{-1}.

6.2.3.1 Effect of bed depth

The removal performance of both As(III) and As(V) of the selected adsorbents (NOIS, sand and murum) were investigated at different bed depth. The bed depth of adsorbent in column is strongly affects the effluent quantity as well as the quality. Increasing the bed depth of adsorbent, volume of treated water at breakthrough is increased. It was noticed that, effluent arsenic concentration is decreased with increasing of bed depth. Hence, minimum bed height is required to achieve the desire effluent arsenic concentration. Fig.6.1 is shows the effects of bed depth on arsenic [both As(III) and As(V)] sorption by NOIS, sand and murum . From the Fig. 6.1, it is evident that treated water volume increased with increasing bed height of the column. Bed height is directly proportional to the contact time and the amount of mass of the adsorbent present in the column that indicate more bed height of the columns results better performance of the column (Seko et al., 2004; Sharma et al., 2010; Maiti et al., 2010). The Fig. 6.1 also shows that, the arsenic removal efficiency was found more for the higher bed depth due to more contact time. In the Fig. 6.1, it can be also that the breakthrough curves are steeper for column with less bed depth. This is because of the columns with smaller bed depth are quickly exhausted compared to the others. The results also corroborate that

NOIS sorbent can treat much higher amount of arsenic polluted water which indicates NOIS adsorbent can be promising arsenic removal filter media. Total adsorbed arsenic quantity, treated water volume at different breakthrough point, column exhausted time, breakthrough time, column performance and adsorption capacity at different bed depth of the adsorbents were presented in Table 6.1. The results indicate that NOIS and murum can meet the desire breakthrough concentration (10 μgL^{-1}) for bed depth of 7.5 cm which was the minimum bed depth used for column experiment but sand could not reach that level even with 45 cm bed depth for both As(III) and As(V) species.

Table 6.1. Effect of column bed depth on arsenic sorption by NOIS, sand and murum at 5ml min^{-1} flow rate.

Adsorbent	As species	Bed depth (cm)	t_B (h)		t_E (h)	V_B (L)		V_E (L)	EBCT (min)	CP (%)	M_{ads} (µg)	q_e (µg g^{-1})
			10µgL^{-1}	50µgL^{-1}		10µgL^{-1}	50µgL^{-1}					
NOIS	As(III)	7.5	456	552	888	136.8	165.6	266.4	7.36	75.29	40115.38	397.68
		15	840	984	1560	252	295.2	468	14.73	79.36	74285.55	368.21
		30	1824	2040	2664	547.2	612	799.2	29.45	83.47	133422.5	330.67
		45	2736	3120	3792	820.8	936	1137.6	44.18	80.36	196721.8	325.03
	As(V)	7.5	600	708	1176	180	212.4	352.8	7.36	72.13	50897.16	504.56
		15	1080	1272	2208	324	381.6	662.4	14.73	70.53	93435.59	463.13
		30	2256	2568	3840	676.8	770.4	1152	29.45	73.97	170421.6	422.36
		45	3504	4008	5328	1051.2	1202.4	1598.4	44.18	82.56	263917.94	436.05
Sand	As(III)	7.5	-	4	14.5	-	1.2	4.35	7.36	52.19	454.06	8.17
		15	-	9	23.5	-	2.7	7.05	14.73	54.72	771.5273	6.94
		30	-	23	53	-	6.9	15.9	29.45	61.4	1952.474	8.78
		45	-	35	81	-	10.5	24.3	44.18	58.12	2824.493	8.47
	As(V)	7.5	-	6	18	-	1.8	5.4	7.36	54.43	587.89	10.58
		15	-	15.5	36.5	-	4.65	10.95	14.73	58.14	1273.17	11.45
		30	-	36	73	-	10.8	21.9	29.45	67.1	2939.11	13.22
		45	-	56	117	-	16.8	35.1	44.18	64.33	4516.29	13.54
Murum	As(III)	7.5	9	24	63	2.7	7.2	18.9	7.36	61.2	2313.25	38.31
		15	30	48	114	9	14.4	34.2	14.73	63.02	4310.33	35.70
		30	42	120	186	12.6	36	55.8	29.45	73.03	8150	33.75
		45	120	186	300	36	55.8	90	44.18	66.02	11883.92	32.80
	As(V)	7.5	27	48	108	8.1	14.4	32.4	7.36	63.22	4096.58	67.85
		15	78	144	234	23.4	43.2	70.2	14.73	70.8	9940.41	82.32
		30	168	288	444	50.4	86.4	86.4	29.45	70.72	18839.74	78.01
		45	264	432	588	79.2	129.6	176.4	44.18	75.49	26632.5	73.52

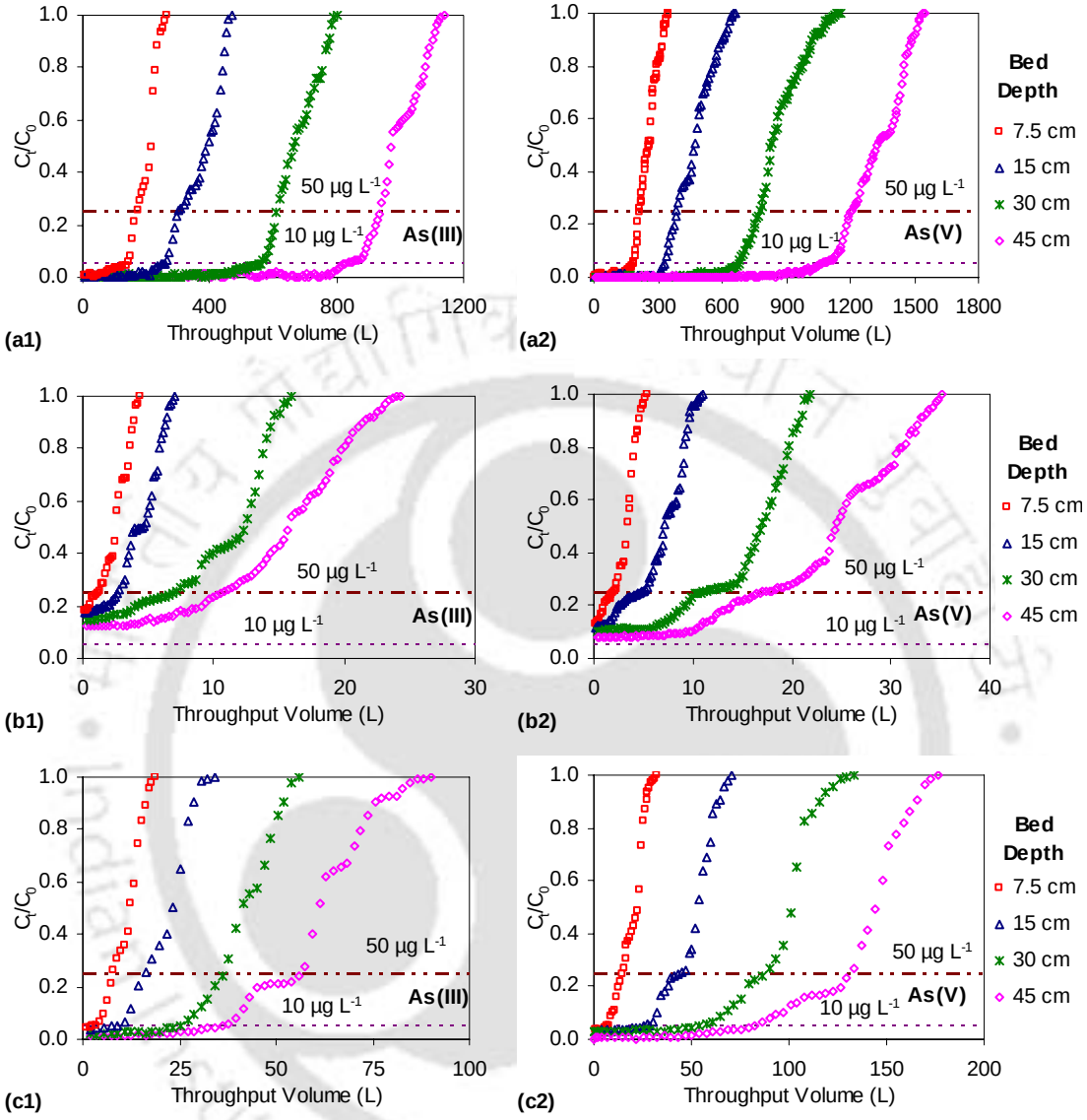

Fig. 6.1. Effect of bed depth on arsenic [both As(III) and As(V)] adsorption by (a) NOIS, (b) sand and (c) murum [Q = 5ml min^{-1}, C_0 = 200 µg L^{-1} and φ = 2.5 cm].

6.2.3.2 Effect of flow rate

The effect of flow rate was investigated at 5, 10 and 15 ml min^{-1} volumetric flow rate against 45 cm height of NOIS, sand and murum adsorbent bed. The experiment was conducted for both As(III) and As(V) species with influent concentration of 200 µg L^{-1} at normal temperature and the corresponding breakthrough curves are shown in Fig. 6.2.

The performances of the selected adsorbent bed at different flow rates are shown in Table6.2. From the Table 6.2 and Fig. 6.2, it can be observed that the adsorption capacity is higher for lower flow rate for the all of the studied adsorbents that was in agreement with the findings of published literature. This can be explained by the fact that at lower flow rate the contact time is more (it can be seen in Table 6.2) which results in low diffusion of solute into the pores of the sorbent (Baral, 2009).

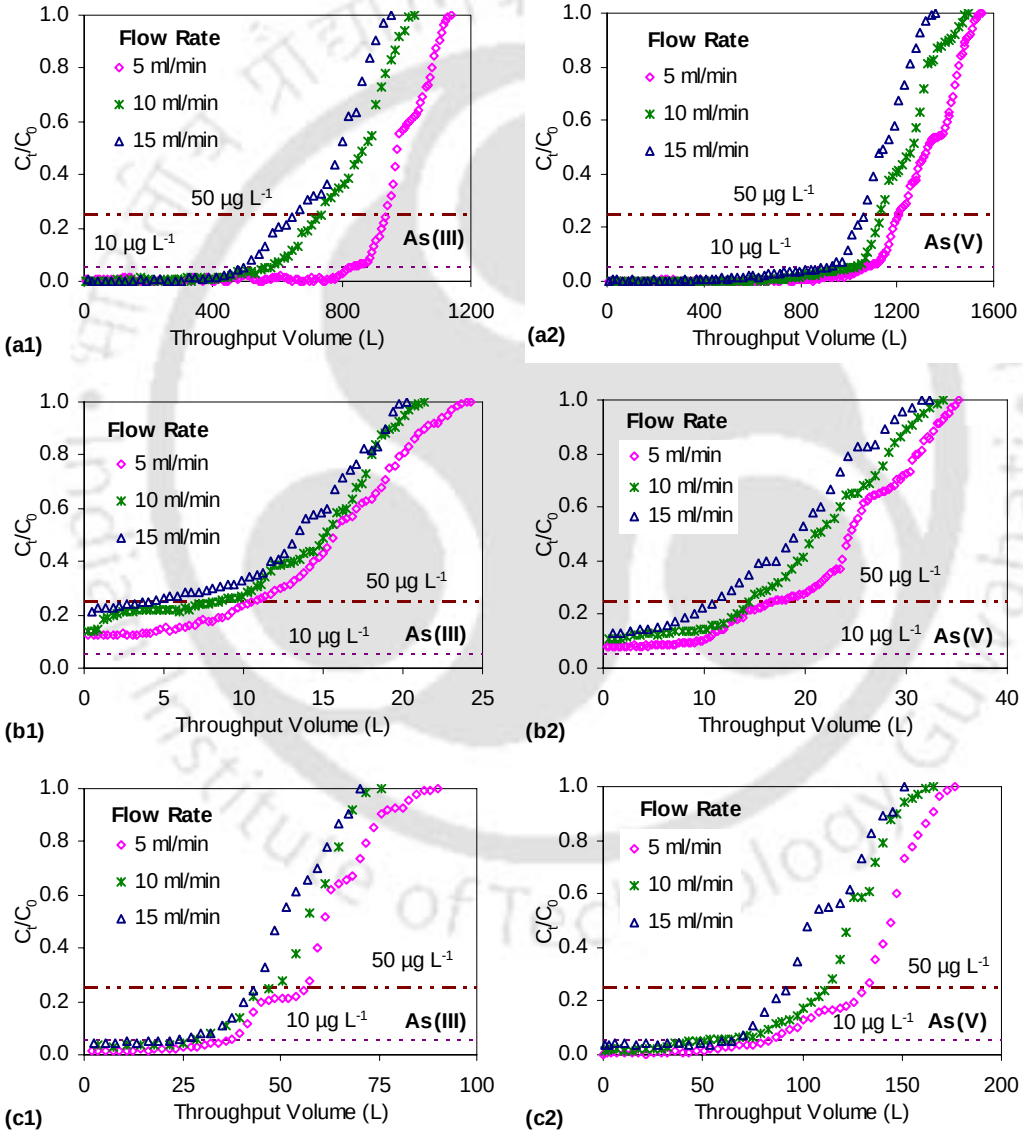

Fig. 6.2. Effect of flow rate on arsenic [both As(III) and As(V)] adsorption onto (a) NOIS, (b) sand and (c) murum [x = 45 cm, C_0 = 200 µg L^{-1} and φ = 2.5 cm].

Table 6.2. Effect of flow rate on arsenic sorption by NOIS, sand and murum. (Bed depth =45 cm, C_0 = 200 µg L^{-1}, ID = 2.5 cm).

Adsorbent	As species	Flow Rate	t_B (h)		t_E (h)	V_B (L)		V_E (L)	EBCT (min)	CP (%)	M_{ads} (µg)	q_e (µg g^{-1})
			10 µg L^{-1}	50 µg L^{-1}		10 µg L^{-1}	50 µg L^{-1}					
NOIS	As(III)	5	2736	3120	820.8	936	4237.34	1137.6	44.18	80.36	196721.8	325.03
		10	912	1224	1704	547.2	734.4	1022.4	22.09	80.46	164518.3	271.82
		15	528	720	1056	475.2	648	950.4	14.73	79.13	150412.3	248.52
	As(V)	5	3504	4008	5328	1051.2	1202.4	1598.4	44.18	82.56	263917.94	436.05
		10	1656	1872	2496	993.6	1123.2	1497.6	22.09	81.92	245373.84	405.41
		15	984	1176	1512	885.6	1058.4	1360.8	14.73	74.47	225201.74	372.09
Sand	As(III)	5	-	35	81	-	10.5	24.3	44.18	58.12	2824.493	8.47
		10	-	13.5	35.5	-	8.1	21.3	22.09	57.87	2465.39	7.39
		15	-	4.5	22.5	-	4.05	20.25	14.73	54.9	2223.63	6.67
	As(V)	5	-	56	117	-	16.8	35.1	44.18	64.33	4516.29	13.54
		10	-	24	56	-	14.4	33.6	22.09	58.59	3937.48	11.80
		15	-	16	40	-	14.4	36	14.73	56.03	4033.87	12.09
Murum	As(III)	5	120	186	300	36	55.8	90	44.18	66.02	11883.92	32.80
		10	42	78	126	25.2	46.8	75.6	22.09	70.72	10693.21	29.52
		15	15	48	78	13.5	43.2	70.2	14.73	70.21	9857.6	27.21
	As(V)	5	264	432	588	79.2	129.6	176.4	44.18	75.49	26632.5	73.52
		10	72	186	276	43.2	111.6	165.6	22.09	71.94	23828.14	65.78
		15	66	102	168	59.4	91.8	151.2	14.73	70.53	21329.12	58.88

6.2.3.3 Effect of initial arsenic concentration

The adsorption performances of the selected adsorbents (NOIS, sand and murum) were investigated at various influent arsenic [As(III) or As(V)] concentrations varying from 100 μg L^{-1} to 300 μg L^{-1} and at 5 ml min^{-1} flow rate. The corresponding arsenic removal parameters such as treatment time and treated water volume at different breakthrough point, arsenic removal capacity and column performance were presented in Table 6.3 and Fig. 6.3 which show the comparison plots of breakthrough curves for different inlet arsenic spiked solution. It can be observed from Fig. 6.3 that the breakthrough curve for lower inlet arsenic concentration appears earlier than its higher inlet concentration. This is due to the fact that higher concentration of arsenic saturates the adsorbent bed early, thereby shortens the bed breakthrough time. It can be seen from Table 6.3 that the breakthrough time and exhaustion time is less for lower inlet arsenic concentration. The column performances and the adsorption capacity also decreased with increase in arsenic concentration in influent. The breakthrough time (at 10 μg L^{-1} breakthrough point) of the NOIS column bed was decreased from 3120 to 492 h with increasing inlet As(III) concentration from 100 μg L^{-1} to 300 μg L^{-1}. Similar kinds of results were obtained for other adsorbents for both species of arsenic feed inlet solutions. Overall presence of higher arsenic in feed water affects on removal capacity of arsenic, column performance as well as treatment efficiency of the adsorbent bed.

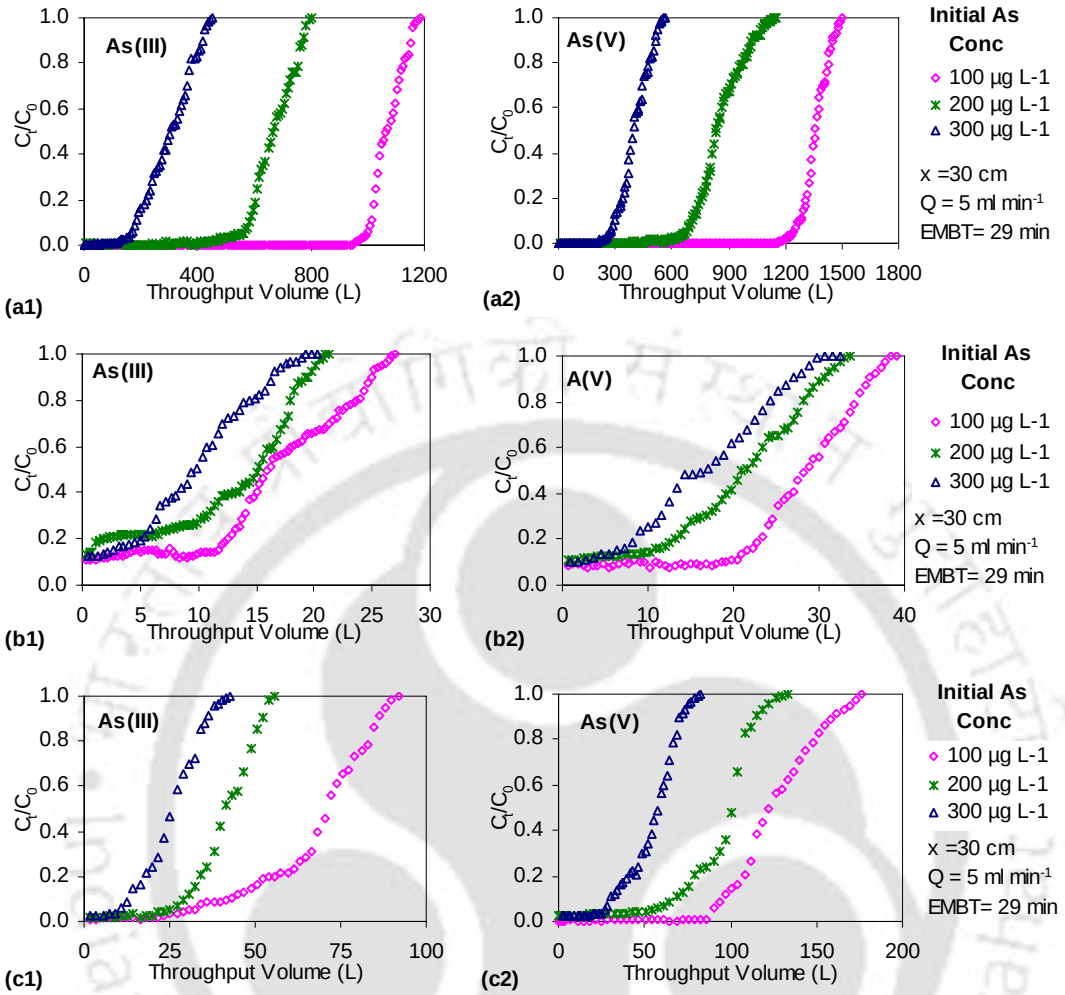

Fig. 6.3. Effect of initial arsenic [both As(III) and As(V)] concentration on arsenic removal by: (a) NOIS, (b) sand and (c) murum [x = 30 cm, Q = 5ml min^{-1} and φ = 2.5 cm].

Table 6.3. Effect of initial arsenic concentration on arsenic sorption by NOIS, sand and murum.

Adsorbent	As species	Bed depth (cm)	Initial As Conc. (µg L^{-1})	t_B (h)		t_E (h)	V_B (L)		V_E (L)	EBCT (min)	CP (%)	M_{ads} (µg)	q_e (µg g^{-1})
				10 µg L^{-1}	50 µg L^{-1}		10 µg L^{-1}	50 µg L^{-1}					
NOIS	As(III)	30	100	3120	3552	3960	936.0	1065.6	1188.0	29.45	90.32	107296	177.28
		30	200	1824	2040	2664	547.2	612.0	799.2	29.45	83.47	133423	220.44
		30	300	492	674	1508	147.8	202.2	452.4	29.45	66.63	90432	149.41
	As(V)	30	100	4248	4512	4992	1274.4	1353.6	1497.6	29.45	80.14	136172	224.99
		30	200	2256	2568	3840	676.8	770.4	1152.0	29.45	73.97	170422	281.58
		30	300	864	1080	1848	259.2	324.0	554.4	29.45	71.62	120660	199.36
Sand	As(III)	30	100	-	53	90	-	15.9	27.0	29.45	59.42	1604	4.81
		30	100	-	23	53	-	6.9	15.9	29.45	61.40	1952	5.85
		30	100	-	8	40	-	2.4	12.0	29.45	51.44	1852	5.55
	As(V)	30	100	-	94	128	-	28.2	38.4	29.45	69.56	2671	8.01
		30	200	-	36	73	-	10.8	21.9	29.45	67.10	2939	8.81
		30	300	-	24	102	-	7.2	11.0	29.45	51.67	4743	14.22
Murum	As(III)	30	100	138	234	306	41.4	70.2	91.8	29.45	73.62	6758	18.66
		30	200	42	120	186	12.6	36.0	55.8	29.45	73.03	8150	22.50
		30	300	24	54	156	7.2	16.6	46.8	29.45	54.19	7608	21.00
	As(V)	30	100	312	408	588	93.6	122.4	176.4	29.45	71.44	12603	34.79
		30	200	168	288	444	50.4	86.4	86.4	29.45	70.72	18840	52.01
		30	300	72	120	276	21.6	36.0	82.8	29.45	65.64	16304	45.01

6.2.3.4 Application of the BDST model

Bed depth service time model (BDST) was applied to the experimental data to study the breakthrough behavior of arsenic sorption onto NOIS, sand and murum and estimating characteristics parameters, K_a and N_0 from the model. BDST model can also predict the service time of column rum before breakthrough for a given influent arsenic concentration, bed depth and loading rate of influent. Estimated bed depth (x) and the corresponding service time (t_s) values were plotted in Fig. 6.4 for both 10 µg L^{-1} and 50 µg L^{-1} desired effluent concentrations against the selected adsorbents. Linear plot of bed depth and service time represented in the BDST model are made according to Equation [6.11]. Respective coefficients i.e. slope (a) and intercept (b) of the BDST model for the all studied adsorbents are presented in Table 6.4. The corresponding values of K_a and N_0 estimated from the slope (a) and intercept (b) of the liner plot of BDST model [Equation (6.12) and (6.13)] are summarized in Table 6.5. High correlation values (R^2) nearly approaching '1' for all the adsorbents except for As(III) adsorption by murum, indicate that BDST model is the best fit model. The model can be used for determination of service time for different influent arsenic concentration as well as different loading rate. In some cases, the BDST plots at different breakthrough are not parallel to each other. Similar results can also be observed for chromium adsorption by PANI jute (Kumar and Chakraborty, 2009) and adsorption of arsenate using untreated laterite (Maiti et al., 2008).

Table 6.4. Coefficients of BDST equation of various adsorbents at different breakthrough (Q = 5 ml min^{-1}, C_0 = 200 µg L^{-1}, ID = 2.5 cm and v = 61.12 ml h^{-1} cm^{-2}).

Adsorbent	Arsenic species	v ((ml h^{-1} cm^{-2}))	C_0 (µg L^{-1})	C_B = 10 µg L^{-1}		C_B = 50 µg L^{-1}	
				a	B	a	b
NOIS	As(III)	61.12	200	61.61	-37.83	69.04	-8.95
	As(V)	61.12	200	77.99	-41.08	88.27	-12.61
Sand	As(III)	61.12	200	-	-	0.84	-2.80
	As(V)	61.12	200	-	-	1.34	-4.26
Murum	As(III)	61.12	200	2.75	-16.68	4.41	-12.92
	As(V)	61.12	200	6.27	-18.61	10.09	-17.90

All of these experiments and literature findings suggested that BDST plots might not be parallel for all different breakthrough points. Requirements of minimum bed depth

to achieve desired effluent concentration for all the selected adsorbents were determined using the Equation 6.10 and presented in Table 6.5. Results show that for the higher desired breakthrough concentration, lower critical bed depth is required. Requirement of critical bed depth is less for As(V) compared to the As(III) due to high affinity of As(V) to the adsorbents.

Table 6.5. BDST model parameters of various adsorbents at different breakthrough (Q = 5 ml min^{-1}, C_0 = 200 µg L^{-1}, ID = 2.5 cm and v = 61.12 ml h^{-1} cm^{-2}).

Adsorbent	As species	Breakthrough = 10µg L^{-1}				Breakthrough = 50µg L^{-1}			
		N_0 (µg L^{-1})	K_a x10^{-5} (L µg^{-1}h^{-1})	x_0 (cm)	R^2	N_0 (µg L^{-1})	K_a x10^{-5} (L µg^{-1}h^{-1})	x_0 (cm)	R^2
NOIS	As(III)	753109	38.92	0.61	0.9989	843933	61.38	0.13	0.9988
	As(V)	953319	35.83	0.53	0.9983	1078948	43.56	0.14	0.9982
Sand	As(III)	-	-	-	-	10303	196.42	3.32	0.9979
	As(V)	-	-	-	-	16367	128.86	3.18	0.9999
Murum	As(III)	33562	88.27	6.07	0.8879	53865	42.53	2.93	0.9974
	As(V)	76653	79.11	2.97	0.9997	123308	30.69	1.77	0.9972

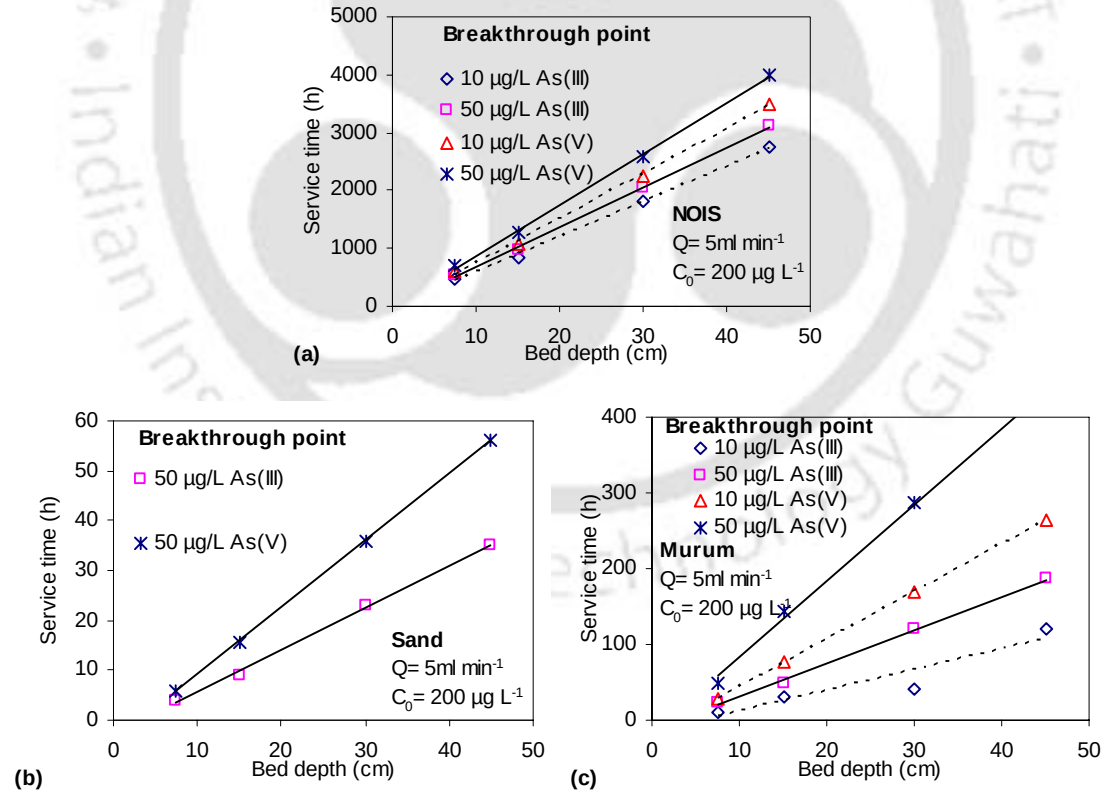

Fig. 6.4. Bed depths versus service time plot at various breakthrough points for the selected adsorbents: (a) NOIS, (b) sand and (c) murum.

6.2.3.5 Application of the Thomas model

The Thomas model was applied to the column data to investigate the breakthrough behavior of As(III) and As(V) onto NOIS, sand and murum. The statistical parameters *i.e.* k_{Th} and q_0 values were determined by plotting of $ln(C_0/C_t\text{-}1)$ against $t=(V_t/Q)$ using column experiment data.

Table 6.6. Coefficients of Thomas model of arsenic sorption on various adsorbents at different bed depth and flow rate.

Adsorbent	Variable	As(III)			As(V)		
		k_{Th} (ml µg^{-1} min^{-1})	q_0 (µg g^{-1})	R^2	k_{Th} (ml µg^{-1} min^{-1})	q_0 (µg g^{-1})	R^2
	Bed Depth						
NOIS	45	0.0005	325.94	0.9500	0.0003	436.42	0.9524
	30	0.0006	332.34	0.9176	0.0004	423.26	0.9823
	15	0.0006	369.03	0.8519	0.0004	462.30	0.9825
	7.5	0.0013	396.53	0.9405	0.0009	507.85	0.9732
Sand	45	0.0099	9.16	0.8827	0.0059	14.47	0.9272
	30	0.0123	9.62	0.8033	0.0101	14.27	0.8324
	15	0.0260	7.53	0.8593	0.0221	12.51	0.8721
	7.5	0.0368	8.71	0.9134	0.0398	11.49	0.9447
Murum	45	0.0035	32.84	0.9439	0.0017	74.65	0.8845
	30	0.0050	33.91	0.9544	0.0024	76.66	0.9309
	15	0.0080	33.73	0.8991	0.0034	82.08	0.9343
	7.5	0.0083	39.76	0.9714	0.0069	63.42	0.9385
	Flow Rate						
NOIS	5	0.0005	325.94	0.9500	0.0003	436.42	0.9524
	10	0.0006	269.68	0.8890	0.0007	407.80	0.9875
	15	0.0008	247.93	0.9126	0.0011	374.96	0.9739
Sand	5	0.0099	9.16	0.8827	0.0059	14.47	0.9272
	10	0.0187	8.07	0.8216	0.0123	12.60	0.9103
	15	0.0191	6.93	0.7843	0.0213	10.81	0.7331
Murum	5	0.0034	32.97	0.9505	0.0017	74.65	0.8845
	10	0.0068	29.19	0.9090	0.0030	64.06	0.8920
	15	0.0080	27.95	0.9614	0.0046	60.67	0.9831

Moderate to high value of coefficient of determination (R^2 value ranges from 0.7331to 0.9875) indicate that Thomas model is fitted reasonably well to the experimental values. Predicted values of Thomas rate constant (k_{Th}) and maximum adsorption capacity (q_0) for

the selected adsorbents at different bed depth and different flow rate are presented in Table 6.6. It can be seen from the results as sown in the tables (Table 6.1, Table 6.2, Table 6.3 and Table 6.6) the calculated maximum adsorption capacity and experimental adsorption capacities were found almost identical for the all adsorbents. This is also the evidence of obeying Tomas equation. As the bed depth is reduced, Thomas rate constant is increased whereas the adsorption capacity is reduced. Opposite trend was observed for the flow rate i.e. increasing of flow rate decreases adsorption capacity and increase in Thomas rate constant. The above findings conclude that the external and internal diffusion is not the rate-limiting step for the column sorption (Baral et al., 2009).

6.2.3.6 Application of the Yoon-Nelson model

Yoon-Nelson Model (Yoon and Nelson, 1984) is a simple model and applicable for investigation of breakthrough behavior of column sorption experimental data. This model predicts the treatment time (τ) to remove arsenic upto 50% of the column influent concentration instead of exhaustion time. The value of the modeled parameter τ and k_{YN} were determined from the slope and intercept of linear plot of $ln[C_t/(C_0-C_t)]$ against time (t) and represented in Table 6.7. The coefficient of determination value (R^2) exhibited the good fit of experimental data of the column studies to the Yoon-Nelson model. The experimental treatment time (τ_{exp}) and the predicted treatment time (τ_{cal}) for the $C_0/2$ effluent concentration were found almost same for all the adsorbents which is also evidence of good fit of the experimental data to the model. Results as shown in Table 6.7 indicate that with increase in flow rate and decrease in bed depth, τ values decrease and k_{YN} increase. Maximum τ value was found for As(V) sorption on to NOIS.

Table 6.7. Predicted Yoon-Nelson model parameters of arsenic sorption on various adsorbents with different bed depth and flow rate.

Adsorbent	Variable	As(III)				As(V)			
		k_{YN} (h^{-1})	τ_{cal} (h)	τ_{exp} (h)	R^2	k_{YN} (h^{-1})	τ_{cal} (h)	τ_{exp} (h)	R^2
	Bed Depth								
NOIS	45	0.0063	3292.15	3240.00	0.9500	0.0036	4408.02	4320	0.9524
	30	0.0072	2237.88	2208.00	0.9176	0.0045	2844.98	2760	0.9500
	15	0.0067	1242.46	1148.00	0.8519	0.0051	1556.48	1584	0.9825
	7.5	0.0154	667.52	602.00	0.9405	0.0102	854.93	912	0.9732
Sand	45	0.1189	50.90	52.00	0.8827	0.0709	80.42	81.00	0.9272
	30	0.1478	35.64	41.00	0.8033	0.1211	52.90	56.00	0.8324
	15	0.3116	13.96	15.00	0.8593	0.2648	23.18	23.50	0.8721
	7.5	0.4416	8.07	8.50	0.9134	0.4777	10.65	11.00	0.9447
Murum	45	0.0421	198.25	198.00	0.9439	0.0198	450.72	480.00	0.8845
	30	0.0596	136.50	132.00	0.9544	0.0291	308.58	336.00	0.9309
	15	0.0959	67.88	78.00	0.8991	0.0414	165.19	174.00	0.9343
	7.5	0.1243	37.14	39.00	0.9518	0.0823	63.82	75.00	0.9385
	Flow Rate								
NOIS	5	0.0063	3292.15	3240.00	0.9500	0.0036	4408.02	4320.00	0.9524
	10	0.0077	1361.95	1440.00	0.8890	0.0078	2059.52	2088.00	0.9875
	15	0.0101	834.76	864.00	0.9126	0.0127	1262.41	1272.00	0.9739
Sand	5	0.1189	50.90	52.00	0.8827	0.0709	80.42	81.00	0.9272
	10	0.1121	44.87	50.00	0.8216	0.0736	70.02	70.00	0.9103
	15	0.0762	38.54	43.50	0.7843	0.0851	60.09	63.00	0.7331
Murum	5	0.0403	199.07	198.00	0.9505	0.0198	450.72	480.00	0.8845
	10	0.0819	88.13	90.00	0.9090	0.0355	193.40	204.00	0.8920
	15	0.0963	56.25	54.00	0.9614	0.0550	122.11	114.00	0.9831

Fig. 6.5 is showing the comparison plots of experimental breakthrough curves and predicted breakthrough curves that are generated using Thomas model and Yoon-Nelson model for different bed depth. From the figure it can be seen that the both the predicted breakthrough curves overlap to each other for all the adsorbents and they are well interpreting the experimental data except for sand. The experimental effluent concentrations for both As(III) and As(V) were found higher than the modeled effluent concentrations.

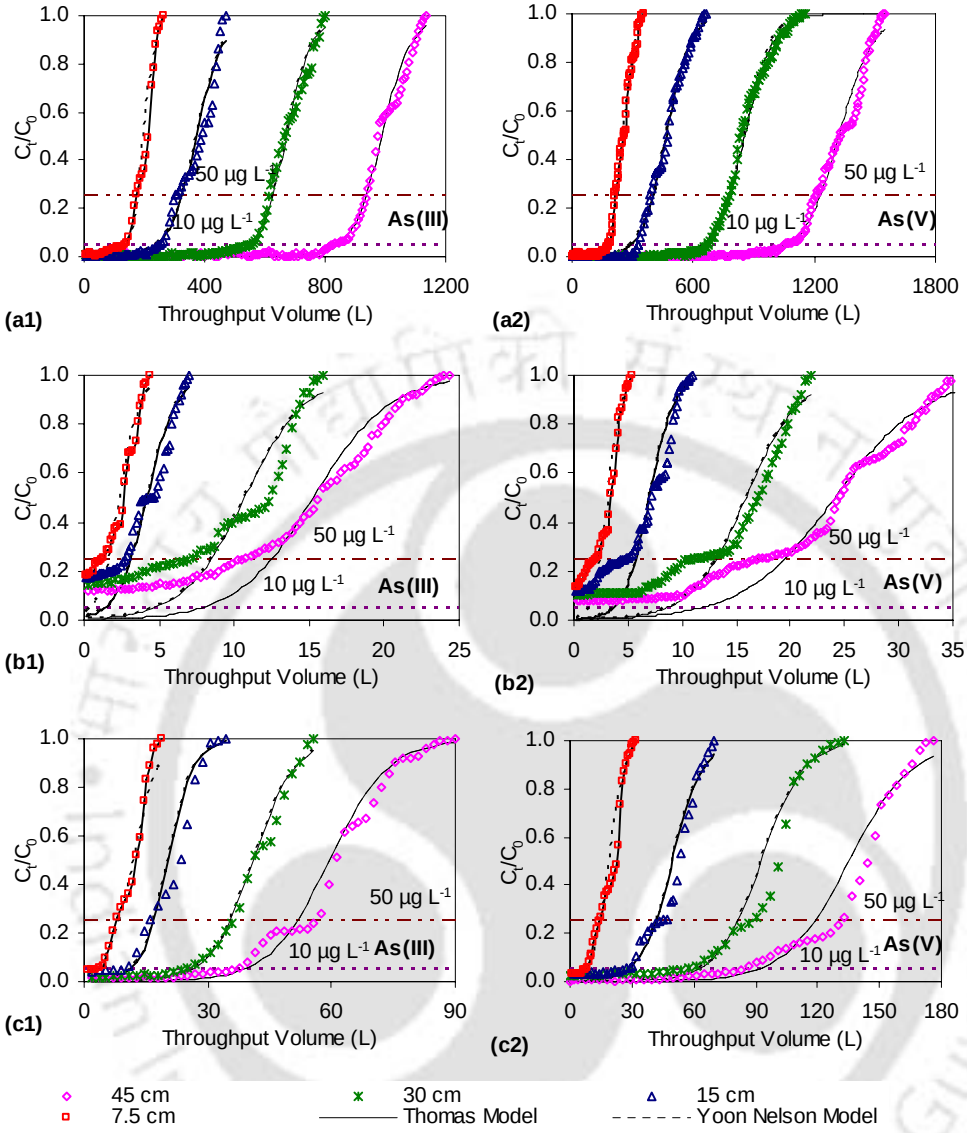

Fig. 6.5. Experimental and modeled breakthrough profiles of arsenic adsorption onto: (a) NOIS, (b) sand and (c) murum.

6.2.3.7 Theoretical breakthrough curve

The theoretical breakthrough curve was generated with initial arsenic concentration of 5 µg L^{-1} following concept of Michaels as follows:

1. Initially, the equilibrium line is drawn assuming various C_e values and calculating corresponding q_e values using Freundlich adsorption isotherm.

2. An operating line was drawn passing through the origin and (200, q_e^*) as shown in Fig. 6.6 (a).
3. A graph of $(C\text{-}C^*)^{-1}$ versus C was plotted. The area under the curve represents the integration value of the Equation (6.21) [shown in Fig. 6.6 (b)].
4. Using Equation 6.23, the theoretical breakthrough curves were generated by plotting of C/C_0 versus $(V\text{-}V_B)/(V_E\text{-}V_B)$ as shown in Fig. 6.6 (c).

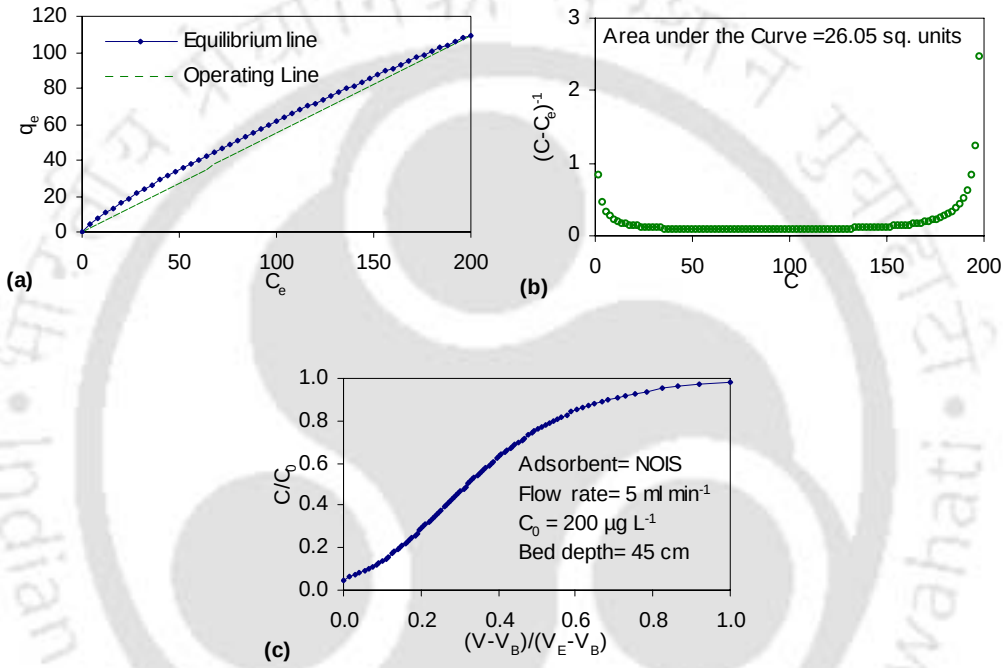

Fig. 6.6. (a) Equilibrium and operating lines to predict the breakthrough curve. (b) Curve to evaluate for determination of theoretical breakthrough curve of As(III). (c) Theoretical breakthrough curve.

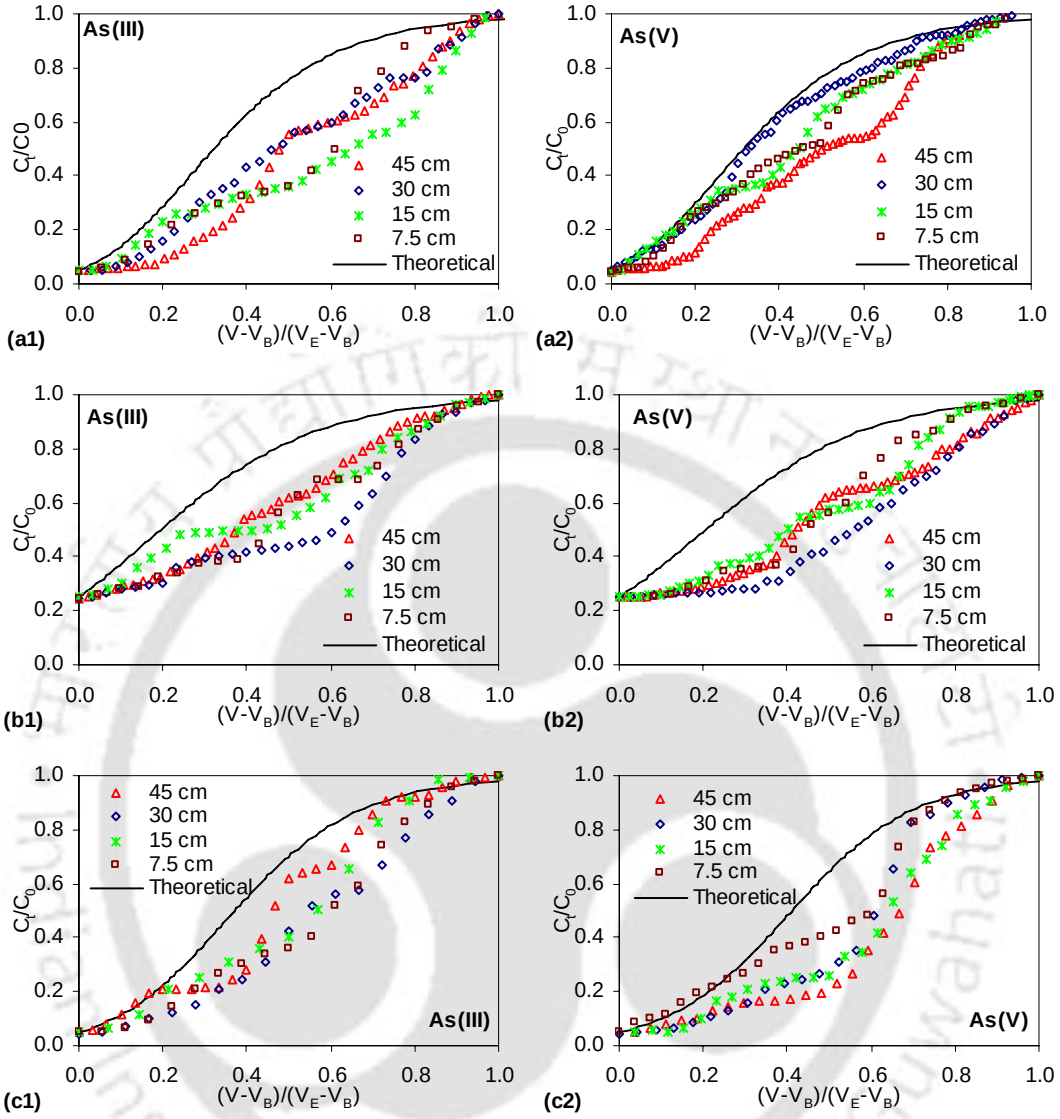

Fig. 6.7. Theoretical breakthrough of arsenic adsorption [As(III) and As(V)] onto (a) NOIS, (b) sand and (c) murum (C_0 = 200 µg L^{-1}, Q = 5 ml min^{-1}).

Theoretical breakthrough curves were generated using the data obtained from the batch isotherm study and compared with the experimental breakthrough curve. Freundlich adsorption isotherm which was the best fit isotherm for all the adsorbents was used to develop the theoretical breakthrough curve. Compared plot of theoretical and experimental breakthrough curve is shown in Fig. 6.7 for the both arsenic species [As(III) and As(V)] adsorption onto NOIS, sand and murum. Compared studies of the breakthrough curves indicate that the experimental plots of C_0/C_t increased gradually

with the increase of $(V-V_B)/(V_E-V_B)$ whereas the theoretical breakthrough curve increased sharply. The overall the experimental breakthrough curves are not following exactly the theoretical breakthrough curve pattern.

Except the theoretical breakthrough curve, all other models (BDST model, Thomas model and Yoon-Nelson model) are well representing the column experimental studies. As it is discussed earlier, the BDST model can predict the service time of column run for a given effluent concentration and loading rate, this is applied to design the pilot scale and field scale filter.

6.3 Co-precipitation test

It is already established that the groundwaters of Brahmaputra floodplains contain higher amount iron in ferrous form. When the groundwater comes in contact of atmosphere, the ferrous iron converted into ferric iron in the presence of atmospheric oxygen. The ferric iron formed flocs which quite capable to adsorb aqueous arsenic. The detailed theory is discussed in section 2.5.8 (Chapter 2). In this chapter an attempt is taken to observe the behavior of iron at normal pH with respect to time and different molar ratio. At 1:100 molar ratio of As and Fe^{3+}, the kinetic study was performed. The results (Fig. 6.8) indicated that iron adsorbed more quantity of As(V) than As(III). Fig. 6.8 indicated that the ferric flocs were precipitated very slowly upto 150 minutes but arsenic sorption process was continued upto 90 minutes. Figures [Fig. 6.8 (a) and (b)] corroborate that arsenic sorption was fully dependent on the density of the ferric flocs remained in the solutions. After 150 minutes of sorption, 25.90% of As(III) was removed by ferric flocs where as 40.94% of As(V) adsorbed by the flocs.

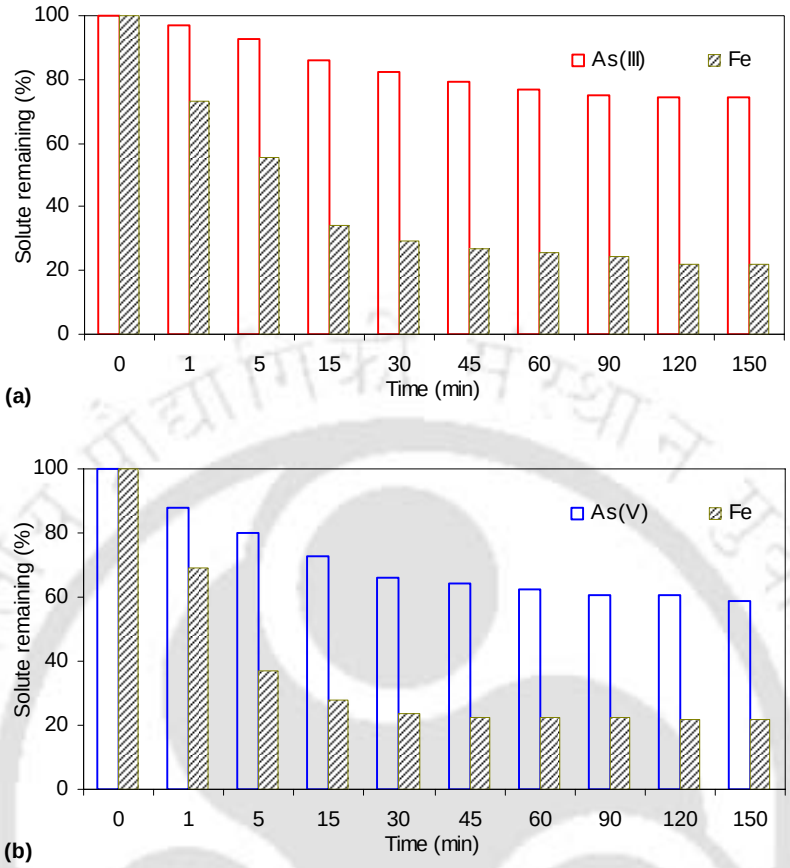

Fig. 6.8. Co-precipitation test with respect to time (Initial arsenic concentration = 4µM, pH=7, Volume of sample = 1L, molar ratio of As and iron = 1:100).

A comparative study was conducted to observe the effect of molar ratio of As to Fe^{3+} on arsenic sorption in the aqueous solution (Fig. 6.9). The arsenic removal efficiency was increased with the increase of molar ratio. As(V) removal efficiency was found to be more compared to the As(III). The maximum removal efficiency (61.09%) was noticed at 1:200 molar ratio in case of As(V). The results pointing that the aqueous iron is quite capable to remove arsenic but can not reduce it to its permissible limit (10 µg L^{-1}).

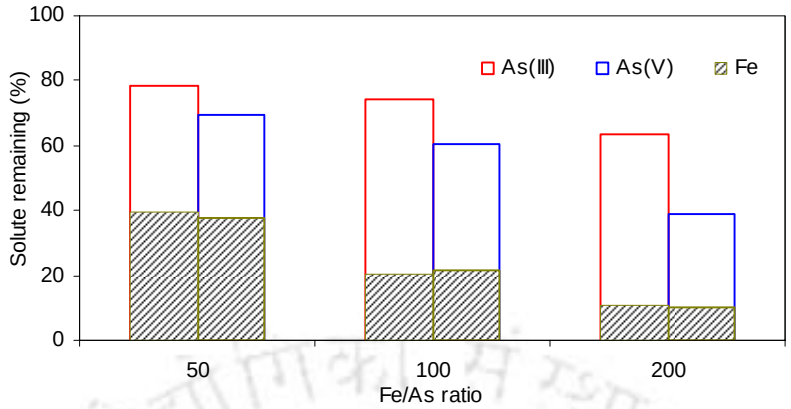

Fig. 6.9. Co-precipitation test with respect molar ratio (Initial arsenic concentration = 4μM, pH=7, volume of sample = 1L, contact time = 150 min).

6.4 Arsenic desorption and regeneration studies

Recently, management of arsenic waste is a big issue. For any adsorption process, it is necessary to recover the adsorbate as well regenerate the adsorbent. Maximum recovery of arsenic can reduce the toxicity level of the spent adsorbent and sludge management will be easy. Again after regeneration, reuse of the adsorbent will reduce the filtration cost. Literatures corroborate that from few past decades various acid and base have been used as desorbing agent. Appropriate strength of HCl, HNO_3 or NaOH can recover the arsenic more than 90% from aluminum-loaded Shirasu-zeolite (Xu et al., 2002), red mud (Genc-Fuhrman et al., 2005), synthetic zeolites (Chutia et al., 2009), coconut coir pith (Anirudhan, 2007), Fe(III)-treated biomass of Staphylococcus xylosus (Aryal et al., 2010) and biomass (Pandey et al., 2009). Form the Fig. 6.10 and Table 6.8, it can be seen that at higher strength (6N), NaOH, HCl and HNO_3 as reagent both arsenic species [As(III) and As(V)] can be recovered successfully from all the studied adsorbents (NOIS, sand, red soil and murum). But the recovery of arsenic is decreased with the dilution of desorbing agents. From comparative study it can be observed that performance of NaOH is more and at 0.5N strength, more than 90% arsenic recovery was recorded. From the results and considering the chemical cost 0.5N NaOH can be use as optimum elution dose.

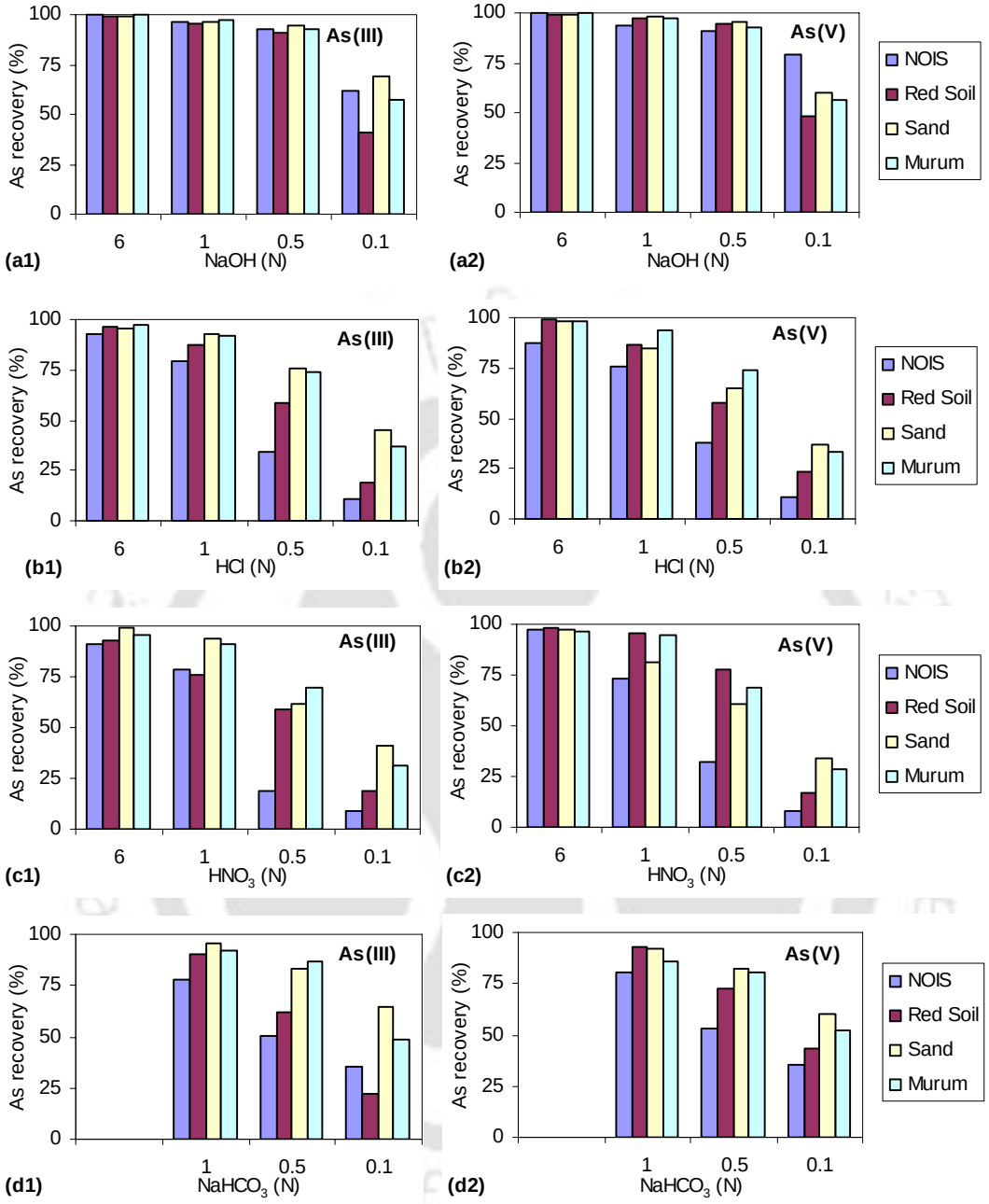

Fig. 6.10. Arsenic recovery from the adsorbents using different elution: (a) NaOH, (b) HCl, (c) HNO_3, (d) $NaHCO_3$.

Table 6.8. Recovery efficiency of As(III) and As(V) by various desorption solutions.

Adsorbent	Desorbing Agent	Strength (N)	As(III)		As(V)	
			Adsorption (%)	Recovery (%)	Adsorption (%)	Recovery (%)
NOIS	NaOH	6	92.84	99.64	95.98	99.66
		1	93.01	96.81	96.10	93.73
		0.5	92.70	92.88	96.53	91.03
		0.1	92.05	61.65	95.95	79.09
	HCl	6	92.19	92.45	95.94	87.52
		1	92.20	78.97	96.28	76.11
		0.5	92.53	34.57	95.90	38.11
		0.1	91.83	10.93	95.93	11.04
	HNO_3	6	92.78	91.31	96.24	97.64
		1	92.59	78.30	96.08	72.95
		0.5	93.06	19.13	96.53	32.05
		0.1	92.11	8.64	96.31	8.23
	$NaHCO_3$	1	92.70	78.30	96.06	80.73
		0.5	92.49	50.53	96.20	52.68
		0.1	92.64	34.98	96.70	35.41
Red Soil	NaOH	6	79.86	99.50	84.35	99.29
		1	80.27	95.06	85.04	97.41
		0.5	79.86	90.54	84.93	94.58
		0.1	79.92	41.25	85.59	47.77
	HCl	6	79.72	96.09	84.48	99.39
		1	79.15	87.51	85.05	86.16
		0.5	80.00	58.42	85.66	57.26
		0.1	79.89	19.20	85.18	23.79
	HNO_3	6	80.27	92.93	84.51	98.15
		1	79.51	76.08	84.48	95.90
		0.5	79.85	59.13	85.19	77.80
		0.1	79.38	18.60	84.93	16.94
	$NaHCO_3$	1	79.22	90.54	84.58	93.01
		0.5	79.52	61.88	84.90	72.28
		0.1	79.87	22.49	84.61	43.37
Sand	NaOH	6	47.18	99.42	70.54	99.38
		1	46.49	100.19	71.56	98.46
		0.5	48.39	94.27	69.64	95.78
		0.1	49.36	68.75	71.49	60.13
	HCl	6	46.36	95.07	70.69	97.90
		1	47.05	92.48	71.70	84.36
		0.5	46.88	75.57	71.64	65.19
		0.1	46.34	44.83	71.90	37.13
	HNO_3	6	46.61	98.71	71.19	97.65
		1	47.09	94.03	71.61	81.46
		0.5	47.71	61.78	71.74	60.60
		0.1	47.40	41.19	72.05	33.59
	$NaHCO_3$	1	46.39	95.39	71.34	91.68
		0.5	47.04	83.07	71.19	82.74
		0.1	46.88	64.69	71.45	59.87

Adsorbent	Desorbing Agent	Strength (N)	As(III)		As(V)	
			Adsorption (%)	Recovery (%)	Adsorption (%)	Recovery (%)
Murum	NaOH	6	79.65	99.61	87.24	99.84
		1	80.48	97.56	87.73	97.62
		0.5	80.28	92.46	87.89	92.85
		0.1	80.11	57.29	87.04	56.53
	HCl	6	80.34	96.98	87.18	98.61
		1	79.63	91.70	86.61	93.58
		0.5	79.95	74.28	87.01	73.68
		0.1	80.24	36.94	87.95	33.13
	HNO_3	6	80.29	95.42	87.64	96.75
		1	79.85	91.52	87.24	94.50
		0.5	79.96	69.89	87.58	68.90
		0.1	80.09	31.29	87.84	28.53
	$NaHCO_3$	1	80.28	92.26	87.48	85.77
		0.5	80.05	86.37	87.24	80.73
		0.1	79.75	49.03	87.33	51.89

To determine the effect of contact time on desorption process, kinetic studies were performed using 0.5N NaOH solution (Table 6.9 and Fig. 6.11). From the results it can be seen that arsenic recovery increases over the time and reached at equilibrium after 60 min. Initially, desorption rate was rapid and it reached up to 30-40% within 5 min. At equilibrium 95-99% of arsenic desorption was observed.

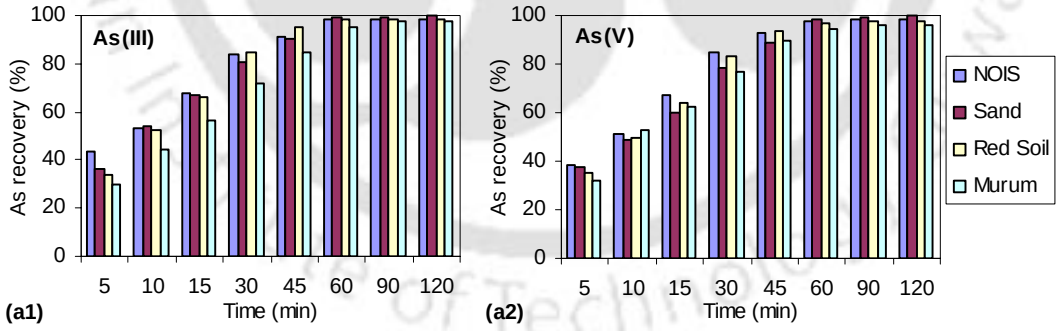

Fig. 6.11. Effect of contact time on arsenic desorption from the adsorbents (NOIS, sand, red soil and murum) using 0.5N NaOH solution: (a1) As(III) adsorption and (a2) As(V) adsorption. Matrix: C_0 = 200 µg L^{-1}; adsorbent dose= 0.35g/35ml; contact time = 4 hr.; Desorbing agent solution: 2 bed volume of 0.5N NaOH and Temperature = 25^0C.

Table 6.9. Effect of contact time on arsenic desorption from NOIS, sand, red soil and murum using 0.5N NaOH solution.

Adsorbent	Time (min)	As(III)		As(V)	
		Arsenic Adsorption (%)	As Recovery (%)	Arsenic Adsorption (%)	As Recovery (%)
NOIS	5	93.48	43.61	96.06	38.27
	10	93.39	52.87	95.70	51.38
	15	93.58	67.65	95.89	66.91
	30	93.41	84.22	95.36	84.52
	45	93.68	91.34	96.18	93.09
	60	93.29	98.33	95.74	97.86
	90	93.18	98.48	96.05	98.01
	120	93.21	98.61	95.99	98.29
Sand	5	46.35	36.46	71.70	37.60
	10	46.75	54.39	71.23	49.00
	15	46.45	66.87	72.35	59.62
	30	45.45	80.80	71.33	78.13
	45	46.45	90.20	71.95	89.12
	60	45.48	99.12	71.50	98.04
	90	45.63	99.37	72.33	99.22
	120	44.95	99.61	71.88	99.81
Red Soil	5	73.18	33.69	83.44	35.27
	10	73.38	52.73	82.86	49.57
	15	73.23	65.79	83.39	64.32
	30	72.73	84.63	82.85	83.52
	45	73.23	94.95	83.43	93.27
	60	72.74	98.66	83.68	96.94
	90	72.81	98.23	83.18	97.42
	120	72.48	98.59	83.40	97.54
Murum	5	76.76	30.06	85.89	32.22
	10	76.60	43.96	86.48	53.12
	15	76.64	56.65	85.30	62.59
	30	75.58	71.72	86.51	77.14
	45	76.51	84.74	85.46	89.91
	60	76.68	95.34	85.66	94.48
	90	76.43	97.24	85.59	96.32
	120	77.18	97.59	85.95	96.36

The kinetic data of arsenic desorption experiments were modeled to describe the desorption rate and maximum desorption capacity. High coefficient of determination values (R^2) and low standard error (SE) are ensuring that desorption processes for all of the adsorbents are obeying pseudo second order reaction model (Table 6.10). Modeled maximum desorption capacity (q_e) was found almost similar to the experimental value for the all cases.

Table 6.10. Coefficients of a pseudo-second-order kinetic model fitting of arsenic desorption kinetics.

Adsorbent	As(III)				As(V)			
	q_e (µg g^{-1})	K_{s2} (g µg^{-1} min^{-1})	R^2	SE	q_e (µg g^{-1})	K_{s2} (g µg^{-1} min^{-1})	R^2	SE
NOIS	19.86	0.0064	0.9985	0.66	20.56	0.0057	0.9982	0.67
Sand	9.79	0.0119	0.9979	0.27	15.96	0.0055	0.9979	0.47
Red Soil	15.66	0.0073	0.9970	0.62	17.86	0.0060	0.9974	0.66
Murum	17.12	0.0040	0.9973	0.48	18.22	0.0055	0.9986	0.42

The desorption experiments also conducted for the column spent adsorbents to observe the variation in arsenic recovery. The amount of adsorbed arsenic in column spent adsorbents is more than the batch sorption that can affect on desorption efficiency. In Table 4, maximum As(III) recovery (88.34%) for NOIS and As(V) recovery (98.84%) for sand can be observed. The data of Table 6.8 and Table 11 indicate that arsenic desorption of column spent adsorbents are little less than the batch spent adsorbent. It may be possible that 0.5N strength of NaOH is not sufficient to dissolve higher quantity of arsenic that present in the column spent adsorbent; higher strength of desorbing agent may be required to achieve more arsenic recovery efficiency.

Table 6.11. Desorption of several column spent adsorbents using 0.5N NaOH solution.

Adsorbent	As(III)			As(V)		
	As in adsorbent (µg)	As desorbed (µg)	As Recovery (%)	As in adsorbent (µg)	As desorbed (µg)	As Recovery (%)
NOIS	62.54	55.25	88.34	113.26	103.51	91.39
Sand	4.00	3.52	88.18	8.37	7.69	91.84
Red soil	16.25	13.90	85.53	26.04	23.22	89.18
Murum	13.76	12.05	87.59	24.02	21.13	87.94

When the column adsorbents after adsorption are exhausted; it is essential to recover the arsenic and regenerate the adsorbents. To recover the arsenic from the spent adsorbents of column, elution test was performed using 0.5N NaOH solution at 18 ml min^{-1} flow rate.

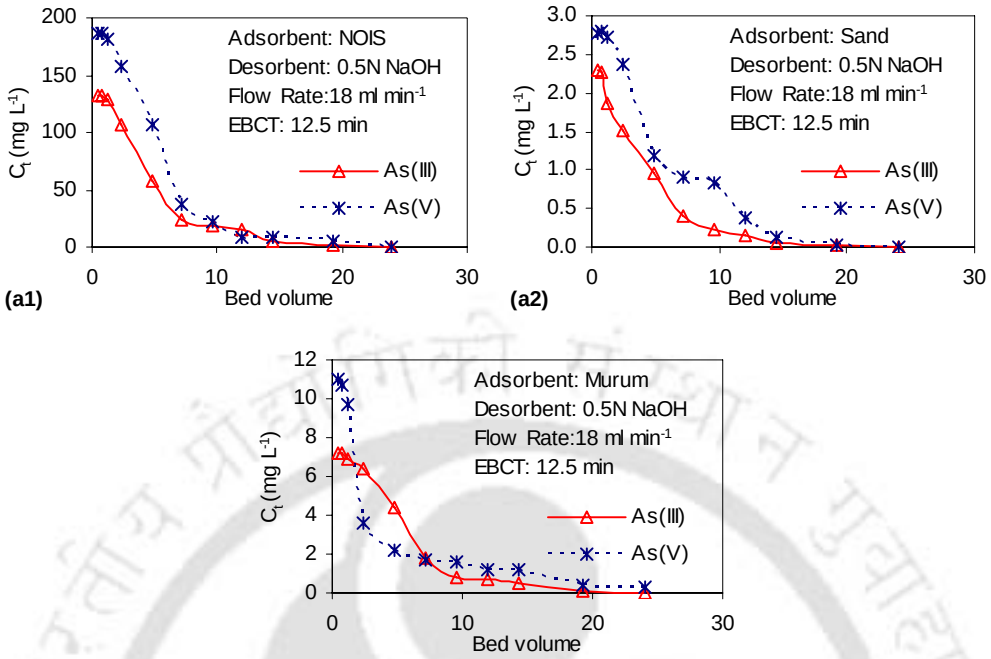

Fig.6.12. As(III) and As(V) desorption profile using 0.5N NaOH: (a1) NOIS, (a2) sand and (a3) murum.

Table 6.12. Summary of the results of adsorption-desorption of As(III) and As(V) onto NOIS, sand and murum.

Adsorbent	As(III)			As(V)		
	As Loaded (mg)	As Desorbed (mg)	Elution Efficiency (%)	As Loaded (mg)	As Desorbed (mg)	Elution Efficiency (%)
NOIS	196.72	164.33	83.53	293.98	248.85	84.65
Sand	2.82	2.51	88.90	4.52	4.06	89.82
Murum	11.88	10.29	86.57	13.67	11.87	86.78

From the Fig. 6.12, it is clear that initially both arsenic species [As(III) and As(V)] desorbed higher quantity in 0.5N NaOH solution thereafter it reduced with the time. Fig. 4 also shows that in less than 15 bed volume, almost the entire amount of both As(III) and AS(V) species were almost completely desorbed from the all of the three selected beds (NOIS, sand and murum). However, to calculate the maximum desorption capacity of eluting agent, upto 24 bed volume of arsenic desorption was calculated. The amount of arsenic desorbed form the adsorbent was calculated as the area under the desorption profile. The Table 6.12, confirmed that almost 90% arsenic was recovered during the elution test from all of the selected adsorbents and for both As(III) and As(V).

The desorption capacity of the eluting agent was found little higher in the batch mode than the column mode; it may be due to higher contact time and better contact of eluting agent with the spent adsorbent.

6.5 Summary

To estimate the performance of NOIS, sand and murum column experiments were performed in continuous mode. Bed volume of NOIS was found be excellent compared to the other adsorbents. BDST model, Thomas model and Yoon-Nelson model can describe the column experimental data. BDST model was applied to predict the service time of the adsorbents for a give loading rate breakthrough concentration. Co-precipitation test corroborate that iron flocs can remove a certain percent of arsenic but can not meet the desirable permissible limit. 2 bed volume of 0.5N NaOH solution can be use as eluent to recover the arsenic from spend adsorbents.

Chapter 7

Development of Arsenic Removal Filter for Arsenic Contaminated Areas of Brahmaputra Floodplain

7.1 Introduction

The chapter deals with the design and development of the arsenic removal filter (ARF) for the arsenic contaminated areas of Assam, India. The objective of this chapter consists of two parts. The performance testing of the developed porous media is discussed at the first part. The second part talked about the development procedure of the arsenic removal filter and its performance testing for the arsenic challenged water.

7.2 Development of porous media

From the earlier chapters (Chapter 5-6) it was established that red soil is a good adsorbent and has high removal efficiency for both arsenic species [As(III) and As(V)] sorption from solution in batch as well as column studies. The uptake capacity of arsenic and removal efficiency ensured that it could be used as an adsorbent for removal of arsenic species from groundwater. Red soil particles are very fine that easily mixed with water which increases the turbidity of the effluent. The retention time of red soil particles are very high and it is difficult to separate the same from water by gravitational method. Due to clayey and sticky nature, red soil particles can be easily moulded into desired shape. Porous media using the red soil particles can only use if burnt to form a compacted solid which is capable in filtering arsenic contaminated water.

7.2.1 Theory

Batch experimental studies were conducted to determine the maximum adsorption of the circular porous disk (CPD). To determine equilibrium time of arsenic sorption onto CPD, batch kinetic study was performed. The adsorption capacities of the CPDs were determined using the following equation (Crini, 2008; Hamdaoui, 2006):

$$q_t = \frac{(C_0 - C_t)V}{m} \tag{7.1}$$

Where, q_t = Adsorption capacity of disk (µg g^{-1})

C_0 = Initial concentration of the solution (µg L^{-1})

V = Volume of the arsenic spiked solution (ml)

m = Weight of the CPD (g)

In continuous mode the loading rate of the pot was calculated from the following equation:

$$v = \frac{Q}{A_s} \tag{7.2}$$

Where, Q is the discharge, v the loading rate and A_s the surface area of the internal side of the filter.

7.2.2 Optimization of the circular porous disk (CPD)

For initial trial circular porous disks (CPD) were prepared with different proportion of red soil and wheat husk mix. Design key parameters such as :i) porosity; ii) water content; iii) loading rate; iv) turbidity and v) arsenic [for both As(III) and As(V)] removal capacity were estimated for the each disk and findings of the same were presented in Table 7.1. The results showed that the key parameters checked against design they increase with the increase of wheat husk and red soil. However, beyond the 0.6:1 proportion ratio, the red soil lost its biding properties which affected on shaping of mould to desired shape. At 0.55:1 ratio of wheat husk to the red soil, the CPD was achieved sufficient amount of loading rate and decent arsenic removal efficiency. The turbidity value of the effluent was found within the safe limit (5 NTU). The biding property of red soil at 0.55:1 proportion remained perfect showing no change. It may be

concluded that using the 0.55:1 ratio of wheat husk and red soil the filter could be workable. Further batch and column experiments were conducted on CPDs with same ratio of wheat husk and red soil to determine the equilibrium time and adsorption capacity.

Table 7.1. Estimated design key parameters of the CPD (prepared using different proportionate red soil and wheat husk).

Red soil and wheat husk ratio	Porosity (fraction)	Water content (fraction)	Loading rate ($cm^3min^{-1}cm^{-2}$)	Effluent Turbidity (NTU)	As removal efficiency (%)	
					As(III)	As(V)
0.05	0.17	0.09	0.000	0.00	67.90	80.58
0.1	0.18	0.09	0.000	0.00	67.50	81.68
0.15	0.20	0.11	0.000	0.00	70.20	84.30
0.2	0.23	0.12	0.009	0.00	70.55	83.15
0.25	0.25	0.13	0.015	0.00	73.10	86.23
0.3	0.29	0.14	0.020	0.10	74.50	88.75
0.35	0.27	0.15	0.028	0.30	77.20	89.28
0.4	0.31	0.16	0.034	0.30	79.20	90.58
0.45	0.33	0.17	0.046	0.40	80.75	93.83
0.5	0.36	0.18	0.054	0.60	82.60	95.33
0.55	**0.39**	**0.20**	**0.060**	**0.70**	**83.15**	**97.50**
0.6	0.40	0.20	0.069	0.70	83.85	98.38
0.65	0.41	0.21	0.082	0.90	83.78	97.50
0.7	0.42	0.22	0.098	1.40	84.55	98.15

7.2.3 Pore sizes of CPD

To estimate the pore sizes of the CPD, FESEM images were investigated. The image (Fig. 7.1) shows that the pores, present inside the CPD, are in irregular in shape and size. The diameter of the pores is not consistence throughout their length. Size of the pores confirmed that the CPDs are quite capable to remove the suspended particles from aqueous solution.

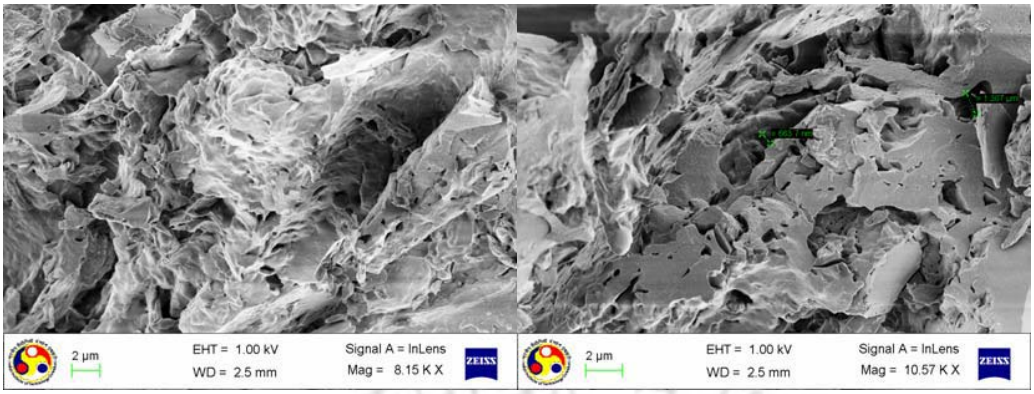

Fig. 7.1. FESEM images of CPD.

7.2.4 Findings of the batch experiments of CPD

Batch experiments were performed to optimize the adsorption capacity of the sorbent with respect to pH, adsorbent dose and equilibrium time. Effect of pH, kinetic studies and equilibrium studies of arsenic sorption on CPD (prepared using 0.55:1 proportion of wheat husk and red soil) were also conducted using distilled water at 25^0C. The observations made from the experimental results were described below.

7.2.4.1 Effect of pH

The effect of pH on both As(III) and As(V) sorption were examined and presented in Fig. 7.2. It was observed that sorption of both As(III) and As(V) ions onto the surface of CPD are sensitive with respect to pH of the solution. Adsorption of both arsenic species rapidly decreased beyond pH 8. In acidic media negligible variation was observed for both of the arsenic species sorption. However in higher acidic condition the arsenic adsorption capacity is decreased for both arsenic species. pH ranges from 3.54 to 7.52 were found to be optimum range for both arsenic species removal from the solution. Optimum pH for both As(III) and As(V) sorption was found as 6.86 and the corresponding adsorption capacities are 6.75 µg g^{-1} and 7.67 µg g^{-1} respectively.

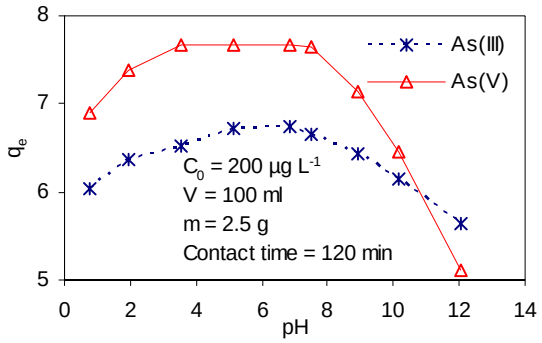

Fig. 7.2. Effect of initial pH on the removal of arsenic [As(III) and As(V)] by CPD at initial As concentration of 200 µg L^{-1}, adsorbent dose 25 g L^{-1}, volume of As spiked solution 100ml, shaking speed 200 rpm and temperature 25^0C.

7.2.4.2 Kinetic study of CPD

The kinetic studies of As(III) and As(V) adsorption onto the surface of the CPD were performed at various time interval in the ranges2.5 to 120 min (Fig.7.3). It was noticed from the Fig. 7.3 that the initial part of the curves were steep due to rapid bulk diffusion onto sorbent. Later on the steepness of curves was decreased which indicated end of the bulk diffusion and pore diffusion was the rate-limiting step at this stage. The end portions of the curves became parallel to the x-axis as it reached at the equilibrium concentration.. It was also observed From Fig. 7.3 that the removal efficiencies of As(III) and As(V) were achieved at rate of 74.88% and 85.50% respectively within first 20 minutes time. Whereas maximum removal efficiencies were estimated 85.80% for As(III) and 95.05% for As(V) at equilibrium time.

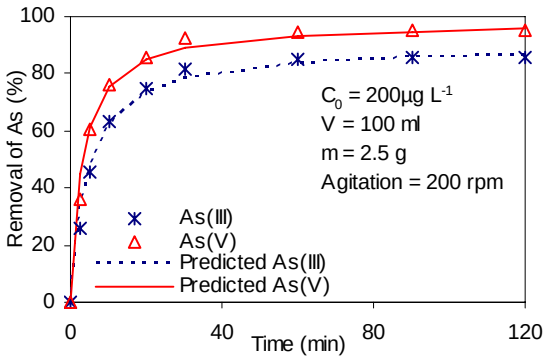

Fig. 7.3. Effect of contact time on arsenic sorption by the surface of CPD. [Matrix: C_0= 200µg L^{-1}, adsorbent dose= 25g L^{-1}, V= 100 ml, pH =7, shaking speed= 200rpm and temp.= 25 ± 1^0C].

Table 7.2. Pseudo second order reaction model parameters for arsenic sorption onto CPD.

Adsorbent	As Species	q_e (µg g^{-1})	K_{s2} (g µg^{-1} min^{-1})	R^2
CPD	As(III)	7.175	0.0320	0.9993
	As(V)	7.839	0.0428	0.9997

To estimate the adsorption kinetic rate, several adsorption models (first order reaction model, second order reaction model and pseudo-second order reaction model) were applied to the kinetic data (not shown here). Amongst all of the models, pseudo-second order reaction model was found to be the best-fit model in the kinetic study. Pseudo-second order reaction model parameters presented in Table 7.2 with high correlation coefficient (R^2) values 0.9993 and 0.9997 of As(III) and As(V) respectively. This indicated good fit of pseudo-second order reaction equation to the kinetic data. Again from the comparison plots of the experimental data and predicted data (Fig 7.3) it can be concluded that the model represented well the experimental kinetics data for both As(III) and As(V) sorption. The maximum adsorption capacities were found 7.175 and 7.839 µg g^{-1} for As(III) and As(V) respectively.

7.2.4.3 Equilibrium study of CPD

The effect of adsorbent dose in terms of removal efficiency on the removal of As(III) and As(V) presented in Fig 7.4 showed that with increase in adsorbent dose there was increase in arsenic removal efficiencies due to larger surface area. The experimental data were tested for fit with commonly used models such as the Langmuir and Freundlich model. The best fit model parameters for As(III) and As(V) adsorption isotherms as shown in Table 7.3 the correlation coefficient values were found above 0.98 against Langmuir and Freundlich model and considered an indication of good fit. In Freundlich model, the maximum adsorption capacities for both As(III) and As(V) were found little higher i.e. 16.76 and 19.55 µg g^{-1} respectively.

Table 7.3. Langmuir and Freundlich adsorption isotherm constants for As(III) and As(V) sorption onto CPD.

As Species	Langmuir model				Freundlich model			
	q_m (µg g^{-1})	b (L μg^{-1})	R^2	R_L	q_m (µg g^{-1})	K_F ($\mu g^{1-(1/n)} L^{1/ng-1}$)	n	R^2
As(III)	13.93	0.060	0.9871	0.08	16.76	1.924	2.45	0.9838
As(V)	15.92	0.092	0.9802	0.05	19.55	2.926	2.79	0.9818

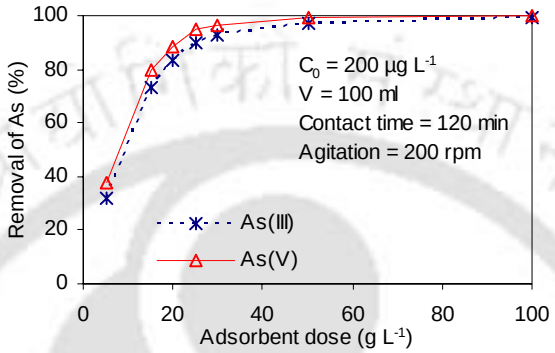

Fig. 7.4. Isotherm data for As(III) and As(V) sorption onto the surface of CPD. [Matrix: C_0= 200 µg L^{-1}, contact time= 120 min, V= 100 ml, pH =7, shaking speed= 200rpm and temperature= 25±1^{0}C].

7.2.4.4 Column study of CPD

The column studies were conducted with 40 cm constant water head to observe the breakthrough behavior of the optimized CPD (wheat husk and red soil ratio is 0.55:1). Constant water head was maintained to keep the loading rate constant (as the loading rate is directly proportional to the applied water head). Column studies were performed with different inlet arsenic concentrations i.e. 100, 200 and 300 µg L^{-1}. Flow rate and EBCT were maintained at 0.58 ml min^{-1} and 16.67 min respectively. Breakthrough behavior of As(III) and As(V) shown in Fig. 7.5 indicated that breakthrough point reached quickly for higher inlet arsenic concentrations than with lower inlet arsenic concentrations. Effluent quality could not meet 10 µg L^{-1} (WHO guideline value) but the CPD columns were capable to reduce arsenic concentration below 50 µg L^{-1} for all cases. Different breakthrough parameters of CPD correspondence to the inlet arsenic concentrations were represented in Table 7.4. The breakthrough time (t_{50}) and time of exhaustion (t_E) for 200 µg L^{-1} As(III) concentration were obtained as 40 h and 67 h, respectively. The corresponding values for As(V) sorption were 73 h and 139 h. Adsorption capacities (q_e)

obtained by the integration of the area above breakthrough curve were 56.17, 53.24 µg g^{-1} and 51.59 for 100, 200 and 300 µg g^{-1} As(III) concentrations respectively. The corresponding q_e values for As(V) sorption are 34.33, 32.62 and 23.95µg g^{-1} respectively. The decrease in breakthrough time as well as exhaustion time at higher initial concentration may be due to the rapid exhaustion of the sorption sites. The breakthrough curve was dispersed and breakthrough time came late at lower arsenic concentrations, saturation of the bed appeared faster at higher concentrations (Bhakat et al., 2006).

Table 7.4. Effect of inlet arsenic concentrations on arsenic sorption by CPD at 0.58 ml min^{-1} of flow rate and 16.67 min of EBCT.

Inlet As concentration	As species	t_{50} (h)	t_E (h)	V_{50} (L)	V_E (L)	*CP (%)*	M_{ads} (µg)	q_e (µg g^{-1})
100	As(III)	23	143	0.80	4.95	56.17	301.56	15.83
200	As(III)	40	67	1.39	2.32	53.24	280.29	14.71
300	As(III)	9	49	0.31	1.70	51.59	262.69	13.79
100	As(V)	193	289	6.68	10.01	65.33	653.97	34.33
200	As(V)	73	139	2.53	4.81	64.53	621.32	32.62
300	As(V)	25	73	0.87	2.53	60.14	456.18	23.95

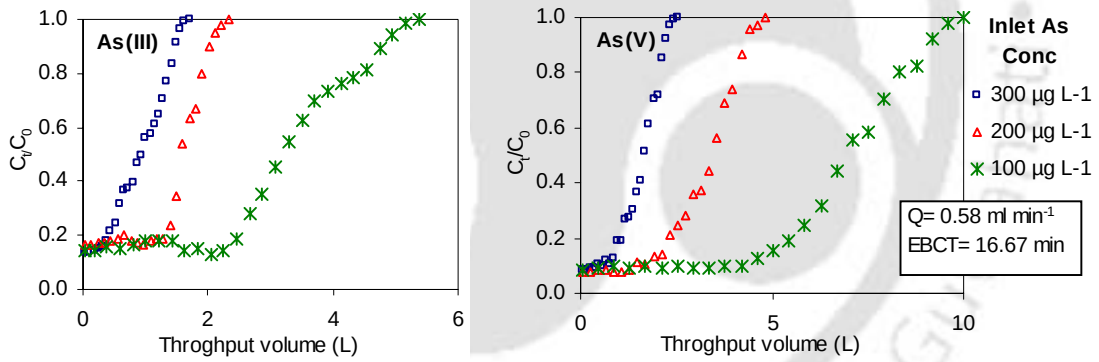

Fig. 7.5. Effect of inlet arsenic concentration on arsenic sorption by CPD [matrix: passage = 3.5 cm, depth = 0.9 cm, pH of solution = 7 and temperature = 21.6^{0}C].

7.2.5 Performance testing of porous pot

To observe the variation of arsenic sorption by field developed porous media and laboratory made CPD, two porous pots were made and they were tested for arsenic adsorption capacities and loading rates. The outer diameter and height of the pot were measured as 15.438 cm 12.4 cm respectively. The external height of the porous zone was 7.6cm. Inside surface of the pot was determined by assuming 1 cm thick pot and

spherical in shape. Internal surface area of the pot was calculated as 278.63 cm^2. The effluent discharges of the two pots were 16.17 and 15.83 ml min^{-1}. The corresponding loading rates were 0.059$cm^3min^{-1}cm^{-2}$ and 0.056$cm^3min^{-1}cm^{-2}$ which were slightly lower than discharge (0.06) of the optimized CPD. To check the turbidity removal efficiency, 100 NTU strength of standard solution was allowed to pass through the porous pot. The turbidity of the effluent was found as 0.4 NTU which is well within the permissible limit.

For testing of arsenic removal capacity of the pots, column studies were performed. Influent flow rate of the pots were maintained at 15 ml min^{-1} during the column study to prevent overflow, which was slightly lower than discharge of the pots. Column studies were performed using 200 µg L^{-1} of As(III) or As(V) spiked solutions. The breakthrough curves of the continuous mode studies were shown in Fig. 7.6 of arsenic sorption onto the surface of the porous pots. The calculated EBCT value was 18.58 min. The breakthrough curves related parameters was summarized in Table 7.5. Breakthrough time and exhaustion time for As(III) sorption were 24 and 72 h respectively. The corresponding throughput volumes were 21.6 and 64.8 L. Similar way the breakthrough time and exhaustion time for As(V) were 84 and 126 h and the correspondence throughput volumes are 75.6 and 113.4 L respectively. Adsorption capacities (q_e) for As(III) and As(V) are found to be 11.82 and 29.74 µg g^{-1} respectively which are slightly lower than the estimated q_e values of CPD. From the results of the porous pot, it can be concluded that the performance of field level porous pot was almost similar to the laboratory prepared CPD. Results of CPDs and porous pots assuring that the pilot scale filter can be developed based on the experimental results.

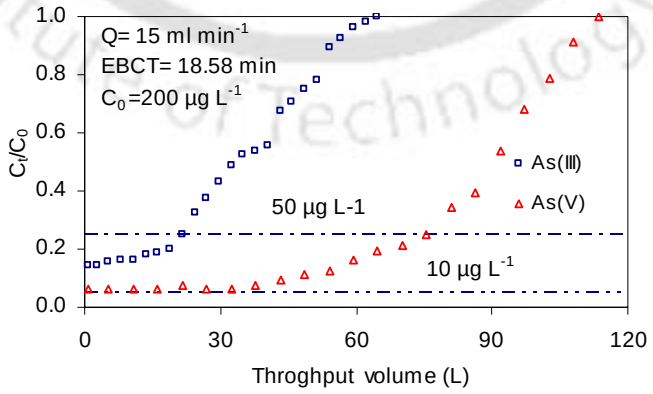

Fig. 7.6. Breakthrough curves of As(III) and As(V) sorption on porous pot. [Matrix: C_0= 200 µg L^{-1}, EBCT = 18.58 min and Q = 15 ml min^{-1}].

Table 7.5. Estimated breakthrough curves parameters of arsenic sorption by porous pot.

As species	t_{50} (h)	t_E (h)	V_{50} (L)	V_E (L)	CP (%)	M_{ads} (µg)	q_e (µg g^{-1})
As(III)	24	72	21.60	64.80	50.30	6519.37	11.82
As(V)	84	126	75.60	113.40	72.35	16408.45	29.74

7.3 Design and performance testing of arsenic removal filter (ARF)

7.3.1 Design approach

From the literature survey and in our present work it was already established that groundwater of 18 districts of Assam is highly contaminated with arsenic. Groundwater also contained huge quantity of ferrous iron in maximum places. Physical survey indicated that to overcome the iron problem in drinking water, the semi urban and rural people were using sand filter since last few decades. From our present study as also in the literatures, it was already established that the sand filter can remove arsenic upto a certain limit but not to the desirable limit of 10 µg L^{-1}. However, sand can remove arsenic successfully from the water along with other adsorbents. Adaptation of a new technology by the users was big challenge for the filter developer. Arsenic is a tasteless, odorless and colorless element and makes no apparent feeling to human while consuming arsenic contaminated water. Its reaction to human body is very slow and takes several years to diagnosis its effect medically. Visible affects of arsenic could be noticed after accumulation in body damaging human organs. Furthermore in developing countries like India arsenic testing in rural sector is still considered to be a big challenge. Capital expenditure of a filter and cost of filtered water is a big issue for the rural people. People are not willing to pay much for safe drinking water unless otherwise there is any change in color/taste of water. So, when a technology is applied for household level or community level it is observed that after a time period people stop using it due to lack of their awareness and affordability as well. The aim of the present study is to develop an arsenic removal filter for household level using locally available adsorbents. Attempt is also taken to design arsenic removal filter based on the locally available adsorbents; like sand, NOIS, red soil and murum. Porous media using red soil and wheat husk was

developed which can control the loading rate, turbidity and also upto a certain degree of arsenic contamination.

Before designing the filter adsorption parameters such as kinetics of arsenic sorption, arsenic removal mechanism, equilibrium time and adsorption capacity of the each adsorbent were evaluated. Effects of pH and co-ions on arsenic sorption for individual adsorbent were evaluated. Optimization of the flow rate was developed for removal of arsenic as well as suspended particles on porous media. Column experiments were performed with each of the adsorbents at different bed depth, different loading rate and different inlet arsenic concentration to determine breakthrough behavior. These were also made to find out service time at breakthrough, exhaustion time of adsorbent bed, adsorption kinetics, column performance and adsorption capacity of the column. From batch experimental results it was found that all of the adsorbents are quite capable to remove arsenic from water. NOIS is found as promising adsorbent for removal of arsenic from water. Effects of pH and major ions on arsenic sorption were also evaluated. The results corroborate that arsenic sorption is optimum at normal pH and no adverse effect were seen due to the presence of co-ions at natural level pH found in groundwater. From the column experiments, the bed volume of NOIS was found to perform at satisfactory level (more than 3000 bed volume). On the other hand bed volumes of other three adsorbents are quite low compared to the NOIS. Removal efficiency of adsorbents with both As(III) and As(V) were tested, the results showed that the adsorbents were more efficiently removing As(V) than As(III). Based on the batch and column experimental results the porous filter was developed and appropriate adsorbents were selected to design the arsenic removal unit.

7.3.2 Development of porous filter

One porous filtration unit was developed to remove the arsenic from water which consists of two chambers and had already discussed in the previous chapter (Chapter 3). Volumetric capacity of the filter was found to be 9.5 L. Lower portion of the upper chamber was made porous through which the effluent will be filtrated. Schematic diagram of the porous portion of the filter is shown in Fig. 7.7. Internal surface area is

determined assuming the porous portion was a part of a sphere. Loading rate of the filter was determined in the similar way as determined for porous pot. Total arsenic adsorption capacity of the porous filter was calculated using the adsorption capacity of the porous pot.

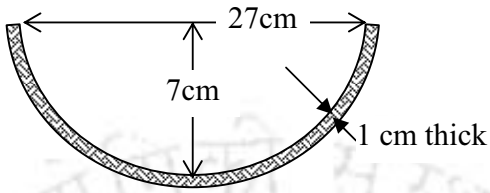

Fig. 7.7. Schematic diagram of the porous portion of the designed filter.

The properties of the porous filter are described below:

Height of the porous zone = 7 cm

Width of the porous zone = 27 cm

Thickness of the porous zone = 1 cm

Internal surface area of the porous zone = 726.49 cm^2

Volume of the porous zone = 2183.54 ml

Average discharge of the filter= 40.33 ml min^{-1}

Average volumetric loading rate of the porous filter = 0.056 ml min^{-1} or 3.331 ml h^{-1} cm^{-2}

Total adsorption capacity of As(III) = 17002.48 µg

Total adsorption capacity of As(V) = 42779.51 µg

7.3.3 Estimation and selection of appropriate adsorbents for design the arsenic removal filter

The arsenic removal unit for household level is designed based on the requirement of water quantity in monthly basis, effluent water characteristics i.e. arsenic concentration below 10 µg L^{-1}. From previous literature and the present study, it is evident that groundwater of Assam contains higher level of iron that also helps removal of arsenic to safe level in filtered water by co-precipitation technique and adsorption. Although iron helps on arsenic sorption from groundwater, it was not taken into account for developing arsenic removal filter since presence of iron at higher level in every case seems uncertain. In the rural and semi-urban area, the requirement of water for cooking and drinking

purpose is approximately 5 L per capita per day (Ahmed, 2001; Jain et al., 2007; Indiresan, 1996; Gleick, 1996). Assuming each family consist of five members; the requirement of water is 25 L per family per day. If the filter is designed for a run time of 4 months, the filter is supposed to treat 3000 L of water (assuming 30 days in a month) before breakthrough (10 µg L^{-1}). Requirements of each of the adsorbents were quantified to meet the treated water volume before breakthrough for the design period of 4 months. Requirements of individual adsorbents were estimated using BDST model assuming that discharge through each adsorbent is same as the discharge measured for the porous filter. It was also assumed that the adsorbents were placed in cylindrical column diameter identical to the diameter of the topmost portion of the porous media. The basic criteria to determine the bed depth and corresponding bed volume are described below:

Arsenic concentration in feed water = 200 µg L^{-1}

Breakthrough arsenic concentration = 10 µg L^{-1}

Design period of the filter run = 4 month

Water consumption rate = 5 L per person per day

Water consumption per family (Assuming 5 member per family) = 25 L

Total volume of water that have to treat within the design period = 3000 L

Discharge of the filter (measured) = 2420 ml h^{-1}

Diameter of adsorbent media inside the filter = 27 cm

Cross sectional area of the column = 572.56 cm^2

Loading rate of the filter = 4.227 ml h^{-1} cm^{-2}

Estimated service of the filter run = 1239.67 h

Table 7.6. Predicted BDST model parameters for the design period of filter run.

Adsorbent	Arsenic species	v_2 (ml h^{-1} cm^{-2})	C_2 (µg L^{-1})	C_F (µg L^{-1})	a_2	b_2	x (cm)	V_a (L)
NOIS	As(III)	4.23	200	10	890.97	-37.83	1.43	0.82
	As(V)	4.23	200	10	1127.83	-41.08	1.14	0.65
Sand	As(III)	4.23	200	10	12.19	-7.50	102.32	58.58
	As(V)	4.23	200	10	19.36	-11.42	64.61	37.00
Murum	As(III)	4.23	200	10	39.71	-16.68	31.64	18.12
	As(V)	4.23	200	10	90.68	-18.61	13.88	7.94
Red Soil	As(III)	4.23	200	10	144.61	-44.00	8.88	5.08
	As(V)	4.23	200	10	161.96	-36.00	7.88	4.51

Required bed depth and the corresponding volume of the adsorbents to meet the effluent characteristics within the design period of filter run was estimated using BDST model. BDST model parameters which calculated from the column experiments were used to predict the require bed depth of the individual adsorbents for the 4.23 ml h^{-1} cm^{-2} loading rate, 10 µg L^{-1} breakthrough concentration and 1239.67 h service time. Predicted bed depth and correspondening volume of the adsorbents is summarized in Table 7.6. Results show that the requirement of bed depth is higher for As(III) sorption than As(V) sorption for the studied adsorbents. Predicted bed depths for As(III) adsorption onto individual adsorbents i.e. NOIS, sand, murum and red soil are 1.43, 102.32, 31.64 and 8.88 cm. Corresponding adsorbents volumes were 0.82, 58.58, 18.12 and 5.08 L and volumetric capacity of the porous filter was 9.5 L. Thus maximum volume of the filter will be occupied by red soil and very little space will be available for influent. Predicted volumes of sand and murum were found to be more than the filter capacity. This problem can be resolved by increasing filter capacity (i.e. total volume). Manufacturing cost of the filter is directly proportional to the volume of filter, which indicates that the capital cost will be increased with increase in capacity of the filter. Again, increasing the capacity of the filter, weight of the filter will be increased which may be difficult in handling the filter. Red soil permeability of soil was very low which can reduce the flirtation rate of the designed filter. In addition to above the particles of red soil are very fine which can hinder passing of water through filter pores. Hence designing gravity flow filter using red soil is an arduous work. Red soil can be used as an arsenic removal adsorbent in up flow mode filters only. Volumetric requirement of NOIS was 0.82 L, which found to be quite low than other studied adsorbents. That can be used as arsenic removal adsorbent media.

7.3.4 Arsenic sorption mechanism of NOIS

The adsorption of arsenic onto the surface of the NOIS was investigated using FESEM images, FTIR Spectra and XRD Spectra.

Due to its highly amorphous nature, no prominent peak is obtained in XRD spectra in case of NOIS [Fig. 7.8 (a)]. The prominent peak of maghemite in XRD spectra

obtained from NOIS (after adsorption of arsenic), confirming the bonding of arsenic on the surface of NOIS [Fig. 7.8 (b)].

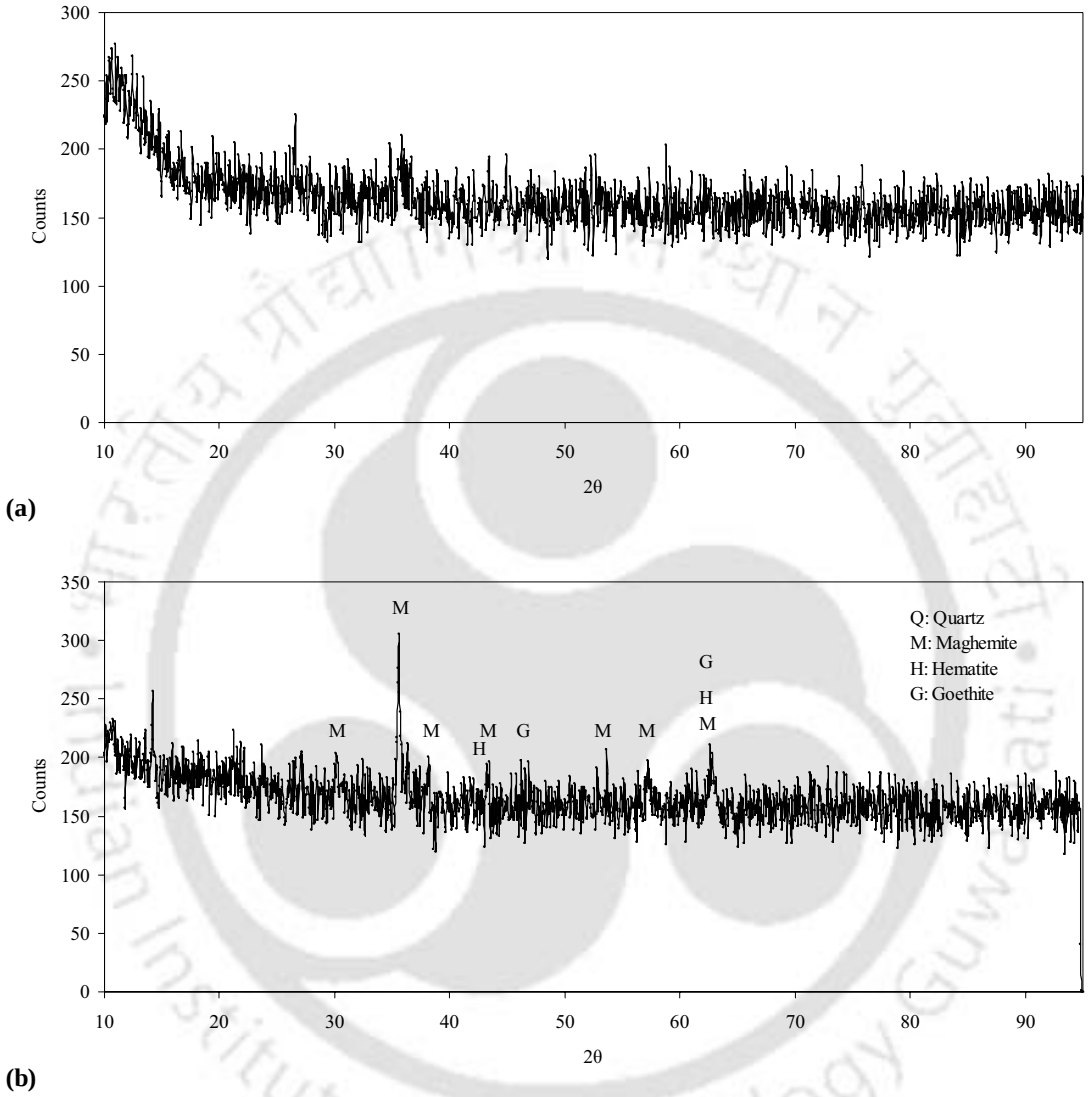

Fig. 7.8. XRD patterns of (a) NOIS before adsorption and (b) NOIS after adsorption of arsenic.

Fig. 7.9 (a) shows that NOIS is highly amorphous in nature. Several different types and different shaped compounds are present in the surface of NOIS particles. The FESEM images [Fig. 7.9 (a)] confirmed that the NOIS particles were amorphous in nature, which may facilitate better arsenic removal. From Fig. 7.9 (b), it can be noticed that arsenic is deposited layer wise on the surface and also inside the voids of NOIS

particles. The shapes of the particles present in the NOIS are changed due to adsorption of arsenic on their surfaces.

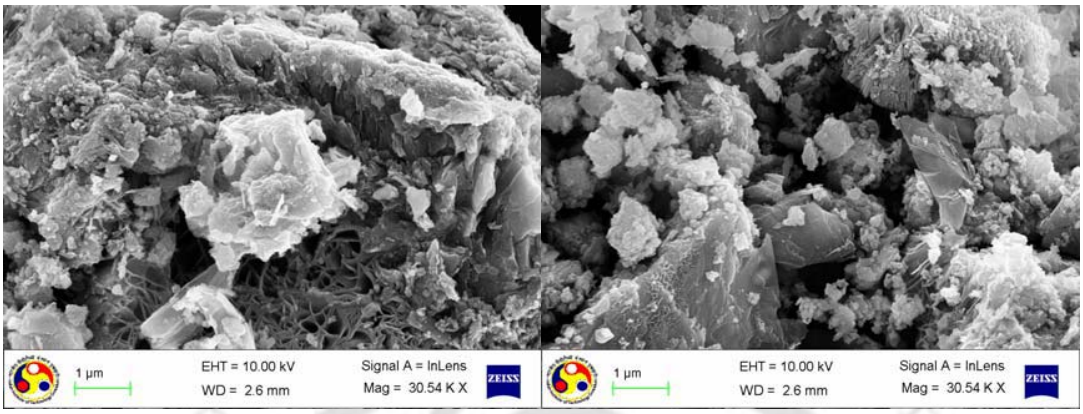

(a)

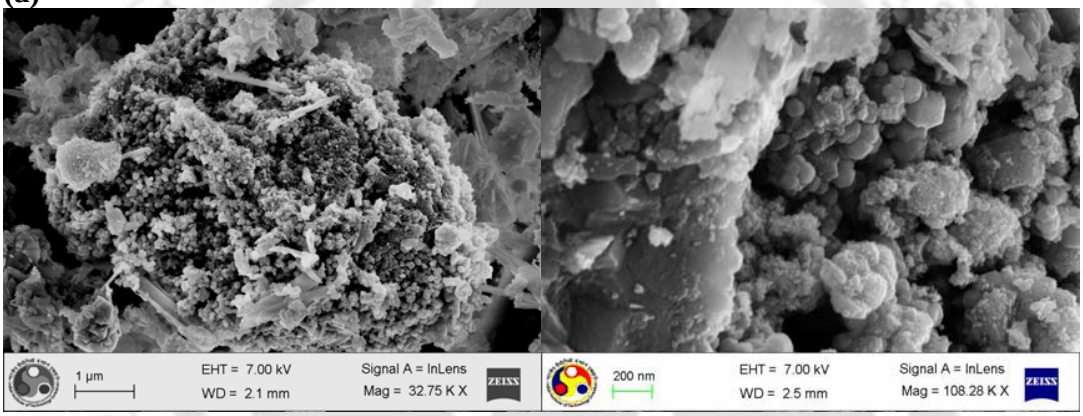

(b)

Fig. 7.9. SEM images of NOIS: (a) before arsenic adsorption and (b) after arsenic adsorption.

The FTIR spectra (Fig. 7.10) at 3434 cm^{-1} and 3436 cm^{-1} (nearby 3400) for the NOIS before and after adsorption of arsenic respectively, can be assigned to the outer –OH stretching vibrations coordinated to trivalent cation (Fe^{3+} or Al^{3+}) in the octahedral layer (Liu et al., 2010) and the corresponding IR peaks at 1637 cm^{-1} and 1632 cm^{-1} due to –OH bending vibration (Anbalagan et al., 2010). IR spectrum at 597 cm^{-1} confirmed that NOIS contain α-Fe_2O_3 whereas IR spectra at 562 indicated the presence of γ-Fe_2O_3 in the NOIS after adsorption of arsenic (Suresh et al., 2009). Again 880 cm^{-1} peak represented $AsO(OH)_2^-$ species (Partey et al., 2008) confirming the presence of arsenic in the adsorbent. After adsorption, the prominent peaks of IR spectra at vibration mode (1000-450 cm^{-1}) were in agreement with the adsorption process.

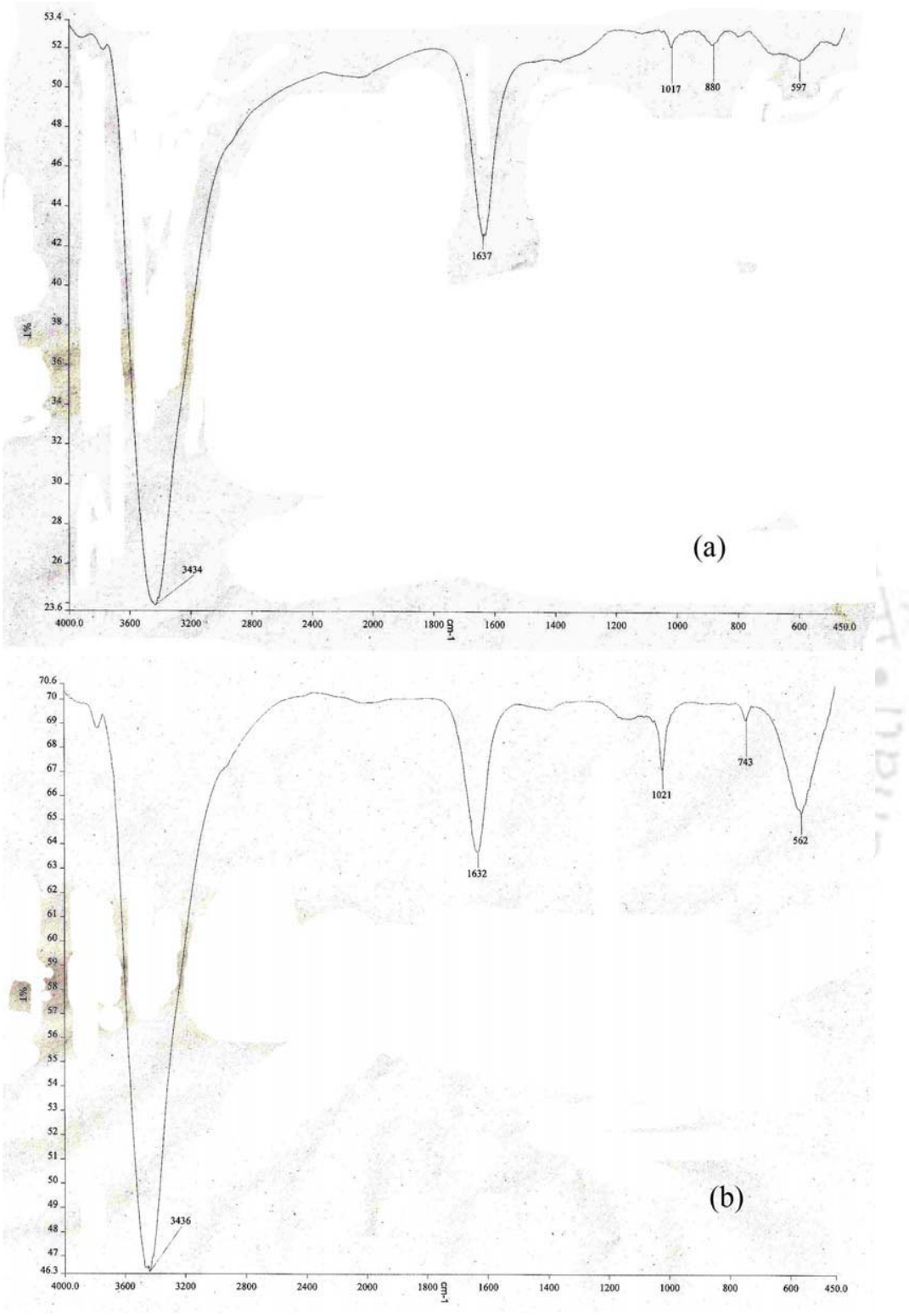

Fig. 7.10. FTIR Spectra of NOIS (a) before and (b) after adsorption of arsenic.

7.3.5 Prediction of service time and development of arsenic removal filter

Performance is the important criteria for development of arsenic removal filter. It was already established that NOIS a good adsorbent for arsenic removal and a bed depth 0.82 cm required for As(III) sorption from water. NOIS is applied for removal of arsenic from the contaminated influent in the filtration unit. Shape of the developed porous filter is considered an important factor for design the adsorption capacity of the filter. Porous media was constructed in spherical shape to accommodate inside the clay pot to regulate water flow and as adsorbent also. Topmost porous portion was measured as 27 cm in diameter, 7 cm in height with a surface area of 726.5 cm^2. It was already established that the porous media cannot meet desired effluent arsenic concentration (below 10 $\mu g\ L^{-1}$) in 200 $\mu g\ L^{-1}$ inlet arsenic concentration. Therefore it is necessary to adsorb the influent arsenic before it reaches the exterior boundary of porous media. The filter should be designed in such a way that the NOIS will adsorb major portion of arsenic to its potential before the breakthrough threshold is reached. Effluent will encounter the porous media in arsenic safe stage only. Thus the bed of NOIS should be placed on the upper surface of the porous media. Sand is a good filtration media which also adsorbs arsenic to a certain extent and easily locally available. The volumetric capacity of the porous portion of the upper chamber of the arsenic removal filter is 2.2 L. Before placing of NOIS inside the filter, the porous portion of the filter is filled with sand to cover the porous portion of the filter. The porous portion is covered using sand to avoid the direct contact of influent with the porous portion of the chamber. 2.5 L of sand is applied to the filter, which is little higher than the required volume. This sand layer will help to reduce the possible clogging problem of the porous media arising out of the presence of turbidity or due to settlement of ferric iron. 1L volume of NOIS was placed in a perforated nylon bag with a diameter of 32 cm and 10 cm height. The nylon bag has a pervious bottom (nylon mesh 100) and impervious sides (like parachute cloth). The mass of applied NOIS was 2.74 kg and the corresponding bed depth was 1.75 cm which was higher than the designed bed depth of 0.82 cm. Diameter of the nylon bag was kept little bigger than the maximum filter diameter to prevent the channel flow between the passage of filter wall and nylon bag. The nylon bag along with the appropriate quantity of NOIS was placed above the top

of sand bed inside the filter. Fig.7.11 is showing the schematic diagram of vertical cross section of the lower portion of the filtration unit that represented the arrangement of sand and NOIS inside the filter.

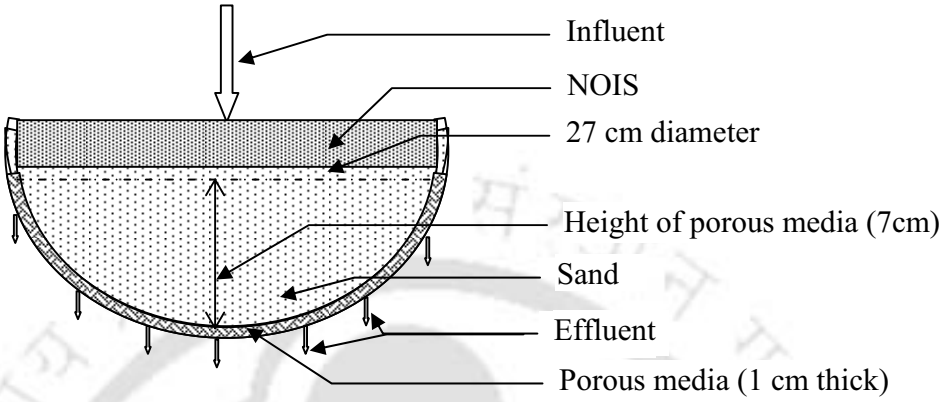

Fig. 7.11. Schematic diagram of vertical cross section of lower portion of the arsenic removal filtration device.

The porous portion of the filter was filled with sand and NOIS bed was placed above the sand bed (Fig. 7.11). The applied influent will pass through the NOIS bed initially when arsenic would be adsorbed in this bed itself. Thereafter, the effluent will pass through the sand bed before passing through the porous media. The filtrated water will be accumulated and stored in the lower chamber. Filtered water can be used directly for drinking purpose and cooking purpose. The characteristics of the arsenic removal filter are summarized in Table 7.7.

Table 7.7. Characteristics of the designed domestic arsenic removal filter.

Parameters	Magnitude
Capacity of Filter	9.5 L in either chamber
Material of construction	Red soil
Adsorbent media	NOIS
Filtration media	Sand
Service	Removal of arsenic from water
Flow rate	40.33 ml min^{-1}
Medium volume	1.00 L
Quantity of adsorbent	2.74 kg
Contact time	24.80 minutes
Daily operation time of filter	10.33 h
Maximum water treatment capacity of filter	58 L

To determine the service time of the filter run, it was assumed that only NOIS adsorbs arsenic and the other materials (sand and porous media) considered being inert. Service time of applied NOIS was determined using BDST model. The BDST equations for arsenic sorption onto NOIS at 200 µg L^{-1} inlet arsenic concentration, 10 µg L^{-1} breakthrough concentration and 4.23 ml h^{-1} cm^{-2} loading rate calculated as:

For As(III) $$t_s = 890.97x - 37.83 \quad (7.3)$$

As(V) $$t_s = 1127.83x - 41.08 \quad (7.4)$$

The predicted service times for 1.75 cm bed of NOIS for As(III) and As(V) sorption were 1518.28 h and 1928.72 h respectively. As the maximum amount of arsenic present in groundwater was in As(III) form, the lower value i.e. 1518.28 h was accounted to predict the column run. The corresponding treated water volume of the filter was 3673.56 L. If 25 L is the water requirement per family per day then the filter will run for 147 days or 4 month 27 days (assuming 30 days in a month). BDST model can also predict the service time for different concentration of arsenic feed water. The predicted BDST equation for the different inlet As(III) concentration (C_2) of the designed filter calculated as:

$$t_s = 890.97\frac{200}{C_2}x - 37.83\left(\frac{200}{C_2}\right)\frac{\ln(C_2/10-1)}{\ln(200/10-1)} \quad (7.5)$$

The Equation [7.5] can be rewritten as:

$$t_s = 178194\frac{x}{C_2} - 2569.59\frac{\ln(C_2/10-1)}{C_2} \quad (7.6)$$

The predicted service times and the corresponding treated water volumes and bed volumes for the different inlet arsenic concentrations are presented in Table 7.8.

Table 7.8. Predicted performance for different inlet As(III) concentration of the designed arsenic removal filter (ARF).

Influent As concentration ($\mu g\ L^{-1}$)	Service time (h)	Volume of treated water (L)	Volume of treated water (Bed Volume)	Design period of filter (days)
50	6153	14891	14891	596
100	3056	7395	7395	296
200	1518	3674	3674	147
300	1009	2441	2441	98
500	602	1458	1458	58
1000	299	725	725	29

From the Table 7.8, it can be observed that the service time of the filter is dependent on the influent quality. Filter life decreases with the increase in feed water arsenic concentration. Results showed that in case of 50 $\mu g\ L^{-1}$ influent arsenic concentrations, the filter remain active for more than one year whereas with 100 $\mu g\ L^{-1}$ inlet arsenic concentration the filter can remove arsenic successfully for more than nine months without any interruption. Even with 1 $mg\ L^{-1}$ of arsenic contaminated feed water, the filter can remove arsenic approximately for one month.

7.3.6 Performance testing of the designed arsenic removal filter units using synthetic arsenic spiked solution

Performance of arsenic removal filter was tested in pilot scale with the designed arsenic removal filtration unit. To test the arsenic removal efficiency of the designed filter, the predicted quantities of sand (2.5 L) and NOIS (1.46 L) were placed inside the arsenic removal porous unit. 200 $\mu g\ L^{-1}$ strength of synthetic As(III) spiked solution applied to the filter at 25 $ml\ min^{-1}$ flow rate. Arsenic challenge water was prepared using tap water of Environmental Engineering Laboratory, IIT Guwahati. Appropriate volume of stock As(III) solution was added to the measured tap water and mixed properly to produce synthetic arsenic spiked solution. Filtered water was collected in lower chamber of the filter. Water sampling was carried out for 24 h time interval to estimate the arsenic concentration in the filtered water and assayed for arsenic concentration. Results are depicted in Fig. 7.12 which is showing the breakthrough behavior of arsenic removal

filter. The corresponding breakthrough parameters of the designed filter are represented in Table 7.9.

Table 7.9. Performance of the designed arsenic removal filter.

t_B (h)		t_E (h)	V_B (L)		V_E (L)	CP (%)	M_{ads} (µg)	q_e (µg g^{-1})
10 µg L^{-1}	50 µg L^{-1}		10 µg L^{-1}	50 µg L^{-1}				
2520	2736	3600	3780	4104	5400	82.79	894176	326

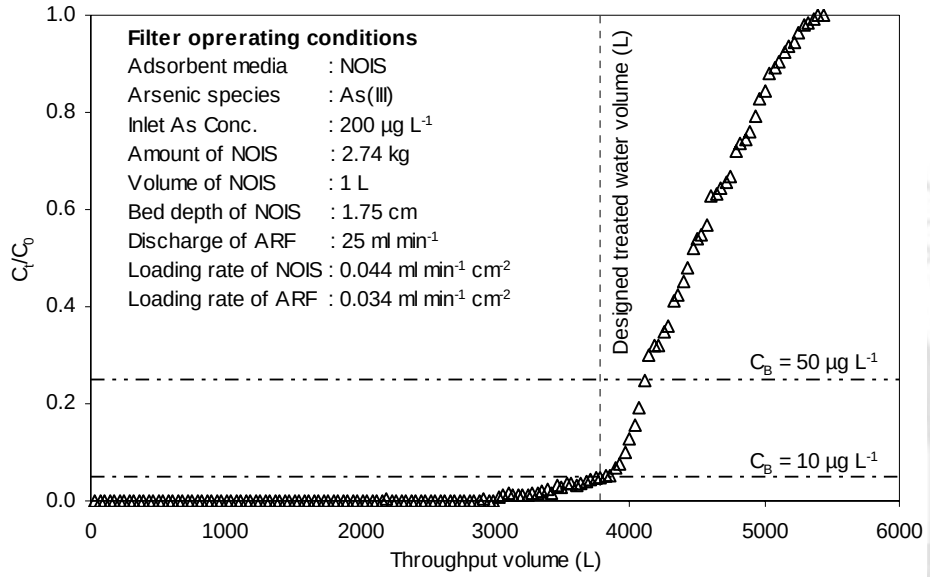

Fig. 7.12. Breakthrough behavior of designed arsenic removal filter.

The Fig. 7.12 shows the breakthrough behavior of As(III) sorption by the designed filter. At the initial stage of the filtration, 100% arsenic removal efficiency can be seen. After 3780 L of water treatment, the arsenic concentration reached at 10 µg L^{-1} breakthrough concentration. Thereafter arsenic concentration in the effluent gradually increased and after 3600 h, the filter bed is completely exhausted. Service times for the 10 µg L^{-1} and 50 µg L^{-1} of breakthrough concentration were 2520 h and 2736 h respectively and the corresponding treated water volumes were 3780 and 4104 L respectively. The throughput volume at 10 µg L^{-1} breakthrough was 3780 L, which was found to be higher than the predicted treated water volume (3674 L). Arsenic removal capacity of the filter designed which was based only on the NOIS. However sand and the porous media also participated on sorption of arsenic to a small extent. Adsorption capacity in arsenic removal filter was observed to be little higher than the predicted

capacity. The results of the designed filter ensure that the ARF will successfully remove arsenic for the design period of the filter run for the arsenic affected area of Brahmaputra floodplains.

7.3.7 Possible problems associated with the using of the domestic filter

Because of high iron content of the arsenic bearing natural ground water in most situations in Brahmaputra floodplains, there will be gradual accumulation of iron hydroxide precipitates upon the filter medium that will result in reduction of flow through the bed. Moreover, the porous media, which is acting as flow controlling device, may also get clogged due to accumulation of iron hydroxide precipitates. Hence, whenever significant reduction in output (filtration rate) will be observed, the NOIS bed, sand bed and the porous pot may be cleaned to restore the flow rate. For cleaning of NOIS and sand bed, the materials may be washed several times in the bucket filled with normal water. The iron precipitates get detached from the bed or bag and get suspended in the water. The water may have to be changed several times (around 5 times) till most of the precipitates are washed out and the water remains almost clear. Using a Scotch Brite or similar plastic scouring pad, scrape the surface of the porous media in an up and down motion to remove the contaminants that have collected on the surface. Use enough pressure to remove a small layer of the porous media on the inner surface of the pot. After cleaning the surface, rinse the pot in cold water to wash away the contaminant. Field experience suggest that washing of the medium may be needed once in a month, though that depends on iron content in the raw water and the volume of water treated. The washing process can be undertaken by users.

7.4 Cost analysis

Socio-economic status and severity of manifestations are correlated which are found all over the world. Poor people are suffer more as they are relatively more exposed to contaminated water with high arsenic level and have little or no choice of alternative solutions. Further, poverty is associated with lack of food and nutrition increasing

venerability. Rich households have better access to information on alternative solution and have more financial capacity to spend for alternative arsenic free water (Sarkar, 2007). Most of the arsenic-affected areas in India and Bangladesh are rural, where the lack of awareness and weaker economic status makes sustainability of any arsenic removal filter more uncertain.

Operational and maintenance issues and costs are particularly challenging. In view of required types of services, cost of a filter and affordability towards filtration for a low income villager must be carefully evaluated.

Cost per liter of water = Cost incurred for investment in purchasing a filter ÷ Liters of water treated till exhaustion of bed. The total cost of the filter developed in this study is shown in Table 7.10.

Table 7.10. Estimated total cost of the filter

Sl.No	**Description**	**Quantity**	**Value (in Rupees)**	**Cost (in Rupees)**
1	Earthen chambers	2 nos.	40.00 per piece	80.00
2	Sand	2.5 L	500.00 per m^3	12.50
3	NOIS	3 kg	20.00 per kg	60.00
4	Perforated nylon bag	1 piece	10.00 per piece	10.00
Grand total				162.50

With Rs. 162.50 investment, a villager can procure an arsenic removal filter which will provide him 3780 liters of safe water initially in the first phase of the filter.

Therefore, initially the cost per liter of water $= \frac{162.50}{3780} = Rs$ 0.0430 i.e. 4 paisa approximately.

Average water consumption per head per day has been 5 litres approximately for drinking and cooking. If it is considered that a average family consists of 4 family members, then arsenic safe water requirement will be 20 liters per day. Thus calculated daily expenditure will be 80 paisa. In a month the family spends Rs 24.00, which seems to be around 1.4 % of the monthly income even if the family head lives below BPL. In its

Ninth Five-Year Plan (1997–2002), BPL (below poverty line) for rural areas in India was set at annual family income less than Rs.20,000 (Wikipedia). The water expenditures of a family should not exceed 2 % of the family income (AWWA 2000, Klawitter 2003). Thus, the cost seems to be justifiable vis-a-vis the income of an average rural family under BPL.

The bed is exhausted after 189 days if water is filtered at the rate of 20 liters per day or after about six months time interval. Even after exhaustion of the filter media, the chamber remains intact. So only the partial cost of chamber may be calculated in evaluating water cost. If it is considered that earthen chamber has a service life of 2 years, then the 2^{nd}, 3^{rd} & 4^{th} cycle of operation (after exhaustion of the 1^{st} cycle) will lower down the cost of water. During these periods, cost per litre of water will be $\frac{72.50}{3780} = Rs$ 0.019 i.e. 2 paisa approximately.

It is believed that an initial investment of Rs 162.50 by a BPL villager is possible to avail safe water. After exhaustion of the filter media, it is possible for a villager to afford Rs.72.50 for replacing the whole media.

The adsorbents can be regenerated with 0.05N NaOH solution. To regenerate the adsorbents, 2 bed volume of 0.5N NaOH solution is required as shown in the section 6.4.

So, total volume requirement of chemical = 1L x 2 = 2 L 0.5N NaOH solution.

NaOH required for regeneration of the spent adsorbent = 2*0.5*40 g = 40 g

Cost of 40 g NaOH = (130*40)/50 = Rs.10.40

Assuming that the adsorbents will be regenerated for 3 times, the cost will be involved approximately Rs. 31.20.

After installation of the filter, only chemical cost will be involved in the filtration device.

So, the water cost after each regeneration will be = $\frac{10.40}{3780} * 100 = Rs$ 0.275 per hundred liter of water.

Thus, the monthly cost of the treated water will be = Rs. 1.65 which is quite reasonable.

Including the chemical cost, the investment of money for the arsenic removal filter in every two years will be (assuming 3 times regeneration) = Rs. 162.50 + Rs. 10.40*3

= Rs. 193.70

Therefore yearly filtration cost should be = Rs. 96.85

≈ Rs. 100.00

Cost analysis suggests that by spending hundred rupees, one can get arsenic free safe water for a year. This amount involved in the ARF is affordable even for the people who are living below the poverty level. Table 2.4 suggests that the developed filter will provide the lowest priced filter for arsenic removal in the study area as well as to other similar parts of Assam. Simplicity of the design, cost involvement and arsenic removal efficiency indicate that the filtration device will be easily accepted by the community.

7.5 Summary

Circular porous disks (CPD) were prepared in laboratory scale and were optimized. The arsenic removal porous filter was prepared for the field level, based on the laboratory scale performance of the CPD. To remove arsenic from aqueous solution, NOIS has been used as adsorbent. Sand was used in the filter as filtration media primarily to reduce the turbidity load of the porous media. The performance of the filter was tested in the laboratory using arsenic challenged water. Results assured that the newly developed arsenic removal filter can remove arsenic successfully and satisfactorily for the inlet arsenic concentration of 200 µg L^{-1}. The cost involvement confirmed that the ARF is generally affordable for the rural people of Brahmaputra floodplains affected by arsenic contamination of groundwater sources.

Chapter 8

CONCLUSIONS

8.1 Conclusions

At the onset as a preparation step towards developing an appropriate treatment system for arsenic affected sources, delineation of unsafe aquifers in the study area (Madhupur block of Nalbari district in Assam, India) was carried out to determine the arsenic contamination level and to quantify geochemical properties of groundwater. The following conclusions were made from this part of the research:

- Groundwater of the study area was severely affected with arsenic contamination. Out of 48 samples, 98% samples exceeded the drinking water permissible limit of arsenic (10 µg L-1) according to WHO guidelines, 88% samples contained arsenic beyond the BIS permissible limit (IS 10500:1991) of 50 µg L-1 and 46% samples contained more than 100 µg L-1 of arsenic concentration.
- The groundwater of the study area was predominantly Na-Ca-HCO3 type.
- The co-existing ions such as major cations, iron, phosphate and bicarbonates apparently played significant roles on arsenic mobilization in the aquifer of the study area.
- Seasonal variations of arsenic were significant; the maximum arsenic concentration was observed in the month of March.

To prevent the consumption of arsenic contaminated water, an arsenic removal filter was attempted using locally available, low cost and affordable materials *i.e.* red soil, sand, NOIS and murum. The adsorption and desorption characteristics of the materials were investigated in batch and continuous mode. From the research conducted, the following conclusions were made:

- The adsorbents (red soil, sand, NOIS and murum) were more efficient on adsorbing arsenic in acidic media than in alkali media. The sorption rate of As(V) were more sensitive to the pH of the aqueous medium than the As(III) sorption.

- Kinetic study revealed that both the arsenic species [As(III) and As(V)] for all adsorbents reached the equilibrium concentration within 3 hours and maximum arsenic sorption was achieved by the adsorbents within 2 hours.
- Pseudo second order reaction rate model was found to be the best fit model to delineate both As(III) and As(V) sorption mechanisms for each adsorbent. The arsenic sorption process was controlled by film diffusion followed by intraparticle diffusion.
- The arsenic adsorption capacity (q_t) was temperature dependent and inverse to the temperature of the solute. The arsenic sorption process was feasible, spontaneous and exothermic in nature.
- From the interpretation of the equilibrium data, the isotherm models can be arranged in the order of excellent fit as: Freundlich> Redlich-Peterson> Langmuir> Temkin> Dubinin-Radushkevich. The maximum adsorption capacity (q_m) was found to be highest for NOIS [155.60 µg g^{-1} for As(III) and 245.10µg g^{-1} for As(V)]. The adsorbents can be ordered according to adsorption capacity as: NOIS>red soil>murum>sand.
- The initial strength of arsenic in the aqueous medium influenced the sorption capacity of the adsorbents. At higher concentration, Ca^{2+} and Mg^{2+} ions slightly enhanced As(III) and As(V) adsorption capacity onto the adsorbents. Fe^{2+} helped to adsorb As(V) but resisted As(III) sorption. Both As(III) and As(V) adsorption onto the adsorbents were adversely affected by the presence of PO_4^{3-} and HCO_3^{2-} anions but no significant variation on arsenic sorption was observed for SO_4^{2-} ion. The coexisting ions were found to have negligible interference on the arsenic adsorption within their normal range as exist in ground water.
- Bed depth, flow rate and initial arsenic concentrations played significant roles in arsenic sorption at continuous mode. With increase of bed depth, the bed volume of adsorbents increased. In case of flow rate and initial arsenic strength, the bed volume of adsorbents decreased.
- The adsorption capacity (q_e) was found to be higher for NOIS [397.68 µg g^{-1} for As(III) and 504.56 µg g^{-1} for As(V)], than murum [38.31 µg g^{-1} for As(III) and 67 µg g^{-1} for As(V)] and lowest for sand [8.17 µg g^{-1} for As(III) and 10.58 µg g^{-1} for

As(V)] at 7.5 cm bed depth, 5 ml m^{-1} flow rate and 200 µg L^{-1} inlet arsenic concentration in continuous mode.

- BDST model, Thomas model and Yoon-Nelson model could well represent the column experimental data except the theoretical breakthrough curve.
- Co-precipitation experiments indicated that iron flocs can remove a certain percent of arsenic but cannot meet the desirable permissible limit (10 µg L^{-1}).
- Desorption/regeneration tests evaluated that 2 bed volume 0.5N NaOH solution can be used as eluent to regenerate the arsenic from spent adsorbents.
- XRD patterns, FESEM images and FTIR spectra confirmed that arsenic sorption onto NOIS is a physicochemical process.

A household level arsenic removal porous filter was developed using red soil (to develop porous media), NOIS (as adsorbent) and sand (as filtration media). The following conclusions are made from this part of the research:

- 0.55:1 proportion of wheat husk and red soil was found to be most effective ratio for development of the porous media.
- 2.5L of sand and 1L of NOIS were used inside the filter as filtration media and arsenic sorption media respectively.
- The volumetric capacity of the designed filter is 9.5 L in each chamber. The filter can fulfill the drinking water need of an average family conveniently.
- The throughput volume of the designed removal filter at 10 µg L^{-1} breakthrough was 3780 L, which was found to be higher than the predicted treated water volume (3674 L). The results assured that the arsenic removal filter can serve arsenic free water within the design period of four months efficiently and safely.
- The implementation cost of the filter was estimated to be Rs. 162.50 which will be affordable for low income people.

8.2 Scope of future research

In the present study, an arsenic removal filter was developed based on the geochemistry of groundwater it's potential for treatment of arsenic and needs of the consumers. The groundwater quality along with arsenic contamination level of the study

area was examined during four different seasons throughout the year. To check the persistence of arsenic severity in the study area, future research can be focused upon:

1. Quantification of arsenic present in the sediment within the aquifer zone.
2. Batch sequential study to estimate the exchangeable arsenic species present in the sediment which may leach out from sediment to the aquifer zone.
3. Determination of mobilization technique of arsenic in the groundwater system.

In the arsenic removal filter, untreated naturally oxidized iron scrap was used as adsorbent. It was observed that shape and size of NOIS particles influenced their arsenic sorption capacity. Again, arsenic adsorption capacity is also depends on the chemical composition of the NOIS particles and ionic form of iron compounds present in the particles. The porous media, which is developed using red soil and wheat husk, can be optimized by controlling shape and size of the wheat husk. The depth of the porous media also may play significant role on removing of arsenic and turbidity which was not tested during the present research. The porous portion of the filter was made in rounded shape to make the filter in Kolsi shape. The designed filter was tested using synthetic arsenic spiked solution. To improve the adsorption capacity of the filter, the future research work can be carried out involving:

1. Evaluations of performance of arsenic removal filter with the real groundwater.
2. Chemical treatment of NOIS to enhance the arsenic adsorption capacity.
3. Optimization of shape and size of NOIS particles to improve adsorption capacity.
4. Evaluation of arsenic sorption capacity of red soil in continuous mode.
5. Process description of regeneration mechanism of the adsorbents.
6. Development of technique for stabilization of the spent adsorbent.
7. Surface complexation study of the adsorbents to determine process involvement in sorption process.
8. Optimization the depth and porosity of the porous media for better removal of arsenic turbidity.
9. Study on the possible clogging problem of the adsorbent bed arising out of the presence of turbidity or due to settlement of ferric iron.

References

1. Abernathy, C. O., Thomas, D. J., and Calderon, R. L. (2003). "Health effects and risk assessment of arsenic." Journal of Nutrition, 133(5 SUPPL. 2), 1536S-1538S.
2. Ahamed, S., Kumar Sengupta, M., Mukherjee, A., Amir Hossain, M., Das, B., Nayak, B., Pal, A., Chandra Mukherjee, S., Pati, S., Nath Dutta, R., Chatterjee, G., Mukherjee, A., Srivastava, R., and Chakraborti, D. (2006). "Arsenic groundwater contamination and its health effects in the state of Uttar Pradesh (UP) in upper and middle Ganga plain, India: A severe danger." Science of The Total Environment, 370(2-3), 310-322.
3. Aharoni, C., Sideman, S., and Hoffer, E. (1979). "Adsorption of Phosphate Ions by Collodion-Coated Alumina." Journal of Chemical Technology and Biotechnology, 29(7), 404-412.
4. Ahmed Feroze, Paper 3: Arsenic Mitigation Technologies in South and East Asia, Volume II Technical Report on Arsenic Contamination of Groundwater in South and East Countries. Link:http://siteresources.worldbank.org/INTSAREGTOPWATRES/Resources/ArsenicVolII_PaperIII.pdf
5. Ahmed, K. (2004). "Arsenic enrichment in groundwater of the alluvial aquifers in Bangladesh: an overview." Applied Geochemistry, 19(2), 181-200.
6. Ahmed, K. M., Bhattacharya, P., Hasan, M. A., Akhter, S. H., Alam, S. M. M., Bhuyian, M. A. H., Imam, M. B., Khan, A. A., and Sracek, O. (2004). "Arsenic enrichment in groundwater of the alluvial aquifers in Bangladesh: an overview." Applied Geochemistry, 19(2), 181-200.
7. Ahmed, M. F. (2001). "An Overview of Arsenic Removal Technologies in Bangladesh and India." Technologies for Arsenic Removal from Drinking Water, B. U. o. E. a. Technology;, and U. N. University, eds.Dhaka, Bangladesh
8. Alshaebi, F. Y., Yaacob, W. Z. W., and Samsudin, A. R. (2010). "Removal of Arsenic from Contaminated Water by Selected Geological Natural Materials." Australian Journal of Basic and Applied Sciences(4), 4413-4422.
9. Anawar, H. M., Akai, J., and Sakugawa, H. (2004). "Mobilization of arsenic from subsurface sediments by effect of bicarbonate ions in groundwater." Chemosphere, 54(6), 753-762.
10. Anbalagan, G., Prabakaran, A., and Gunasekaran, S. (2010). "Spectroscopic characterization of indian standard sand." Journal of Applied Spectroscopy, 77(1), 86-94.
11. Anirudhan, T. S., and Radhakrishnan, P. G. (2009). "Kinetic and equilibrium modelling of Cadmium(II) ions sorption onto polymerized tamarind fruit shell." Desalination, 249(3), 1298-1307.
12. Anirudhan, T. S., and Unnithan, M. R. (2007). "Arsenic(V) removal from aqueous solutions using an anion exchanger derived from coconut coir pith and its recovery." Chemosphere, 66(1), 60-66.
13. Annadurai, G., and Krishnan, M. R. V. (1996). "Adsorption of basic dye using chitin." Indian J. Env. Prot., 16(6), 444-449.

14. Antia, D. D. J. (2010). "Sustainable Zero-Valent Metal (ZVM) Water Treatment Associated with Diffusion, Infiltration, Abstraction, and Recirculation." Sustainability, 2(9), 2988-3073.
15. Aptel, P., and Buckley, C.A. (1996). "Categories of Membrane Operations," Chapter in Water Treatment Membrane Processes, McGraw Hill, 1996. American Water Works Research Foundation, Lyonnaise des Eaux, Water Research Commision of South Africa, 1996.
16. Arslan-Alaton, I., Kabdaşli, I., Vardar, B., and Tünay, O. (2009). "Electrocoagulation of simulated reactive dyebath effluent with aluminum and stainless steel electrodes." Journal of hazardous materials, 164(2-3), 1586-1594.
17. Aryal, M., Ziagova, M., and Liakopoulou-Kyriakides, M. (2010). "Study on arsenic biosorption using Fe(III)-treated biomass of Staphylococcus xylosus." Chemical Engineering Journal, 162(1), 178-185.
18. Asta, M. P., Cama, J., Martinez, M., and Gimenez, J. (2009). "Arsenic removal by goethite and jarosite in acidic conditions and its environmental implications." Journal of hazardous materials, 171(1-3), 965-972.
19. ASTDR (2007). "Toxicological Profile for Arsenic." Department of Health and Human Services, Public Health Service Agency for Toxic Substances and Disease Registry, US.
20. Awuah, E., Morris, R. T., Owusu, P. A., Sundell, R., and Lindstrom, J. (2009). "Evaluation of simple methods of arsenic removal from domestic water supplies in rural communities." Desalination, 248(1-3), 42-47.
21. Ayoob, S., Gupta, A. K., and Bhakat, P. B. (2007). "Analysis of breakthrough developments and modeling of fixed bed adsorption system for As(V) removal from water by modified calcined bauxite (MCB)." Separation and Purification Technology, 52(3), 430-438.
22. Badruzzaman, M., Westerhoff, P., and Knappe, D.R.U. (2004). "Intraparticle diffusion and adsorption of arsenate onto granular ferric hydroxide (GFH)." Water Research, 38 (18), 4002-4012.
23. Bajpai, S., and Chaudhuri, M. (1999). "Removal of arsenic from ground water by manganese dioxide-coated sand." Journal of Environmental Engineering, 125(8), 782-784.
24. BAMWSP, DFID, and WATERAID (2001). "Rapid Assessment of Household Level Arsenic Removal Technologies, Phase-I and Phase-II - Final Reports." Surrey: WS Atkins International Limited.
25. Banerjee, K., Amy, G. L., Prevost, M., Nour, S., Jekel, M., Gallagher, P. M., and Blumenschein, C. D. (2008). "Kinetic and thermodynamic aspects of adsorption of arsenic onto granular ferric hydroxide (GFH)." Water research, 42(13), 3371-3378.
26. Baral, S. S., Das, N., Ramulu, T. S., Sahoo, S. K., Das, S. N., and Chaudhury, G. R. (2009). "Removal of Cr(VI) by thermally activated weed Salvinia cucullata in a fixed-bed column." Journal of hazardous materials, 161(2-3), 1427-1435.
27. Barringer, J. L., Reilly, P. A., Eberl, D. D., Blum, A. E., Bonin, J. L., Rosman, R., Hirst, B., Alebus, M., Cenno, K., and Gorska, M. (2011). "Arsenic in sediments, groundwater, and streamwater of a glauconitic Coastal Plain terrain, New Jersey, USA—Chemical "fingerprints" for geogenic and anthropogenic sources." Applied Geochemistry, 26(5), 763-776.

28. Berg, M., Luzi, S., Trang, P. T. K., Viet, P. H., Giger, W., and Stüben, D. (2006). "Arsenic removal from groundwater by household sand filters: Comparative field study, model calculations, and health benefits." Environmental Science and Technology, 40(17), 5567-5573.
29. Bhakat, P. B., Gupta, A. K., Ayoob, S., and Kundu, S. (2006). "Investigations on arsenic(V) removal by modified calcined bauxite." Colloids and Surfaces A: Physicochemical and Engineering Aspects, 281(1-3), 237-245.
30. Bhattacharya, P., Mukherjee, A., and Mukherjee, A. B. (2011). "Arsenic in Groundwater of India." Encyclopedia of Environmental Health, O. N. Editor-in-Chief: Jerome, ed., Elsevier, Burlington, 150-164.
31. BIS (1993). Indian Drinking Water Standards. Indian Standard Specifications For Drinking Water.
32. Bohart, G. S., and Adams, E. Q. (1920). "Some aspects of the behavior of charcoal with respect to chlorine." Journal of the American Chemical Society, 42(3), 523-543.
33. Brammer, H., and Ravenscroft, P. (2009). "Arsenic in groundwater: A threat to sustainable agriculture in South and South-east Asia." Environment international, 35(3), 647-654.
34. Cabal, B., Ania, C. O., Parra, J. B., and Pis, J. J. (2009). "Kinetics of naphthalene adsorption on an activated carbon: comparison between aqueous and organic media." Chemosphere, 76(4), 433-438.
35. Camacho, L. M., Parra, R. R., and Deng, S. (2011). "Arsenic removal from groundwater by MnO2-modified natural clinoptilolite zeolite: Effects of pH and initial feed concentration." Journal of hazardous materials, 189(1-2), 286-293.
36. Carberry, J. J. (1976). "Chemical and catalytic reaction engineering." McGraw-Hill, New York, 156-171.
37. Chabani, M., Amrane, A., and Bensmaili, A. (2006). "Kinetic modelling of the adsorption of nitrates by ion exchange resin." Chemical Engineering Journal, 125(2), 111-117.
38. Chakraborti, D. (2011). "Arsenic: Occurrence in Groundwater." Encyclopedia of Environmental Health, O. N. Jerome, ed., Elsevier, Burlington, 165-180.
39. Chakravarty, S., Dureja, V., Bhattacharyya, G., Maity, S., and Bhattacharjee, S. (2002). "Removal of arsenic from groundwater using low cost ferruginous manganese ore." Water research, 36(3), 625-632.
40. Chadha, D. K. (1999). A proposed new diagram for geochemical classification of natural waters and interpretation of chemical data. Hydrogeology Journal, 7(5), 431-439.
41. Chang, C. F., Chang, C. Y., Chen, K. H., Tsai, W. T., Shie, J. L., and Chen, Y. H. (2004). "Adsorption of naphthalene on zeolite from aqueous solution." Journal of colloid and interface science, 277(1), 29-34.
42. Chen, C. Y., Chang, T. H., Kuo, J. T., Chen, Y. F., and Chung, Y. C. (2008). "Characteristics of molybdate-impregnated chitosan beads (MICB) in terms of arsenic removal from water and the application of a MICB-packed column to remove arsenic from wastewater." Bioresource technology, 99(16), 7487-7494.

43. Chen, J., Li, Y., Long, Q., Wei, Z., and Chen, Y. (2011). "Improving the selective flotation of jamesonite using tannin extract." International Journal of Mineral Processing, 100(1-2), 54-56.
44. Chen, R., Zhi, C., Yang, H., Bando, Y., Zhang, Z., Sugiur, N., and Golberg, D. (2011). "Arsenic (V) adsorption on Fe3O4 nanoparticle-coated boron nitride nanotubes." Journal of colloid and interface science, 359(1), 261-268.
45. Chen, S., Yue, Q., Gao, B., and Xu, X. (2010). "Equilibrium and kinetic adsorption study of the adsorptive removal of Cr(VI) using modified wheat residue." Journal of colloid and interface science, 349(1), 256-264.
46. Chen, Y., Parvez, F., Gamble, M., Islam, T., Ahmed, A., Argos, M., Graziano, J. H., and Ahsan, H. (2009). "Arsenic exposure at low-to-moderate levels and skin lesions, arsenic metabolism, neurological functions, and biomarkers for respiratory and cardiovascular diseases: Review of recent findings from the Health Effects of Arsenic Longitudinal Study (HEALS) in Bangladesh." Toxicology and Applied Pharmacology, 239(2), 184-192.
47. Chen, Y. N., Chai, L. Y., and Shu, Y. D. (2008). "Study of arsenic(V) adsorption on bone char from aqueous solution." Journal of hazardous materials, 160(1), 168-172.
48. Cheng, H., Hu, Y., Luo, J., Xu, B., and Zhao, J. (2009). "Geochemical processes controlling fate and transport of arsenic in acid mine drainage (AMD) and natural systems." Journal of hazardous materials, 165(1-3), 13-26.
49. Cheng, T., Hammond, D. E., Berelson, W. M., Hering, J. G., and Dixit, S. (2009). "Dissolution kinetics of biogenic silica collected from the water column and sediments of three Southern California borderland basins." Marine Chemistry, 113(1-2), 41-49.
50. Cheng, T., Jiang, Y., Zhang, Y., and Liu, S. (2004). "Prediction of breakthrough curves for adsorption on activated carbon fibers in a fixed bed." Carbon, 42(15), 3081-3085.
51. Chenxi, Li. (2008). "Batch and bench-scale fixed-bed column evaluations of heavy metal removals from aqueous solutions and synthetic landfill leachate using low-cost natural adsorbents." M.S. Thesis, Queen's University, Kingston, Ontario, Canada, 42.
52. Cheremisinoff, N. P. (2002). "Prevention and Control Hardware." Handbook of Air Pollution Prevention and Control, Butterworth-Heinemann, Woburn, 389-497.
53. Cheung, W. H., Szeto, Y. S., and McKay, G. (2007). "Intraparticle diffusion processes during acid dye adsorption onto chitosan." Bioresource technology, 98(15), 2897-2904.
54. Choksi, P. M., and Joshi, V. Y. (2007). "Adsorption kinetic study for the removal of nickel (II) and aluminum (III) from an aqueous solution by natural adsorbents." Desalination, 208(1-3), 216-231.
55. Chowdhury, M. R. I., and Mulligan, C. N. (2011). "Biosorption of arsenic from contaminated water by anaerobic biomass." Journal of hazardous materials, 190(1-3), 486-492.
56. Choy, K. K., Ko, D. C., Cheung, C. W., Porter, J. F., and McKay, G. (2004). "Film and intraparticle mass transfer during the adsorption of metal ions onto bone char." Journal of colloid and interface science, 271(2), 284-295.

57. Chutia, P., Kato, S., Kojima, T., and Satokawa, S. (2009). "Arsenic adsorption from aqueous solution on synthetic zeolites." Journal of hazardous materials, 162(1), 440-447.
58. Clifford, D. A., Ghurye, G., and Tripp, A. R. (1999). "Development of an Anion Exchange Process for Arsenic Removal from Water." Arsenic Exposure and Health Effects III, R. C. Willard, O. A. Charles, and L. C. Rebecca, eds., Elsevier Science Ltd, Oxford, 379-387.
59. Craw, D. (2005). "Potential anthropogenic mobilisation of mercury and arsenic from soils on mineralised rocks, Northland, New Zealand." Journal of environmental management, 74(3), 283-292.
60. Crini, G. (2008). "Kinetic and equilibrium studies on the removal of cationic dyes from aqueous solution by adsorption onto a cyclodextrin polymer." Dyes and Pigments, 77(2), 415-426.
61. Crittenden, J. C., Reddy, P. S., Arora, H., and Hand, J. T. D. W. (1991). "Predicting GAC performance with Rapid Small-Scale Column Tests." Journal AWWA, Jan, 83(1), 77.
62. Cundy, A. B., Hopkinson, L., and Whitby, R. L. D. (2008). "Use of iron-based technologies in contaminated land and groundwater remediation: A review." Science of The Total Environment, 400(1-3), 42-51.
63. Curko, J., Mijatovic, I., Matosic, M., Jakopovic, H. K., and Bosnjak, M. U. "As(V) removal from drinking water by coagulation and filtration through immersed membrane." Desalination, In Press, Corrected Proof.
64. Das, B., Hazarika, P., Saikia, G., Kalita, H., Goswami, D. C., Das, H. B., Dube, S. N., and Dutta, R. K. (2007). "Removal of iron from groundwater by ash: A systematic study of a traditional method." Journal of hazardous materials, 141(3), 834-841.
65. Datta, D. V., and Kaul, M. K. (1976). "Arsenic content of drinking water in villages in Northern India. A concept of arsenicosis." The Journal of the Association of Physicians of India, 24(9), 599-604.
66. Davis, H. T., Marjorie Aelion, C., McDermott, S., and Lawson, A. B. (2009). "Identifying natural and anthropogenic sources of metals in urban and rural soils using GIS-based data, PCA, and spatial interpolation." Environmental Pollution, 157(8-9), 2378-2385.
67. Debasish, M., Debaraj, M., and Kyung Ho, P. (2008). "A laboratory scale study on arsenic(V) removal from aqueous medium using calcined bauxite ore." Journal of Environmental Sciences, 20(6), 683-689.
68. Devi, R., Alemayehu, E., Singh, V., Kumar, A., and Mengistie, E. (2008). "Removal of fluoride, arsenic and coliform bacteria by modified homemade filter media from drinking water." Bioresource technology, 99(7), 2269-2274.
69. Dixit, S., and Hering, J. G. (2003). "Comparison of arsenic(V) and arsenic(III) sorption onto iron oxide minerals: Implications for arsenic mobility." Environmental Science and Technology, 37(18), 4182-4189.
70. Djeribi, R., and Hamdaoui, O. (2008). "Sorption of copper(II) from aqueous solutions by cedar sawdust and crushed brick." Desalination, 225(1-3), 95-112.
71. Do Carmo Freitas, M., Pacheco, A. M. G., and Ventura, M. G. (2004). "Anthropogenic sources of PM2.5's arsenic, lead, mercury and nickel in northern

metropolitan Lisbon, Portugal." Nuclear Instruments and Methods in Physics Research Section B: Beam Interactions with Materials and Atoms, 219-220(0), 153-156.

72. Drahota, P., and Filippi, M. (2009). "Secondary arsenic minerals in the environment: a review." Environment international, 35(8), 1243-1255.
73. Dubinin, M. M., and Radushkevich, L. V. (1947). "Equation of the characteristic curve of activated charcoal." Chem. Zentr., 1(1), 875-889.
74. Duker, A. A., Carranza, E. J. M., and Hale, M. (2005). "Arsenic geochemistry and health." Environment international, 31(5), 631-641.
75. Eckenfelder, W.W. (2000). "Industrial Water Pollution Control." McGraw-Hill Series in Water Resources and Environmental Engineering; 3rd ed.; McGraw-Hill Higher Education, 584.
76. Enmark, G., and Nordborg, D. "Arsenic in the groundwater of the Brahmaputra floodplains, Assam, India – Source, distribution and release mechanisms." Minor Field Study 131, Uppsala University, Sweden, august, 2007.
77. Fan, Q.-h., Li, P., Chen, Y.-f., and Wu, W.-s. (2011). "Preparation and application of attapulgite/iron oxide magnetic composites for the removal of U(VI) from aqueous solution." Journal of hazardous materials, 192(3), 1851-1859.
78. Fazal, M. A., Kawachi, T., and Ichion, E. (2001). "Validity of the latest research findings on causes of groundwater arsenic contamination in Bangladesh." Water International, 26(3), 380-389.
79. Ferguson, J. F., and Gavis, J. (1972). "A review of the arsenic cycle in natural waters." Water research, 6(11), 1259-1274.
80. Fernandez-Jimenez, A., Macphee, D. E., Lachowski, E. E., and Palomo, A. (2005). "Immobilization of cesium in alkaline activated fly ash matrix." Journal of Nuclear Materials, 346(2-3), 185-193.
81. Ferreccio, C., Gonzalez, C., Milosavjlevic, V., Marshall, G., and Sancha, A. M. (1999). "Exposure to arsenic in air and drinking water: Results of a study in Chile." IAHS-AISH Publication (260), 29-30.
82. Fields, K., Chen, A., and Wang, L. (2000). "Arsenic Removal from Drinking Water by Iron Removal Plants." EPA/600/R-00-086. Cincinnati, OH.
83. Fields, K., Sorg, T., Chen, A., and Wang, L. "Long-Term Evaluation of Arsenic Removal in Conventional Water Treatment Systems." Proc., Inorganics Contaminants Workshop 2000.
84. Foo, K. Y., and Hameed, B. H. (2010). "Insights into the modeling of adsorption isotherm systems." Chemical Engineering Journal, 156(1), 2-10.
85. Freundlich, H. M. F. (1906). "Over the adsorption in solution." J. Phys. Chem, 57, 385-470.
86. Fuller, C. C., Davis, J. A., and Waychunas, G. A. (1993). "Surface chemistry of ferrihydrite: Part 2. Kinetics of arsenate adsorption and coprecipitation." Geochimica et Cosmochimica Acta, 57(10), 2271-2282.
87. Garai, R., Chakraborty, A. K., Dey, S. B., and Saha, K. C. (1984). "Chronic arsenic poisoning from tube-well water." Journal of the Indian Medical Association, 82(1), 34-35.
88. Genc-Fuhrman, H., Bregnhoj, H., and McConchie, D. (2005). "Arsenate removal from water using sand--red mud columns." Water research, 39(13), 2944-2954.

89. Ghurye, G. L., Clifford, D. A., and Tripp, A. R. (2004). "Pilot study of an iron coagulation-direct microfiltration process for arsenic removal from groundwater." Journal of American Water Works Association, 96 (4), 143-152.
90. Gleick, P. H. (1996). "Basic water requirements for human activities: meeting basic needs." Water International, 21(2), 83-92.
91. Goldberg, S., and Johnston, C. T. (2001). "Mechanisms of arsenic adsorption on amorphous oxides evaluated using macroscopic measurements, vibrational spectroscopy, and surface complexation modeling." Journal of colloid and interface science, 234(1), 204-216.
92. Goldberg, S., Johnston, C. T., Suarez, D. L., and Lesch, S. M. (2007). "Chapter 9 Mechanism of Molybdenum Adsorption on Soils and Soil Minerals Evaluated Using Vibrational Spectroscopy and Surface Complexation Modeling." Developments in Earth and Environmental Sciences, O. B. Mark, and B. K. Douglas, eds., Elsevier, 235-266.
93. Goldberg, S., Su, C., and Forster, H. S. (1998). "Sorption of Molybdenum on Oxides, Clay Minerals, and Soils: Mechanisms and Models." In: E.A. Jenne (Ed). "Adsorption of Metals by Geomedia: Variables, Mechanisms, and Model Applications." Proc. Am. Chem. Soc. Symp., Academic Press, San Diego, CA, 401-426.
94. Gottinger, A. M., Wild, D. J., McMartin, D., Moldovan, B., and Wang, D. "Development of an iron-amended biofilter for removal of arsenic from rural Canadian prairie potable water." 333-344.
95. Greenberg, A. E., Clesceri, L. S., and Eaton, A. D. (1998). Standard Methods for the Examination of Water and Wastewater.
96. Guha Mazumder, D., and Dasgupta, U. B. "Chronic arsenic toxicity: Studies in West Bengal, India." The Kaohsiung Journal of Medical Sciences, In Press, Corrected Proof.
97. Guha Mazumder, D. N. (2005). "Effect of chronic intake of arsenic-contaminated water on liver." Toxicology and Applied Pharmacology, 206(2), 169-175.
98. Guha Mazumder, D. N., Ghose, N., Mazumder, K., Santra, A., Lahiri, S., Das, S., Basu, A., and Smith, A. H. (2003). "Natural history following arsenic exposure: A study in an arsenic endemic area of West Bengal, India." Arsenic Exposure and Health Effects V, R. C. Willard, O. A. Charles, L. C. Rebecca, and J. T. David, eds., Elsevier Science B.V., Amsterdam, 381-389.
99. Guin, D., and Manorama, S. V. (2008). "Room temperature synthesis of monodispersed iron oxide nanoparticles." Materials Letters, 62(17-18), 3139-3142.
100. Gupta, V. K., Agarwal, S., and Saleh, T. A. (2011). "Chromium removal by combining the magnetic properties of iron oxide with adsorption properties of carbon nanotubes." Water research, 45(6), 2207-2212.
101. Gupta, V. K., Saini, V. K., and Jain, N. (2005). "Adsorption of As(III) from aqueous solutions by iron oxide-coated sand." Journal of colloid and interface science, 288(1), 55-60.
102. Haiying, Z., Youcai, Z., and Jingyu, Q. (2011). "Utilization of municipal solid waste incineration (MSWI) fly ash in ceramic brick: Product characterization and environmental toxicity." Waste Management, 31(2), 331-341.

103. Hajjaji, W., Jeridi, K., Seabra, P., Rocha, F., Labrincha, J. A., and Jamoussi, F. (2009). "Composition and properties of glass obtained from Early Cretaceous Sidi Aich sands (central Tunisia)." Ceramics International, 35(8), 3229-3234.
104. Halsey, G. D. (1952). "The Role of Surface Heterogeneity in Adsorption." Advances in Catalysis, 4(C), 259-269.
105. Hamdaoui, O. (2006). "Batch study of liquid-phase adsorption of methylene blue using cedar sawdust and crushed brick." Journal of hazardous materials, 135(1-3), 264-273.
106. Hamdaoui, O., Saoudi, F., Chiha, M., and Naffrechoux, E. (2008). "Sorption of malachite green by a novel sorbent, dead leaves of plane tree: Equilibrium and kinetic modeling." Chemical Engineering Journal, 143(1-3), 73-84.
107. Haque, S., Ji, J., and Johannesson, K. H. (2008). "Evaluating mobilization and transport of arsenic in sediments and groundwaters of Aquia aquifer, Maryland, USA." Journal of contaminant hydrology, 99(1-4), 68-84.
108. Harvey, C. F., Ashfaque, K. N., Yu, W., Badruzzaman, A. B. M., Ali, M. A., Oates, P. M., Michael, H. A., Neumann, R. B., Beckie, R., Islam, S., and Ahmed, M. F. (2006). "Groundwater dynamics and arsenic contamination in Bangladesh." Chemical Geology, 228(1-3), 112-136.
109. Heithmar, E., Momplaisir, G. M., and Rosal, C. "Arsenic speciation methods for studying the environmental fate of organoarsenic animal feed additives." 709-711.
110. Hem, J. D. (1985). "Study and interpretation of the chemical characteristics of natural water." US Geological Survey Water-Supply Paper, 2254.
111. Hering, J. G. (1996). "Risk assessment for arsenic in drinking water: limits to achievable risk levels." Journal of hazardous materials, 45(2-3), 175-184.
112. Ho, Y. S., and McKay, G. (1998). "The kinetics of sorption of basic dyes from aqueous solution by sphagnum moss peat." Canadian Journal of Chemical Engineering, 76(4), 822-827.
113. Hobbins, William B. (1982). “Arsenic determination by hydride generation.” Varian Instruments at Work, AA-22
114. Holm, T. R., and Wilson, S. D. (2006). "Chemical Oxidation for Arsenic Removal." Midwest Technology Assistance Center for Small Public Water Systems TR06-05: Champaign, Illinois.
115. Hopenhayn-Rich, C., Browning, S. R., Hertz-Picciotto, I., Ferreccio, C., Peralta, C., and Gibb, H. (2000). "Chronic arsenic exposure and risk of infant mortality in two areas of Chile." Environmental Health Perspectives, 108(7), 667-673.
116. Horneman, A., van Geen, A., Kent, D. V., Mathe, P. E., Zheng, Y., Dhar, R. K., O'Connell, S., Hoque, M. A., Aziz, Z., Shamsudduha, M., Seddique, A. A., and Ahmed, K. M. (2004). "Decoupling of As and Fe release to Bangladesh groundwater under reducing conditions. Part I: Evidence from sediment profiles." Geochimica et Cosmochimica Acta, 68(17), 3459-3473.
117. Hung, D. Q., Nekrassova, O., and Compton, R. G. (2004). "Analytical methods for inorganic arsenic in water: a review." Talanta, 64(2), 269-277.
118. Indiresan, P. V. (1996). "Driving Force – Impedances: Technology Vision 2020." Technology Information Forecasting and Assessment Council, New Delhi.
119. IS:10500 (1991). "Guidelines for Drinking Water Quality Standards." Bureau of Indian Standards (BIS).

120. Islam, M., Mishra, P. C., and Patel, R. (2011). "Arsenate removal from aqueous solution by cellulose-carbonated hydroxyapatite nanocomposites." Journal of hazardous materials, 189(3), 755-763.
121. Jalali, M., and Khanlari, Z. (2008). "Effect of aging process on the fractionation of heavy metals in some calcareous soils of Iran." Geoderma, 143(1-2), 26-40.
122. Jessen, S., Larsen, F., Koch, C. B., and Arvin, E. (2005). "Sorption and desorption of arsenic to ferrihydrite in a sand filter." Environmental Science and Technology, 39(20), 8045-8051.
123. Joarder, M. A. M., Raihan, F., Alam, J. B., and Hasanuzzaman, S. (2008). "Regression analysis of ground water quality data of Sunamganj District, Bangladesh." International Journal of Environmental Research, 2(3), 291-296.
124. Jonsson, L., and Lundell, L. (2004). "Targeting safe aquifers in regions with arsenic-rich groundwater in Bangladesh: case study in Matlab Upazila." Minor Field Studies, Swedish University of Agricultural Sciences, Uppsala, 60.
125. Junyapoon, S. (2005). "Use of zero-valent iron for waste water treatment." KMITL. Science Technology Journal, 5, 587-595.
126. Kar, S., Maity, J. P., Jean, J.-S., Liu, C.-C., Nath, B., Yang, H.-J., and Bundschuh, J. (2010). "Arsenic-enriched aquifers: Occurrences and mobilization of arsenic in groundwater of Ganges Delta Plain, Barasat, West Bengal, India." Applied Geochemistry, 25(12), 1805-1814.
127. Karim, M. M. (2000). "Arsenic in groundwater and health problems in Bangladesh." Water research, 34(1), 304-310.
128. Kartinen, E. O., and Martin, C. J. (1995). "An overview of arsenic removal processes." Desalination, 103(1-2), 79-88.
129. Khan, A. H., Rasul, S. B., Munir, A. K. M., Alauddin, M., Habibuddowlah, M., and Hussam, A. "On two simple arsenic removal methods for groundwater of Bangladesh." Proc., In Proceedings of the Bangladesh Environmental Network Conference, 1-12.
130. Kim, J., and Benjamin, M. M. (2004). "Modeling a novel ion exchange process for arsenic and nitrate removal." Water research, 38(8), 2053-2062.
131. Kim, M.-J., and Nriagu, J. (2000). "Oxidation of arsenite in groundwater using ozone and oxygen." The Science of the total environment, 247(1), 71-79.
132. Kim, Y., Kim, C., Choi, I., Rengaraj, S., and Yi, J. (2004). "Arsenic Removal Using Mesoporous Alumina Prepared via a Templating Method." Environmental Science and Technology, 38(3), 924-931.
133. Kookana, R. S., and Naidu, R. (1998). "Effect of soil solution composition on cadmium transport through variable charge soils." Geoderma, 84(1-3), 235-248.
134. Kumar, P. A., and Chakraborty, S. (2009). "Fixed-bed column study for hexavalent chromium removal and recovery by short-chain polyaniline synthesized on jute fiber." Journal of hazardous materials, 162(2-3), 1086-1098.
135. Kumaresan, M., and Riyazuddin, P. (2001). "Overview of speciation chemistry of arsenic." Current Science, 80(7), 837-846.
136. Kundu, S., and Gupta, A. K. (2007). "As(III) removal from aqueous medium in fixed bed using iron oxide-coated cement (IOCC): Experimental and modeling studies." Chemical Engineering Journal, 129(1-3), 123-131.

137. Kundu, S., and Gupta, A. (2006). "Arsenic adsorption onto iron oxide-coated cement (IOCC): Regression analysis of equilibrium data with several isotherm models and their optimization." Chemical Engineering Journal, 122(1-2), 93-106.
138. Kundu, S., and Gupta, A. K. (2005). "Analysis and modeling of fixed bed column operations on As(V) removal by adsorption onto iron oxide-coated cement (IOCC)." Journal of colloid and interface science, 290(1), 52-60.
139. Kundu, S., Kavalakatt, S. S., Pal, A., Ghosh, S. K., Mandal, M., and Pal, T. (2004). "Removal of arsenic using hardened paste of Portland cement: batch adsorption and column study." Water research, 38(17), 3780-3790.
140. Lagergren, S. (1898). "zur theoric der sogenannten adsorption geloster stoffe." Kungliga Svenska Vetenskapsakademiens Handlinga(24), 1-39.
141. Leupin, O. X., and Hug, S. J. (2005). "Oxidation and removal of arsenic (III) from aerated groundwater by filtration through sand and zero-valent iron." Water research, 39(9), 1729-1740.
142. LeVan, M. D., and Vermeulen, T. (1984). "Channeling and bed-diameter effects in fixed-bed adsorber performance." A.I.Ch.E. Symposium Series, 80(233), 34–43.
143. Lien, H.-L., and Wilkin, R. T. (2005). "High-level arsenite removal from groundwater by zero-valent iron." Chemosphere, 59(3), 377-386.
144. Liu, C., Li, F., Li, X., Zhang, G., and Kuang, Y. (2006). "The effect of iron oxides and oxalate on the photodegradation of 2-mercaptobenzothiazole." Journal of Molecular Catalysis A: Chemical, 252(1-2), 40-48.
145. Liu, K., Chen, Q., Hu, H., and Yin, Z. (2010). "Characterization and leaching behaviour of lizardite in Yuanjiang laterite ore." Applied Clay Science, 47(3-4), 311-316.
146. Liu, Z.-r., Chen, X.-s., Zhou, L.-m., and Wei, P. (2009). "Development of a first-order kinetics-based model for the adsorption of nickel onto peat." Mining Science and Technology (China), 19(2), 230-234.
147. Mahanta, C., Choudhury, R., Borah, P., Sailo, L., Mondal, S., Saikia, L., and Alam, W. "Monitoring and Surveillance of Groundwater Arsenic Contamination in the Brahmaputra Floodplain in Assam." ASCE, 442-442.
148. Mahanta, C., Pathak, N., Bhattacharya, P., Enmark, G., and Nordborg, D. "Source, Distribution and Release Mechanisms of Arsenic in the Groundwater of Assam Floodplains of Northeast India." ASCE, 78-78.
149. Mahanta, C., Pathak, N., Choudhury, R., Borah, P., and Alam, W. "Quantifying the spread of arsenic contamination in groundwater of the brahmaputra floodplains, Assam, India: A threat to public health of the region." 1804-1813.
150. Maiti, A., Basu, J. K., and De, S. (2010). "Experimental and kinetic modeling of As(V) and As(III) adsorption on treated laterite using synthetic and contaminated groundwater: Effects of phosphate, silicate and carbonate ions." Chemical Engineering Journal.
151. Maiti, A., Sharma, H., Basu, J. K., and De, S. (2009). "Modeling of arsenic adsorption kinetics of synthetic and contaminated groundwater on natural laterite." Journal of hazardous materials, 172(2-3), 928-934.
152. Maji, S. K., Pal, A., and Pal, T. (2008). "Arsenic removal from real-life groundwater by adsorption on laterite soil." Journal of hazardous materials, 151(2-3), 811-820.

153. Maji, S. K., Pal, A., Pal, T., and Adak, A. (2007). "Modeling and fixed bed column adsorption of As(III) on laterite soil." Separation and Purification Technology, 56(3), 284-290.
154. Maji, S. K., Pal, A., Pal, T., and Adak, A. (2007). "Sorption kinetics of arsenic on laterite soil in aqueous medium." Journal of Environmental Science and Health, Part A, 42(7), 989-996.
155. Malana, M. A., Qureshi, R. B., and Ashiq, M. N. (2011). "Adsorption studies of arsenic on nano aluminium doped manganese copper ferrite polymer (MA, VA, AA) composite: Kinetics and mechanism." Chemical Engineering Journal, 172(2-3), 721-727.
156. Malik, A. H., Khan, Z. M., Mahmood, Q., Nasreen, S., and Bhatti, Z. A. (2009). "Perspectives of low cost arsenic remediation of drinking water in Pakistan and other countries." Journal of hazardous materials, 168(1), 1-12.
157. Mall, I. D., Srivastava, V. C., and Agarwal, N. K. (2006). "Removal of Orange-G and Methyl Violet dyes by adsorption onto bagasse fly ash—kinetic study and equilibrium isotherm analyses." Dyes and Pigments, 69(3), 210-223.
158. Mall, I. D., Srivastava, V. C., Agarwal, N. K., and Mishra, I. M. (2005). "Adsorptive removal of malachite green dye from aqueous solution by bagasse fly ash and activated carbon-kinetic study and equilibrium isotherm analyses." Colloids and Surfaces A: Physicochemical and Engineering Aspects, 264(1-3), 17-28.
159. Mamisahebei, S., Jahed Khaniki, G. R., Torabian, A., Nasseri, S., and Naddafi, K. (2007). "Removal of arsenic from an aqueous solution by pretreated waste tea fungal biomass." Iranian Journal of Environmental Health Science and Engineering, 4(2), 85-92.
160. Mandal, S., Padhi, T., and Patel, R. K. (2011). "Studies on the removal of arsenic (III) from water by a novel hybrid material." Journal of hazardous materials, 192(2), 899-908.
161. Mane, V. S., Deo Mall, I., and Chandra Srivastava, V. (2007). "Kinetic and equilibrium isotherm studies for the adsorptive removal of Brilliant Green dye from aqueous solution by rice husk ash." Journal of environmental management, 84(4), 390-400.
162. Manna, B., and Ghosh, U. C. (2007). "Adsorption of arsenic from aqueous solution on synthetic hydrous stannic oxide." Journal of hazardous materials, 144(1-2), 522-531.
163. Matheson, L. J., Goldberg, W. C., Bostick, W. D., and Harris, L. (2003). "Analysis of Uranium-Contaminated Zero Valent Iron Media Sampled from Permeable Reactive Barriers Installed at U.S. Department of Energy Sites in Oak Ridge, Tennessee, and Durango, Colorado." Handbook of Groundwater Remediation using Permeable Reactive Barriers, L. N. David, J. M. Stan, C. F. Christopher, and A. D. James, eds., Academic Press, San Diego, 343-367.
164. Mathews, A. P., and Weber W.J, Jr. (1976). "Physical, chemical wasterwater treatment." AIChE Symp. Ser, 166(73), 91-98.
165. Mathieu, J. L. (2010). "Arsenic remediation of drinking water using iron-oxide coated coal bottom ash."
166. Mazumder, D. N. G. (2003). "Chronic arsenic toxicity: Clinical features, epidemiology, and treatment: Experience in West Bengal." Journal of

Environmental Science and Health - Part A Toxic/Hazardous Substances and Environmental Engineering, 38(1), 141-163.

167. Mazumder, D. N. G., De, B. K., Santra, A., Dasgupta, J., Ghosh, N., Roy, B. K., Ghoshal, U. C., Saha, J., Chatterjee, A., Dutta, S., Haque, R., Smith, A. H., Chakraborty, D., Angle, C. R., and Centeno, J. A. (1999). "Chronic Arsenic Toxicity: Epidemiology, Natural History and Treatment." Arsenic Exposure and Health Effects III, R. C. Willard, O. A. Charles, and L. C. Rebecca, eds., Elsevier Science Ltd, Oxford, 335-347.
168. McArthur, J. M., Banerjee, D. M., Hudson-Edwards, K. A., Mishra, R., Purohit, R., Ravenscroft, P., Cronin, A., Howarth, R. J., Chatterjee, A., Talukder, T., Lowry, D., Houghton, S., and Chadha, D. K. (2004). "Natural organic matter in sedimentary basins and its relation to arsenic in anoxic ground water: the example of West Bengal and its worldwide implications." Applied Geochemistry, 19(8), 1255-1293.
169. McNeill, L. S., and Edwards, M. (1995). "Soluble arsenic removal at water treatment plants." Journal AWWA, 84(5), 105–113.
170. McNeill, L. S., and Edwards, M. (1997). "Predicting as removal during metal hydroxide precipitation." Journal / American Water Works Association, 89(1), 75-86.
171. Melita, L., and Popescu, M. (2008). "Removal of Cr (VI) from industrial water effluents and surface waters using activated composite membranes." Journal of Membrane Science, 312(1-2), 157-162.
172. Mendelovici, E., Yariv, S., and Villalba, R. (1979). "Aluminum-bearing geothite in veneulan laterites." Clays and Clay Minerals, 27 (5), 368-372.
173. Meng, X., Bang, S., and Korfiatis, G. P. (2000). "Effects of silicate, sulfate, and carbonate on arsenic removal by ferric chloride." Water research, 34(4), 1255-1261.
174. Meng, X., Korfiatis, G. P., Christodoulatos, C., and Bang, S. (2001). "Treatment of arsenic in Bangladesh well water using a household co-precipitation and filtration system." Water research, 35(12), 2805-2810.
175. Michaels, A. S. (1952). "Simplified method of interpreting kinetic data in fixed-bed ion exchange." Ind. Eng. Chem., 44(8), 1922-1930.
176. Milton, A. H., and Rahman, M. (2002). "Respiratory effects and arsenic contaminated well water in Bangladesh." International Journal of Environmental Health Research, 12(2), 175-179.
177. Mohan, D., and Pittman, C. U., Jr. (2007). "Arsenic removal from water/wastewater using adsorbents--A critical review." Journal of hazardous materials, 142(1-2), 1-53.
178. Mohapatra, M., Rout, K., Singh, P., Anand, S., Layek, S., Verma, H. C., and Mishra, B. K. (2011). "Fluoride adsorption studies on mixed-phase nano iron oxides prepared by surfactant mediation-precipitation technique." Journal of hazardous materials, 186(2-3), 1751-1757.
179. Mondal, P., Majumder, C. B., and Mohanty, B. (2008a). "Treatment of arsenic contaminated water in a laboratory scale up-flow bio-column reactor." Journal of hazardous materials, 153(1-2), 136-145.
180. Mondal, P., Majumder, C. B., and Mohanty, B. (2008b). "Effects of adsorbent dose, its particle size and initial arsenic concentration on the removal of arsenic, iron and

manganese from simulated ground water by Fe3+ impregnated activated carbon." Journal of hazardous materials, 150(3), 695-702.
181. Moore, M. M., Harrington-Brock, K., and Doerr, C. L. (1997). "Relative genotoxic potency of arsenic and its methylated metabolites." Mutation Research/Reviews in Mutation Research, 386(3), 279-290.
182. Nacèra, Y., and Aicha, B. (2006). "Equilibrium and kinetic modelling of methylene blue biosorption by pretreated dead streptomyces rimosus: Effect of temperature." Chemical Engineering Journal, 119(2-3), 121-125.
183. Namdeo, M., and Bajpai, S. K. (2008). "Investigation of hexavalent chromium uptake by synthetic magnetite nanoparticles." Electronic Journal of Environmental, Agricultural and Food Chemistry, 7(7), 3082-3094.
184. Namdeo, M., and Bajpai, S. K. (2009). "Investigation of hexavalent chromium uptake by synthetic magnetite nanoparticles." Electronic Journal of Environmental, Agricultural and Food Chemistry, 8(5), 367-381.
185. Nath, B., Jean, J.-S., Lee, M.-K., Yang, H.-J., and Liu, C.-C. (2008). "Geochemistry of high arsenic groundwater in Chia-Nan plain, Southwestern Taiwan: Possible sources and reactive transport of arsenic." Journal of contaminant hydrology, 99(1-4), 85-96.
186. Nehrenheim, E., and Gustafsson, J. P. (2008). "Kinetic sorption modelling of Cu, Ni, Zn, Pb and Cr ions to pine bark and blast furnace slag by using batch experiments." Bioresource technology, 99(6), 1571-1577.
187. Ng, J. C., Wang, J., and Shraim, A. (2003). "A global health problem caused by arsenic from natural sources." Chemosphere, 52(9), 1353-1359.
188. Nguyen, T.V., Vigneswaran, S., Ngo, H.H., Pokhrel, D., Viraraghavan, T. (2006). "Specific treatment technologies for removing arsenic from water." Eng. Life Sci., 6(1), 86–90.
189. Nicolli, H. B., Bundschuh, J., García, J. W., Falcón, C. M., and Jean, J.-S. (2010). "Sources and controls for the mobility of arsenic in oxidizing groundwaters from loess-type sediments in arid/semi-arid dry climates – Evidence from the Chaco–Pampean plain (Argentina)." Water research, 44(19), 5589-5604.
190. Nishide, T., Yamaguchi, H., and Mizukami, F. (1995). "Crystal modulation of tungsten oxide gels and films prepared by the sol-gel process using 2,4-pentanedione as an organic ligand." Journal of Materials Science, 30(19), 4946-4949.
191. Nomanbhay, S. M., and Palanisamy, K. (2005). "Removal of heavy metal from industrial wastewater using chitosan coated oil palm shell charcoal." Electronic Journal of Biotechnology, 8(1), 43-53.
192. Örnek, A., Özacar, M., and Sengil, I. A. (2007). "Adsorption of lead onto formaldehyde or sulphuric acid treated acorn waste: Equilibrium and kinetic studies." Biochemical Engineering Journal, 37(2), 192-200.
193. Paluszkiewicz, C., Holtzer, M., and Bobrowski, A. (2008). "FTIR analysis of bentonite in moulding sands." Journal of Molecular Structure, 880(1-3), 109-114.
194. Pandey, P. K., Choubey, S., Verma, Y., Pandey, M., and Chandrashekhar, K. (2009). "Biosorptive removal of arsenic from drinking water." Bioresource technology, 100(2), 634-637.

195. Parga, J. R., Cocke, D. L., Valenzuela, J. L., Gomes, J. A., Kesmez, M., Irwin, G., Moreno, H., and Weir, M. (2005). "Arsenic removal via electrocoagulation from heavy metal contaminated groundwater in La Comarca Lagunera México." Journal of hazardous materials, 124(1-3), 247-254.
196. Parida, K., and Das, J. (1996). "Studies on ferric oxide hydroxides: II. Structural properties of goethite samples (α-FeOOH) prepared by homogeneous precipitation from Fe(NO3)3 solution in the presence of sulfate ions." Journal of colloid and interface science, 178(2), 586-593.
197. Partey, F., Norman, D., Ndur, S., and Nartey, R. (2008). "Arsenic sorption onto laterite iron concretions: Temperature effect." Journal of colloid and interface science, 321(2), 493-500.
198. Pe-Piper, G. (1982). Geochemistry, tectonic setting and metamorphism of mid-Triassic volcanic rocks of Greece. Tectonophysics, 85(3), 253-272.
199. Perrott, K. W., Smith, B. L., and Mitchell, B. D. (1976). "Effect of pH on the reaction of sodium fluoride with hydrous oxides of silicon, aluminum, and iron, and with poorly ordered aluminosilicate." Journal of Soil Science, 27, 348-356.
200. Petrusevski, B., Sharma, S.K., Kruis, F., Omeruglu, P., Schippers, J.C. (2002). "Family filter with iron-coated sand: solution for arsenic removal in rural areas." Water Sci. Technol.: Water Supply, 2 (5–6), 127–133.
201. Pillewan, P., Mukherjee, S., Roychowdhury, T., Das, S., Bansiwal, A., and Rayalu, S. (2011). "Removal of As(III) and As(V) from water by copper oxide incorporated mesoporous alumina." Journal of hazardous materials, 186(1), 367-375.
202. Postma, D., Jessen, S., Hue, N. T. M., Duc, M. T., Koch, C. B., Viet, P. H., Nhan, P. Q., and Larsen, F. (2010). "Mobilization of arsenic and iron from Red River floodplain sediments, Vietnam." Geochimica et Cosmochimica Acta, 74(12), 3367-3381.
203. Pozo, C., Bildstein, O., Raynal, J., Jullien, M., and Valcke, E. (2007). "Behaviour of silicon released during alteration of nuclear waste glass in compacted clay." Applied Clay Science, 35(3-4), 258-267.
204. Predoi, D. (2007). "A study on iron oxide nanoparticles coated with dextrin obtained by coprecipitation." Digest Journal of Nanomaterials and Biostructures, 2(1), 169-173.
205. Puttamraju, P., and SenGupta, A. K. (2006). "Evidence of tunable on-off sorption behaviors of metal oxide nanoparticles: Role of ion exchanger support." Industrial and Engineering Chemistry Research, 45(22), 7737-7742.
206. Qu, D., Wang, J., Hou, D., Luan, Z., Fan, B., and Zhao, C. (2009). "Experimental study of arsenic removal by direct contact membrane distillation." Journal of hazardous materials, 163(2-3), 874-879.
207. Qu, R., Sun, C., Wang, M., Ji, C., Xu, Q., Zhang, Y., Wang, C., Chen, H., and Yin, P. (2009). "Adsorption of Au(III) from aqueous solution using cotton fiber/chitosan composite adsorbents." Hydrometallurgy, 100(1-2), 65-71.
208. Rahaman, M. S., Basu, A., and Islam, M. R. (2008). "The removal of As(III) and As(V) from aqueous solutions by waste materials." Bioresource technology, 99(8), 2815-2823.

209. Rahman, M., Tondel, M., Ahmad, S. A., Chowdhury, I. A., Faruquee, M. H., and Axelson, O. (1999). "Hypertension and arsenic exposure in Bangladesh." Hypertension, 33(1 I), 74-78.
210. Ranjan, D., Talat, M., and Hasan, S. H. (2009). "Biosorption of arsenic from aqueous solution using agricultural residue 'rice polish'." Journal of hazardous materials, 166(2-3), 1050-1059.
211. Raven, K. P., Jain, A., and Loeppert, R. H. (1998). "Arsenite and arsenate adsorption on ferrihydrite: Kinetics, equilibrium, and adsorption envelopes." Environmental Science and Technology, 32(3), 344-349.
212. Redlich, O., and Peterson, D. L. (1959). "A useful adsorption isotherm." Journal of Physical Chemistry, 63(6), 1024.
213. Reichenberg, D. (1953). "Properties of ion-exchange resins in relation to their structure. III. Kinetics of exchange." Journal of the American Chemical Society, 75(3), 589-597.
214. Reza, R., and Singh, G. (2010). "Heavy metal contamination and its indexing approach for river water." International Journal of Environmental Science and Technology, 7(4), 785-792.
215. Rom, W. N., Varley, G., Lyon, J. L., and Shopkow, S. (1982). "Lung cancer mortality among residents living near the El Paso smelter." British Journal of Industrial Medicine, 39(3), 269-272.
216. Rosenboom, J. W., Bangladesh. Arsenic Policy Support, U., Great Britain. Dept. for International Development, B., and Bangladesh, U. (2004). Not just red or green : an analysis of arsenic data from 15 upazilas in Bangladesh, Govt. of the People's Republic of Bangladesh, Ministry of Local Govt., Rural Development, and Co-operatives, Dept. of Public Health & Engg., Arsenic Policy Support Unit, Dhaka.
217. Rostamian, R., Najafi, M., and Rafati, A. A. (2011). "Synthesis and characterization of thiol-functionalized silica nano hollow sphere as a novel adsorbent for removal of poisonous heavy metal ions from water: Kinetics, isotherms and error analysis." Chemical Engineering Journal, 171(3), 1004-1011.
218. Roychowdhury, T., Uchino, T., Tokunaga, H., and Ando, M. (2002). “Arsenic and other heavy metals in soils from an arsenic-affected area of West Bengal, India.” Chemosphere, 49(6), 605-618.
219. Ruan, H. D., Frost, R. L., Kloprogge, J. T., and Duong, L. (2002). "Infrared spectroscopy of goethite dehydroxylation: III. FT-IR microscopy of in situ study of the thermal transformation of goethite to hematite." Spectrochimica Acta - Part A Molecular and Biomolecular Spectroscopy, 58(5), 967-981.
220. Ruthven, D. M. (1984). Principles of Adsorption and Adsorption Processes, JohnWiley, New York.
221. Sabbatini, P., Yrazu, F., Rossi, F., Thern, G., Marajofsky, A., and Fidalgo de Cortalezzi, M. M. (2010). "Fabrication and characterization of iron oxide ceramic membranes for arsenic removal." Water research, 44(19), 5702-5712.
222. Saha, K. C. (1984). "Melanokeratosis from arsenic contaminated tubewell water." Indian journal of dermatology, 29(4), 37-46.
223. Sahabi, D. M., Takeda, M., Suzuki, I., and Koizumi, J.-i. (2009). "Adsorption and abiotic oxidation of arsenic by aged biofilter media: Equilibrium and kinetics." Journal of hazardous materials, 168(2-3), 1310-1318.

224. Sampson, M.L., Bostick, B., Chiew, H., Hagan, J.M., Shantz, A. (2008). "Arsenicosis in Cambodia: Case studies and policy response." Applied Geochemistry, 23(11), 2977-2986.
225. Sankararamakrishnan, N., Kumar, P., and Singh Chauhan, V. (2008). "Modeling fixed bed column for cadmium removal from electroplating wastewater." Separation and Purification Technology, 63(1), 213-219.
226. Sarkar, B., Venkateswralu, N., Rao, R. N., Bhattacharjee, C., and Kale, V. (2007). "Treatment of pesticide contaminated surface water for production of potable water by a coagulation-adsorption-nanofiltration approach." Desalination, 212(1-3), 129-140.
227. Sarkar, M., Banerjee, A., Pramanick, P., and Sarkar, A. (2007). "Design and operation of fixed bed laterite column for the removal of fluoride from water." Chemical Engineering Journal, 131(1-3), 329-335.
228. Sarkar, S., Blaney, L. M., Gupta, A., Ghosh, D., and SenGupta, A. K. (2007). "Use of ArsenXnp, a hybrid anion exchanger, for arsenic removal in remote villages in the Indian subcontinent." Reactive and Functional Polymers, 67(12), 1599-1611.
229. Scott, K. N., Green, J. F., Do, H. D., and Mclean, S. J. (1995). "Arsenic Removal by Coagulation." Journal AWWA, 87(4), 114–126.
230. Seko, N., Basuki, F., Tamada, M., and Yoshii, F. (2004). "Rapid removal of arsenic(V) by zirconium(IV) loaded phosphoric chelate adsorbent synthesized by radiation induced graft polymerization." Reactive and Functional Polymers, 59(3), 235-241.
231. Senthil Kumar, P., Ramalingam, S., Senthamarai, C., Niranjanaa, M., Vijayalakshmi, P., and Sivanesan, S. (2010). "Adsorption of dye from aqueous solution by cashew nut shell: Studies on equilibrium isotherm, kinetics and thermodynamics of interactions." Desalination, 261(1-2), 52-60.
232. Sharma, A., Verma, N., Sharma, A., Deva, D., and Sankararamakrishnan, N. (2010). "Iron doped phenolic resin based activated carbon micro and nanoparticles by milling: Synthesis, characterization and application in arsenic removal." Chemical Engineering Science, 65(11), 3591-3601.
233. Sharma, V. K., and Sohn, M. (2009). "Aquatic arsenic: Toxicity, speciation, transformations, and remediation." Environment international, 35(4), 743-759.
234. Sidle, Wotten, and Murphy (2001). "Provenance of geogenic arsenic in the Goose River basin, Maine, USA." Environmental Geology, 41(1), 62-73.
235. Signes-Pastor, A. J., Mitra, K., Sarkhel, S., Hobbes, M., Burló, F., De Groot, W. T., and Carbonell-Barrachina, A. A. (2008). "Arsenic speciation in food and estimation of the dietary intake of inorganic arsenic in a rural village of West Bengal, India." Journal of Agricultural and Food Chemistry, 56(20), 9469-9474.
236. Singh, T. S., and Pant, K. K. (2004). "Equilibrium, kinetics and thermodynamic studies for adsorption of As(III) on activated alumina." Separation and Purification Technology, 36(2), 139-147.
237. Siripitayakunkit, U., Visudhiphan, P., Pradipasen, M., and Vorapongsathron, T. (1999). "Association between Chronic Arsenic Exposure and Children's Intelligence in Thailand." Arsenic Exposure and Health Effects III, R. C. Willard, O. A. Charles, and L. C. Rebecca, eds., Elsevier Science Ltd, Oxford, 141-149.

238. Smedley, P. L., and Kinniburgh, D. G. (2002). "A review of the source, behaviour and distribution of arsenic in natural waters." Applied Geochemistry, 17(5), 517-568.
239. Smedley, P. L., Knudsen, J., and Maiga, D. (2007). "Arsenic in groundwater from mineralised Proterozoic basement rocks of Burkina Faso." Applied Geochemistry, 22(5), 1074-1092.
240. Smedley, P. L., Nicolli, H. B., Macdonald, D. M. J., Barros, A. J., and Tullio, J. O. (2002). "Hydrogeochemistry of arsenic and other inorganic constituents in groundwaters from La Pampa, Argentina." Applied Geochemistry, 17(3), 259-284.
241. Smith, E., Naidu, R., and Alston, A. M. (1998). "Arsenic in the Soil Environment: A Review." Advances in Agronomy, L. S. Donald, ed., Academic Press, 149-195.
242. Srivastava, V., Weng, C. H., Singh, V. K., and Sharma, Y. C. (2011). "Adsorption of nickel ions from aqueous solutions by nano alumina: Kinetic, mass transfer, and equilibrium studies." Journal of Chemical and Engineering Data, 56(4), 1414-1422.
243. Strawn, D., Doner, H., Zavarin, M., and McHugo, S. (2002). "Microscale investigation into the geochemistry of arsenic, selenium, and iron in soil developed in pyritic shale materials." Geoderma, 108(3-4), 237-257.
244. Sun, G. (2004). "Arsenic contamination and arsenicosis in China." Toxicology and Applied Pharmacology, 198(3), 268-271.
245. Supapong, S., Phanthumchinda, K., and Srirattanaban, J. (2004). "Nerve conduction studies in chronic arsenic poisoning patients." Journal of the Medical Association of Thailand, 87(SUPPL. 2), S207-S212.
246. Suresh, B., Sowmya, T., and Sankaranarayanan, S. R. (2009). "Synthesis of Iron oxide from metallurgical wastes." Journal of Mining and Metallurgy, Section B: Metallurgy, 45 (1), B(1), 127-130.
247. Taylor, P. R., Qiao, Y. L., Schatzkin, A., Yao, S. X., Lubin, J., Mao, B. L., Rao, J. Y., McAdams, M., Xuan, X. Z., and Li, J. Y. (1989). "Relation of arsenic exposure to lung cancer among tin miners in Yunnan Province, China." British Journal of Industrial Medicine, 46(12), 881-886.
248. Temkin, M. I., and Pyzhev, V. (1940). "Kinetics of ammonia synthesis on promoted iron catalysts." Acta Physicochim. USSR, 12(3), 327-356.
249. Thomas, H. C. (1944). "Heterogeneous ion exchange in a flowing system." Journal of the American Chemical Society, 66(10), 1664-1666.
250. UNISEF (2008). "Arsenic Primer Guidance for UNICEF Country Offices on the Investigation and Mitigation of Arsenic Contamination." Water, Environment and Sanitation Section Programme DivisionUNICEF, New York.
251. USEPA (2000). “Technologies and Costs for Removal of Arsenic from Drinking Water.” Report prepared by ICI, Malcolm Pirnie and the Cadmus Group for USEPA Office of EPA 815-R-00-028.
252. Vaclavikova, M., Gallios, G., Hredzak, S., and Jakabsky, S. (2008). "Removal of arsenic from water streams: an overview of available techniques." Clean Technologies and Environmental Policy, 10(1), 89-95.
253. Vahter, M. (1999). "Variation in Human Metabolism of Arsenic." Arsenic Exposure and Health Effects III, R. C. Willard, O. A. Charles, and L. C. Rebecca, eds., Elsevier Science Ltd, Oxford, 267-279.

254. Valencia-Trejo, E., Villicaña-Méndez, M., Alfaro-Cuevas-Villanueva, R., Garnica-Romo, M. G., and Cortés-Martínez, R. (2010). "Effect of Temperature on the Removal of Arsenate from Aqueous Solutions by Titanium Dioxide Nanoparticles." Journal of Applied Sciences in Environmental Sanitation, 5, 171-184.
255. Voice, T. C., and Weber, W. J. (1983). "Sorption of hydraulic compounds by sediments, solids and suspended solids – I, theory and background." Water research, 17, 1433 – 1441.
256. W.J., W., and Morris, J. C. (1963). "Kinetics of adsorption on carbon from solution." J. Sanit. Eng. Div. ASCE(89), 31-60.
257. Wang, S., and Mulligan, C. N. (2006). "Occurrence of arsenic contamination in Canada: Sources, behavior and distribution." Science of The Total Environment, 366(2-3), 701-721.
258. Waychunas, G. A., Rea, B. A., Fuller, C. C., and Davis, J. A. (1993). "Surface chemistry of ferrihydrite: Part 1. EXAFS studies of the geometry of coprecipitated and adsorbed arsenate." Geochimica et Cosmochimica Acta, 57(10), 2251-2269.
259. Weber Jr., W. J., Voice, T. C., and Jodellah, A. (1983). Adsorption of humic substances: the effects of heterogeneity and system characteristics, American Water Works Association, Denver, CO, ETATS-UNIS.
260. Weber, T. W., and Chakravorti, R. K. (1974). "PORE AND SOLID DIFFUSION MODELS FOR FIXED-BED ADSORBERS." AIChE Journal, 20(2), 228-238.
261. Weber, W. J. (1972). "Adsorption in Physicochemical Processes for Water Quality Control." R.L. Metcalf, and J. N. Pitts, eds., Wiley Interscience, NY, 199-259.
262. WHO (1993). "Guidelines for Drinking Water Quality (2nd Edition, Vol. I): Health Criteria and Supporting Information." Recommendations, World Health Organization, Geneva, Switzerland World Health Organization, Geneva, Switzerland, 41-42.
263. Wu, F.-C., Tseng, R.-L., and Juang, R.-S. (2009). "Characteristics of Elovich equation used for the analysis of adsorption kinetics in dye-chitosan systems." Chemical Engineering Journal, 150(2-3), 366-373.
264. Xie, X., Wang, Y., Ellis, A., Su, C., Li, J., and Li, M. (2011). "The sources of geogenic arsenic in aquifers at Datong basin, northern China: Constraints from isotopic and geochemical data." Journal of Geochemical Exploration, 110(2), 155-166.
265. Xu, Y.-h., Nakajima, T., and Ohki, A. (2002). "Adsorption and removal of arsenic(V) from drinking water by aluminum-loaded Shirasu-zeolite." Journal of hazardous materials, 92(3), 275-287.
266. Young Hee, Y., and Nelson, J. H. (1984). "Application of gas adsorption kinetics I. A theoretical model for respirator cartridge service life." American Industrial Hygiene Association Journal, 45(8), 509-516.
267. Yuh-Shan, H. (2004). "Citation review of Lagergren kinetic rate equation on adsorption reactions." Scientometrics, 59(1), 171-177.
268. Zhao, X., Zhang, B., Liu, H., and Qu, J. (2010). "Removal of arsenite by simultaneous electro-oxidation and electro-coagulation process." Journal of hazardous materials, 184(1-3), 472-476.
269. Zhou, D., Zhang, L., Zhou, J. and Guo, S. (2004). "Cellulose/chitin beads for adsorption for heavy metals in aqueous solution." Water Research, 38, 2643-2650.

270. Zhu, H., Jia, Y., Wu, X., and Wang, H. (2009). "Removal of arsenic from water by supported nano zero-valent iron on activated carbon." Journal of hazardous materials, 172(2-3), 1591-1596.
271. Zierold, K. M., Knobeloch, L., and Anderson, H. (2004). "Prevalence of chronic diseases in adults exposed to arsenic-contaminated drinking water." American Journal of Public Health, 94(11), 1936-1937.

APPENDIX A

(Delineation of Unsafe Aquifers in a Major Arsenic Contaminated Area of Madhupur Block in Nalbari District, Assam)

Table A.1. Groundwater sampling points in the study area (Madhupur Block in Nalbari district in Assam, India).

Well No.	Name of Village	Name of Habitation	Pin Point Location	Type of Source	Depth (m)	Latitude	Longitude
1	Banshi Bhaga	Sulmari Supa	583 No. Banabhag Sholmari L.P. School	TP	31	26.501083	91.395117
2	Banshi Bhaga	Sulmari Supa	Natun Dehar Mauza H.S. School	SHP	22	26.501350	91.395083
3	Banshi Bhaga	Sulmari Supa	Shankardev Girls School (M.E.)	TP	26	26.501533	91.395717
4	Banshi Bhaga	Sulmari Supa	Upendra Narayan L.P. School	TP	21	26.501433	91.396250
5	Baranagar Banikuchi	Bhakatpara Suba	3 No. Masjid	HTW	32	26.466633	91.368483
6	Baranagar Banikuchi	Bhakatpara Suba	Farzan Ali	HTW	39	26.463483	91.367700
7	Baranagar Banikuchi	Bhakatpara Suba	Hasmat Ali	HTW	39	26.472633	91.374617
8	Baranagar Banikuchi	Shilakuchi Suba	717 no. L.P. School	HTW	29	26.460067	91.366517
9	Baranagar Banikuchi	Shilakuchi Suba	Samsher Ali	HTP	21	26.462817	91.373183
10	Barkhetri Banekuchi	Dakshin Suba	Milan L.P. School	SHP	39	26.461117	91.392133
11	Barkhetri Banekuchi	Barkhetri Banekuchi	313 No. L.P. School	SHP	29	26.463500	91.389867
12	Barkhetri Banekuchi	Barkhetri Banekuchi	Namgarh	SHP	21	26.463500	91.389867
13	Barkhetri Banekuchi	Kakoti Para Suba	1 No Masjid	TP	29	26.470367	91.390200
14	Barkhetri Banekuchi	Kakoti Para Suba	Ahmed Ali	TP	29	26.470483	91.390200
15	Barkhetri Banekuchi	Kakoti Para Suba	Gonain Ghar	TP	29	26.473367	91.389767
16	Barkhetri Banekuchi	Kakoti Para Suba	Naam Ghar	TP	29	26.472917	91.380567
17	Barkhetri Banekuchi	Kakoti Para Suba	PHED Dept of Banekuchi	TP	29	26.470550	91.390767
18	Barkhetri Banekuchi	Kakoti Para Suba	Rabin Barman	TP	31	26.472217	91.390000
19	Barkhetri Banekuchi	Kakoti Para Suba	Taroni Barman	TP	31	26.473330	91.394517

Well No.	Name of Village	Name of Habitation	Pin Point Location	Type of Source	Depth (m)	Latitude	Longitude
20	Burinagar	Bill Par Supa	Haser Ali	SHP	29	26.477417	91.403033
21	Burinagar	Bill Par Supa	Janata M.E. School	HTW	39	26.484800	91.404967
22	Burinagar	Bill Par Supa	Naresh Ali	TP	21	26.481650	91.403700
23	Burinagar	Bill Par Supa	Primary Health Centre	HTW	39	26.488117	91.407133
24	Burinagar	Bill Par Supa	Vijaya Barman	HTW	29	26.489083	91.407217
25	Burinagar	Chencharghat	787 Chencharghat L.P. School	SHP	39	26.469917	91.401683
26	Burinagar	Chencharghat	Fuleshwari Buro	SHP	37	26.471383	91.395117
27	Burinagar	Chencharghat	Ganesh Boro	TP	29	26.468167	91.398883
28	Burinagar	Chencharghat	Jamal Ali	TP	31	26.469450	91.395517
29	Burinagar	Chencharghat	Mahesh Deuri	SHP	39	26.470500	91.395050
30	Danguapara	Banekuchi	Ambikadevi Vidya Niketan	M-II	30	26.478750	91.393167
31	Danguapara	Banekuchi	Binay Das	SHP	39	26.479067	91.392633
32	Danguapara	Bargasa Suba	Chandramohan Patowari	SHP	39	26.475767	91.389083
33	Danguapara	Bargasa Supa	Bargasa Hari Mandir	SHP	39	26.487667	91.395917
34	Danguapara	Bargasa Supa	Bargasa LP School	SHP	39	26.488650	91.395417
35	Danguapara	Bargasa Supa	Lakhy Deka	SHP	21	26.48865	91.395417
36	Danguapara	Bargasa Supa	Praneswar Barman	M-II	42	26.491733	91.396433
37	Danguapara	Deka Para Supa	Birendranath Buiya	HTW	29	26.474533	91.387917
38	Danguapara	Deka Para Supa	Jaycharan Deka	SHP	39	26.473417	91.382967
39	Danguapara	Deka Para Supa	Parikhyit Deka	SHP	39	26.481267	91.392433
40	Danguapara	Paschim Suba	Dangapara 3 no. L.P. School	TP	39	26.477067	91.381033
41	Danguapara	Paschim Suba	Hyder Ali	HTW	30	26.475733	91.378050
42	Danguapara	Paschim Suba	Jay Nur	TP	29	26.474833	91.377883
43	Danguapara	Paschim Suba	Paschim Danguapara Maszid	TP	30	26.478100	91.380233
44	Danguapara	Sulmari Supa	813 No LP School	SHP	39	26.480867	91.389283
45	Haripur	Haripur	Haripur L.P. School	HTW	29	26.456500	91.404950
46	Pub Nambarbag	Chamtiya para	Chamtiya para L.P. School	SHP	29	26.483617	91.370567
47	Rajakhat Banekuchi	Shilakuchi Suba	5 no Maszid	TP	29	26.455933	91.364617
48	Rajakhat Banikuchi	Shilakuchi Suba	Jainal Ahmed	HTW	29	26.455317	91.372533

Table A.2. Physicochemical characteristics of the groundwater in the study area – Fist water sampling (on dated 20/06/2008).

Well No	Temp-rature	pH	EC	TDS	As	Fe	Ca	Na	K	Mg	Mn	HCO_3	Cl	F	PO_4	SO_4	NO_3
1	28.8	6.73	174	160	81.40	12.08	14.66	17.40	1.35	3.23	0.52	130	5	0.24	0.87	0.62	1.32
2	28.0	6.36	140	130	50.27	5.90	10.43	13.58	1.06	2.52	0.27	90	7	0.32	0.67	0.05	1.42
3	28.3	6.66	173	160	74.22	11.93	14.56	17.70	1.15	3.54	0.50	118	4	0.12	1.39	0.00	0.94
4	27.2	6.69	164	150	124.52	13.55	23.30	24.00	1.33	4.88	0.94	190	4	0.05	0.97	0.35	1.21
5	29.8	6.90	181	170	71.30	9.22	27.89	25.67	1.95	6.73	0.14	172	10	0.21	1.12	0.48	1.29
6	28.2	6.70	169	160	38.80	7.44	20.60	17.40	1.81	4.06	0.38	116	14	0.12	0.46	0.45	0.86
7	26.4	6.70	183	170	91.60	14.40	25.67	29.11	1.60	5.42	0.20	178	12	0.02	1.32	0.48	0.50
8	28.6	6.60	168	160	91.30	11.99	32.67	36.16	1.83	3.53	0.63	216	12	0.09	1.65	0.45	0.72
9	27.2	6.70	167	150	46.20	4.61	12.80	11.00	1.59	4.40	0.34	80	15	0.01	0.85	0.48	1.19
10	27.0	6.80	287	230	105.10	9.40	20.80	20.97	2.18	7.46	0.48	142	14	0.04	0.83	0.42	1.43
11	28.4	6.90	269	210	114.70	5.82	29.46	29.46	1.68	7.87	0.70	202	11	0.12	1.06	0.56	1.21
12	26.6	7.10	260	210	98.30	12.16	26.82	26.82	1.61	7.51	0.82	198	10	0.13	0.71	0.42	1.02
13	27.0	6.70	184	130	72.96	12.74	27.07	28.43	1.06	3.86	0.43	182	10	0.02	1.12	0.11	0.79
14	27.9	6.80	182	130	133.40	10.84	30.12	26.80	1.32	3.71	0.50	156	17	0.00	1.46	0.14	0.63
15	27.9	6.80	274	220	85.14	13.83	31.15	25.97	1.38	5.93	0.64	186	15	0.00	1.21	0.23	0.84
16	29.4	6.70	180	130	117.30	8.30	28.43	27.00	1.20	3.26	0.87	172	14	0.12	0.65	1.35	1.26
17	29.4	6.80	186	130	51.97	13.09	28.45	29.88	1.27	2.99	0.67	188	10	0.34	0.85	0.25	1.02
18	27.1	6.90	363	280	166.25	16.26	30.35	26.00	1.76	7.84	0.98	198	13	0.13	1.35	0.53	0.75
19	26.6	6.60	380	280	150.30	16.70	34.20	27.07	1.86	5.31	0.76	210	10	0.13	1.22	1.80	0.89
20	28.8	6.56	146	130	124.22	8.35	36.00	24.44	1.42	2.73	0.64	190	5	0.24	1.07	0.24	0.81
21	27.9	6.76	158	120	85.43	12.14	23.80	23.69	1.33	3.04	0.39	162	3	0.31	0.99	0.05	0.73
22	28.3	6.75	289	240	235.16	19.30	40.80	37.00	1.75	8.22	1.17	284	4	0.52	1.83	0.65	1.31
23	28.0	6.67	162	150	161.00	13.70	29.50	30.00	1.38	3.55	0.71	196	4	0.29	1.68	0.27	1.20
24	28.4	6.69	167	150	145.12	13.84	34.50	34.50	1.55	3.59	0.90	246	4	0.00	1.82	0.35	1.01
25	26.2	6.71	180	166	126.68	13.04	37.70	22.09	1.54	5.04	0.39	230	5	0.00	1.33	0.32	1.34
26	22.2	6.57	175	160	161.44	16.70	38.00	21.70	1.66	6.07	0.90	226	5	0.13	1.56	0.16	1.42
27	27.7	6.68	167	140	67.43	11.32	13.21	19.32	1.43	2.13	0.64	122	7	0.12	0.34	0.24	1.35
28	28.1	6.73	188	150	128.43	10.32	22.90	33.60	1.54	2.74	0.85	184	11	0.39	0.64	0.35	1.32
29	27.8	6.74	180	170	124.11	12.60	27.90	19.00	1.43	5.55	0.76	180	5	0.34	1.72	0.19	1.23

Well No	Temp-rature	pH	EC	TDS	As	Fe	Ca	Na	K	Mg	Mn	HCO_3	Cl	F	PO_4	SO_4	NO_3
30	26.4	6.74	280	230	176.00	13.70	36.80	24.96	1.44	8.06	1.14	242	4	0.12	1.69	0.05	0.97
31	26.3	6.78	187	160	96.43	9.54	21.41	26.43	1.35	2.41	0.35	150	8	0.00	0.56	0.46	0.89
32	26.6	6.74	183	160	123.23	8.44	19.31	30.40	1.46	3.35	0.75	156	9	0.21	0.83	0.43	0.67
33	27.7	6.56	175	160	62.87	6.10	15.29	17.10	1.44	4.01	0.30	114	5	0.00	0.87	0.59	0.35
34	29.2	6.18	152	140	130.86	16.23	20.27	23.89	1.75	3.19	0.80	148	12	0.00	1.16	0.24	0.53
35	28.0	6.56	185	170	109.74	15.59	17.87	19.60	1.61	5.44	1.00	150	5	0.12	1.13	0.05	0.51
36	28.2	6.73	168	150	55.16	9.65	13.76	18.80	1.37	2.81	0.65	124	7	0.13	1.13	0.19	0.78
37	27.0	6.67	259	210	78.03	14.75	16.01	19.30	1.31	4.15	0.62	142	8	0.02	0.59	0.24	0.83
38	27.0	7.41	285	240	86.00	3.32	16.45	20.90	1.67	3.27	0.64	110	7	0.00	0.84	1.26	0.64
39	26.5	6.70	194	180	93.50	14.23	17.90	16.67	1.24	6.53	0.68	152	12	0.00	1.29	0.48	0.79
40	26.5	6.70	180	167	97.40	15.10	33.90	25.58	1.93	6.75	0.55	212	10	0.03	0.94	0.45	1.20
41	26.2	6.80	180	170	48.10	9.60	28.02	22.40	1.60	4.90	0.61	168	12	0.21	0.40	0.48	1.07
42	27.2	6.90	179	170	28.80	4.30	12.00	15.30	1.71	4.17	0.36	84	14	0.12	0.48	0.51	0.89
43	26.9	6.60	182	170	36.50	8.30	25.58	12.60	1.84	3.40	0.56	140	11	0.29	0.84	0.48	0.69
44	27.7	6.70	183	160	161.00	13.38	34.30	29.70	1.61	4.70	0.64	218	5	0.16	1.05	0.00	1.32
45	28.2	6.71	184	170	187.00	17.60	33.10	33.80	1.55	6.28	1.09	238	5	0.21	1.37	0.19	1.06
46	27.1	6.90	183	170	104.00	9.91	34.85	34.85	1.68	3.80	0.60	208	16	0.16	1.65	0.45	1.27
47	29.0	6.70	177	170	83.10	14.01	27.59	24.87	1.80	5.75	0.65	190	10	0.07	1.10	0.48	0.85
48	26.5	6.50	183	170	5.70	4.21	12.80	13.70	1.39	3.14	0.08	86	11	0.04	0.55	0.48	0.64

Note: The unit of As is µg L^{-1}, Temperature is degree centigrade (^{0}C), Depth is m, EC is µS cm^{-1}, ORP is mV and the unit of the other water quality parameters are mg L^{-1}.

Table A.3. Physicochemical characteristics of the groundwater in the study area – Second water sampling (on dated 18/09/2008).

Well No	Temp-rature	pH	EC	TDS	As	Fe	Ca	Na	K	Mg	Mn	HCO_3	Cl	F	PO_4	SO_4	NO_3
1	24.5	6.76	170.6	150	66.77	9.05	14.00	16.36	1.47	2.80	0.53	104	6	0.02	0.14	0.54	1.44
2	24.3	6.25	125.4	110	60.23	5.36	10.80	14.67	0.99	1.64	0.63	86	4	0.25	0.28	0.15	0.94
3	23.5	6.59	160.3	140	91.78	10.02	30.00	16.64	1.25	3.01	1.12	158	5	0.32	0.36	0.14	0.82
4	25.3	6.63	160.4	140	104.88	10.74	28.80	28.60	1.43	4.40	1.10	188	6	0.14	0.47	0.30	1.01
5	23.6	6.60	172.5	150	98.21	7.00	24.70	24.49	1.78	5.91	0.94	160	10	0.08	1.70	0.54	1.40
6	23.4	6.65	160.2	140	48.84	5.93	26.70	31.59	1.66	4.16	0.97	162	12	0.66	1.25	0.37	0.93
7	23.6	6.72	180.0	160	107.13	11.31	23.00	28.22	1.50	4.70	0.88	158	10	0.14	1.47	0.52	0.97
8	24.5	6.62	159.0	140	98.11	8.49	25.50	34.39	1.72	2.80	0.86	180	10	0.25	0.78	0.37	0.83
9	22.7	6.56	158.6	140	26.39	3.15	13.60	16.20	1.06	3.66	0.59	98	12	0.00	1.22	0.56	0.99
10	24.3	6.78	216.0	190	108.83	7.47	19.00	19.63	2.04	6.29	0.81	123	12	0.00	1.66	0.29	1.53
11	24.7	6.92	203.0	180	110.25	5.19	25.60	28.22	1.56	6.80	0.95	164	10	0.00	1.22	0.41	1.26
12	24.8	7.02	203.0	180	80.60	9.28	21.70	25.61	1.47	6.40	0.90	177	8	0.42	0.84	0.55	0.93
13	24.3	6.54	136.1	120	63.04	9.48	24.20	27.48	1.02	3.28	0.92	156	8	0.32	1.66	0.23	1.08
14	22.9	6.85	160.4	140	116.15	9.26	23.70	26.07	1.23	2.84	0.97	140	14	0.42	1.85	0.30	1.22
15	23.7	6.74	222.3	190	69.31	10.06	29.30	28.32	1.30	5.09	1.10	176	13	0.36	1.55	0.39	1.07
16	23.6	6.72	161.7	140	55.92	6.69	26.90	27.85	1.10	2.63	1.07	156	12	0.04	0.87	1.13	0.92
17	23.8	6.85	163.4	140	42.81	10.12	27.50	26.36	1.20	2.30	1.08	176	8	0.77	0.29	0.38	0.67
18	24.7	6.39	281.4	240	143.03	13.33	29.30	26.00	1.64	11.20	1.17	244	10	0.24	1.71	0.40	1.29
19	24.6	6.56	275.3	240	137.90	12.93	30.00	25.42	1.75	4.73	1.18	202	9	0.12	1.36	0.85	1.18
20	24.8	6.60	126.7	110	105.19	7.53	31.60	26.07	1.37	3.14	1.01	204	6	0.22	0.87	0.38	0.94
21	24.5	6.70	154.2	140	70.45	10.41	13.00	22.71	1.28	3.42	0.79	120	4	0.00	1.39	0.17	1.00
22	24.3	6.80	240.3	210	201.95	15.98	39.30	37.30	1.83	7.31	1.42	274	4	0.00	2.50	0.55	1.25
23	24.8	6.63	149.8	130	111.67	11.42	28.00	23.74	1.33	2.95	1.11	176	6	0.21	1.78	0.16	1.02
24	24.5	6.64	156.1	140	119.49	11.65	30.30	30.60	1.60	3.00	1.03	186	8	0.00	2.63	0.42	0.88
25	24.9	6.70	195.6	170	100.33	11.08	15.30	20.00	1.45	3.66	0.78	127	6	0.00	2.02	0.25	0.39
26	24.5	6.52	168.5	150	140.98	13.58	32.00	28.00	1.71	5.76	1.07	208	6	0.33	2.01	0.08	0.22
27	24.3	6.63	157.4	140	52.11	8.73	15.10	18.00	1.33	1.78	0.83	113	6	0.24	0.63	0.28	0.98
28	24.7	6.70	180.0	160	101.49	8.95	35.50	26.30	1.63	2.34	1.33	182	9	0.00	0.87	0.39	1.19

Well No	Temp-rature	pH	EC	TDS	As	Fe	Ca	Na	K	Mg	Mn	HCO_3	Cl	F	PO_4	SO_4	NO_3
29	23.5	6.71	216.0	190	99.99	10.53	31.60	29.30	1.35	4.92	1.27	196	6	0.11	2.02	0.23	1.54
30	23.6	6.48	204.0	180	140.25	10.90	36.30	23.08	1.53	7.13	1.26	210	8	0.00	1.69	0.13	1.43
31	23.6	6.70	204.0	180	75.19	7.28	20.20	25.33	1.31	2.06	0.74	141	8	0.00	0.45	0.57	0.73
32	23.6	6.70	158.6	140	115.50	6.88	18.00	20.93	1.54	2.91	0.69	128	7	0.00	0.72	0.36	0.86
33	23.8	6.51	173.4	150	49.46	5.49	14.00	18.50	1.35	3.60	0.59	124	6	0.22	0.76	0.69	0.48
34	23.7	6.23	144.2	130	102.26	13.16	19.00	22.62	1.79	2.48	0.73	140	10	0.21	1.22	0.32	0.92
35	23.4	6.50	155.0	140	84.45	11.88	15.80	18.41	1.54	4.64	0.64	138	8	0.32	1.43	0.21	0.95
36	23.3	6.78	155.0	140	40.81	7.89	12.80	17.76	1.29	2.34	0.69	112	8	0.00	1.28	0.29	0.89
37	23.7	6.70	190.2	170	118.26	11.21	27.80	23.00	1.24	3.75	0.93	180	10	0.00	2.02	0.37	1.39
38	23.8	7.25	234.9	210	58.39	3.49	15.10	19.91	1.60	3.00	0.63	117	12	0.24	0.77	0.98	0.62
39	23.8	6.66	180.2	160	42.38	11.04	17.00	15.70	1.17	5.72	0.79	130	10	0.00	1.45	0.63	0.92
40	23.4	6.66	195.8	170	83.88	11.19	26.40	23.93	1.84	6.28	1.02	172	9	0.00	1.05	0.54	1.11
41	24.2	6.75	205.0	180	36.05	6.15	26.90	31.78	1.53	4.31	0.97	204	10	0.14	0.42	0.57	0.70
42	24.2	6.85	170.3	150	25.22	2.69	20.30	26.00	1.29	4.36	0.80	146	12	0.00	0.44	0.60	0.58
43	24.1	6.63	182.4	160	26.44	6.26	23.10	19.91	1.19	2.06	0.99	130	10	0.00	0.95	0.54	0.67
44	24.6	6.70	175.3	150	106.43	11.51	32.10	29.70	1.47	4.40	1.30	204	6	0.42	1.32	0.13	1.39
45	24.6	6.68	182.2	160	125.47	13.73	38.80	27.70	1.46	5.67	1.27	232	6	0.00	1.58	0.25	1.38
46	24.1	6.92	172.6	150	42.25	7.52	16.00	25.40	1.57	3.38	0.75	132	14	0.25	1.76	0.38	1.30
47	24.1	6.64	158.2	140	66.35	9.81	25.90	23.93	1.65	5.25	0.88	182	8	0.00	1.21	0.45	0.96
48	24.2	6.46	180.0	160	0.00	1.76	13.60	16.20	1.03	2.33	0.35	72	12	0.05	0.63	0.42	0.47

Note: The unit of As is µg L^{-1}, Temperature is degree centigrade (^{0}C), Depth is m, EC is µS cm^{-1}, ORP is mV and the unit of the other water quality parameters are mg L^{-1}.

Table A.4. Physicochemical characteristics of the groundwater in the study area – Third water sampling (on dated 16/12/2008).

Well No	Temp-rature	pH	EC	TDS	ORP	As	Fe	Ca	Na	K	Mg	Mn	HCO_3	Cl	F	PO_4	SO_4	NO_3
1	22.4	6.45	168	140	-187	89.60	14.26	9.36	25.60	0.96	2.35	0.96	124	8	0.36	1.20	0.04	1.35
2	21.3	6.53	153	130	-210	96.30	7.36	11.32	28.40	1.02	3.36	0.35	136	6	0.36	1.26	0.05	0.98
3	21.3	6.12	176	150	-222	160.50	11.25	27.90	19.36	1.45	2.45	0.36	142	10	0.45	1.20	1.10	1.12
4	22.5	6.35	176	150	-180	145.60	10.42	11.25	21.80	1.25	3.01	0.43	114	7	0.20	0.65	0.36	1.01
5	22.3	6.36	180	150	-172	204.57	16.90	15.66	24.90	2.07	5.63	1.44	152	8	0.60	1.56	0.68	0.46
6	21.5	6.38	165	140	-186	120.90	3.10	12.80	27.00	1.34	3.80	0.73	124	11	0.12	0.91	0.47	0.00
7	21.3	6.45	165	140	-210	230.30	15.60	28.00	26.50	2.37	6.17	1.38	188	10	0.20	1.62	0.51	0.68
8	22.0	6.45	153	135	-196	155.37	6.56	13.91	27.20	1.90	3.28	0.24	124	9	0.00	0.56	0.05	0.39
9	21.2	6.25	162	140	-180	47.84	3.53	13.30	16.40	1.34	3.00	0.31	88	10	0.00	0.47	0.24	0.27
10	22.3	6.35	230	190	-175	148.65	9.38	24.35	31.26	1.56	3.29	0.35	164	10	0.31	1.36	0.35	1.02
11	23.5	6.26	216	180	-231	145.60	8.15	29.35	22.86	1.65	3.26	0.36	165	11	0.36	0.98	1.42	0.78
12	22.8	7.02	236	200	-189	118.19	8.96	21.23	21.82	1.13	2.46	0.39	123	13	0.12	0.86	0.29	0.34
13	22.9	6.78	186	150	-195	100.60	9.50	12.60	25.20	1.22	1.50	0.30	112	10	1.14	0.41	0.70	2.36
14	23.6	6.34	146	120	-165	165.32	9.61	21.53	21.35	1.36	4.36	0.86	146	11	0.30	0.61	0.28	1.65
15	22.8	6.53	243	210	-195	96.36	10.36	21.36	21.36	1.78	3.65	0.68	136	13	0.00	0.76	0.15	1.36
16	21.9	6.45	190	160	-165	77.95	8.47	13.16	23.62	1.76	2.72	0.51	108	9	0.50	0.44	0.45	1.22
17	23.5	6.42	143	120	-178	65.28	12.67	8.50	20.20	1.15	3.24	0.42	96	15	0.11	1.01	0.03	1.00
18	23.4	6.01	213	180	-210	198.65	15.50	16.69	26.20	1.94	4.35	1.14	154	15	0.10	1.35	0.35	1.13
19	24.5	6.35	226	190	-211	180.36	9.25	19.36	24.69	1.12	2.78	1.16	138	9	0.26	0.68	0.12	0.45
20	22.9	6.35	176	150	-201	143.26	6.35	25.10	20.36	1.25	2.38	0.45	146	7	0.23	0.26	0.16	1.20
21	23.6	6.35	146	120	-186	98.45	9.38	10.35	20.36	1.23	6.00	0.25	134	5	0.12	0.75	0.01	0.96
22	23.1	6.13	167	140	-183	282.42	17.30	33.60	28.10	2.31	6.33	1.49	202	15	1.40	1.65	0.62	0.75
23	22.8	6.25	176	145	-199	148.26	13.10	14.38	25.63	1.95	4.10	0.47	130	12	0.40	1.41	0.29	0.23
24	23.7	6.42	183	140	-201	167.28	10.62	27.90	24.40	1.25	2.31	0.68	188	7	0.10	0.63	0.24	0.46
25	22.7	6.24	153	130	-198	134.70	10.90	14.70	20.60	1.53	2.97	0.29	112	8	1.10	0.16	0.47	0.39
26	23.0	6.35	193	160	-191	201.02	11.58	27.90	25.50	2.12	5.49	1.22	172	12	0.50	1.40	0.37	1.23
27	22.4	6.11	167	140	-232	75.50	11.30	17.10	21.70	1.32	1.72	0.70	118	13	0.47	1.30	0.10	2.14
28	22.3	6.01	186	160	-201	128.00	8.10	14.50	20.60	1.38	2.39	0.45	106	11	0.93	1.67	0.61	2.23

Well No	Temp-rature	pH	EC	TDS	ORP	As	Fe	Ca	Na	K	Mg	Mn	HCO_3	Cl	F	PO_4	SO_4	NO_3
29	21.4	6.34	168	140	-226	134.48	10.70	13.09	24.84	1.78	3.57	0.38	124	8	0.20	1.30	0.17	0.39
30	22.9	6.38	243	210	-211	196.35	15.10	23.00	21.80	1.36	4.44	0.94	180	9	0.10	0.92	0.11	0.45
31	22.3	6.08	157	140	-201	118.10	12.60	19.70	23.20	1.14	2.55	0.29	146	11	0.17	1.38	0.65	1.82
32	22.7	6.35	242	210	-231	174.33	13.19	17.32	26.00	2.14	5.89	1.06	150	10	0.20	1.49	0.44	0.56
33	21.9	6.35	118	100	-185	73.10	8.00	15.50	25.00	1.32	1.68	0.35	122	12	0.66	0.54	0.53	1.81
34	22.8	6.28	196	160	-207	139.81	12.36	13.48	19.36	1.96	2.36	0.81	115	10	0.34	0.65	0.36	0.01
35	22.6	6.53	138	120	-201	115.80	8.51	14.76	22.90	2.12	3.87	0.96	126	8	0.80	1.28	0.37	0.64
36	22.7	6.62	186	150	-196	59.36	12.36	13.38	16.68	1.36	3.68	0.82	123	8	0.10	0.89	0.01	0.30
37	22.7	6.15	193	160	-211	228.36	18.60	29.00	29.00	2.46	6.24	1.16	224	9	0.12	1.36	0.25	0.86
38	22.6	6.32	190	160	-201	76.32	11.26	13.62	16.38	1.12	2.38	0.41	98	12	0.00	0.46	0.12	1.12
39	22.4	6.32	212	180	-201	65.60	12.50	14.35	17.53	1.30	2.13	0.42	118	9	0.65	0.13	0.23	0.45
40	22.8	6.61	163	140	-213	112.03	15.25	25.39	24.36	1.68	2.39	0.26	156	15	0.12	0.89	0.34	0.34
41	22.9	6.46	176	150	-187	56.32	2.40	11.62	14.92	1.34	2.86	0.73	78	7	0.23	0.67	0.42	1.15
42	22.8	6.73	156	130	-178	45.38	11.35	13.36	13.46	1.14	4.65	0.46	102	10	0.32	0.32	0.38	0.65
43	23.1	6.31	196	170	-203	46.78	5.80	23.65	19.60	1.46	2.36	0.79	140	11	0.12	0.84	0.37	1.25
44	24.1	6.11	112	90	-196	105.70	14.30	17.90	20.60	1.65	2.44	0.49	142	8	0.07	0.50	0.92	0.67
45	23.7	6.25	175	150	-216	105.70	12.50	17.10	20.90	1.43	3.51	0.53	130	14	1.00	0.65	0.47	0.17
46	23.1	6.12	175	160	-193	67.90	7.30	14.20	27.30	1.74	5.45	0.48	146	9	0.00	0.78	0.43	0.34
47	24.6	6.35	165	130	-213	100.00	7.70	14.30	24.20	1.32	2.32	0.60	136	7	0.73	1.00	0.60	0.00
48	22.4	6.12	201	170	-196	5.70	4.21	10.30	15.20	1.08	2.12	0.08	74	11	0.00	0.34	0.48	0.85

Note: The unit of As is µg L^{-1}, Temperature is degree centigrade (^{0}C), Depth is m, EC is µS cm^{-1}, ORP is mV and the unit of the other water quality parameters are mg L^{-1}.

Table A.5. Physicochemical characteristics of the groundwater in the study area – Fourth water sampling (on dated 06/03/2009).

Well No	Temp-rature	pH	EC	TDS	ORP	As	Fe	Ca	Na	K	Mg	Mn	HCO_3	Cl	F	PO_4	SO_4	NO_3
1	25.2	6.12	163	150	-248	132.37	13.85	13.52	22.22	1.86	2.49	0.51	108	10	0.43	1.40	3.07	2.02
2	25.6	6.28	140	150	-240	45.26	12.25	6.60	19.36	1.45	4.56	0.35	102	8	0.65	0.64	0.10	1.68
3	25.5	6.26	162	150	-251	170.28	14.74	12.96	22.66	1.88	2.62	0.52	114	9	0.70	1.40	1.22	1.25
4	25.4	6.12	145	130	-237	166.16	16.19	14.36	21.00	1.89	2.75	0.61	134	8	0.16	0.60	0.54	0.87
5	25.3	6.50	176	160	-255	213.54	14.70	19.00	27.72	2.36	6.23	0.82	170	8	0.23	1.23	0.12	0.59
6	25.1	6.54	169	176	-252	125.30	8.25	7.60	20.00	1.85	5.62	0.53	108	16	0.15	0.62	0.53	0.35
7	25.3	6.19	157	140	-251	240.81	21.00	32.40	26.22	1.98	4.27	1.03	210	10	0.21	0.60	0.71	0.36
8	25.6	6.35	153	155	-240	165.00	12.36	28.30	31.02	1.69	6.15	0.45	220	12	0.35	0.72	0.23	1.58
9	25.5	6.20	210	195	-244	71.17	18.50	14.00	26.20	2.13	11.70	1.24	188	9	0.78	1.20	0.78	0.21
10	25.2	6.38	257	215	-244	312.86	20.40	29.60	29.00	2.16	11.60	0.98	236	11	0.86	1.87	1.24	2.65
11	25.6	6.47	223	195	-236	257.11	12.30	18.04	31.00	2.00	8.28	0.83	180	12	1.05	1.20	1.10	0.39
12	25.6	6.40	210	172	-216	231.00	17.10	21.21	25.10	1.86	7.26	0.69	164	12	0.84	1.02	1.10	0.25
13	25.1	6.22	163	150	-241	103.66	11.70	13.17	16.00	1.62	3.54	0.30	114	10	1.06	1.40	0.56	0.32
14	25.3	6.10	157	140	-235	166.68	11.11	13.14	24.19	1.96	2.29	0.40	112	11	1.85	1.00	0.10	0.17
15	24.1	6.36	185	170	-234	175.68	15.06	17.03	24.30	1.85	4.33	0.63	140	9	0.28	1.20	0.80	0.01
16	25.9	6.42	180	185	-216	85.88	15.36	9.40	30.26	1.65	6.38	0.36	140	14	0.45	1.21	0.15	1.52
17	25.3	6.29	161	150	-234	121.68	12.34	13.50	24.70	1.79	2.05	0.76	112	13	0.54	1.20	0.75	1.69
18	24.1	6.44	213	210	-247	202.80	15.46	20.10	29.00	2.31	9.29	1.08	198	8	0.65	1.40	0.46	1.12
19	25.0	6.34	176	160	-250	183.08	14.08	15.24	24.87	1.82	6.01	0.36	148	10	0.42	0.80	0.54	0.27
20	24.6	6.17	146	130	-231	150.63	13.39	13.15	22.46	1.95	1.73	0.76	112	12	1.52	1.00	1.22	0.21
21	25.4	6.26	157	130	-219	163.07	10.12	11.60	22.55	1.88	2.17	0.45	112	8	0.35	1.00	1.27	2.27
22	26.2	6.42	157	165	-222	288.26	18.00	23.56	30.25	2.36	7.26	1.11	182	14	1.45	1.75	0.23	0.96
23	24.7	6.22	155	140	-231	83.19	8.09	13.93	23.25	1.90	1.39	0.66	114	10	0.54	0.60	0.90	1.99
24	24.0	6.26	231	210	-240	250.63	14.79	32.60	29.50	1.77	6.30	0.73	210	9	0.93	1.36	0.41	2.36
25	26.5	6.25	180	190	-240	135.25	12.36	19.57	25.26	1.95	8.32	0.65	180	8	0.41	0.91	0.21	1.60
26	26.3	6.45	175	176	-236	224.56	14.02	15.36	22.25	1.56	6.32	0.36	145	8	0.35	0.56	0.35	1.65
27	24.7	6.24	151	160	-249	85.69	8.10	16.25	23.75	1.64	4.23	0.45	140	15	0.46	0.32	0.26	2.45
28	24.1	6.22	156	140	-240	146.66	13.15	14.15	22.68	1.70	2.54	0.44	122	10	1.40	1.00	0.83	1.49

Well No	Temp-rature	pH	EC	TDS	ORP	As	Fe	Ca	Na	K	Mg	Mn	HCO_3	Cl	F	PO_4	SO_4	NO_3
29	25.4	6.45	153	155	-245	135.84	16.05	18.36	24.69	1.84	8.63	0.25	176	8	0.65	1.42	0.41	1.47
30	25.2	6.29	198	180	-237	208.86	12.61	16.60	22.48	1.91	5.70	1.13	132	12	0.78	1.60	0.97	2.14
31	24.5	6.12	131	145	-231	127.24	11.26	19.36	27.26	1.65	3.65	0.25	144	10	0.00	1.40	0.39	1.95
32	25.8	6.15	143	150	-236	186.54	12.36	26.38	23.15	1.23	5.36	1.21	160	9	0.41	1.47	0.31	1.86
33	26.7	6.38	260	220	-230	133.21	19.00	26.60	30.40	2.70	15.90	1.20	248	11	0.61	1.68	0.15	2.01
34	25.2	6.11	172	160	-232	142.14	16.84	16.74	22.00	2.11	3.58	0.94	156	11	0.75	0.80	0.56	0.01
35	26.3	6.11	158	140	-232	122.24	9.78	12.54	23.62	2.39	1.71	0.57	112	10	0.29	1.00	0.51	0.94
36	25.7	6.11	156	140	-225	87.41	11.01	14.40	22.94	1.93	2.35	0.66	120	11	0.81	1.00	0.44	0.27
37	26.8	6.40	211	193	-250	237.33	12.44	18.70	26.10	2.64	13.40	0.89	210	8	0.26	1.60	0.37	1.02
38	25.4	6.35	158	150	-225	77.44	12.82	15.30	20.70	1.83	2.26	0.44	114	10	0.85	1.00	0.85	0.35
39	26.6	6.14	167	150	-238	76.36	16.80	15.32	20.70	1.95	4.13	0.86	142	6	0.91	1.00	0.78	0.38
40	25.0	5.97	169	150	-243	138.61	15.17	12.24	25.38	1.76	3.30	0.42	112	14	1.59	1.40	0.17	0.26
41	25.8	6.36	194	175	-245	173.56	15.51	12.77	22.00	2.00	5.64	0.97	134	10	0.29	0.60	0.83	1.23
42	26.4	6.10	189	175	-239	174.98	13.96	18.20	22.99	1.77	4.09	0.19	136	11	0.21	0.60	0.12	0.96
43	25.7	6.16	175	160	-241	135.77	16.60	11.67	23.35	2.01	5.40	0.58	146	7	0.28	1.00	0.19	1.36
44	27.0	6.19	163	150	-240	118.23	15.01	16.30	24.30	2.00	5.16	0.64	146	9	0.12	0.80	0.75	0.21
45	25.7	6.24	160	170	-204	84.68	14.65	19.02	22.36	1.52	7.26	0.56	140	16	1.20	0.75	0.56	0.35
46	25.2	6.24	175	160	-257	111.23	10.66	12.77	21.54	1.72	4.80	1.16	112	13	0.24	1.60	1.17	1.06
47	24.2	6.47	145	131	-241	113.56	10.83	13.57	23.28	1.52	0.94	0.57	118	9	0.12	0.40	1.14	1.02
48	26.1	5.89	170	166	-240	82.77	12.54	15.24	21.34	1.88	5.80	0.89	140	11	0.39	0.45	0.51	1.45

Note: The unit of As is µg L^{-1}, Temperature is degree centigrade (^{0}C), Depth is m, EC is µS cm^{-1}, ORP is mV and the unit of the other water quality parameters are mg L^{-1}.

Table A.6. Physicochemical characteristics of the groundwater in the study area – Fifth water sampling (on dated 11/06/2009).

Well No	Temp-rature	pH	EC	TDS	ORP	As	Fe	Ca	Na	K	Mg	Mn	HCO_3	Cl	F	PO_4	SO_4	NO_3
1	29.3	6.25	200.0	170	-202	92.35	13.30	17.00	24.30	2.33	3.73	0.39	130	12	0.21	1.22	1.32	1.02
2	28.7	6.31	212.0	180	-214	52.23	11.30	18.80	21.50	1.87	5.78	0.25	166	12	0.15	0.36	0.30	1.02
3	28.8	6.44	185.0	160	-187	98.25	14.10	17.50	24.30	2.13	4.68	0.31	140	11	0.43	0.24	0.94	0.25
4	28.9	6.25	175.0	150	-174	45.30	7.90	16.30	23.00	2.25	4.00	0.78	134	10	0.00	0.25	0.73	0.36
5	28.7	6.54	215.0	180	-188	164.91	17.20	21.30	25.80	3.11	5.20	1.32	182	11	0.35	1.77	0.27	1.07
6	29.6	6.63	226.0	180	-196	81.49	7.10	24.40	29.00	2.43	7.24	0.25	178	17	0.05	0.11	0.45	0.85
7	29.8	6.24	152.3	130	-178	145.08	15.20	16.80	28.90	2.21	3.88	1.04	150	12	0.12	1.43	0.80	0.14
8	30.4	6.58	196.3	160	-202	75.29	11.50	23.60	32.50	1.98	7.83	0.36	202	13	0.36	0.42	0.37	1.02
9	30.6	6.34	205.6	170	-231	44.91	7.80	16.70	24.70	2.43	5.49	0.22	144	10	0.52	0.36	0.70	1.11
10	30.7	6.47	249.0	210	-112	224.16	13.00	20.00	31.00	2.36	9.07	1.48	186	12	1.02	1.55	1.14	1.15
11	30.1	6.50	285.6	230	-180	215.09	15.20	22.10	28.10	2.74	9.60	1.38	200	13	0.74	2.01	0.91	0.25
12	30.2	6.38	178.6	150	-178	149.72	16.70	18.80	21.00	1.72	5.60	0.96	162	13	0.22	0.85	1.23	0.12
13	29.5	6.12	222.3	180	-215	76.56	11.00	16.00	18.10	2.10	4.61	0.47	122	11	0.93	1.25	0.70	0.63
14	28.6	6.24	200.0	170	-226	94.82	10.10	15.20	25.80	2.16	3.73	0.66	134	13	1.55	1.33	0.35	0.52
15	30.5	6.36	226.4	190	-175	143.46	13.40	19.80	22.30	2.01	3.44	0.71	156	11	0.42	1.25	0.87	0.44
16	29.4	6.42	240.3	200	-186	79.36	14.50	29.00	22.60	1.90	5.60	0.29	182	15	0.00	0.93	0.35	0.72
17	29.5	6.22	186.2	160	-167	65.89	10.80	17.00	23.20	2.10	3.29	0.83	146	14	0.00	1.02	0.83	0.33
18	29.4	6.42	260.0	230	-236	176.48	14.50	22.60	30.80	2.41	8.20	1.36	208	10	0.72	1.11	0.39	0.14
19	29.8	6.34	202.0	170	-221	163.84	12.60	17.70	27.00	2.16	3.80	1.22	160	12	0.12	1.47	0.68	0.72
20	29.1	6.11	180.6	150	-203	129.37	11.10	15.70	24.90	2.13	3.29	1.75	144	14	0.36	0.93	1.11	1.25
21	28.4	6.20	182.9	150	-201	91.28	9.40	14.70	24.90	2.11	2.40	1.36	138	10	0.72	0.75	1.37	1.02
22	28.2	6.25	214.6	180	-214	241.26	17.70	25.60	28.50	2.56	9.26	1.22	208	16	0.22	1.96	0.14	1.14
23	27.6	6.05	188.5	160	-186	42.39	7.10	17.80	26.00	2.13	2.71	0.28	140	12	0.36	0.17	0.75	0.85
24	27.8	6.24	182.6	240	-234	154.39	13.70	20.50	30.80	2.05	4.98	1.02	186	10	0.72	1.22	0.56	0.93
25	29.5	6.29	245.6	210	-178	137.09	10.60	22.50	22.80	2.21	6.88	1.08	168	10	0.25	0.56	0.41	1.48
26	27.6	6.50	225.6	190	-172	159.78	12.50	18.50	33.00	1.87	4.54	0.81	170	9	0.32	1.97	0.56	1.85
27	31.5	6.30	210.0	180	-221	34.26	12.10	20.50	25.70	2.05	5.56	0.40	156	14	0.14	0.63	0.48	0.42

Well No	Temp-rature	pH	EC	TDS	ORP	As	Fe	Ca	Na	K	Mg	Mn	HCO_3	Cl	F	PO_4	SO_4	NO_3
28	31.5	6.31	188.0	160	-218	134.05	11.50	22.60	21.70	2.13	4.61	0.99	140	11	1.02	1.24	0.95	1.25
29	29.3	6.48	210.0	180	-176	94.33	14.30	21.00	26.40	2.16	7.32	0.82	190	9	0.36	1.66	0.57	1.01
30	29.3	6.32	260.0	220	-205	186.52	18.80	21.00	24.00	2.76	4.54	1.02	164	13	0.55	1.84	0.69	0.58
31	29.3	6.23	190.3	160	-179	106.38	10.10	22.80	28.50	2.03	4.80	1.32	172	11	0.00	1.52	0.22	0.43
32	29.6	6.37	190.3	160	-184	135.26	11.80	28.90	25.70	1.67	6.95	0.86	180	10	0.22	1.63	0.48	0.17
33	29.4	6.52	271.3	230	-173	55.27	13.70	22.60	21.70	2.38	6.72	0.63	162	12	0.14	1.38	0.31	0.42
34	29.5	6.22	207.6	180	-219	127.37	15.50	20.10	25.00	2.46	4.34	0.47	174	13	0.32	0.49	0.79	0.33
35	29.8	6.21	190.8	160	-231	78.37	8.40	16.30	21.00	2.64	3.20	1.33	120	11	0.22	1.33	0.61	0.42
36	29.6	6.21	176.0	150	-211	75.69	10.20	16.50	24.30	2.18	3.71	0.88	130	13	0.14	1.42	0.54	0.82
37	28.7	6.43	270.6	230	-204	224.62	16.90	27.60	27.20	2.43	8.34	1.19	224	11	0.42	1.71	0.54	0.9
38	28.6	6.36	184.5	160	-178	46.39	12.10	19.20	22.30	1.65	3.27	0.54	128	13	0.66	0.89	0.93	0.25
39	29.4	6.15	210.0	170	-233	67.65	14.90	17.20	22.80	2.11	3.17	0.76	134	8	0.72	1.05	0.50	0.68
40	29.8	6.32	210.0	170	-201	96.26	13.90	15.70	26.80	1.92	2.59	0.92	138	15	1.22	1.27	0.39	0.95
41	30.2	6.53	224.6	190	-177	112.36	13.40	14.90	24.50	2.21	4.88	0.63	142	11	0.05	0.36	0.93	1.02
42	30.5	6.14	214.5	180	-203	156.38	12.00	25.60	24.30	1.90	3.27	1.21	160	12	0.03	1.39	0.31	0.72
43	29.6	6.14	196.7	170	-226	87.37	13.40	13.70	25.50	2.20	4.73	0.92	152	9	0.25	0.66	0.41	0.74
44	29.4	6.14	182.6	160	-204	87.49	13.10	14.70	25.30	2.13	4.20	0.49	148	10	0.00	0.47	0.85	1.53
45	29.7	6.26	230.0	190	-196	71.36	11.70	17.30	24.00	1.87	6.40	1.22	136	15	0.75	0.66	0.70	1.25
46	29.5	6.26	215.3	180	-186	91.74	8.70	15.40	23.80	1.96	3.37	0.55	122	12	0.33	1.45	1.05	1.64
47	29.6	6.52	180.4	150	-212	76.52	9.50	16.30	25.00	1.65	2.40	0.73	130	11	0.00	0.39	0.91	0.53
48	29.6	6.23	210.0	180	-194	2.38	8.10	13.60	12.60	2.15	2.67	0.28	86	12	0.00	0.34	0.62	0.37

Note: The unit of As is µg L^{-1}, Temperature is degree centigrade (^{0}C), Depth is m, EC is µS cm^{-1}, ORP is mV and the unit of the other water quality parameters are mg L^{-1}.

Table A.7. Physicochemical characteristics of the groundwater in the study area – Sixth water sampling (on dated 06/09/2009).

Well No	Temp-rature	pH	EC	TDS	ORP	As	Fe	Ca	Na	K	Mg	Mn	HCO_3	Cl	F	PO_4	SO_4	NO_3
1	28.3	6.02	149	140	-197	111.72	10.83	15.15	23.19	1.57	2.04	0.47	120	8	1.12	0.75	0.19	0.29
2	28.1	6.50	140	120	-202	68.25	10.23	15.26	16.35	1.65	4.21	0.56	130	5	0.62	1.46	0.12	1.65
3	27.3	6.18	145	130	-200	148.13	12.72	14.62	22.67	1.52	3.53	0.52	118	11	0.00	1.77	0.17	1.46
4	27.8	6.11	101	90	-185	43.84	4.80	8.25	10.25	1.16	1.02	0.36	50	15	0.00	0.25	0.17	0.00
5	27.3	6.51	152	130	-191	214.10	19.50	25.20	26.26	2.11	5.71	0.76	184	12	0.03	1.78	0.17	1.09
6	27.2	6.61	138	120	-180	134.00	0.41	11.43	25.63	1.52	4.21	0.79	112	9	0.02	0.51	0.46	0.00
7	27.6	6.71	142	120	-184	195.28	6.95	14.08	20.79	2.20	5.25	0.95	112	11	0.61	1.59	0.75	1.12
8	27.2	6.49	132	120	-193	165.00	7.95	14.08	27.14	1.68	5.14	0.72	140	10	0.28	1.71	0.12	1.49
9	28.6	6.85	165	140	-202	56.25	12.02	26.35	23.58	2.28	5.36	0.11	160	14	0.75	0.58	0.55	0.89
10	31.00	6.25	151	130	-206	276.36	24.20	26.90	31.19	1.74	7.81	1.01	226	7	1.33	2.17	0.66	0.67
11	27.8	6.50	154	130	-195	243.27	22.60	24.80	23.70	2.07	6.31	0.69	209	10	1.51	2.58	0.73	1.69
12	28.1	7.20	236	180	-194	175.06	8.23	22.67	27.30	1.58	3.65	0.65	152	15	0.32	1.25	0.52	0.76
13	27.4	6.39	146	130	-196	87.38	11.05	10.75	26.39	1.44	2.10	0.42	122	9	0.93	2.28	0.39	2.36
14	27.5	6.45	142	130	-187	131.88	13.86	11.33	24.78	1.53	2.19	0.56	120	10	0.00	1.43	0.49	1.99
15	28.3	6.90	242	180	-198	161.25	10.23	21.98	21.21	2.36	6.56	0.96	148	15	0.00	1.35	0.32	1.71
16	27.5	6.70	139	120	-213	146.35	10.25	18.28	21.26	1.25	3.96	0.74	144	11	0.42	1.25	0.21	1.52
17	27.7	6.58	143	130	-185	115.74	14.56	10.48	28.49	1.61	3.20	0.70	138	8	0.00	1.13	0.83	2.06
18	28.8	6.75	165	150	-211	191.97	11.66	24.85	27.30	2.03	7.37	0.61	170	12	0.37	1.68	0.27	2.69
19	28.7	6.70	314	240	-210	173.25	21.40	16.25	28.50	1.45	3.26	0.87	150	12	0.65	2.28	0.35	0.90
20	28.9	6.68	138	120	-215	135.26	21.60	20.20	19.36	1.58	3.12	0.72	156	7	0.72	1.25	0.39	1.46
21	27.8	6.30	129	120	-184	123.88	9.35	11.60	20.46	1.74	2.62	0.45	102	11	0.86	1.97	0.19	2.65
22	28.4	6.47	135	120	-197	303.36	22.60	28.60	35.00	2.61	8.85	1.02	216	16	1.42	2.58	0.81	0.56
23	26.7	6.35	138	120	-191	47.51	8.71	14.51	21.68	1.32	2.17	0.64	114	10	0.42	0.11	0.29	0.27
24	27.5	6.40	138	120	-205	164.11	15.05	12.71	18.01	1.59	3.80	0.77	112	8	0.14	1.05	0.51	2.03
25	26.9	6.35	145	130	-209	151.46	12.27	13.28	19.27	1.66	3.20	0.38	114	10	1.05	0.28	0.15	0.39
26	27.5	6.39	143	130	-193	160.58	8.86	15.78	24.22	1.80	3.53	0.38	120	7	1.05	3.05	0.75	0.25
27	27.3	6.37	138	120	-203	50.19	2.40	14.85	21.10	1.51	1.89	0.54	90	14	0.35	1.15	0.19	2.14

Well No	Temp-rature	pH	EC	TDS	ORP	As	Fe	Ca	Na	K	Mg	Mn	HCO_3	Cl	F	PO_4	SO_4	NO_3
28	27.2	6.43	135	120	-201	142.34	9.44	11.71	21.89	1.44	2.15	0.57	116	10	0.77	1.44	0.46	2.23
29	27.6	6.45	150	130	-191	146.45	10.91	13.03	23.94	1.45	2.70	0.32	122	3	0.70	2.28	0.66	2.84
30	29.6	6.21	180	160	-213	207.62	21.80	24.88	26.35	1.94	6.49	0.83	188	10	1.87	2.08	0.54	1.06
31	29.4	6.22	158	140	-210	124.05	10.78	18.40	24.18	1.45	2.91	0.48	136	9	0.00	1.20	0.34	1.82
32	28.4	6.38	168	150	-200	165.70	10.22	22.41	21.14	1.79	4.66	1.10	146	7	0.40	1.37	0.24	1.82
33	28.6	6.26	141	130	-209	60.16	8.80	16.11	23.80	1.46	1.86	0.54	110	10	0.44	1.62	0.15	1.81
34	29.2	6.18	152	140	-203	130.86	16.23	20.27	23.89	1.75	3.19	0.80	148	12	0.14	0.15	0.24	0.00
35	28.7	5.98	158	140	-197	106.36	24.44	13.19	18.85	1.54	3.03	0.45	118	18	0.00	0.06	0.10	0.00
36	27.5	6.34	128	120	-205	136.63	13.57	11.50	19.80	1.50	2.66	0.55	110	10	0.00	0.16	0.22	0.00
37	29.5	6.62	210	180	-217	267.84	13.96	32.70	38.52	2.69	9.74	0.80	242	10	1.21	1.88	0.19	1.80
38	29.5	6.36	148	130	-195	56.73	13.32	15.01	12.90	1.45	1.47	0.44	100	8	0.51	1.25	0.17	2.63
39	28.8	6.07	142	130	-209	74.99	15.07	17.92	20.88	1.64	2.44	0.78	128	10	1.24	0.25	0.10	0.38
40	28.9	6.40	139	120	-210	106.80	13.13	15.69	23.13	1.46	1.84	0.41	124	14	0.00	1.29	0.00	1.50
41	29.8	6.52	146	130	-189	156.76	16.67	17.18	17.80	1.44	3.09	0.25	126	11	0.73	0.12	0.17	0.30
42	28.8	6.36	137	120	-194	170.01	13.48	20.04	18.13	2.10	4.94	0.51	134	10	0.10	1.98	0.34	0.78
43	29.7	6.21	147	130	-204	123.12	15.30	18.82	21.07	1.77	3.14	0.54	136	9	0.19	0.12	0.22	0.20
44	28.2	6.28	145	130	-212	102.38	12.54	16.90	21.26	1.81	2.67	0.60	130	6	0.00	0.23	0.61	0.67
45	27.7	6.39	150	130	-193	91.18	10.40	15.80	19.25	1.65	3.74	0.72	124	12	1.00	0.27	0.29	0.17
46	27.8	6.34	135	120	-184	108.21	6.97	11.05	29.97	1.58	2.68	0.79	134	8	0.00	2.37	0.34	2.27
47	27.2	6.50	153	130	-194	81.86	9.26	12.62	24.41	1.53	2.70	0.65	128	7	0.52	0.85	0.49	0.00
48	28.5	6.80	180	150	-186	8.05	5.02	13.00	18.46	1.67	2.19	0.12	90	12	0.00	0.46	0.59	1.56

Note: The unit of As is µg L^{-1}, Temperature is degree centigrade (^{0}C), Depth is m, EC is µS cm^{-1}, ORP is mV and the unit of the other water quality parameters are mg L^{-1}.

APPENDIX B

(Development of Arsenic Removal Filter)

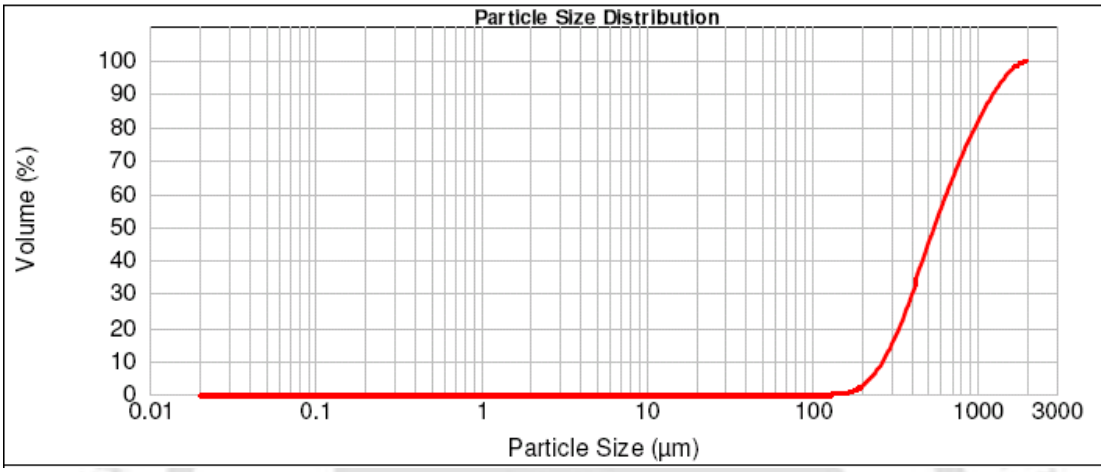

Fig. B.1. Particle size distribution plot of sand.

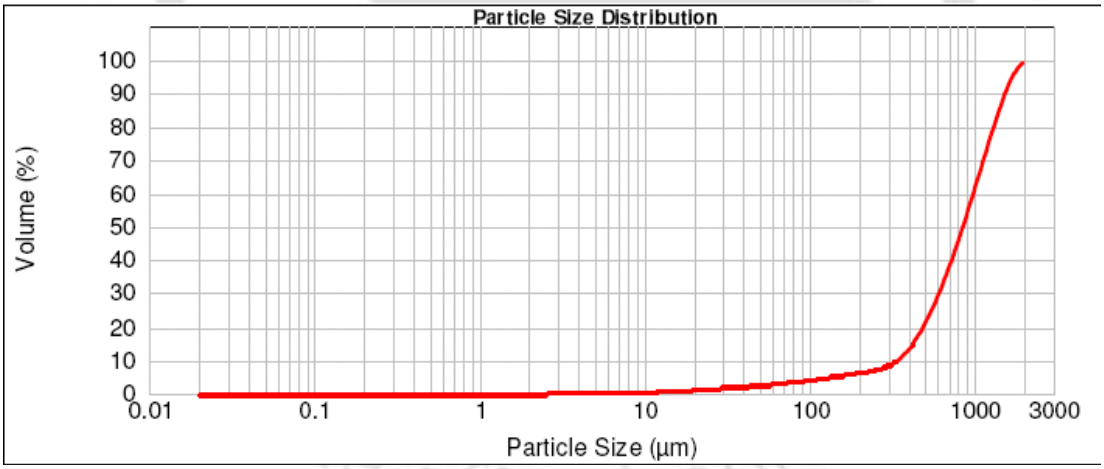

Fig. B.2. Particle size distribution plot of NOIS.

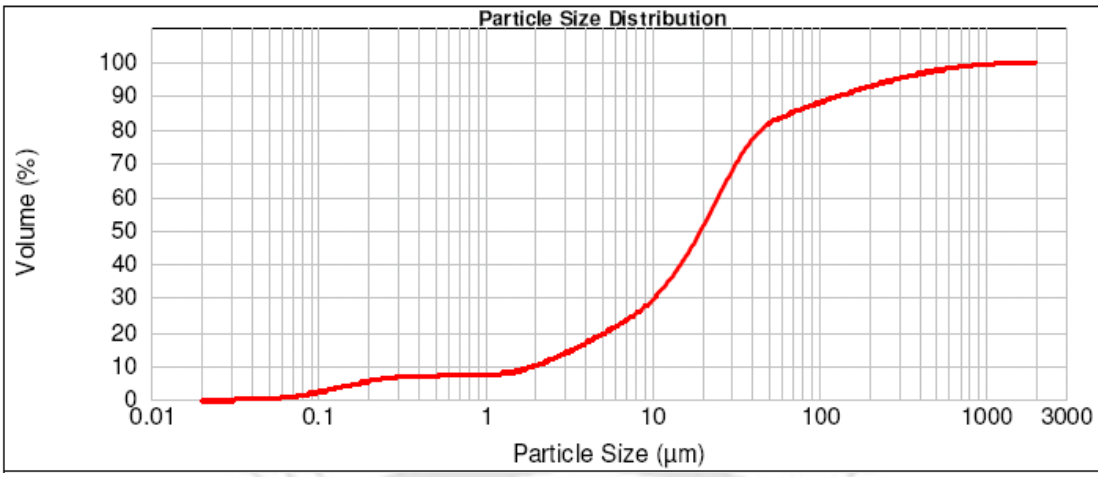

Fig. B.3. Particle size distribution plot of red soil.

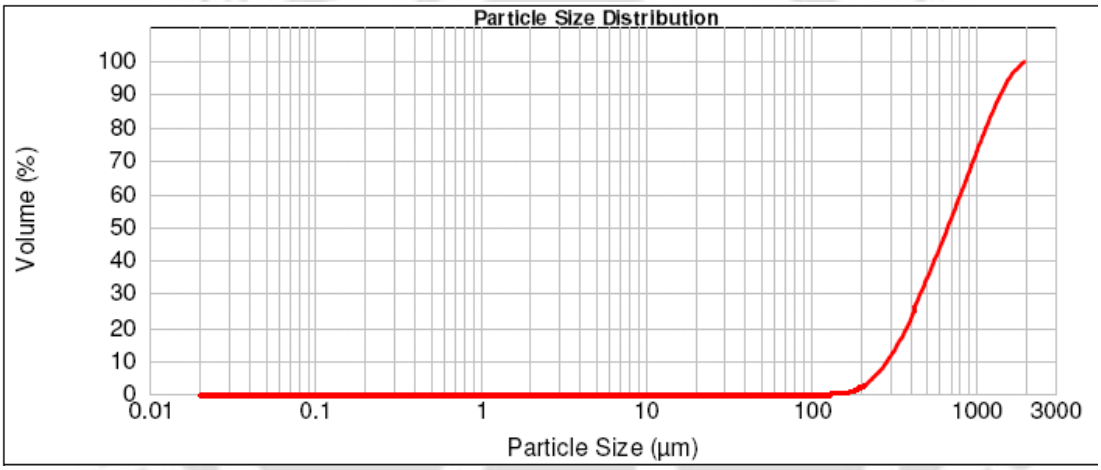

Fig. B.4. Particle size distribution of murum.

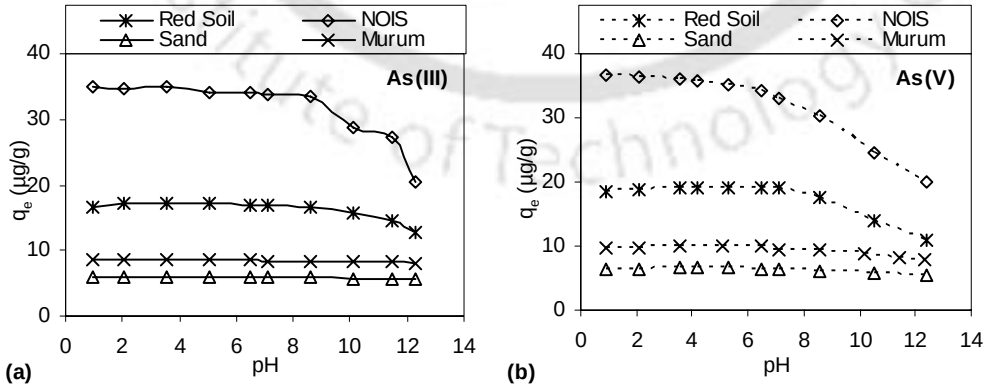

Fig. B.5. Effect of pH on arsenic adsorption by the selected adsorbents.

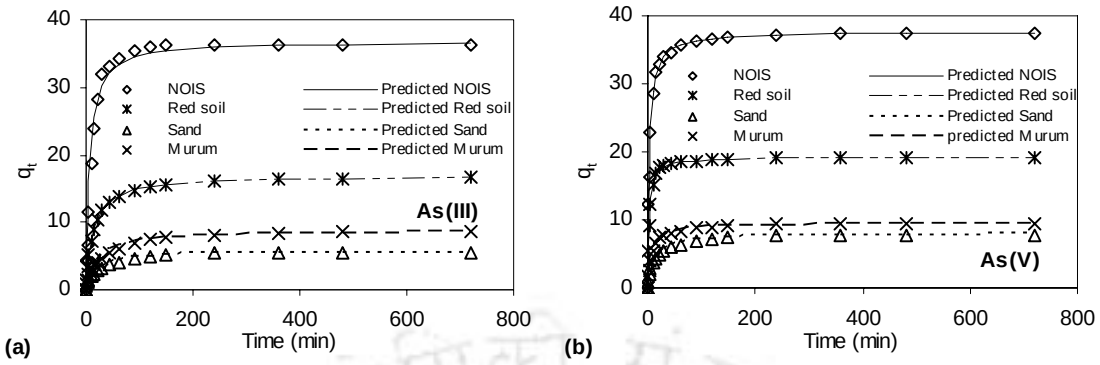

Fig. B.6. Test of pseudo second order reaction model for arsenic adsorption onto different adsorbents.

Table B.1. Langmuir and Freundlich parameters of the selected adsorbents.

Adsorbent	As Species	Langmuir isotherm				Freundlich isotherm			
		q_m (µg g^{-1})	b (L μg^{-1})	R^2	RL	K_F ($\mu g^{1-(1/n)}$ $L^{1/ng-1}$)	n	q_m (µg g^{-1})	R^2
Red soil	As(III)	21.9	0.014	0.991	0.27	0.9	1.8	17.8	0.991
	As(V)	46.4	0.012	0.993	0.29	1.2	1.5	40.3	0.987
Sand	As(III)	17.2	0.007	0.999	0.43	0.3	1.6	10.3	0.993
	As(V)	23.8	0.014	0.994	0.27	0.9	1.7	19.7	0.992
NOIS	As(III)	155.6	0.006	0.967	0.44	1.4	1.2	109.7	0.998
	As(V)	245.1	0.006	0.929	0.47	1.7	1.2	166.9	0.999
Murum	As(III)	37.2	0.006	0.997	0.44	0.5	1.4	23.3	0.990
	As(V)	25.2	0.019	0.990	0.21	1.3	1.9	22.9	0.991

Table B.2. Water quality parameters of the arsenic challenged water used for performance testing of the designed filter.

Water quality parameter	**Concentration**
pH	6.72
Temperature (Degree C)	24.3
EC (µS cm-1)	162
Turbidity (NTU)	2
Na (mg L-1)	34
K (mg L-1)	1.3
Ca (mg L-1)	46
Mg (mg L-1)	5.6
Mn (mg L-1)	2.2
As (µg L-1)	200
HCO_3 (mg L-1)	186
Cl (mg L-1)	12
SO_4 (mg L-1)	1.2
PO_4 (mg L-1)	bdl

Table B.3. Designed arsenic removal filter experimental data.

Time (hr)	Through put Volume (L)	Bed Volume	Effluent As Conc (µg L^{-1})
24	36	24.66	0.00
48	72	49.32	0.00
72	108	73.97	0.00
96	144	98.63	0.00
120	180	123.29	0.00
144	216	147.95	0.00
168	252	172.60	0.00
192	288	197.26	0.00
216	324	221.92	0.00
240	360	246.58	0.00
264	396	271.23	0.00
288	432	295.89	0.00
312	468	320.55	0.00
336	504	345.21	0.00
360	540	369.86	0.00
384	576	394.52	0.00
408	612	419.18	0.00
432	648	443.84	0.00
456	684	468.49	0.00
480	720	493.15	0.00
504	756	517.81	0.00
528	792	542.47	0.00
552	828	567.12	0.00
576	864	591.78	0.00
600	900	616.44	0.00
624	936	641.10	0.00
648	972	665.75	0.00
672	1008	690.41	0.00
696	1044	715.07	0.00
720	1080	739.73	0.00
744	1116	764.38	0.00
768	1152	789.04	0.00
792	1188	813.70	0.00
816	1224	838.36	0.00
840	1260	863.01	0.00
864	1296	887.67	0.00
888	1332	912.33	0.00
912	1368	936.99	0.00
936	1404	961.64	0.00
960	1440	986.30	0.00
984	1476	1010.96	0.00
1008	1512	1035.62	0.00
1032	1548	1060.27	0.00
1056	1584	1084.93	0.00
1080	1620	1109.59	0.00
1104	1656	1134.25	0.00
1128	1692	1158.90	0.00
1152	1728	1183.56	0.00
1176	1764	1208.22	0.00
1200	1800	1232.88	0.00
1224	1836	1257.53	0.00
1248	1872	1282.19	0.00
1272	1908	1306.85	0.00
1296	1944	1331.51	0.00
1320	1980	1356.16	0.00
1344	2016	1380.82	0.00
1368	2052	1405.48	0.12
1392	2088	1430.14	0.15
1416	2124	1454.79	0.31
1440	2160	1479.45	0.22
1464	2196	1504.11	0.42
1488	2232	1528.77	0.39
1512	2268	1553.42	0.27
1536	2304	1578.08	0.15
1560	2340	1602.74	0.32
1584	2376	1627.40	0.26
1608	2412	1652.05	0.14
1632	2448	1676.71	0.08
1656	2484	1701.37	0.31
1680	2520	1726.03	0.26
1704	2556	1750.68	0.18
1728	2592	1775.34	0.34
1752	2628	1800.00	0.00
1776	2664	1824.66	0.20
1800	2700	1849.32	0.04
1824	2736	1873.97	0.27
1848	2772	1898.63	0.11
1872	2808	1923.29	0.06
1896	2844	1947.95	0.04
1920	2880	1972.60	0.03
1944	2916	1997.26	0.41
1968	2952	2021.92	0.11
1992	2988	2046.58	0.22
2016	3024	2071.23	1.75
2040	3060	2095.89	2.20
2064	3096	2120.55	2.98
2088	3132	2145.21	2.05
2112	3168	2169.86	2.80
2136	3204	2194.52	2.35
2160	3240	2219.18	2.73
2184	3276	2243.84	3.08
2208	3312	2268.49	3.25
2232	3348	2293.15	4.23
2256	3384	2317.81	4.88
2280	3420	2342.47	3.40
2304	3456	2367.12	6.18
2328	3492	2391.78	5.45
2352	3528	2416.44	6.90
2376	3564	2441.10	7.13
2400	3600	2465.75	6.45
2424	3636	2490.41	7.43
2448	3672	2515.07	8.13
2472	3708	2539.73	8.53
2496	3744	2564.38	9.45
2520	3780	2589.04	9.35
2544	3816	2613.70	10.10
2568	3852	2638.36	10.68
2592	3888	2663.01	13.63
2616	3924	2687.67	15.23
2640	3960	2712.33	20.00
2664	3996	2736.99	26.00
2688	4032	2761.64	31.53
2712	4068	2786.30	38.20
2736	4104	2810.96	49.58
2760	4140	2835.62	59.75
2784	4176	2860.27	63.70
2808	4212	2884.93	63.70
2832	4248	2909.59	69.40
2856	4284	2934.25	72.00
2880	4320	2958.90	82.30
2904	4356	2983.56	85.10
2928	4392	3008.22	90.30
2952	4428	3032.88	96.00
2976	4464	3057.53	104.00
3000	4500	3082.19	108.00
3024	4536	3106.85	110.00
3048	4572	3131.51	113.70
3072	4608	3156.16	126.00
3096	4644	3180.82	126.60
3120	4680	3205.48	128.60
3144	4716	3230.14	131.50
3168	4752	3254.79	133.50
3192	4788	3279.45	144.40
3216	4824	3304.11	147.20
3240	4860	3328.77	148.80
3264	4896	3353.42	152.00
3288	4932	3378.08	158.50
3312	4968	3402.74	166.00
3336	5004	3427.40	168.40
3360	5040	3452.05	176.10
3384	5076	3476.71	178.80
3408	5112	3501.37	181.20
3432	5148	3526.03	185.00
3456	5184	3550.68	187.10
3480	5220	3575.34	189.00
3504	5256	3600.00	192.40
3528	5292	3624.66	196.10
3552	5328	3649.32	197.10
3576	5364	3673.97	198.54
3600	5400	3698.63	200.00